EVALUATION OF THE USE OF COVERS FOR REDUCING ACID GENERATION FROM STRATHCONA TAILINGS

MEND Project 2.25.3

September 1997

**EVALUATION OF THE USE OF COVERS
FOR REDUCING ACID GENERATION
FROM STRATHCONA TAILINGS
7777-112
MEND Project 2.25.3**

Final Report

This work was funded under the Canada-Ontario Mineral Development Agreement

Prepared For:

Glen Hall
Supervisor Environmental Affairs
Falconbridge Limited
Sudbury Operations
Falconbridge, Ontario

and Michael P. Sudbury
Director Environmental Affairs
Falconbridge Limited
Toronto, Ontario

Prepared By:

Lakefield Research Limited
P.O. Bag 4300, 185 Concession Street
Lakefield, Ontario
K0L 2H0

April, 1997

TABLE OF CONTENTS

LIST OF TABLES

LIST OF FIGURES

LIST OF APPENDICES

EXECUTIVE SUMMARY

An evaluation of the effectiveness of organic covers in reducing acid generation from sulphidic tailings was conducted. The materials evaluated were: lime-stabilized sewage sludge (LSSS), municipal solid waste (MSW) compost, and peat. One inorganic material, desulphurized tailings (DST), was included in the evaluation for comparative purposes, due to the potential for production of this material at operating mining properties. The evaluation included three components: physical and chemical characterization of the tailings and cover materials, salt migration column tests, and pilot-scale cells.

Material characterization indicated that the tailings were more finely grained and had a lower hydraulic conductivity than the LSSS, compost and peat. The compost and peat tended to decompose and compact with time. The LSSS, compost and peat were more readily drained than the tailings.

Surface evaporation decreased with increasing cover depth. The DST and peat had the highest evaporation rates and these materials also exhibited a significant increase in conductivity at the surface. A direct relationship between evaporation and salt accumulation was apparent. A capillary barrier did not affect the rate of evaporation.

Pilot cell testing indicated a reduction in acid generation in tailings beneath the LSSS cover. The pH of the pore water and leachate increased, while the level of dissolved metals and sulphate decreased. The LSSS demonstrated a high oxygen consuming ability and maintained over 90% water saturation throughout the cover depth.

The DST cover maintained high moisture levels, inhibiting the movement of oxygen and water into the underlying tailings. The high air entry value and low hydraulic conductivity resulted in reduced volumes of leachate. High evaporation rates and desiccation cracking were observed, however, indicating that DST would be unsuitable as a single cover material.

Further work would be recommended to determine the effects of an evaporative barrier on evaporative losses, salt migration and crack formation.

The results of the program indicated that LSSS and DST offer the greatest potential for reducing metal and sulphate loading from oxidized tailings. The benefits of utilizing LSSS are based on chemical changes within the tailings pore water, while the benefits of DST are physical, namely, low hydraulic conductivity and a high degree of saturation.

SOMMAIRE

On résume dans ce rapport les résultats d'un projet pilote, d'une durée d'un an, qui avait été conçu pour évaluer l'efficacité de diverses matières organiques comme couvertures permettant de limiter ou de réduire l'impact sur l'environnement du drainage minier acide provenant des résidus acidogènes. Lakefield Research Limited a conclu un contrat avec Falconbridge Limited pour effectuer ces travaux dans le cadre du programme de Neutralisation des eaux de drainage dans l'environnement minier (NEDEM). Trois matières de couverture ont été testées: boues d'épuration stabilisées à la chaux, compost de déchets solides municipaux et tourbe. Des résidus désulfurés, une matière de couverture inorganique, ont aussi été utilisés lors de l'étude, et ce, à des fins de comparaison et en raison de la production potentielle de volumes importants de ce matériau sur les sites miniers en exploitation.

Le programme d'essais comprenait trois volets: caractérisation des résidus et de la matière de couverture, détermination en colonne de la migration des sels et tests en cellule à l'échelle pilote. Les déterminations en colonne de la migration des sels et les tests en cellule à l'échelle pilote ont, tous les deux, permis d'évaluer le système couverture-résidus.

On a procédé à une caractérisation chimique, physique, minéralogique et hydrogéologique des résidus oxydés, des résidus de pyrrhotine et des matières de couverture. Une analyse multi-éléments a révélé que les résidus oxydés présentaient une teneur en aluminium, en calcium, en magnésium et en sodium de 3 à 4 fois plus élevée que les résidus de pyrrhotine. Des concentrations semblables de cadmium, de cobalt, de chrome, de cuivre, de manganèse et de plomb ont été mesurées dans les résidus oxydés et dans les résidus de pyrrhotine. Les concentrations de nickel et de zinc étaient plus élevées dans les résidus de pyrrhotine que dans les résidus oxydés. Les concentrations de fer et de soufre total dans les résidus oxydés étaient de 38 % et de 19 %, respectivement, alors qu'elles étaient de 53 % et de 31 % dans les résidus de pyrrhotine.

Le compost, la tourbe et la matière capillaire présentaient une distribution granulométrique plus grossière, tandis que les résidus oxydés, les résidus désulfurés, les résidus de pyrrhotine et les boues d'épuration stabilisées à la chaux étaient constitués de grains beaucoup plus fins. La taille granulométrique de 80 % des matières tamisées était de 3022 µm dans le cas de la matière capillaire, de 2835 µm dans le cas du compost, de 2653 µm dans le cas de la tourbe, de 170 µm dans le cas des résidus oxydés, de 130 µm dans le cas des résidus désulfurés, de 76 µm dans le cas des boues d'épuration stabilisées à la chaux et de 34 µm dans le cas des résidus de pyrrhotine.

La teneur volumique en humidité au moment de la réception était de 158 % pour la tourbe, de 32 % pour les boues d'épuration stabilisées à la chaux et de 13 % pour le compost. La valeur calculée de la porosité était de 71 % dans le cas des boues d'épuration stabilisées à la chaux, de 59 % dans le cas du compost et de 60 % dans le cas de la tourbe.

L'analyse minéralogique a révélé que la pyrrhotine constituait le principal minéral sulfuré des résidus oxydés (75-80 % de sulfures, en volume) et des résidus de pyrrhotine (>90 % de sulfures, en volume).

Des mesures in situ réalisées à la surface des couvertures dans les cellules pilotes ont indiqué que la conductivité hydraulique ne changeait pas après un an d'essais réalisés sur les résidus oxydés ($2,0 \times 10^{-5}$ cm/s), les résidus désulfurés ($3,5 \times 10^{-5}$ cm/s) et les boues d'épuration stabilisées à la chaux (3×10^{-3} cm/s). Toutefois, la conductivité hydraulique diminuait d'un ordre de grandeur à la surface de la couverture de compost (de $2,1 \times 10^{-1}$ à $2,6 \times 10^{-2}$ cm/s) et de la couverture de tourbe (de $6,8 \times 10^{-2}$ à $4,8 \times 10^{-3}$ cm/s). La décomposition et le compactage étaient, estime-t-on, responsables de cette diminution observée dans les valeurs de conductivité hydraulique.

Les valeurs d'entrée d'air (AEV), qui ont été estimées à partir des courbes de drainage, étaient de 450 cm de H_2O pour les résidus oxydés, de 525 cm de H_2O pour les résidus désulfurés, de 100 cm de H_2O pour les boues d'épuration stabilisées à la chaux, de 25 cm de H_2O pour le compost et de 15 cm de H_2O pour la tourbe. Ces valeurs indiquent que les résidus oxydés et les résidus désulfurés peuvent retenir de l'eau sous une succion beaucoup plus intense que les boues d'épuration stabilisées à la chaux, le compost et la tourbe. Le drainage procéderait plus rapidement dans les boues d'épuration stabilisées à la chaux, dans le compost et dans la tourbe que dans les résidus.

Le flux d'évaporation a été mesuré en laboratoire, et il a été déterminé qu'au cours des sept premiers jours le rapport entre l'évaporation réelle et l'évaporation potentielle était en moyenne de 0,75 pour les résidus oxydés, de 0,893 pour les résidus désulfurés, de 0,831 pour les boues d'épuration stabilisées à la chaux, de 0,869 pour le compost et de 0,843 pour la tourbe.
Ces rapports ont servi lors du calcul de la perte d'eau par évaporation dans les cellules pilotes durant les mesures du bilan hydrique des cellules.

La teneur en carbone organique total (COT) de trois matières de couverture organiques a été déterminée au début et à la fin de l'essai en cellule pilote d'une durée d'un an. La teneur initiale était de 1,68 % dans le cas des boues d'épuration stabilisées à la chaux, de 20,1 % dans le cas du compost et de 23,1 % dans le cas de la tourbe. Après un an d'essais, la COT était la même dans les boues d'épuration stabilisées à la chaux, tandis qu'il y avait eu diminution d'environ 69 % et 29 % à une profondeur de 15 cm et de 45 cm dans la couverture de compost, respectivement, et d'environ 4 % et 16 % à une profondeur de 15 cm et de 45 cm dans la couverture de tourbe, respectivement.

Un essai d'incubation à court terme et une modélisation ont été effectués sur des boues d'épuration stabilisées à la chaux semblables à celles utilisées lors des essais en cellule pilote et sur un mélange constitué de ces boues d'épuration et de résidus désulfurés. L'essai d'incubation n'a révélé aucune trace de décomposition manifestée par un dégagement de dioxyde de carbone. Le dosage, avant et après l'essai, du COT et du carbone organique soluble laisse supposer qu'il n'y avait décomposition que dans les boues d'épuration stabilisées à la chaux et non dans le mélange constitué de boues d'épuration et de résidus désulfurés. La modélisation des résultats des dosages du COT permet de prévoir un taux annuel de décomposition de 16 % pour les boues d'épuration stabilisées à la chaux, au cours des deux premières années, dans des conditions climatiques semblables à celles qui règnent dans la région de Sudbury.

Après deux ans, lorsque toute la matière organique facilement décomposable aura été épuisée, le taux de décomposition diminuera considérablement. Selon des estimations grossières, environ 80

% du COT sera transformé en dioxyde de carbone après dix ans. Le mélange constitué de boues d'épuration sèches stabilisées à la chaux et de résidus désulfurés est très résistant à la décomposition.

Lors de la détermination en colonne de la migration des sels, on a observé que la vitesse d'évaporation en surface diminuait au fur et à mesure qu'augmentait la profondeur de la couverture. Parmi les matières de couverture examinées, les résidus désulfurés et la tourbe présentaient les vitesses d'évaporation les plus élevées, tandis que les boues d'épuration stabilisées à la chaux et le compost présentaient les vitesses les plus faibles. La plus grosse augmentation de conductivité électrique a aussi été observée à la surface des couvertures de résidus désulfurés et de tourbe, tandis que la plus faible a été notée dans le compost et les boues d'épuration stabilisées à la chaux, ce qui laisse supposer l'existence d'une relation directe entre l'évaporation et l'accumulation de sel à la surface. Le sel accumulé à la surface était surtout constitué de sulfate, de fer et de magnésium.

La vitesse d'évaporation dépendait de la teneur en humidité près de la surface des couvertures. Au fur et à mesure qu'augmentait la profondeur de la couverture, la teneur en humidité à la surface diminuait, entraînant ainsi une réduction de la vitesse d'évaporation et une faible augmentation correspondante de la conductivité électrique.

La conductivité électrique élevée des boues d'épuration stabilisées à la chaux n'était reliée, estime-t-on, ni à la vitesse d'évaporation ni à la migration vers la surface des sels en provenance des résidus oxydés sous-jacents, mais dépendait plutôt de la dissolution des sels présents dans les boues d'épuration. Les sels responsables de l'augmentation de conductivité électrique étaient surtout constitués de calcium, de magnésium, de sulfate et probablement d'ions bicarbonate et hydroxyle.

L'utilisation de barrières capillaires pour réduire la migration des sels vers la surface était efficace dans le cas d'une couverture de 0,15 m, mais non dans le cas d'une couverture de 0,5 m et de 1,0 m de profondeur. La barrière capillaire n'avait aucun effet perceptible sur la vitesse d'évaporation. Les barrières capillaires ne permettaient pas de réduire efficacement l'accumulation de sels dans la couverture épaisse, en raison de l'ascension capillaire provoquée par le compactage et l'utilisation d'un matériau à granularité étalée.

Lors des essais en cellule pilote d'une durée d'un an, on a observé des effets positifs sur la réduction de la quantité d'acide produite sous la couverture constituée de boues d'épuration stabilisées à la chaux. Il y avait augmentation du pH et de la teneur en carbone organique dissous dans l'eau interstitielle et diminution de la teneur en sulfate et en métaux dissous dans l'eau interstitielle des résidus oxydés sous la couverture de boues d'épuration stabilisées à la chaux. On a aussi observé, dans la cellule pilote comportant une couverture de boues d'épuration stabilisées à la chaux, une augmentation du pH du lixiviat et une diminution de la concentration de sulfate et de métaux dissous dans le lixiviat, ainsi qu'un apport moindre dans l'environnement de sels provenant des résidus oxydés sous-jacents. L'alcalinité élevée des boues d'épuration stabilisées à la chaux contribuait à l'augmentation de pH observée dans l'eau interstitielle et le lixiviat. D'autres processus microbiens qui consomment de l'acide (par exemple, la réduction des sulfates par les bactéries sulfatoréductrices) contribuent également à l'augmentation du pH. La

diminution des teneurs en sulfate et en métaux des résidus oxydés sous-jacents était peut-être le résultat (1) de la précipitation du fer sous forme d'hydroxyde ferrique et du sulfate sous forme de sulfate de calcium hydraté et (2) de la précipitation des sulfures métalliques par l'intervention de bactéries sulfatoréductrices. Les boues d'épuration stabilisées à la chaux pouvaient consommer beaucoup d'oxygène et restaient saturées à plus de 90 % dans l'ensemble de l'épaisseur de la couverture.

Comme on l'a mentionné plus haut, les boues d'épuration stabilisées à la chaux comportent de nombreux avantages, mais elles suscitent aussi certaines inquiétudes dont: pH très élevé (>12) et conductivité électrique élevée, ce qui constitue un environnement difficile pour les plantes; concentrations de cuivre élevées dans l'eau interstitielle des boues d'épuration stabilisées à la chaux; concentrations élevées de phosphore total dans l'eau interstitielle et les lixiviats des boues d'épuration stabilisées à la chaux; et concentrations élevées de phénol dans le lixiviat.

La couverture de résidus désulfurés était efficace également pour réduire l'apport de substances dans l'environnement, en maintenant un taux élevé d'humidité et en freinant l'infiltration de l'oxygène et de l'eau vers les résidus sous-jacents. Les résidus désulfurés présentaient une valeur d'entrée d'air élevée (510 cm de H2O) et une faible conductivité hydraulique (de l'ordre de 10-5 cm/s) et conservaient un degré de saturation à plus de 90 % dans l'ensemble de l'épaisseur de la couverture. Ces caractéristiques alliées aux faibles concentrations de sels dans la couverture ont entraîné une diminution des volumes de lixiviat provenant des résidus oxydés sous-jacents. Les résidus désulfurés ne convenaient pas, estimait-on, comme matière de couverture unique, en raison de la vitesse élevée d'évaporation et de la formation subséquente dans la couverture de fissures permettant à l'oxygène de migrer directement jusqu'aux résidus oxydés sous-jacents. Cette migration directe de l'oxygène est peut-être responsable de l'augmentation, indicative de l'oxydation en cours, des concentrations de fer et de sulfate observée dans l'eau interstitielle des résidus oxydés sous-jacents.

Le compost possédait une grande capacité de consommation d'oxygène et présentait un pH alcalin. Toutefois, la teneur en carbone organique dissous et le pH de l'eau interstitielle des résidus oxydés sous-jacents ne changeaient pas, mais sa teneur en sulfate et en fer augmentait, ce qui permet de supposer que le lixiviat provenant de la couverture n'avait pas interagi positivement avec les résidus sous-jacents. Le compost maintenait un degré de saturation d'environ 60 % et pouvait piéger toute la précipitation qui le pénétrait, ce qui entraînait dans l'environnement un important apport de sels en provenance des résidus oxydés sous-jacents.

Parmi les matières organiques utilisées comme couverture qui ont été soumises à des essais, c'est la tourbe qui semble posséder les caractéristiques les moins favorables. La tourbe n'exerçait aucun effet sur la migration de l'oxygène, en raison de son incapacité de consommer l'oxygène et de maintenir un niveau de saturation suffisant pour réduire la vitesse d'infiltration de l'oxygène. Tout comme dans le cas des résidus désulfurés et du compost, les concentrations de sulfate et de fer dans l'eau interstitielle des résidus oxydés sous-jacents demeuraient élevées et le pH de l'eau interstitielle des résidus restait inférieur à 4,0. De plus, tout comme dans le cas du compost, les cellules de tourbe entraînaient, dans l'environnement, un apport élevé de sels provenant des résidus oxydés sous-jacents.

D'après les résultats obtenus jusqu'ici, on peut conclure que ce sont les boues d'épuration stabilisées à la chaux et les résidus désulfurés qui permettraient, semble-t-il, de réduire le plus l'apport, dans l'environnement, de sulfate et de métaux dans l'eau se déplaçant par migration à partir des résidus oxydés sous-jacents.

Vu la nature des résidus oxydés (c.-à-d. présence d'oxydants subsistant après une oxydation préalable; limite des sulfates réductibles), il est nécessaire d'évaluer l'efficacité des matières de couverture à réduire la formation d'acide sur une période plus longue. Il a donc été recommandé de poursuivre le contrôle des couvertures constituées de boues d'épuration stabilisées à la chaux, de résidus désulfurés et de compost.

Comme il se peut que d'importants volumes de résidus désulfurés soient produits à des sites d'exploitation minière et comme les caractéristiques de couverture observées dans le cadre du présent programme d'essais sont favorables, nous examinons des méthodes qui permettraient de réduire les pertes par évaporation des résidus désulfurés et la fissuration qui en découle. La présence d'une barrière empêchant l'évaporation à partir des résidus désulfurés permettrait très probablement de réduire les pertes par évaporation, l'accumulation de sels en surface et la formation de fissures.

Une barrière empêchant l'évaporation assurerait aussi une protection contre l'érosion et, ainsi, permettrait de maintenir l'intégrité physique du système de couverture.

Il est recommandé de procéder sur le terrain à des essais bien conçus, ce qui permettrait d'évaluer de façon plus approfondie la performance des couvertures, en complément des études en laboratoire décrites dans le présent rapport.

1.0   INTRODUCTION

The following report summarizes the results of a one year pilot project designed to investigate the use of various organic materials for covering tailings. Two progress reports on this project have been submitted to MEND and Falconbridge Limited. This is the final report to be submitted to MEND and Falconbridge Limited after the completion of the revised program scope.

The cover-tailings pilot experiments described in this report were commissioned by Falconbridge Limited. Lakefield Research Limited assisted with the design of the pilot tests and, after construction of the required test apparatus, performed the material characterization testing and monitored the cover cell test. Additional analytical and experimental support has been provided by staff at the Noranda Technology Centre (NTC) and various universities including: the University of Saskatchewan, the University of Waterloo, and the Ohio State University.

1.1   Background

Large quantities of organic material are now stockpiled, or may be available in the near future, from urban and industrial sources. A previous study conducted by Pierce (1992) indicated that the cities in Ontario are capable of producing approximately 680,000 tonnes of municipal solid waste (MSW) compost annually and create comparable amounts of sewage sludge, which is currently landfilled. Peat from bogs in the Canadian Shield region, although not a waste material, represents a vast renewable source of organic matter. Peat bogs are often found near base metal and precious metal mines.

These materials may provide effective and affordable solutions to the reclamation of acidic mine tailings. A literature review of the physical and chemical characteristics of MSW

compost and other organic materials (Pierce, 1992) revealed that an organic layer on sulphide tailings could be beneficial in the suppression of tailings oxidation and acidic mine drainage, in the following five ways:

1. _Physical oxygen barrier_ - The organic cover layer may be saturated with water over at least part of its depth. This saturation could be the limiting factor for the rate of oxygen diffusion into the tailings and this rate could be as low as the diffusivity of oxygen in water.

2. _Oxygen-consuming barrier_ - The decomposition of organic materials may create a large biological oxygen demand which would act as a sink for atmospheric oxygen and dissolved oxygen in infiltrating water.

3. _Chemical inhibition_ - Compounds and decomposition products in the organic material that leach into the tailings may inhibit the growth and metabolism of sulphate-producing (acidifying) bacteria.

4. _Chemical amelioration_ - Organic compounds in the organic material may cause the reductive dissolution of iron oxides (either directly or indirectly by providing metabolic substrates for bacteria), the reduction of sulphate, and the prevention of indirect ferrous sulphide oxidation and acid generation.

5. _Reduced water infiltration_ - The decomposition and resultant compaction of an organic cover layer may result in a decreased hydraulic conductivity of the cover. This would result in a subsequent decrease in infiltration, thus decreasing tailings ground water flow.

A potential problem associated with the use of organic materials as covers may be the effect of decomposition products, particularly organic acids, on the solubility (due to weathering of tailings minerals) and on the mobility of dissolved metals (Pierce 1992). In a short term experiment using MSW compost as a cover layer on oxidized tailings, an increase in the

concentrations of trace metals in pore water was observed in some models tested (Pierce et al. 1994). This trace metal increase observed may have been due to metal dissolution or chelation by organics in methods similar to the acid generation process in sulphides; or, the dissolution of previously oxidized and precipitated metals as they are reduced to a sulphide form through soluble phases during the reduction process (reductive dissolution). An example of reductive dissolution would be the transformation of ferric iron hydroxide solids to a mobile ferrous iron. Because ferric hydroxide solids can scavenge many metals, there also exists the potential for the release of these metals when the ferric iron hydroxide solids dissolve.

Even though increases in dissolved metal concentrations were observed in some columns in which compost was mixed with tailings, other columns in which tailings were covered with 5 cm coarse sand and 30 cm compost showed low metal concentrations (Pierce et al. 1994, CIMMER 1994). These columns clearly showed low oxygen and Eh levels and the precipitation of sulphides. Trace metal levels were highest in samples from a mixed compost and tailings layer. This suggests that the close contact between organic decomposition products, bacteria, and tailings was accelerating the release of metals.

The mobilization of metals seen in the compost cover layer experiment (Pierce et al. 1994, CIMMER 1994) may be a transitory phase that will be followed by increasing immobilization of metals by complexation to organic compounds and the formation of metal sulphide precipitates. These processes are mediated primarily by soluble humic acids and by the sulphate-reducing bacteria (SRB) that are found in anoxic environments. These anaerobic microbes require organic compounds, particularly organic acids, for their metabolism. This consumption of organic acids results in an increase in pH which would further enhance the SRB activity. SRB and other bacteria also cause an increase in pH through an acid consuming process, which results in the formation of methane or hydrogen gas. Increasing pH and certain organic compounds also suppress the acid-generating process by inhibiting the growth and activity of the autotrophic iron bacteria *Thiobacillus ferrooxidans* that thrive at the low pH range of 1.5 to 3.5 (Pierce 1992).

Lakefield Research Limited
Environmental Services

The migration of metals as relatively stable, soluble, organo-metal complexes will largely be controlled by the solution pH. Under conditions where the pH of the solution is imposed by factors other than the presence of the organic acids, metal dissolution through complexation will be greater at pH above 5 than at pH below 4. At pH<5, the dissolution of metals will increase with decreasing pH. Consequently, the combined effects of ARD and organic acids on metal dissolution and migration are likely to be very complex. Most peat, compost and lime stabilized sewage sludge generally have pH values above 5. Studies (Pierce et al. 1994) have shown significant pH increases, to as high as 8, as a result of compost covers on previously oxidized, low pH tailings.

Sulphate and iron reduction rates may be limited in a tailings system by a lack of organic substrates for bacterial metabolism. Consequently, an organic cover layer on the tailings may be an important source of carbon compounds for bacteria as decomposition and leaching proceeds. The biological oxygen demand of an aerobic, actively-decomposing organic layer constitutes a strong sink for atmospheric oxygen. This can decrease the oxygen concentration for the ARD oxidation processes in the tailings.

Oxygen consumption in an organic cover layer material will eventually decline as the remaining material becomes more humified and more resistant to further decomposition (Pierce 1992). Therefore, the biological oxygen demand of the organic cover layer will eventually reach a lower level based on a lower input rate of natural carbon compounds and other nutrients into the cover layer. The resistance that the cover layer will still be able to offer to the downward diffusion of atmospheric oxygen will then be determined by its physical properties, especially its depth and gas-filled porosity. Gas-filled porosity, in turn, will be determined by the structural composition of the material and the degree that the pore spaces are filled with water (i.e. water content).

1.2   Purpose & Scope

The purpose of this program was to evaluate the effectiveness of various materials in the elimination or reduction of acid generation and the movement of acidity and heavy metals from tailings ponds. Three organic materials were studied, namely, peat, municipal solid waste (MSW) compost, and lime-stabilized sewage sludge (LSSS). One inorganic material, desulphurized tailings, was studied to provide a contrasting cover layer that may also prove to be cost-effective. The organic materials were believed to have physical and chemical characteristics that will decrease the rates of the acid generation processes in sulphide tailings, or reverse the acid generation processes and cause the precipitation of sulphides. These materials may also decrease the movement of water through the tailings pond (Pierce 1992, Pierce et al. 1994) and are potentially available in large quantities at low costs.

Background information from previous studies has shown that it is important to evaluate the process of organic leachate interaction with tailings. An assessment of the relative production and consumption of organic decomposition products is being conducted for each type of cover material. This balance is being assessed by examining the processes in-situ during the pilot experiments.

The research project had the following objectives:

1. To experimentally compare the effectiveness of organic and inorganic cover layers in reducing acid generation and the mobilization of trace metals from partially oxidized acid generating tailings.

2. To evaluate the extent and rates of upward salt migration in a range of cover materials under worst case conditions, assess the need and effectiveness of a capillary barrier , and to correlate physical characteristics and depth with salt migration.

3. To monitor the organic and inorganic chemistry of three organic and one inorganic tailings cover system in an effort to understand and quantify the aerobic and anaerobic organic degradation rates and processes and their interaction with acid generating tailings.

4. To evaluate the physical characteristics of three organic and one inorganic cover to determine their ability to remain saturated enough to minimize oxygen transport. This would assist in the development of a quantitative relationship to predict the ability of a cover to remain saturated under natural conditions.

The test program included three main components of study:
1. Characterization of Tailings and Cover Materials
2. Salt Migration Columns
3. Pilot Scale Test Cells

2.0   METHODS

The following section details the scope of work and procedures used in the three main components of the test program noted above.

2.1   Sample Preparation

On September 12, 1994, a shipment of 30 drums of Strathcona oxidized tailings was received at Lakefield Research Limited. The drums were emptied onto a clean cement floor and blended by tractor until the tailings colour was homogeneous. This method of blending did not effectively break up the hardpan in the tailings, therefore, fully autogeneous grinding (FAG) was conducted using the Nordberg FAG mill to break up the +100 mm hardpan lumps and to produce the blended oxidized tailings required for pumping into the cover cells.

The first of pilot plant FAG mill circuits (PP1) was setup on September 19, 1994. PP1 involved the weighing, loading and feeding of 100 kg tubs of Strathcona oxidized tailings

into the Norberg mill by feed conveyor. Strathcona mill process water, received from Falconbridge on September 2, 1994, was piped from a tanker truck to the feed chute of the Nordberg mill. The mill discharge pulp slurry was screened at 8 mesh, and the plus 8 mesh screen oversize was recycled, by conveyors, to the mill feed chute. The minus 8 mesh screen undersize slurry was collected into 200 Liter drums.

The Strathcona tailings were fed into the Nordberg FAG mill at a feed rate of 2 tonnes/hour. Mill discharge pulp densities ranged between 1600 g/L and 1960 g/L, with an average pulp density of 1835g/L. One liter samples, of minus 8 mesh Nordberg mill discharge product, were cut and composited every half hour and stored for head sample characterization. Approximately 30 drums of minus 8 mesh blended and pulped tailings were produced in PP1. The flowsheet illustrating this process is presented in Figure 1.

The salt migration columns were filled using 18 of the 30 drums produced during PP1. The remaining 12 drums from PP1 were added as a component of the feed to the mill during subsequent Strathcona oxidized tailings blending pilot plants (PP2 and PP3).

The FAG pilot plant was set up again on October 25/94 to blend a 20 tonne truckload of Strathcona oxidized tailings. The truckload of Strathcona oxidized tailings were first blended on the concrete pad using a tractor and then transported to the Nordberg building for processing in pilot plant runs PP2 and PP3.

PP2 was operated on October 26, 1994, using the same circuit configuration as described in Figure 1. A total of 12.8 tonnes of wet tailings were fed into the mill and eight drums of the PP1 minus 8 mesh tailings were pumped into the feed end of the mill. A head sample of the PP2 run was composited by combining one liter samples of minus 8 mesh product cut every half hour. Mill discharge pulp densities ranged between 1600 g/L and 1860 g/L, with an average pulp density of 1745g/L. The minus 8 mesh mill discharge slurry was collected in drums.

Figure 1. Pilot Plant Flowsheet Configuration

(1) STRATHCONA OXIDIZED TAILINGS,

PP1 • 30 x 45 **gallon** drums

PP2, PP3 • 20 **tonne** truckload

FLOWSHEET

BLENDING STRATHCONA OXIDIZED TAILINGS

DUMP DRUMS/DUMP TRUCK

PP1 oxidized tailings

Blend by tractor and move
into Nordberg Bldg.

Upper Moose
Lake Water

2 Tonne/hr Feedrate

NORDBERG FAG MILL

Conveyor
recycle of
8 mesh
oversize

8 Mesh Screen

Drum @ Pulp Density 1700-1900 g/L
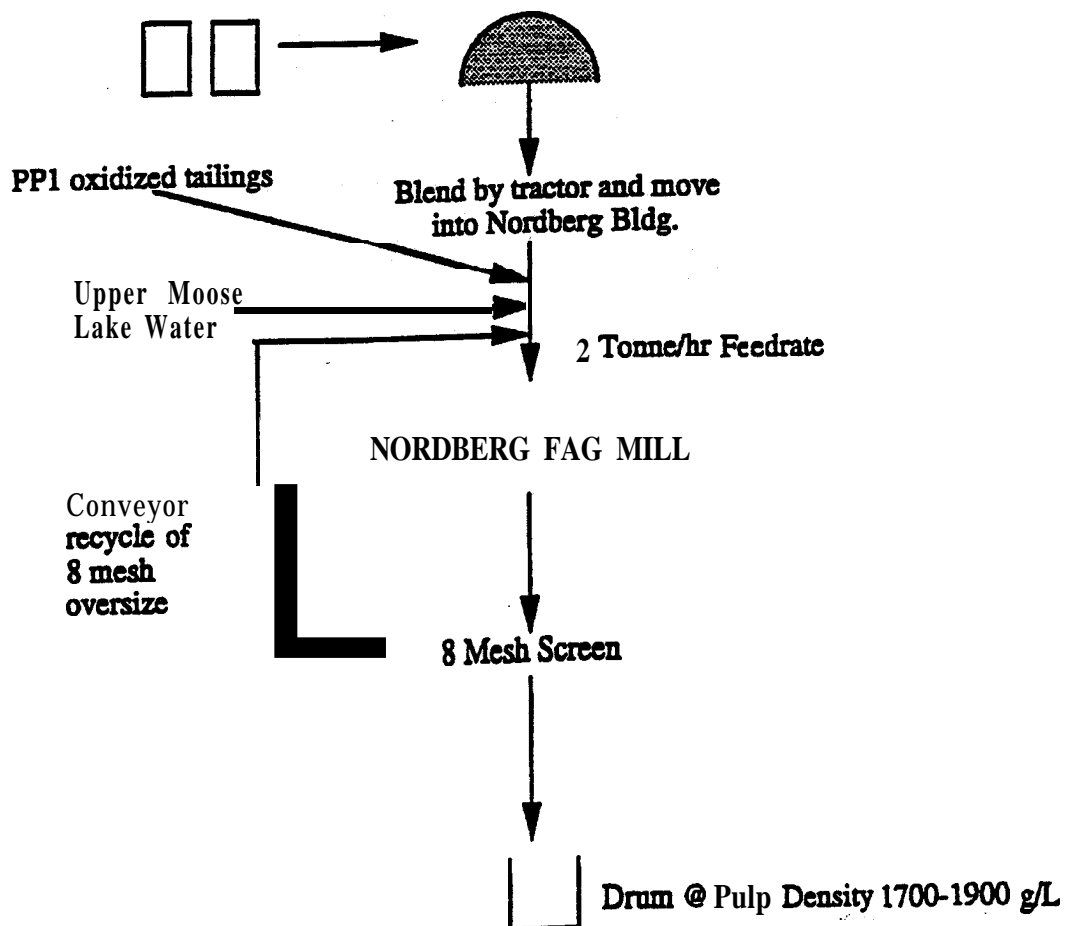
PP3 was operated on October 27, 1994. Four drums of the PP1 minus 8 mesh tailings were pumped into the feed end of the Nordberg mill. To obtain a representative sample of PP3 head, one liter samples of minus 8 mesh product were cut and composited every half hour. The Nordberg mill discharge pulp densities ranged between 1650 g/L and 2060 g/L, with an average pulp density of 1877g/L. The minus 8 mesh mill discharge slurry was collected in drums.

On November 30, 1994, 63 drums containing Strathcona mill cyclone overflow were received at Lakefield Research Limited for desulphurization by flotation. The contents of several randomly selected drums were repulped and pumped into a 1200 liter holding tank. Difficulties in repulping were encountered since some of the drums had a high sand content. These were set aside for future evaluation as required. The repulped material was passed through a 8 mesh screen to prevent plugging of the flotation circuit piping. The pulp density of the slurry was adjusted to 1600 g/L and the slurry was then pumped to a second 1200 liter holding tank that was used to feed the flotation circuit.

The flotation pulp was pumped from the 1200 liter holding tank into a 20 liter, Conditioner 1 tank. The reagents added to Conditioner 1 included 37 to 89 g/t sulphuric acid and 498 to 619 g/t copper sulphate. These reagents were added to activate the iron sulphide minerals in preparation for the flotation collector addition. Between 296 and 376 g/t of A317 xanthate collector were added to the 20L Conditioner 2 tank, to float the iron sulphide minerals. Methyl Isobutyl Carbonyl (MIBC) was added to the rougher and scavenger feed pulps at dosages of 2 to 12 g/t to maintain the desired flotation froth characteristics. The pulp retention times were 1 minute for each conditioner tank and 17 minutes in the flotation cells.

Three pilot plant tests were conducted to produce the desulphurized tailings. Pilot plant test 1 was run to resolve the flotation circuit mechanical problems. Pilot plant tests 2 and 3, showed 89% weight recovery of the feed material reported to the desulphurized tailings at 0.40 and 0.28 % total sulphur grades. The desulphurized tailings final pulp density was approximately 1400 g/L. A total of 56 drums of desulphurized tailings were produced; 28

drums from each of pilot plants 2 and 3. The products were stored in sealed drums until they were required for cover placement.

Lime stabilized sewage sludge (LSSS) was received on October 11, 1994, from Waste Stream Management in Syracuse, New York. Approximately 10 cubic yards of LSSS (2.5 tonnes) was received and placed outside in a sheltered location adjacent to the cover cell laboratory and covered over with black polyethylene. A composite head sample was collected from the LSSS soil by sampling at 4 locations in the pile.

Mature compost was received at Lakefield Research Limited on September 8, 1994, from the Corcan Central Composting Facility, at Millhaven, Ontario. A composite head sample was collected from five locations in the pile, for archiving and testing. The compost pile was wet on surface, but dry below the surface. It was black/brown in colour and had an organic and woody odour. Wood fibres were visible in the compost material.

The peat tested was obtained from a local peat source near Bridgenorth, Ontario. The peat was received in December, 1994. The peat was stored outside in covered 45 gallon drums until the pilot cells were ready for cover application.

2.2   Characterization of the Tailings and Cover Materials

Samples of the tailings and cover materials selected for the test program were characterized chemically, physically, mineralogically, and hydrogeologically. The results of these characterization tests were used to provide a comparison between the various cover materials being tested. Many of these tests were performed at the beginning of the program and repeated at the end of the program.

2.2.1 Chemical Characterization

Multi-element scans by Inductively Coupled Plasma Emission Spectroscopy (ICP-ES) and a whole rock analysis by X-Ray Fluorescence (XRF) were performed on the oxidized tailings and the pyrrhotite tailings at the beginning of the program. The multi-element scan by ICP-ES was also conducted at the end of the program on the oxidized tailings collected from the control cell and from the cover cells and on the pyrrhotite tailings collected from the compost cover cell.

2.2.2 Physical Characterization

Physical characterization tests performed on the cover and tailings materials included:
- particle size distribution using sieve series,
- cyclosizer analyses and hygrometric analyses,
- specific gravity determinations,
- moisture content determinations,
- bulk density determinations and
- porosity calculations.

Additional moisture content testing was added to the scope of the test program to provide data for a comparison of the moisture content, determined by time domain reflectometry (TDR), to the in-situ gravimetric and volumetric moisture contents in the pilot scale test cells. Destructive core sampling was performed using a 50 mm diameter stainless steel core sampler on November 16-17, 1995, and on April 11-12, 1996. Prior to the core sampling, TDR readings were recorded. Core samples were then collected from the same depth intervals as the seven monitoring port levels. The samples were immediately weighed while still encased in their 2" stainless steel liner. The samples were then split in half. One of the split samples was placed in a 60 mL plastic jar and then placed in the freezer for storage. The other half was consumed for gravimetric moisture content and bulk density determinations.

2.2.3 Mineralogical Examination

Mineralogical examination of polished sections of the oxidized tailings and pyrrhotite tailings was conducted at the beginning of the test program. Examinations were conducted again at the end of the test program on the oxidized tailings sampled from the control cell and from the cover cells, to identify any mineralogical changes over time. Examinations were also conducted on samples collected from the interfacial region of the cells to identify any precipitation compounds in this region.

2.2.4 Hydrogeological Testing

Hydrogeological tests performed on the covers and tailings included drainage curve tests, hydraulic conductivity tests and surface evaporation flux tests.

Drainage Curve Tests

Drainage curve tests were conducted on each of the tailings and cover materials. Testing was performed by Noranda Technology Centre (NTC) at the beginning of the test program and by the University of Saskatchewan at the end of the test program.

The method used at NTC for the drainage curve test was the American Society for Testing and Materials (ASTM) method D 2325-68 and D3152-72. The equipment used for this test was set up in two different ways depending on the sample material. The first setup used a model 700-12 air pressure manifold to distribute the air pressure between the two Tempe cells, a model 1000 pressure membrane extractor capable of working pressure in excess of 45 bars and a model of 1500 pressure plate extractor with a working pressure to 15 bars. This equipment was used to test coarse to fine grained materials with medium air entry values, because the ceramic plate in the pressure plate extractor, used to support the sample and allow for drainage, had a 3 bar air entry value. The second setup used a Brainard-Kilman S-500 pneumatic triaxial/permeability control panel to regulate the air pressure to the Tempe

cells. This equipment was used to test materials with low air entry values, such as peat and compost, because the ceramic plate in the Tempe cell had an air entry value of only 0.5 bar.

The test consisted of packing approximately 25 g of material into a rubber ring (1.01 cm high by 5.08 cm in diameter) and then placing on the test surface. When the test surface was covered with a sufficient number of samples (10-14), water was poured onto the test surface until the samples were almost submerged. The samples were left for a minimum 24 hour period to allow for a complete saturation. The excess water was then removed from the test surface. One sample was selected from the test surface for water content determination. The water content determined was considered to be representative of full saturation for the drainage curve test. After the first sample was selected and removed, the cover of the test equipment was secured and the first pressure increment was applied. After 24 hours, the cover of the test equipment was opened, another sample was selected and removed for water content determination. The cover of the test equipment was re-secured and the next pressure increment was applied. This 24 hour sequence was repeated.

A drainage curve was plotted using water content versus pressure increment. Once the air entry value of the material was experimentally determined, the test was stopped. The results from the drainage curve test were then compared to the results from a numerical model. If the results were in agreement, the test was considered terminated. If the results were not in agreement, the test was reverified and repeated as necessary.

At the end of the pilot cell test program, two 2"x 4" core samples were collected from the surface of each pilot cell and sent to the Department of Civil Engineering, University of Saskatchewan (U of S) for the drainage curve tests. Samples were collected from the control cell and the cover cells including LSSS, desulphurized tailings, compost and peat. The method used by the U of S is described below.

A ceramic pressure plate with an air entry value of 1 bar capacity was used for the test. The ceramic plate was saturated initially and remained in a saturated condition as long as the air

entry value of the ceramic plate was not exceeded by air pressure applied to the pressure plate cell. The test specimens were prepared by loading the core samples into a retaining cylinder with minimum disturbance.

Two separate procedures were used for the application of matric suction to the sample in the pressure plate cell.

(1) For matric suction values less than 10 kPa, a water column was used. A 1.5 m long flexible tubing was attached to the outlet drain located at the bottom of the pressure plate cell. The flexible tubing was filled with water. A negative water head, or matric suction was applied to the sample by maintaining the water level in the water column at the required distance below the sample, and the air pressure inlet drain was left open to the atmosphere.

(2) For matric suction values greater than 10 kPa, an air pressure supply was used. A pressure regulator with an accuracy in the range of 1 kPa was used to regulate the air pressure. Air pressure was supplied to the pressure plate cell system via the air pressure inlet tube located at the top of the pressure plate cell. The lower water outlet drain tube was left open to the atmosphere. Water draining from the sample because of the applied air pressure was collected from the water outlet drain. Equilibrium was established when water ceased to drain from the sample. The amount of water collected was weighed. The next increment of air pressure corresponding to the required matric suction value was applied to the pressure plate system and again the water draining from the system was collected until equilibrium suction condition was reached. The process was repeated for each required matric suction value. At the end of the test, the volume-mass properties of the test specimen were determined and used to calculate the water content of the test specimen corresponding to each matric suction increment value along with the amount of water collected from the system at each stage of the test.

In-situ Hydraulic Conductivity Test (Infiltration Test)

The in-situ infiltration tests to determine the hydraulic conductivity of the cover materials were conducted using an air-entry permeameter (AEP). The tests were performed by SRA Environmental at the beginning of the test program and by Noranda Technology Centre at the end of the test program. An apparatus very similar to the Sealed Single-Ring Infiltrometer (SSRI) was used for the testing. The method used is outlined in a paper entitled, "Evaluation of In-Situ Permeability Testing Methods" published in the Journal of Geotechnical Engineering (Vol. 116, No. 2, 1990) written by Neal Fernuik and Moir Haug. The infiltration tests were performed on the surface of the oxidized tailings and cover materials during the week of February 20, 1995 and the week of April 1, 1996.

The AEP consisted of a stainless steel cylindrical ring with an internal diameter of 25 cm and height of 20 cm. A circular trench was dug in the material to be tested that had a circumference which was the same as the cylinder. Several depth measurements of the trench were taken. The trench was then filled with bentonite paste. The infiltrometer was slowly pushed into the bentonite paste creating the seal between the AEP ring and the material being tested. The acrylic cover with all the pipe fittings attached to the cover was replaced and secured in place. Weights were then placed across the AEP to counteract the uplifting forces created by the head of water. Finally the AEP was filled slowly with water until a water level was registered in a graduated pipette. This level was noted with time and the test was considered started.

Readings were taken at regular time intervals. These readings were then entered into a spreadsheet and the gradient and hydraulic conductivity were calculated. The test continued for several hours, until the level in the pipette moved very slowly. At this time, no more readings were taken and the test was considered terminated.

Laboratory Hydraulic Conductivity Test

Core samples (4"x 4" square tube) were taken from the interfacial area between the oxidized tailings and covers at the end of the one year test program. These core samples were sent to the Department of Civil Engineering, University of Saskatchewan for hydraulic conductivity tests using the falling-head permeameter method.

The results of these tests were used to establish whether any changes in the hydraulic conductivity of the cover materials had occurred over time due to compaction, decomposition and/or the production of a precipitated hardpan layer in the interfacial regions.

Evaporative Flux Tests

Two simple flux experiments were conducted, respectively, between July 21, 1995 and August 8, 1995, and between April 8, 1996 and April 29, 1996, to determine the surface evaporative flux of the various cover materials. The test involved setting up small plastic containers (cells) of uniform diameter filled with oxidized tailings and the four different cover materials. Samples were cut from the frozen head samples of each material for use in this test. The inorganic cover materials were slurried to approximate similar densities of those present in the pilot cells. The organic covers were placed and compacted into the cells in a manner similar to their placement in the pilot cells. The evaporative flux cells were then topped up to a uniform height (approximately 6 cm) and completely saturated. The flux cells were placed at the top of their respective pilot cells in the laboratory. For each material tested, a plastic container filled only with deionized water was placed besides the flux cell. Both the flux cell and the plastic container were weighed every day at 8:00 am for the duration of the flux test period. The results of the flux cell tests were used to calculate the actual evaporation rates (AE) of the cover materials. The plastic containers filled with deionized water provided the data useful to calculate the potential evaporation rates (PE) at different locations in the laboratory.

At the end of the evaporative flux tests, materials were oven-dried and the dry weights were recorded. This data provided the moisture contents of the materials after exposure to different evaporation rates.

2.2.5   Other Bench Scale Testing

Potential Evaporation

An evaporation pan was placed in the Strathcona pilot cell lab and another was placed in the salt migration column lab. These pans were placed at a height similar to the height of the pilot cells or the salt migration columns, and were used to monitor the laboratory potential evaporation conditions daily (excluding weekends). The monitoring was conducted between March 7, 1995, and April 1, 1996. The pans were weighed each day at 8:00 am and then topped up to 1000 g.

Humidity and Temperature

The humidity and temperature in the Strathcona pilot cell lab and the salt migration lab were monitored. Each lab was outfitted with a digital humidity and temperature meter. Readings were recorded from the meters twice daily, once at 8:00 am and once at 4:00 pm. The monitoring was conducted between March 7, 1995, and April 1, 1996. The humidity and temperature were also monitored on a 24 hour basis using a mini-drum hygrothermograph. The hygrothermograph was installed in the laboratory and monitoring was initiated on April 10, 1995. This instrument gave a continuous graphical recording of the humidity and temperature over a seven day period. The graph paper was replaced weekly. Plate 1 shows the hygrothermograph and pan evaporation set-up.

Decomposition Rates of Organic Cover Materials

The determination of decomposition rates involved a combination of laboratory analyses at LRL and the performance of longer term incubation tests and computer modeling at Predictive Modeling, Inc., in Arkansas.

Core samples were taken at different cover depths of the organic materials in the pilot cells. These samples were collected at the beginning and at the end of the test program, and analyzed for total organic carbon (TOC) content. The differences in TOC content between the beginning and the end of the test program were used to calculate the decomposition rates of the organic cover materials and their variations with cover depths.

The performance of longer term incubation tests and computer modeling was conducted at Predictive Modeling, Inc., Arkansas, USA. Since Falconbridge Limited considered the application of lime stabilized sewage sludge (LSSS) mixed with desulphurized tailings (DST), the following four different LSSS-DST volume ratio combinations were evaluated: 100% LSSS at the as-received moisture content; 100% LSSS at 50% of the as-received moisture content; 50:50 LSSS: DST; 20:80 LSSS:DST. LSSS was mixed with the DST at the as-received moisture content. Each of the four combinations was loaded into a test tube to simulate a column of material. The test tubes were placed into incubation vessels which had 1 M NaOH carbon dioxide traps, and the incubation vessels were sealed.   The incubation tests were conducted at 25°C for 60 days. Carbon dioxide evolved during the decomposition process was collected in 1 M NaOH traps. The NaOH traps were regularly replaced and analyzed by weak acid titration after the addition of barium chloride.

The computer model, DECOMPOSITION, was used to predict field decomposition rates using the rate constants determined in the incubation tests, which were corrected for the climate in the Sudbury area. The mean monthly temperature and precipitation data for Sudbury between 1951 and 1980 were used. No monthly evaporation data could be obtained, instead, the monthly evaporation data for the Ottawa region was used.

2.3   Salt Migration Columns

In reclaimed tailings ponds, the migration of salts from the tailings to the surface of the overlying covers may result in the impairment to growth of vegetative covers and release of salts to surface runoff resulting in increased metal loadings to the environment. This salt movement is thought to be due to a combination of the capillary movement of water from the tailings and the evaporative flux from the cover layer surface. Salt migration column tests were conducted to determine if the cover materials being studied would be susceptible to upwards salt migration.

2.3.1   Materials

The materials tested included:
1) control (oxidized tailings)
2) peat
3) lime-stabilized sewage sludge
4) desulphurized tailings
5) desulphurized tailings with a capillary barrier (CB)
6) mature compost

The columns were filled with oxidized tailings to a depth of 0.30 m and a water table height of 0.30 m was maintained. Each type of cover tested was placed over the oxidized tailings in layers 0.15 m, 0.50 m, and 1.0 m thick. Therefore, three columns were commissioned for each cover material and control listed above, for a total of eighteen columns.

2.3.2   Apparatus and Column Construction

The salt migration test columns were constructed using 0.6 m diameter Nalgene containers with a 0.3 m constant head (CH) column connected at the base. The columns varied in height

from 0.45 m to 1.5 m (Figure 2). Moose Lake process water was used to top up the CH reservoirs once weekly to maintain a constant water table height in the attached salt migration columns. The volume of water added was recorded. The CH columns were covered with impermeable lids to eliminate evaporative losses.

A filter bed was placed at the bottom of the salt migration columns to ensure that the low hydraulic conductivity of the tailings would not plug the connection between the CH column and the salt migration (SM) column. Several materials were considered for the construction of the filter bed. The filter material was required to have the following characteristics:

1. a higher hydraulic conductivity than the oxidized tailings, to permit unrestricted water flow between the CH and SM columns;

2. physical characteristics suited to retaining the tailings above the filter layer, and

3. chemical neutrality that would not be reactive in an acidic environment, not be acid generating and not introduce salts or other materials into the SM columns through interaction with the make-up water.

The filter materials tested included aquarium gravel, silica sand, and nepheline syenite. The materials were contacted with several milliliters of 1N HCl to determine their reactivity. Both the aquarium gravel and the silica sand reacted within 3 minutes of contact with the HCl. The nepheline syenite reacted less noticeably after a much longer time period (10 minutes).

The nepheline syenite was then subjected to a leach test using the Moose Lake process water (pH 7). This test involved the flushing of the nepheline syenite with standard volumes of Moose Lake process water. The pH of the filtrate was then determined. Results, contained in Appendix A, showed a negligible pH change of the filtrate from contact with the nepheline syenite. The nepheline syenite was then tested using Acid Base Accounting (ABA).

Figure 2. Salt Migration Columns
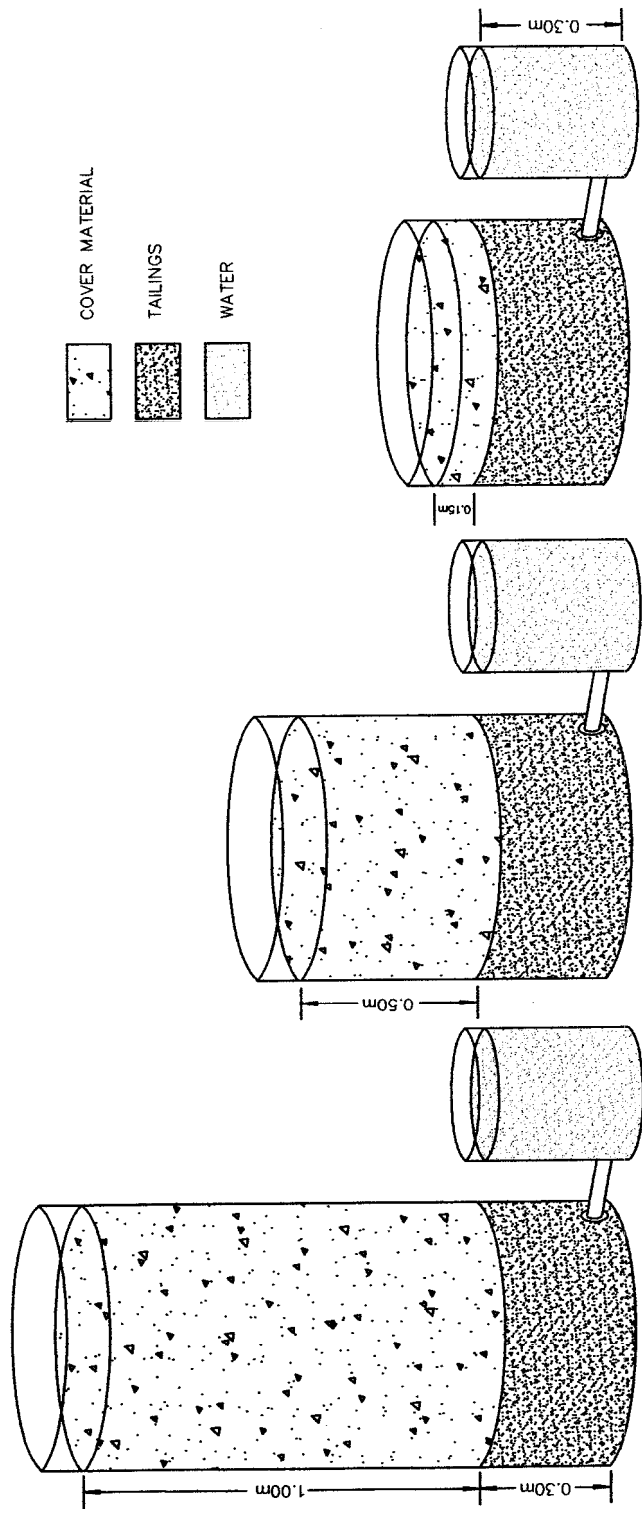
The results of the ABA test work showed the nepheline syenite had the following characteristics:

Common net neutralization potential:	24 t $CaCO_3$/1000 t material
Maximum potential acidity:	0.31 t $CaCO_3$/1000 t material
Total sulphur content:	<0.01 %
Paste pH:	10.2

The nepheline syenite met the prescribed criteria, therefore, it was used as the filter bed material at the base of the SM columns. The filter bed was placed to cover the top of the spigot, which connected the SM and CH reservoirs. A layer of geosynthetic fabric was placed on top of the filter bed as a physical separation between the nepheline syenite and the oxidized tailings. Bench test work conducted to select a suitable geomembrane for use in this program is described in Section 2.4.2.

2.3.3   Column Filling

The SM columns were washed with Moose Lake process water and connected to the CH columns. The nepheline syenite and geomembrane filter bed were placed at the base of the SM columns. The oxidized tailings were then slurried onto the top of the filter bed, to a thickness of 0.30 m. The oxidized tailings were then covered with the respective cover materials. The cover materials were placed to depths of 0.15 m, 0.5 m, and 1.0 m on the oxidized tailings in three separate columns.

The salt migration columns were filled from October 8-12, 1994. Eighteen drums of Strathcona oxidized tailings, blended during PP1, were required to fill the eighteen SM columns to a depth of 0.3 m. Each drum of PP1 tailings was slurried with the mixer prior to addition to the columns. The slurry was then pumped into the columns at a flow rate of 0.25 L/s to 0.35 L/s. The density of the oxidized tailings during filling varied between 1700 g/L and 1900 g/L.

One column for each depth tested was filled with oxidized tailings as a control column. Therefore, three control cells were filled with 0.15 m, 0.5 m, and 1.0 m, respectively of oxidized tailings over the 0.3 m deep oxidized tailings layer. The resultant total tailings depth in these SM columns was 0.45 m, 0.8 m and 1.3 m, with a water table maintained at 0.3 m above the base of the oxidized tailings.

Table 1 summarizes the set up of the SM columns. The columns containing the peat, mature compost, and lime stabilized sewage sludge (LSSS) covers were filled between November 23, and November 25, 1994. These materials were placed in the columns without alteration of moisture content. The entire surface of the cover materials was compacted with a 0.49 kg/cm^2 (7 psi) tamping device after each 40 L addition of material. This procedure was followed to simulate the weight of a small tractor driving on the tailings pond during the spreading of the cover materials. This tamping device consisted of a heavy weight with a handle attached, and was designed to deliver 0.49 kg/cm^2 of pressure. The volume of the LSSS decreased to approximately 70% of its original volume after compaction. The peat volume decreased to about 75% after compaction, and the mature compost decreased to about 65% volume after compaction. The desulphurized tailings cover was added to the columns as a slurry from December 12 to December 16, 1994. The density of the desulphurized tailings varied from approximately 1500 g/L to 1600 g/L. The slurry was approximately 60% solids by volume. A 0.15 m thick capillary barrier of gravel and sand was placed on the Strathcona oxidized tailings before the addition of the desulphurized tailings in three columns. The capillary barrier was also compacted using the 7 psi tamping rod. The difference in volume of the capillary barrier before and after compaction was not measurable.

Forty litres of gravel and sand were required to form each of the 0.15 m thick capillary barriers required in the columns.

Table 1.   Summary of Salt Migration Column Contents

Column	Contents (top to bottom)
Column 1	1.00 m oxidized tailings; 0.30 m oxidized tailings; <1 mm geotextile filter membrane; 0.05 m nepheline syenite filter bed
Column 2	1.00 m LSSS; 0.30 m oxidized tailings; <1 mm geotextile filter membrane; 0.05 m nepheline syenite filter bed
Column 3	1.00 m desulphurized tailings; 0.30 m oxidized tailings; <1 mm geotextile filter membrane; 0.05 m nepheline syenite filter bed
Column 4	1.00 m peat; 0.30 m oxidized tailings; <1 mm geotextile filter membrane; 0.05 m nepheline syenite filter bed
Column 5	1.00 m mature compost; 0.30 m oxidized tailings; <1 mm geotextile filter membrane; 0.05 m nepheline syenite filter bed
Column 6	0.85 m desulphurized tailings; 0.15 m gravel and sand; 0.30 m oxidized tailings; <1 mm geotextile filter membrane; 0.05 m nepheline syenite filter bed
Column 7	0.50 m oxidized tailings; 0.30 m oxidized tailings; <1 mm geotextile filter membrane; 0.05 m nepheline syenite filter bed
Column 8	0.50 m LSSS; 0.30 m oxidized tailings; <1 mm geotextile filter membrane; 0.05 m nepheline syenite filter bed
Column 9	0.50 m desulphurized tailings; 0.30 m oxidized tailings; <1 mm geotextile filter membrane; 0.05 m nepheline syenite filter bed
Column 10	0.50 m peat; 0.30 m oxidized tailings; <1 mm geotextile filter membrane; 0.05 m nepheline syenite filter bed
Column 11	0.50 m mature compost; 0.30 m oxidized tailings; <1 mm geotextile filter membrane; 0.05 m nepheline syenite filter bed
Column 12	0.50 m desulphurized tailings; 0.15 m gravel and sand; 0.30 m oxidized tailings; <1 mm geotextile filter membrane; 0.05 m nepheline syenite filter bed
Column 13	0.15 m oxidized tailings; 0.30 m oxidized tailings; <1 mm geotextile filter membrane; 0.05 m nepheline syenite filter bed
Column 14	0.15 m LSSS; 0.30 m oxidized tailings; <1 mm geotextile filter membrane; 0.05 m nepheline syenite filter bed
Column 15	0.15 m desulphurized tailings; 0.30 m oxidized tailings; <1 mm geotextile filter membrane; 0.05 m nepheline syenite filter bed
Column 16	0.15 m peat; 0.30 m oxidized tailings; <1 mm geotextile filter membrane; 0.05 m nepheline syenite filter bed
Column 17	0.15 m mature compost; 0.30 m oxidized tailings; <1 mm geotextile filter membrane; 0.05 m nepheline syenite filter bed
Column 18	0.15 m desulphurized tailings; 0.15 m gravel and sand; 0.30 m oxidized tailings; <1 mm geotextile filter membrane; 0.05 m nepheline syenite filter bed

To allow the water to drain, the solids were settled overnight. The columns containing the desulphurized tailings cover were re-filled with desulphurized tailings an average of 3 times. Preliminary results showed that tailings added at 1550 g/L settled to a volume of about 70% the original volume. The tailings were expected to dry out and further compact over time. Desulphurized tailings were not compacted using the tamping rod as it was anticipated that a desulphurized tailings cover would not be applied using a tractor but would be pumped on as a slurry.

Plates #2-4 illustrate the Strathcona salt migration columns.

2.3.4   Salt Migration Column Monitoring Methodology

The salt migration columns were monitored for both evaporative water loss and salt movement through the cover materials. The methodology followed is described below.

Evaporative Loss Measurements

The rate of evaporation in the laboratory was measured and compared to field pan evaporation rates. It was anticipated that the laboratory evaporation rates would be higher than those in the field, therefore no artificial means were used to increase the evaporation rates from the salt migration columns.

As water was lost from the SM columns through the evaporative process, the water level in the attached constant head (CH) tank decreased. The CH tanks were monitored on the Friday of each week during the project. The water in the CH tanks was topped up with Moose Lake process water and the volume of water that was added was recorded. The water added to the CH reservoirs was recorded as the evaporative loss from the surface of the salt migration columns.

Column Sampling

Prior to commissioning the columns, a discrete sample volume of each cover material was analyzed for electrical conductivity (EC). The results of these analyses were used to indicate the electrical conductivity of the cover materials at Time 0. As the electrical conductivity of the decant varied with natural salt content, this value was used to measure the relative salt concentration changes within the different cover materials. These data were used to indicate the movement of salts through the cover materials from the underlying oxidized tailings as reflected by increased electrical conductivity concentrations over time.

Time 0, (T_0), was defined as the date when the filling of the columns was completed. T_0 for the oxidized tailings control columns was October 12, 1994. T_0 for the columns with covers was November 25, 1994.

Samples were collected monthly over a four month period. The samples were collected using a stainless steel auger sampler. The samples were collected in duplicate at 15 cm intervals from the surface, within the cover material. The same location was never sampled twice. The samples were placed in 60 mL plastic jars and one of the samples was immediately placed in storage in the freezer. The second sample was sent to the laboratory at Lakefield Research for analysis of the electrical conductivity. The holes left by the sampling were filled with a slurried bentonite mix. The holes were then plugged with a labeled cap, showing the date of sampling.

As noted above, extracted soil samples were collected from all columns at 0.15 m intervals from the surface of the cover. The sampling locations are listed below.

Cover thickness	Sample Collection Depth (from surface)	Sampled Interval

Lakefield Research Limited
Environmental Services

0.15 m	0 m from surface	Surface
	0.15 m	0.10 - 0.15
0.5 m	0 m from surface	Surface
	0.15 m	0.10 - 0.15
	0.30 m	0.25 - 0.30
	0.45 m	0.40 - 0.45
1.0 m	0 m	Surface
	0.15 m	0.10 - 0.15
	0.30 m	0.25 - 0.30
	0.45 m	0.40 - 0.45
	0.60 m	0.55 - 0.60
	0.75 m	0.70 - 0.75

For the determination of electrical conductivity, the samples were dried and 5 g of the dried sample was weighed into a beaker. Fifty milliliters of deionized water were added to each beaker. The mixture was heated for 20 minutes and then allowed to cool. The mixture was transferred into the 100 mL volumetric flask. The beaker was washed with 50 mL deionized water and the wash solution was also transferred into the volumetric flask. The volume was made to 100 mL with deionized water. The electrical conductivity was measured on the decant.

Final destructive core sampling was conducted in the salt migration columns on October 13, 1995, about 11-12 months after the initiation of the salt migration column test. Samples were collected from 0.05 m, 0.45 m and 0.75 m depths below the surface of the 1.0 m cover, from 0.05 m, 0.15 m and 0.45 m depths below the surface of the 0.50 m cover, and from 0.05 m and 0.15 m depths below the surface of the 0.15 m cover. The samples were analyzed for gravimetric and volumetric moisture content, electrical conductivity, total dissolved solids (TDS), pH, SO_4 and metal concentrations (Ni, Cu and Fe). This additional data provided supporting information for the electrical conductivity results collected and would also confirm the migration of salts from underlying oxidized tailings layer.

Shake Flask Test on the LSSS

After the salt migration column test was completed, a modified shake flask test was conducted on the LSSS to determine the contribution of salts in the LSSS to the observed high electrical conductivity. The shake flask test was performed according to "Modified Test for Shake Extraction of Solid Waste with Water, ASTM D3987". Ten grams of dried LSSS were weighed into a 200 mL Erlenmeyer flask, and 50 mL deionized water was added to produce a slurry of 20% solids. A stopper was placed on the flask and agitated at 200 rpm for 24 hours. The flask contents were allowed to settle for half an hour and the supernatant was decanted into a vial. Another 50 mL of deionized water was added into the flask and agitated for another 24 hours. The supernatant was decanted into another vial. The supernatants were analyzed for pH and electrical conductivity, and filtered through 0.45 µm filter for analysis of Ca, Mg, Fe, Al, and P. These five elements were selected because of their high total concentrations present in the LSSS.

2.4 Pilot Cells

Pilot scale models of the Strathcona tailings pond were constructed to simulate post-closure conditions and to allow physical testing of the effects of various cover materials on the underlying oxidized tailings. The results of the pilot cell tests were used to determine the effects of the covers on acid generation and the release of trace metals.

2.4.1 Materials

The eight cover layers treatments which were tested in the pilot scale simulation included:
1) control (only oxidized tailings)
2) peat overlying oxidized tailings
3) lime-stabilized sewage sludge (LSSS) overlying oxidized tailings
4) lime-stabilized sewage sludge with a capillary barrier (LSSS+CB) overlying oxidized tailings

5) desulphurized tailings (DST) overlying oxidized tailings

6) desulphurized tailings with a capillary barrier (DST+CB) overlying oxidized tailings

7) mature compost overlying oxidized tailings

8) mature compost overlying pyrrhotite tailings

2.4.2   Apparatus - Pilot Cell Construction

The pilot scale models (pilot cells) were constructed of 1.25 cm thick sheets of PVC plastic welded together and supported within a frame of angle iron. The pilot cells were 2.5 m long, 1.5 m high and 0.6 m wide (Figure 3). One clear Plexiglas^{TM} sheet formed one long side of the cells (2.5 m by 1.5 m) to permit visual observations of the layered systems. The back, sides and bottom were constructed of opaque PVC. One end of each pilot cell was covered with a geosynthetic filter fabric to allow the cover and tailings layers to drain freely. The fabric was secured into place using PVC strips and a PVC welder. The pilot cells were constructed by Miller Plastics Ltd. of Mississauga, Ontario.

Several tests were conducted to select the optimum filter fabric for use in the cell. The filter fabric was required to allow the slurried tailings to drain without the loss of fine materials. Samples of spunbound (non-woven) and woven geomembrane fabrics were received from Terrafix Environmental Technology Inc. of Rexdale, Ontario for testing. Small diameter (12 cm) columns were constructed to test the ability of various geomembranes to retain tailings and freely drain water. The geomembrane was placed at the base of the columns and the slurried tailings were poured into the top. The water was allowed to flow through the geomembrane into a supporting beaker. The geomembrane selected was a nylon weave material identified as Geotex AMOCO woven geosynthetic M1198 geomembrane material (425 micron opening). This was used for all SM columns, as well as for the free draining ends of the pilot cells.
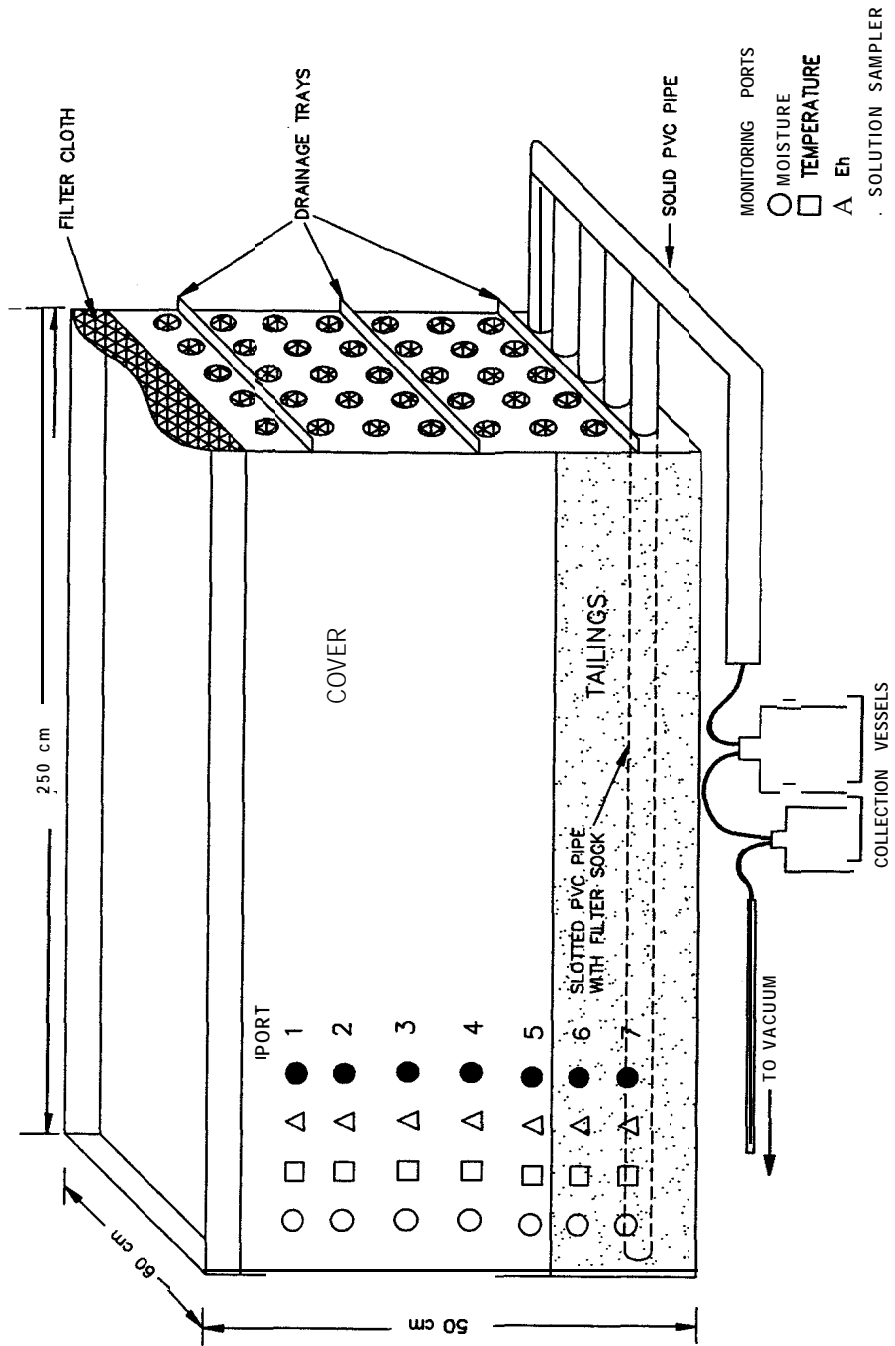
Seven sets of sampling ports and monitoring sensor ports were installed vertically in the Plexiglas™ side of the cells, to allow for the collection of pore water profiles and sensor data

from the cover and oxidized tailings. Two sampling and monitoring ports were installed in the oxidized tailings layer and five sets of ports were installed in the cover layer. The ports were installed at 0.15 intervals vertically in the Plexiglas™. The ports were installed 1.75 m from the cell end covered with the filter fabric to reduce oxygen effects from the drainage end on the data collected.

Stands for the cells were constructed at Maple Grove Metal Works in Norwood, Ontario. The stands were used to permit the elevation of the bottom of the cells to a 1.0 % slope to permit the collection of drainage water and to simulate the slope of the actual Strathcona tailings impoundment.

The cells were modified at Lakefield Research for the installation of the sensors and sampling ports. Holes were drilled and hand filed to the diameter required to fit the moisture sensor probes. The moisture probes consisted of a two probe system. One probe was a stainless steel tube, and the second was a PVC sheathed. These probes were installed during October, 1994. The sheathed tubes were welded in place on the inside of the cells. Both the sheathed and stainless steel tubes were fitted and sealed in place with silicone. Plate #5 shows the inside of the pilot cell set up before filling.

The external assembly of the moisture probes required the manufacture of copper plates and the accurate placement of these plates, washers, diodes, resistors and electrical connections. More detail on the moisture probe system is provided in Section 2.4.4.

Temperature probes, Eh probes, and solution samplers were installed for the bottom monitoring levels in the pilot cells and siliconed in place in October, 1994. The probes and samplers for the upper four monitoring levels were installed as the cells were filled to permit compaction of the covers without damaging the probes.

A mounting bracket was attached to the front of the cells on the metal frame to permit the mounting of a plug-in board for the connection of wires for the Eh, and moisture probes.

These boards permitted the connection of the Eh and moisture probe meters using banana jacks, or BNC connectors, to each monitor level. The temperature probes, plug-in boards, moisture probes, and all associated wiring were assembled on site.

On October 28, 1994, the pilot cells were sealed, cleaned, and leveled for filling. PVC collection trays were installed at the drainage end of the cells to collect runoff water from the surface cover and tailings layer. The collection trays were welded into place at the base of the cells to direct drainage waters into large plastic basins as the cells were filled.

2.4.3 Pilot Cell Filling

Tailings Placement

Strathcona oxidized tailings and pyrrhotite tailings were mixed separately to ensure complete homogenization. The pilot cells were then filled with Strathcona oxidized tailings or pyrrhotite tailings to a depth ranging from 0.5 m to 0.55 m. Samples of the pilot cell drainage were collected and archived for future analysis, if required. A detailed account of the filling is summarized in the following paragraphs.

On October 6-7, 1994, the pyrrhotite (Po) tailings were repulped into two large mixing tanks. A total of 10 barrels of Po tailings were repulped with 1 barrel of Moose Lake process water (pH 7) and circulated between the two mixing tanks using an Emerson Wakeshau pump set at a constant speed.

On October 7, the first batch of Po (Po1) tailings were pumped from the recirculating tanks to fill Pilot Cell #8. Pilot cell #8 was filled at a rate of 1L/sec and, during filling, a head sample was collected for characterization test work.
A relatively low slurry density of the first batch of Po tailings resulted in a requirement for additional Po tailings to be blended and added to pilot cell #8. On October 21, 1994 the second batch of Po tailings (Po2) was received at Lakefield Research and blended in the

mixing tanks. A total of 14 barrels were blended and mixed in this run. The slurry density was recorded at 1800g/L. Po2 tailings were head sampled as they were pumped into pilot cell #8.   Po2 tailings solids were filled into pilot cell #8 to increase the solids level to the required 0.5 m base depth. The pyrrhotite tailings cell was topped up again with Po tailings on November 15, 1994. Any remaining Po2 solids were pumped into drums and placed in storage. A 20 L head sample was collected for NTC for drainage curve test work.

Strathcona oxidized tailings were reslurried and pumped into the remaining seven pilot cells. From October 29 through November 12, 1995, an average of 6 barrels/day of oxidized tailings were pumped into each of the pilot cells.   These were added at a ratio of approximately two barrels of PP2 to four barrels PP3. The cells were topped up with PP3 oxidized tailings to approximately 0.5 metres above the base. At this depth, the top of the tailings layer was located just above the second monitoring level in the cells. Plates #6 through to #7 are photographs showing the filling of the pilot cells.

A peer review meeting was held on November 23, 1994. This review was conducted to review the technical aspects of the pilot cell testing program. Since there were several questions which required input prior to initiating the monitoring program, the application of cover materials was put on hold until the meeting and resultant correspondence was concluded. It was noted during this review that the oxidized tailings or the pyrrhotite tailings remained saturated over their entire thickness due to capillary suction pressures. The minor surface drying which occurred was considered relevant to what would occur in the field.

Computer Modeling and Vacuum System

The major concern identified with the pilot cells during the peer review meeting conducted in November, 1994, was the lack of understanding of the hydraulics of the system.   The University of Saskatchewan were contracted to conduct computer modeling of the cells to verify the flow concepts for the cell and aid in the subsequent interpretation of the data. Computer flow modeling of the pilot cells was conducted by the University of Saskatchewan,

under the direction of Dr. S. Lee Barbour. The objective of the modeling was to illustrate the possible hydraulic performance of the cells for the following conditions:

1. a no flow lower boundary,
2. a lower drainage boundary,
3. various capillary barrier lengths.

The results of the modeling exercise are contained in Appendix B. The main findings of this exercise are summarized below.

- A capillary break does not develop in the pilot cell when the base of the cell is defined as a no flow lower boundary.

- A capillary break will develop in the pilot cell for a lower drainage boundary when a negative pore-water pressure is maintained at the base. The capillary barrier only becomes effective when the negative pore-water pressures in the underlying tailings become greater than the negative pore-water pressure corresponding to the residual water content of the capillary barrier.

- A full capillary break is not achieved for a capillary barrier that extends only part way across the length of the model. Lateral flow develops around the partial capillary barrier for a lower drainage boundary.

- For a cover to remain saturated, the air entry value of the cover must be higher than the negative pore-water pressure, which corresponds to the residual water content of the capillary barrier.

- The extent of water ponding, for a no flow lower boundary, depends on the relative difference between the applied surface flux and the saturated hydraulic conductivity of the tailings.

The schematic results of the modeling for cell constructed with a flow boundary at the bottom of the cell and a capillary barrier running the full length of the cell showed an effective capillary break effect.

Lakefield Research Limited
Environmental Services

Due to the results of the modeling exercise, and at the recommendation of the peer review group, a vacuum drain system was installed at the base of the pilot cells to permit "free drainage" conditions. Since the cells had already been filled, the installation of a porous plate system was not possible. The fragility of porous plate tubes and other shape variations also rendered these unsuitable for installation in the cells.

The vacuum drain system installed was comprised of an internal and an external component. The internal component consisted of four parallel 152 cm lengths of 2.5 cm PVC screen wrapped with nylon filter sock material, and attached to 152 cm lengths of solid pipe. The wrapped screen sections of the pipe were buried in the tailings. The solid pipe extended out of the free draining end of the cells, where it was downsized to 1.25 cm vacuum header. The header was connected to the remainder of the external vacuum system lines, which was constructed of 1.25 cm PVC schedule 40 pipe and fittings.

A 15 L collection flask was attached between the header and the vacuum system lines for the collection and measurement of drainage. A second 5 L overflow flask was also attached, in series, to the 15 L flask to prevent fluids from entering the vacuum system. The vacuum system was constructed with a check valve ahead of each header (i.e. between the cell and the vacuum pump). This check valve was put in place to separate the cell from the other cells in the shared vacuum system in case of pressure loss at a single cell. The vacuum lines ran to a central galvanized steel pressure tank. The pressure tank also had a check valve located between the tank and the vacuum pump. The purpose of this valve was to maintain vacuum in the tank when the pump shut down. This avoided continuous running of the pump. Figure 4 illustrates the vacuum system.
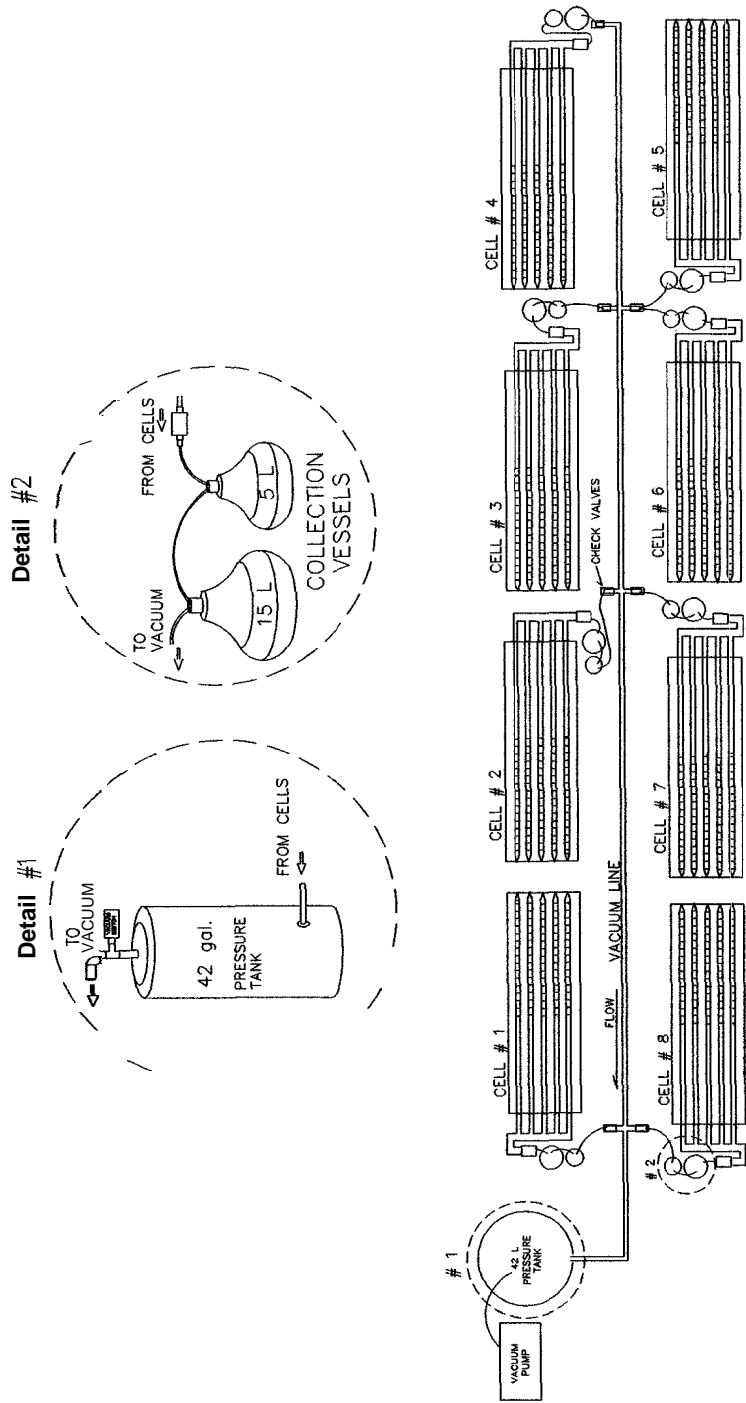
Construction and installation of the vacuum system was initiated on January 18, 1995. The vacuum system was installed in the pilot cells before cover addition but after the addition of the tailings. This encouraged further draining and compaction of the tailings prior to cover application. Vacuum compaction resulted in the development of large cracks at the surface

of the tailings. A steel concrete vibrator (11" long x 7/8" x 7/8" square, connected to a 115V x 9 amp. electric vibrator) was used to reslurry the surfaces and remediate these cracks prior to cover application. Additional oxidized tailings from PP3 were added, where necessary, to increase the tailings thickness to cover the second monitoring level.

Results from the NTC drainage curve test work were used to set the vacuum of 250 cm H_2O, which was lower than the air entry value of the oxidized tailings (450 cm H_2O). The purpose of this vacuum was to bring the tailings to a moisture content similar to that of unsaturated tailings located above the capillary fringe.

Cover Material Placement

Cover materials were placed in available inside storage areas for thawing on January 16, 1995. A lean-to was constructed adjacent to the laboratory to permit thawing of the bulk compost and LSSS materials.

The oxidized tailings or pyrrhotite tailings were then covered with a 0.85 m depth of cover material. The cover materials were placed without modification to their moisture contents. The covers were then compacted to mimic field placement techniques. Where a capillary barrier was used, the oxidized tailings were covered with a 0.15 m capillary barrier of gravel and sand, followed by 0.7 m of the requisite cover material. After filling, the pilot cells were elevated at the non-free draining end to simulate the 1% surface slope of the Strathcona tailings pond. Filling of the cells is described in more detail in Section 2.3.3.

The cover placement in the cells began in January, 1995. The cover application was a very labour intensive task that took over three weeks to complete, with two operating shifts. The addition of slurried tailings, as cover, required the reslurrying and pumping of tailings materials. While materials were being reslurried, the vacuum system installation proceeded and bulk covers were applied manually and compacted. The LSSS, peat, and compost were

manually shoveled into 20 L pails and carried to the cells where they were emptied, spread and compacted.

A pressure of 7 psi was applied to compact the peat, compost and LSSS materials placed in the cells. Temperature, Eh probes, and the solution samplers were installed as 15 cm layers of the solid cover materials were applied. All probes and samplers were silicone sealed after installation.

Final preparation of the pilot cells, prior to commissioning, included the following tasks:

1. During the filling of the cells, some monitoring ports were observed to leak. These were resiliconed as detected.

2. The cells were raised by inserting 1.25 cm thick plates under each back leg to give the 1% slope required to simulate the Strathcona pond slope.

3. Once the cover cells were filled and sloped, the sensors were wired to connect all the sensor cables to the monitoring boards at the front of the cells.

4. PVC drain collection trays and funnels were welded onto the free draining end of the cells. The trays and funnels were installed at the surface of the cover, the interface of the cover and the tailings, and the bottom of the cells. These trays were used to collect discrete discharges from these interfaces.

5. The final hook up of the vacuum system was completed with all check valves, collection bottles, piping, pump and pressure tank connections.

The cells were filled and ready for saturation at the end of February, 1995. The pilot cell contents are summarized in Table 2.

2.4.4 Pilot Cell Monitoring Methodology

Sampling and monitoring of the pilot cells was scheduled for immediately after loading, one week after cell saturation, and then 2 weeks, 1 month, 3 months, 6 months, 9 months and 12 months after cell saturation. The methodology and a brief description of the apparatus used, for each of these scheduled sampling and monitoring events, is provided in the following paragraphs.

Simulated Rain Production

A discussion by the Peer Review Group concerning the nature of the water to use for the simulated rainfall in the test program led to the decision to use the local town water. Lakefield Town water was aerated with a pump for at least twelve hours to remove any chlorine. The pH of the water was then adjusted to 4.2 using a 60/40 mixture of sulphuric (H_2SO_4): nitric (HNO_3) acid. This rain was used for the saturation and rainfall application on the cells. An analysis of the Lakefield Town water was performed to provide background information on the incipient "rainwater" quality. A multi-element ICP-ES scan was performed on the simulated rain water on March 8, 1995, August 17, 1995, and January 8, 1996.

Cover saturation

After the cover materials had been placed over top of the tailings, the cells were subjected to a period of heavy and prolonged rainfall to bring the covers to saturation prior to initialization of the monitoring program. Once the cells were saturated (free water visible at surface), the vacuum system was applied at a suction of 127.8 cm H_2O until no further water flowed freely

from the cells. This procedure was followed to simulate field conditions of tailings and covers located above the water table. The procedure followed is included in Appendix C.

Table 2. **Summary of Pilot Cell Contents**

Height (mm)	Pilot Cell 1	Pilot Cell 2	Pilot Cell 3	Pilot Cell 4	Pilot Cell 5	Pilot Cell 6	Pilot Cell 7	Pilot Cell 8
700	Oxidized Pyrrhotite Tailings	Lime Stabilized Sewage Sludge	Desulphurized Tailings	Mature Compost	Peat	Desulphurized Tailings	Lime Stabilized Sewage Sludge	Mature Compost
150	Oxidized Pyrrhotite Tailings					Cappillary Barrier	Cappillary Barrier	
500	Oxidized Pyrrhotite Tailings	Oxidized Tailings	Oxidized Tailings	Oxidized Tailings	Oxidized Tailings	Oxidized Tailings	Oxidized Tailings	Pyrrhotite Tailings

<u>Rainfall Application</u>

Rainfall was applied once weekly at a rate calculated to approximate the average annual precipitation rate at Sudbury, Ontario. The laboratory pan evaporation rate and the field pan evaporation rate for the Sudbury Airport were used to calculate a ratio of lab:field conditions and this was used to generate the weekly rainfall rate. The procedure followed is included in Appendix D.

The pilot cells were initially rained on individually using a fine mist (600 mL/min.) hose nozzle. This method was used from March 9, 1995, to July 13, 1995. From July 14, 1995 on an automated fine mist rain system was used. This system was composed of a single line spread over four of the cells with twenty-four nozzles (6/cell). The nozzles were calibrated to have the same flow rate. The line was connected to the pump which was set for a specific time based on the total flow output from the nozzles. The volume of water added to each cell was initially calculated to be 15.5L. The volume of water added was adjusted at a later stage of the test program, on a weekly basis, to compensate for changes in the potential evaporation rate in the laboratory.

<u>In-situ Monitoring</u>

In-situ monitoring was conducted for Eh and temperature one week after cell saturation, and then 2 weeks, 1 month, 3 months, 6 months, 9 months and 12 months after cell saturation. The moisture content using TDR was monitored on a more frequent basis including before and after the weekly rainfall events.

Eh Monitoring: Custom Eh probes were produced, which consisted of 1/4" ID acrylic tubing, 22 gauge copper wire and 0.254 mm diameter platinum wire. Each port level (1-7) in the Strathcona pilot cells was outfitted with a permanent Eh probe. These probes were used to measure the redox potential of the material at the different levels.

Lakefield Research Limited
Environmental Services

At the time of monitoring, a temporary reference electrode was inserted into the surface of the each cell and deionized water was added to wet the area to provide the necessary electrical connection through the cover and tailings materials. The Eh probes were then connected to a digital pH/mV/ion meter for readout. The Eh of the cover and tailings materials were monitored in conjunction with the solution sampling events. The Eh was monitored on the same day of solution sampling on February 28, 1995, April 6, 1995, April 13, 1995 and April 28, 1995. The Eh was then monitored one day before the solution sampling event and just prior to rainfall application for the remaining five sampling event.

Temperature: Each port level (1-7) in the Strathcona cells was outfitted with a permanent thermocouple. The thermocouples were used to measure the temperature of the cover and tailings materials at different levels. The thermocouples were connected to a digital thermometer for readout. The temperatures of the Strathcona covers and tailings were monitored in conjunction with the solution sampling events, on the same days as the Eh monitoring events.

Moisture Measurements With Time Domain Reflectometry Moisture Probes - Calibration Curve Test work: Time Domain Reflectometry (TDR) is a recognized method for moisture content analysis in soils. The method relates the time taken for an electrical impulse to travel through a soil to the moisture content, because the moisture content and electrical impulse reflection time are proportional. As the moisture content increases, the time required for the input impulse to travel also increases. TDR values are also a function of the characteristics of the material being measured. Therefore, calibration curves were required for each different material being studied.

Historical difficulties with TDR in highly conductive soils, of which oxidized tailings could be considered an extreme example, have led to the innovative design of a sheathed dual probe system for the measurement of moisture with TDR in conductive soils. Such a dual probe system was designed for use in the pilot cells by Gabel Instruments. Subsequent to the initial probe design involving a 5 cm spacing between the sheathed and unsheathed stainless steel

probes, Mr. Hook of Gabel Instruments conducted testing on samples of tailings provided by Lakefield Research. His test results suggested that, at moisture contents greater than 40% by volume, the calibration curves became non-linear and exponential.

In early November, following further testing at his facilities in Victoria, B.C., Mr. Hook suggested that a probe spacing of 12 cm may give more accurate results than the 5 cm spacing originally configured. The pilot cells had already been built with the 5 cm spacing at this time and the probes had been welded and siliconed in place and the oxidized tailings and pyrrhotite tailings had already been pumped into the majority of the cells.

On November 18, 1994, tests were conducted to compare the moisture content measured using the 12 cm spacing and 5 cm spacing for different materials. Mature Compost and LSSS were analyzed at various moisture contents to determine whether the difference in probe spacings was necessary to the moisture contents expected in these materials. Results showed that the 5 cm spacing would be sufficient to provide a calibration curve useful to the interpretation of the TDR results (Appendix E). The pilot cells were, therefore, left with the 5 cm spacing for filling.

TDR Methodology

Seven TDR probes were permanently installed in each pilot cell at 0.15 m intervals. Measurements were recorded at ports 1, 3, 5 and 7. The TDR system was calibrated before every monitoring session. The moisture content was measured using the TDR system on a weekly basis, one day before and after every rainfall event. The monitoring program was initiated on March 1, 1995, and terminated at the end of one year test program.

A detailed continuous TDR monitoring program was also performed on many of the Strathcona pilot cells. This program involved collecting TDR measurements and oxygen concentration measurements every hour for approximately one week to monitor the migration of water and the depletion of oxygen through the cells as rainfall was applied and water

moved through the system. Cells #3 (desulphurized tailings) and #6 (desulphurized tailings + CB) were monitored continuously from July 31, 1995, to August 4, 1995. Cell #4 (compost over oxidized tailings) was monitored continuously from August 14, 1995, to August 17, 1995. Cells #2 (LSSS) and #7 (LSSS + CB) were monitored continuously from September 11, 1995, to September 15, 1995. Cell #8 (compost over pyrrhotite tailings) was monitored continuously from August 28, 1995, to August 31, 1995.

Water Balance Measurements

The various flows into and out of the pilot cells were recorded to provide data for water balance determinations. These flow data included the rainfall application, pan evaporation, free drainage from the cells and the vacuum drain water. Laboratory relative humidity and temperature were also recorded to supplement the laboratory climatic information.

Free Drainage Water: The free drain water was collected from the cells three times a week. The free drain water was intercepted in drainage trays located at the surface, to collect runoff water; at the interface between the cover and the underlying tailings; and at the base of the tailings layers of each cell. This water was directed into small mouth amber bottles. The free drain water was decanted from the bottles and measured using graduated cylinders one day after a rainfall event, at mid week, and immediately before the next rainfall event.

Vacuum Drainage Water: The vacuum system was connected to stoppered flasks for the collection of the vacuum drained water. During operation of vacuum system, the vacuum drain water was collected from the cells three times a week: one day after rainfall, mid week, and immediately before the next rainfall event. The vacuum ran continuously from March 31, 1995, to July 20, 1995, and then stopped due to possible air flow into the oxidized tailings layer. The vacuum drain water was decanted and measured using graduated cylinders. The measurements were recorded and adjusted into weekly totals.

Solution Sampling

Samples of the pore water in the cells were collected on day 0 (February 28, 1995), one week after saturation (April 6, 1995), two weeks after saturation (April 13, 1995), four weeks after saturation (April 28, 1995), two months after saturation (May 26, 1995), three months after saturation (June 30, 1995), six months after saturation (September 27, 1995), nine months after saturation (December 19, 1995), and 12 months after saturation (March 26, 1996). The pore water samples were collected into vacuum sample tubes. About 60-100 milliliters of solution were sampled from ports 1, 3, 5 and 7. Sometimes the vacuum in the tubes was increased through the connection of vacuum pumps to the tubes to ensure the collection of sufficient solution sample. In some instances insufficient solution sample was available due to low moisture contents. When this occurred, solid samples were taken at those sampling ports from the surface or from the screened end of the pilot cells using a stainless steel auger sampler. The solid samples were immediately sent to the lab for analysis using a saturated extraction procedure (Appendix F). The solution samples were filtered through 0.45 µm for analysis of pH, SO_4, $S^=$, NO_3, DOC, and through 0.1 µm for analysis of Fe (including Fe^{2+} and Fe^{3+}), Ni, Cu, Pb, Mg and total P.

Gas Sampling

In-situ pore gas sampling was added to the program in September, 1995. Pore gas samples were collected from the Strathcona pilot cells on September 26, 1995, November 10, 1995, January 26, 1996 and March 25, 1996. The gas samples were extracted using a syringe, through a stainless steel tube fitted with a septum. All the cells were sampled at ports 1, 3, 5, 6 and 7. Before taking a sample, the gas tubes were purged by extracting 50 mL, and then a 30 mL gas sample was extracted for oxygen (O_2) concentration analysis using an oxygen concentration apparatus (OCA) designed by Dr. R. Nicholson from the University of Waterloo. On March 25, 1996, the concentrations of O_2, CO_2 and CH_4 were measured simultaneously using a Geogroup GA-90 Methane-O_2-CO_2 Analyzer.

Leachate Analysis

Leachate analysis was introduced into the testing program in October, 1995. The leachate samples were collected from the bottom tailings layers during the weeks of the following dates: October 13, 1995, October 31, 1995, November 29, 1995, January 8, 1996, January 29, 1996, February 19, 1996 and March 11, 1996. Runoff water samples were also collected from the surface and at the interface on March 11, 1996. All the samples were filtered through 0.45 µm and analyzed for pH, electrical conductivity, SO_4, and a 24-element scan. On April 11, 1996, additional leachate samples were collected from the bottom tailings layer of the five organic cover cells including LSSS, compost and peat. These samples were analyzed for polycyclic aromatic hydrocarbons (PAHs) and total phenol contents. These analyses were conducted in order to evaluate the effect of covers on the quality of the discharge and to calculate the loading of metals and sulphate.

Crack Filling and Monitoring

Various cover materials and the control oxidized tailings experienced some surficial cracking throughout the duration of the program (Plates #8 and #9). The cracks were monitored approximately every month to note any changes. The cracking was also documented in photographs throughout the program. Some cracks formed due to shrinkage of materials away from the edges of the pilot cells. These cracks were filled with their respective cover materials. The cracks were filled manually by mixing the appropriate cover material with deionized water and pumping or pouring the slurry directly into the cracks.

3.0 RESULTS

The following sections of the report briefly summarize and interpret the results obtained from the three components of the test program: characterization of tailings and cover materials, salt migration columns and pilot scale cover cells.

3.1   Characterization of Tailings and Cover Materials

Samples of tailings and cover materials selected for this test program were subjected to chemical, physical, mineralogical, hydrogeological and specific bench scale tests. These tests were conducted to provide data for the comparison of these materials. Most of these tests were conducted at the beginning of the program and many were performed at the end of the program.

3.1.1   Chemical Characterization

The Strathcona oxidized tailings and fresh pyrrhotite tailings were chemically characterized with a multi-element scan by ICP-ES and a whole rock analysis by XRF.

ICP-ES Scan

The samples of both oxidized tailings and pyrrhotite tailings were digested in a strong acid mixture of HNO_3, HF and $HClO_4$ and the total metal concentrations in the digests were determined by ICP-ES. The results of the multi-element ICP-ES scan are presented in Table 3.

Table 3. Multi-element ICF-ES Scan Results for Oxidized Tailings and Pyrrhotite Tailings at the Beginning and the End of One Year Test Program in the Control Cell and Under Various Cover Materials (Port 6 was located iust below the interface).

Element	Oxidized Tailings									Pyrrhotite Tailings		
	Initial	Control Cell		LSSS	DST	Compost	Peat	DST+CB	LSSS+CB	Initial 1	Initial 2	Compost
		Surface	Port 6	Port 6	Port 6	Port 6	Port 6	Port 6	Port 6			Port 6
Al (g/t)	28000	28800	25200	38000	35600	27500	26600	30100	29900	6400	7000	7000
As (g/t)	320	< 50	< 50	< 50	< 50	< 50	< 50	< 50	< 50	< 30	< 30	< 50
Ba (g/t)	220	185	142	269	230	166	159	212	185	56	57	46
Be (g/t)	< 1.0	< 1.0	< 1.0	< 1.0	< 1.0	< 1.0	< 1.0	< 1.0	< 1.0	< 1.0	< 1.0	< 1.0
Ca (g/t)	16000	17600	15700	20600	21400	18100	15600	18400	16000	4800	5500	5940
Cd (g/t)	25	21	24	18	21	23	23	21	22	44	53	30
Co (g/t)	140	136	145	127	122	142	130	134	137	190	170	159
Cr (g/t)	110	84	81	103	72	82	76	80	79	63	77	72
Cu (g/t)	560	550	505	638	730	558	510	492	502	660	720	650
Fe (g/t)	380000	355000	376000	285000	308000	365000	374000	342000	364000	530000	530000	542000
K (g/t)	-	4580	3690	9700	5630	4590	3480	4220	4650	-	-	1540
La (g/t)	< 50	< 50	< 50	< 50	< 50	< 50	< 50	< 50	< 50	< 5	< 5	< 50
Mg (g/t)	9200	9430	8230	14300	11200	8800	8330	9090	9060	2800	3000	2870
Mn (g/t)	550	528	493	665	581	509	478	512	511	360	400	363
Mo (g/t)	< 20	< 10	< 10	< 10	< 10	< 10	< 10	< 10	< 10	< 30	< 30	< 10
Na (g/t)	10000	10600	9500	13400	13300	10000	9340	10800	10400	2600	2800	2810
Ni (g/t)	4500	4110	4930	3730	3520	4480	4080	4060	4160	8100	7400	6640
P (g/t)	280	341	316	514	419	332	280	349	307	27	100	23
Pb (g/t)	160	37	28	20	32	37	30	31	30	130	120	51
Sb (g/t)	< 20	< 50	< 50	< 50	< 50	< 50	< 50	< 50	< 50	< 20	< 20	< 50
Se (g/t)	< 50	< 50	< 50	< 50	< 50	< 50	< 50	< 50	< 50	< 50	< 50	< 50
Sn (g/t)	< 20	< 20	< 20	< 20	< 20	< 20	< 20	< 20	< 20	< 20	< 20	< 20
Te (g/t)	< 10	< 10	< 10	< 10	< 10	< 10	< 10	< 10	< 10	< 10	< 10	< 10
Y (g/t)	< 10	< 5.0	< 5.0	6.7	6.2	< 5.0	< 5.0	5	< 5.0	< 5.0	< 5.0	< 5.0
Zn (g/t)	150	154	155	166	156	157	152	156	154	360	250	178

Table 3 summarizes the analytical results of the oxidized tailings and the pyrrhotite tailings
from tailings samples collected under the various cover materials at the beginning and at the

end of the one year test program. The concentrations of major elements (Al, Ca, Mg, and Na) were 3-4 times higher in the oxidized tailings than in the pyrrhotite tailings. The concentration of Fe was 38% in the oxidized tailings and 53% in the pyrrhotite tailings. Higher concentrations of Ni and Zn were also noted in the pyrrhotite tailings than in the oxidized tailings. Both tailings types had similar concentrations of Cd, Co, Cr, Cu, Mn and Pb.

After one year under the LSSS cover and DST cover, the concentrations of Al, Ba, Ca, Cu, Mg, Mn, Na, and P in the oxidized tailings increased, while the concentrations of Fe and Ni decreased, and the concentrations of Cd, Co, Cr, Pb and Zn remained unchanged. The total metal concentrations in the oxidized tailings under other cover materials were similar to the initial concentrations or to those concentrations in the control cell (Table 3).

The total metal concentrations in the pyrrhotite tailings under the compost cover for one year were similar to the initial total metal concentrations of the pyrrhotite head sample (Table 3).

Although not included in the original program scope, a head sample of the oxidized tailings was decanted and filtered through a 0.45 µm filter. The filtrate of the oxidized tailings water was found to exhibit high concentrations of Ni (282 mg/L), Fe (4890 mg/L), and SO_4 (11603 mg/L), with an acidic pH value of 3.78. The Fe in the filtrate was in the form of Fe^{2+} .

Whole Rock Analysis

A whole rock analysis was conducted on the oxidized tailings and the pyrrhotite tailings at the beginning of the test program using semi-quantitative XRF method. The elemental concentrations of the major rock forming constituents were determined and expressed as oxides of Si, Al, Fe, Ca, Mg, Na, K, P, Ti, Mn, and Cr. Loss on ignition (LOI) was also determined as part of the whole rock analysis. The results of the whole rock analysis are presented in Table 4. The measured sum of 99.8% for the oxidized tailings was within the acceptable range for the sum of components in the whole rock analysis (98-101%). However,

the whole rock technique is inappropriate for the sulphidic pyrrhotite tailings as the measured sums for both pyrrhotite tailings samples analyzed ranged from 89 to 91% (i.e. below the acceptable range) (Table 4).

Table 4.   Whole Rock Analysis Results

Element	Oxidized Tailings	Pyrrhotite tailings (Po)	Po Replicate
SiO_2 (%)	23.5	4.79	4.99
Al_2O_3 (%)	5.87	1.34	1.41
Fe_2O_3 (%)	46.4	70	71.3
MgO (%)	2.05	0.46	0.51
CaO (%)	2.44	0.74	0.77
Na_2O (%)	1.50	0.34	0.46
K_2O (%)	-	0.09	0.1
TiO_2 (%)	0.39	0.23	0.28
P_2O_5 (%)	0.08	0.02	0.02
MnO (%)	0.09	0.07	0.07
Cr_2O_3 (%)	0.04	0.02	0.03
LOI (%)	16.9	11.2	11.2
Sum (%)	99.8	89.3	91.1
S (%)	18.6	31.7	30.5

With the exception of Fe_2O_3, the percentage of all the other oxide minerals was higher in the oxidized tailings than in the pyrrhotite tailings. The analysis indicated that Fe_2O_3 (46%), SiO_2 (23.5%) and Al_2O_3 (5.9%) were the major components of the oxidized tailings. Minor components of the oxidized tailings included: MgO (2.1%), CaO (2.4%) and Na_2O (1.5%). In the pyrrhotite tailings, Fe_2O_3 accounted for >70% of the oxides, with 4.8% of SiO_2, 1.3% of Al_2O_3, 0.75% of CaO, 0.48% MgO, and 0.40% of Na_2O. The oxidized tailings contained 18.6% S and the pyrrhotite tailings contained 30.5-31.7% S which represented a maximum of 87% of pyrrhotite as FeS. This suggests that the pyrrhotite tailings have a greater acid generating potential than the oxidized tailings.

3.1.2 Physical Characterization

Physical tests and measurements were conducted on all tailings and cover materials. The tests included the determination of specific gravity and grain size distribution using sieve series, cyclosizer analyses and hygrometric analyses. The moisture content and the bulk density were determined for the as-received LSSS, compost and peat. The moisture content was also determined for all the materials after placement in the pilot cells and prior to saturation with simulated rain water.

Grain Size Distribution

Figure 5 illustrates the grain size distribution for all tailings, cover materials and capillary barrier gravel and sand. Materials plotted close to the left of Figure 5 exhibited finer grain sizes, whereas materials plotted on the right of Figure 5 had coarser grain sizes. Peat, compost and gravel and sand exhibited similar coarse grain size distributions. The oxidized tailings, desulphurized tailings, pyrrhotite tailings and LSSS had a finer grain size distribution. The grain sizes of pyrrhotite tailings, desulphurized tailings and LSSS were finer than the oxidized tailings. The 80% passing sizes (d_{80}) for the gravel and sand, compost, peat, oxidized tailings, desulphurized tailings, LSSS, and pyrrhotite tailings, were 3022, 2835, 2653, 170, 130, 76, and 34 μm, respectively.

Fiber size classification was also determined for peat and compost. According to ASTM fiber size designation, coarse fibers are those retained on #8 sieve (2.36 mm), medium fibers are those retained on #20 sieve (0.85 mm) and fine fibers are those passing #20 sieve and retained in pan. The peat had 51.9% coarse fibers, 24.25% medium fibers and 23.85% fine fibers. The compost had 59.89% coarse fibers, 17.92% medium fibers and 22.19% fine fibers. The results indicate that the peat had the higher percentage of medium and fine fibers than the compost. This may be due to the decomposition and formation of humus in the peat material.

Figure 5.   Grain Size Distribution for Tailings and Cover Materials
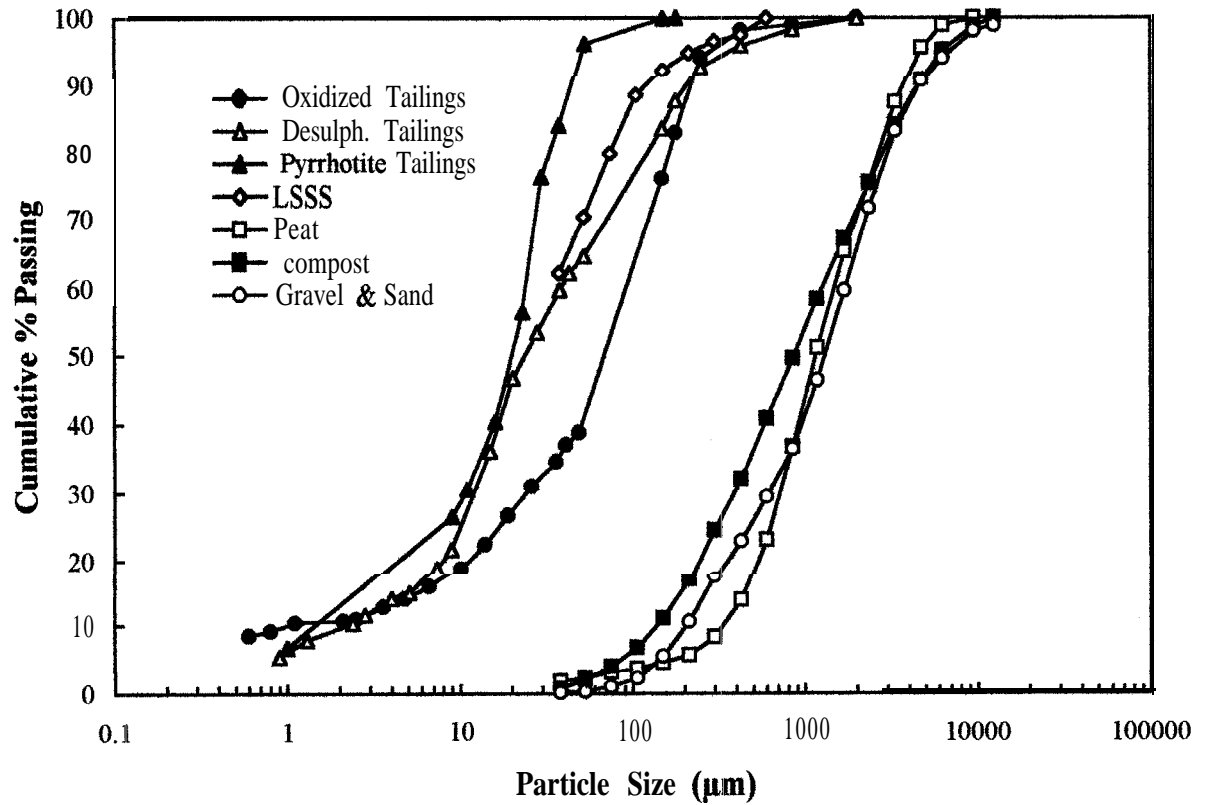
<u>Specific Gravity</u>

The specific gravities of the various materials were: 3.30 g/cm^3 for the oxidized tailings, 4.12 g/cm^3 for the pyrrhotite tailings, 2.90 g/cm^3 for the desulphurized tailings, 2.47 g/cm^3 for the LSSS, 1.73 g/cm^3 for the peat, 1.72 g/cm^3 for the compost, and 2.72 g/cm^3 for the gravel and sand.

<u>Physical Properties of Cover Materials</u>

The physical properties of the as-received LSSS, compost and peat are presented in Table 5. These organic cover materials were low in bulk density (<0.7 g/cm^3), and high in porosity

(>60%). However, the moisture content of these organic materials varied widely. The volumetric moisture contents were 31.6% for the LSSS, 12.6% for compost and 157.9% for peat.

Table 5.   Physical Properties of the As-received Cover Materials

Material	Bulk Density (g/cm^3)	Moisture Content (% by wt.)	Moisture Content (% by vol.)	Porosity (%)
LSSS	0.72	43.9	31.6	70.9
Compost	0.54	23.3	12.6	68.6
Peat	0.69	228.8	157.9	60.1

After placement of the tailings and the cover materials in the pilot cell and two weeks after saturation with simulated acidic rain, solid samples were taken from ports 1 and 3 in the tailings layer and within the cover layer for the gravimetric moisture content determination (Table 6). In comparison with the moisture content in Table 5, a slight increase in moisture content was observed for LSSS, a great increase in moisture content was noted for compost, and a great decrease in moisture content was found for peat after placement, suggesting the LSSS and compost gained moisture and the peat lost moisture during the placement. As the oxidized tailings and the desulphurized tailings (DST) were slurried and pumped into the pilot cells, they maintained relatively high moisture contents. Assuming a bulk density of 1.70 g/cm^3 for both the oxidized tailings and DST, the volumetric moisture content was calculated to be 36.2-41.8% for the oxidized tailings, and 41.3-55.6% for the DST.

Table 6.   Moisture Content of the Oxidized Tailings and the Cover Materials After Placement in the Pilot Cells and Two Weeks After Saturation

Cell	Material	Moisture Content (% by wt)	
		Port 1	Port 3
1	Oxidized tailings	21.3	24.6
2	LSSS	48.6	52.2
3	DST	25.9	24.3
4	Compost	64.7	51.9
5	Peat	77.6	84.7
6	DST	27.5	32.7
7	LSSS	46.2	51.4
8	Compost	70.1	77.1

3.1.3 Mineralogical Examination

X-Ray Diffraction (XRD) analysis was performed on the oxidized tailings to confirm major mineral components. Polished sections of both the oxidized tailings and pyrrhotite tailings were prepared and examined using incident and transmitted light under microscope at 50 to 500x magnification.   The examination was conducted at the beginning of the test and again at the end of the test program. At the end of the test program, samples of the oxidized tailings or pyrrhotite tailings were taken from the interface between the cover materials and the tailings.

Mineralogy of the Oxidized Tailings

The results of the XRD tests on the oxidized tailings are presented in Table 7. The oxidized tailings consisted primarily of minor proportions of pyrrhotite, quartz, goethite, magnetite, plagioclase, and possibly a trace of chlorite.

Table 7.   Results of X-Ray Diffraction for the Oxidized Tailings

Relative Proportion	Mineral	Formula
Minor	Pyrrhotite	$Fe_{(1-x)}S$
Minor	Quartz	SiO_2
Minor	Goethite	$FeO(OH)$
Minor	Magnetite	Fe_3O_4
Minor	Plagioclase	$CaAlSi_3O_8$
Trace	?Chlorite	$Mg_5Al(Si_3Al)O_{10}(OH)_8$

The polished sections of the oxidized tailings were characterized by silicate gangue, pyrrhotite, minor goethite, magnetite, and trace amounts of pyrite, chalcopyrite and pentlandite (Table 8). Pyrrhotite was the major sulphide mineral phase (75-80% of sulphide by volume) and occurred dominantly as: angular liberated particles up to 120 µm in diameter; corroded particles cemented by goethite; and, trace inclusions with silicate gangue. The pyrrhotite exhibited various stages of oxidation, from angular liberated particles with ragged

or microfractured edges, to goethite-rimmed particles, and relict cores within a spongy goethite.

Table 8.   Estimated Relative Proportion of Opaque Minerals in Oxidized Tailings

Mineral	Relative Proportion (% by volume)
Pyrrhotite	75-80
Goethite	5-10
Magnetite	5-10
Pyrite	2-3
Chalcopyrite	1
Pentlandite	< 1

Pyrite was present as a minor sulphide mineral phase (2-3% of sulphide by volume) in the oxidized tailings, and occurred primarily in binary association with pyrrhotite. Other trace sulphide minerals present included chalcopyrite (1% of sulphide by volume) and pentlandite (<1% by volume).

Minor magnetite was present as angular liberated particles commonly 30 to 90 µm in diameter. Magnetite also formed minor particles with silicate gangue, and was present within goethite concretions. Goethite was present as a minor component of the oxidized tailings.

After one year pilot cell testing, samples of oxidized tailings were collected from the control cell and from cells covered with LSSS, DST, compost and peat. Polished thin sections and polished sections of each sample were prepared and examined for general mineral identification and chemical and textural characterization, with special emphasis on the presence or absence of textures indicative of sulphide oxidation. The results of the mineralogical examination are included in Appendix G. The samples of the oxidized tailings collected from the cells covered with LSSS, compost or peat exhibited minor extent of pyrrhotite oxidation, whereas the samples of oxidized tailings collected from the control cell

and from the cells covered with DST, DST+CB or LSSS+CB exhibited minor to moderate extent of pyrrhotite oxidation.

Mineralogy of the Pyrrhotite Tailings

The relative proportion and size of the minerals identified from the pyrrhotite tailings are summarized in Table 9. The polished sections of the pyrrhotite tailings samples showed the mineralogy to consist predominantly of pyrrhotite (90-95% of sulphides by volume) as liberated, irregularly shaped angular grains, with lesser amounts of magnetite and non-opaques. Trace amounts of chalcopyrite, goethite and pentlandite were also identified. Composite grains with variable proportions of pyrrhotite, magnetite, chalcopyrite, and non-opaques were present as a minor component of the sample (5-10% by volume).

Table 9. **Mineralogy of the Pyrrhotite Tailings**

Mineral	Relative Proportion (% by volume)	Size (µm)	Comments
Pyrrhotite $Fe_{1-x} S$	90-95	< 1 to 270	> 90 % liberated typical size: 15-140µm
Magnetite Fe_3O_4	8-10	5-310	> 95% liberated
Chalcopyrite $CuFeS_2$	< 0.5	10-160	> 90 liberated
Goethite $FeO(OH)$	< 0.5	< 5-40	
Pentlandite $(Fe,Ni)_9S_8$	< 0.5	< 10	exsolution lamellae in pyrrhotite
Non-opaques	3-5	< 3-300	typical size: 40-90µm

After one year pilot cell testing, the fresh pyrrhotite tailings, which was covered with compost, exhibited trace oxidation.

3.1.4 Hydrogeological Testing

Hydrogeological tests were conducted on the oxidized tailings and cover materials to determine their ability to retain moisture and permit the flow of water. The tests included surface infiltration tests in the pilot scale test cells to determine the hydraulic conductivity of the materials, and drainage curve tests to determine the air entry values of the materials. The results of these tests are summarized in Table 10. Bench scale evaporative flux tests were also conducted to determine the relative evaporative fluxes for each cover material.

Hydraulic Conductivity Results

Hydraulic conductivity testing was performed at the surface of the oxidized tailings and the covers in the pilot cells immediately following the saturation of the covers, and again at the end of one year test program. Tests were conducted using the infiltrometer which requires pre-saturation of the material being tested. The hydraulic conductivity results exhibited decreasing values for: compost > peat > LSSS > desulphurized tailings = oxidized tailings. The results suggest that incoming waters would infiltrate the compost, peat and LSSS at a relatively faster rate than the desulphurized tailings and oxidized tailings.

Table 10.   Hydraulic Conductivities and Air Entry Values of the Tailings and Cover Materials at the Beginning and the End of One Year Test Program

Cell	Material	Hydraulic Conductivity (cm/s)		Air Entry Value (cm H_2O)	
		Beginning	End	NTC	U. of Sask.
1	Oxidized Tailings	2.0×10^{-5}	2.73×10^{-5}	450	200
2	LSSS	2.8×10^{-3}	4.56×10^{-3}	100	230
3	DST	3.47×10^{-5}	3.84×10^{-5}	525	200
4	Compost	2.1×10^{-1}	2.60×10^{-2}	25	110
5	Peat	6.8×10^{-2}	4.83×10^{-3}	15	100
6	DST+CB	-	2.01×10^{-5}	-	-
7	LSSS+CB	-	5.17×10^{-3}	-	-
8	Compost/Po	-	2.60×10^{-2}	-	-

Note: Hydraulic conductivity was determined in the pilot cells.
Air entry values estimated by NTC were from disturbed samples, and those by University of Saskatchewan from undisturbed samples.

At the end of the test program, the hydraulic conductivity values for the oxidized tailings, desulphurized tailings and LSSS were similar to those measured at the beginning of the test program (Table 10). However, the hydraulic conductivities decreased from 2.1×10^{-1} to 2.6×10^{-2} cm/s for the compost and from 6.8×10^{-2} to 4.83×10^{-3} cm/s for peat. The observed decrease in hydraulic conductivity for the compost and peat may be caused by decomposition and compaction during the testing in the pilot cells.

Air Entry Values

At the beginning of the test program, drainage curve tests were conducted by NTC using both disturbed and consolidated samples. The air entry values, estimated from the drainage curve test work, were: 450 cm H_2O for the oxidized tailings, 525 cm H_2O for desulphurized tailings, 100 cm H_2O for the LSSS, 25 cm H_2O for the compost and 15 cm H_2O for the peat (Table 10). This indicates that the oxidized tailings and desulphurized tailings can hold water under much higher exerted suction than the LSSS, which can hold water under higher applied pressures than compost and peat. Therefore, the peat and compost would be more readily drained than the other materials and would provide a less efficient physical barrier to oxygen infiltration.

At the end of the test program, drainage curve tests were conducted by the University of Saskatchewan using undisturbed samples cored from the pilot cells. The air entry values, estimated from the drainage curve test work, were 200 cm H_2O for the oxidized tailings, 200 cm H_2O for desulphurized tailings, 230 cm H_2O for the LSSS, 110 cm H_2O for the compost and 100 cm H_2O for the peat (Table 10).

The air entry values obtained from NTC were empirically defined air entry values, which are often used in the mathematical description of the soil-water characteristic curves (SWCC). These air entry values are defined as the intersection of the extrapolated straight lines of saturation and gradual decrease in moisture content with applied suctions. This procedure is often used with SWCC for fine-grained soils and other soils with high initial void ratios (e.g.

tailings slurries), because the air entry values may not be obvious from the SWCC. In coarse-grained soils, there is little or no change of the total soil volume when the soil drains. Normally, the empirically defined air entry values are higher than the true air entry values which are defined as the suction at which air first enters the pores of an initially saturated soil. In addition, the air entry values are a function of grain size and dry density (or void ratio).

Evaporative Flux Determinations

Figure 6 shows the evaporation rate vs. time for each material tested. The actual evaporation rate (AE) was compared with the potential evaporation rate (PE) which was measured in the laboratory in a container set beside the AE container at the tops of the respective pilot cells.

All the materials tested were saturated initially and then placed in the laboratory where the pilot cells were located. All the materials exhibited AE rates lower than the PE rates during the three-week test period. The wide difference between the AE and PE was noted only after 17 or 18 days of the testing for the desulphurized tailings, LSSS, peat and compost (Figure 6). The oxidized tailings showed a decreasing trend in AE with time. After about 7 days of testing, the oxidized tailings ceased to lose water, suggesting that the oxidized tailings were either completely dried out or had not been fully saturated initially.

Simulated rain was applied to the surface of the pilot cells every seven days during the test. Assuming that the cover surface of the pilot cells was saturated after rain application, it is estimated that the water loss by evaporation from the cover surface in the pilot cells would be equivalent to that which occurred during the first 7 day results of the evaporative flux test. The average ratio of AE to PE was 0.75 for the oxidized tailings, 0.893 for the desulphurized tailings, 0.831 for the LSSS, 0.869 for the compost and 0.843 for the peat. These ratios were used for the calculation of the water balance in the pilot cell test.

Figure 6.   **Evaporative Rate vs. Time for Different Materials**
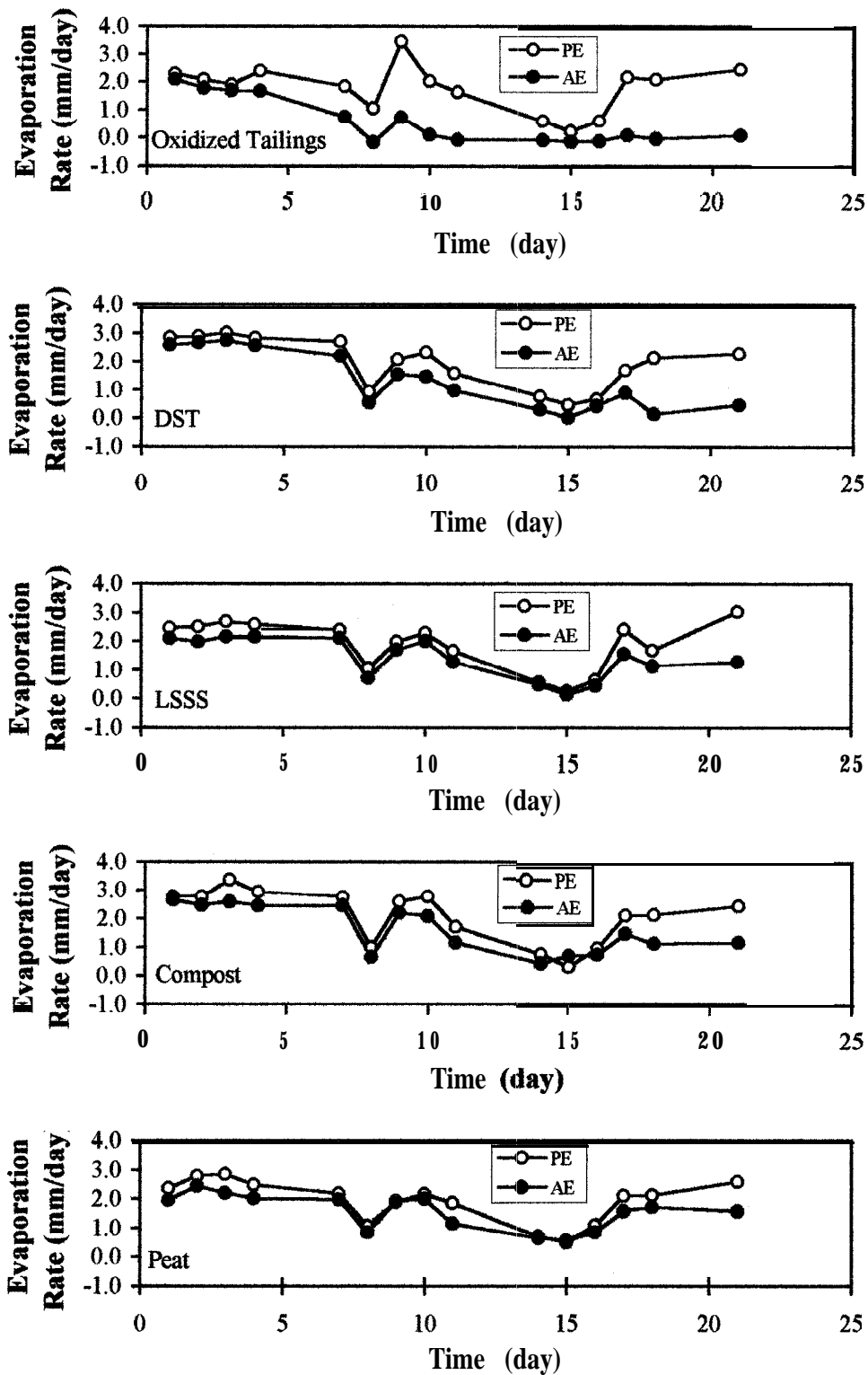
Figure 7 shows the gravimetric moisture content retained by the different materials during the evaporative flux tests. The moisture contents decreased as the evaporation period increased. The moisture contents of both peat and compost decreased at a higher rate throughout the testing period than the LSSS, which in turn decreased at a higher rate than the desulphurized tailings and oxidized tailings. The desulphurized tailings had a higher moisture content than the oxidized tailings initially. The moisture content for the oxidized tailings was 16% by weight or 29% by volume. Assuming that a porosity of 40-50% would be more realistic for tailings, the degree of saturation for the oxidized tailings would be 58-73%. This suggests that the oxidized tailings were not fully saturated. This also points to the difficulty of saturating fine-grained sediments in such experiments.

Figure 8 shows the actual evaporation rate versus the gravimetric moisture content retained by the different materials. All the materials exhibited a general trend: as the moisture content decreased, the AE rate decreased. The fluctuation in the AE rate with moisture may be caused by the variation in temperature and relative humidity in the laboratory.

3.1.5   Other Bench Scale Testing

The bench scale testing program had two components: 1) continuous measurements of relative humidity, temperature and pan evaporation rates in the laboratory area; and 2) determination of the decomposition rates in the organic covers.

The continuous measurements of relative humidity, temperature and pan evaporation rates in the laboratory area were recorded, and the pan evaporation rates were calculated and compared with the pan evaporation rates in the Sudbury area to adjust the amount of simulated rain water applied in the pilot cells.

Figure 7.   Moisture Content vs. Time During the Evaporative Flux Test
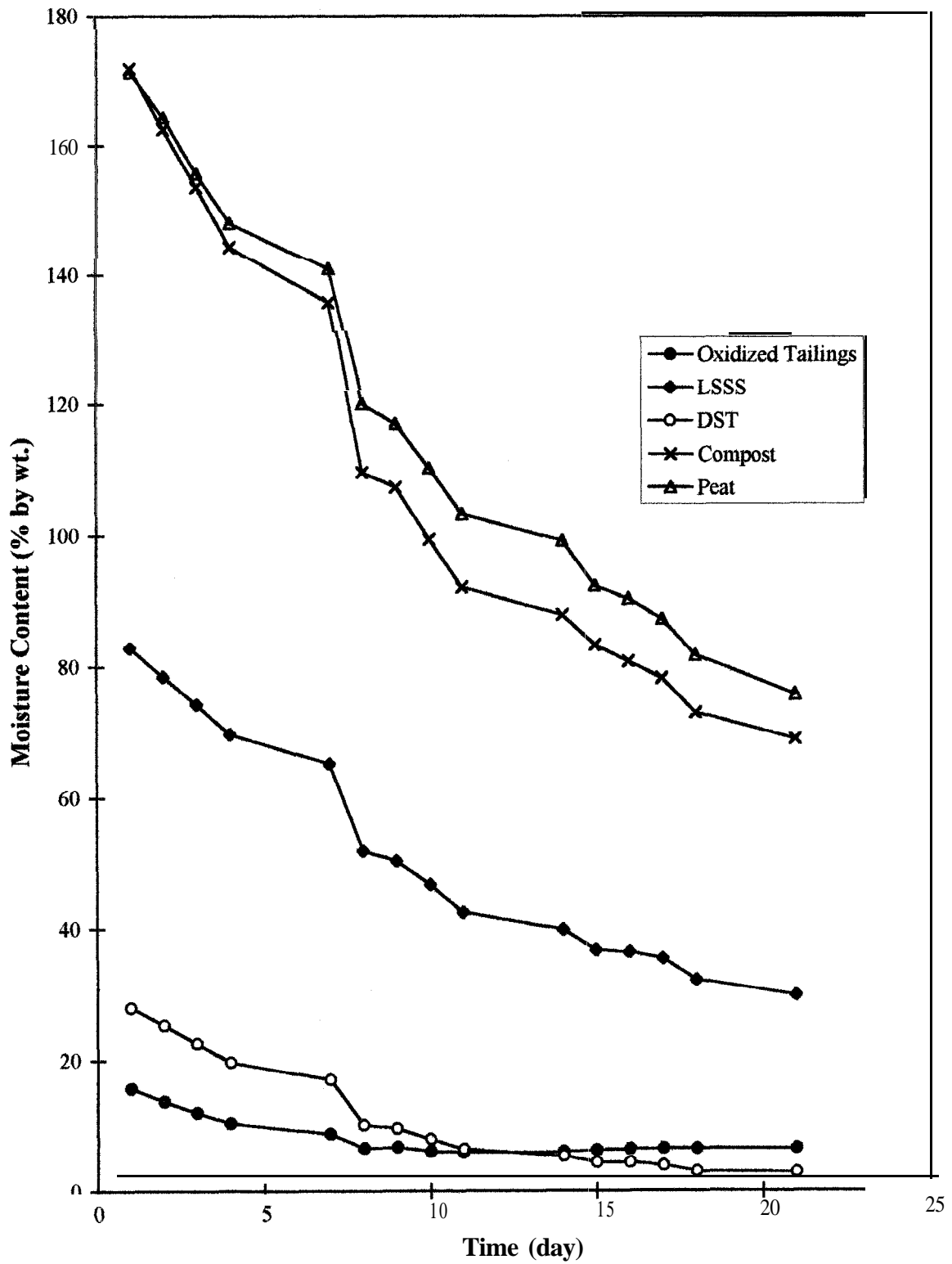
Figure 8.   **Actual Evaporation Rate vs. Moisture Content Retained by Different Materials**
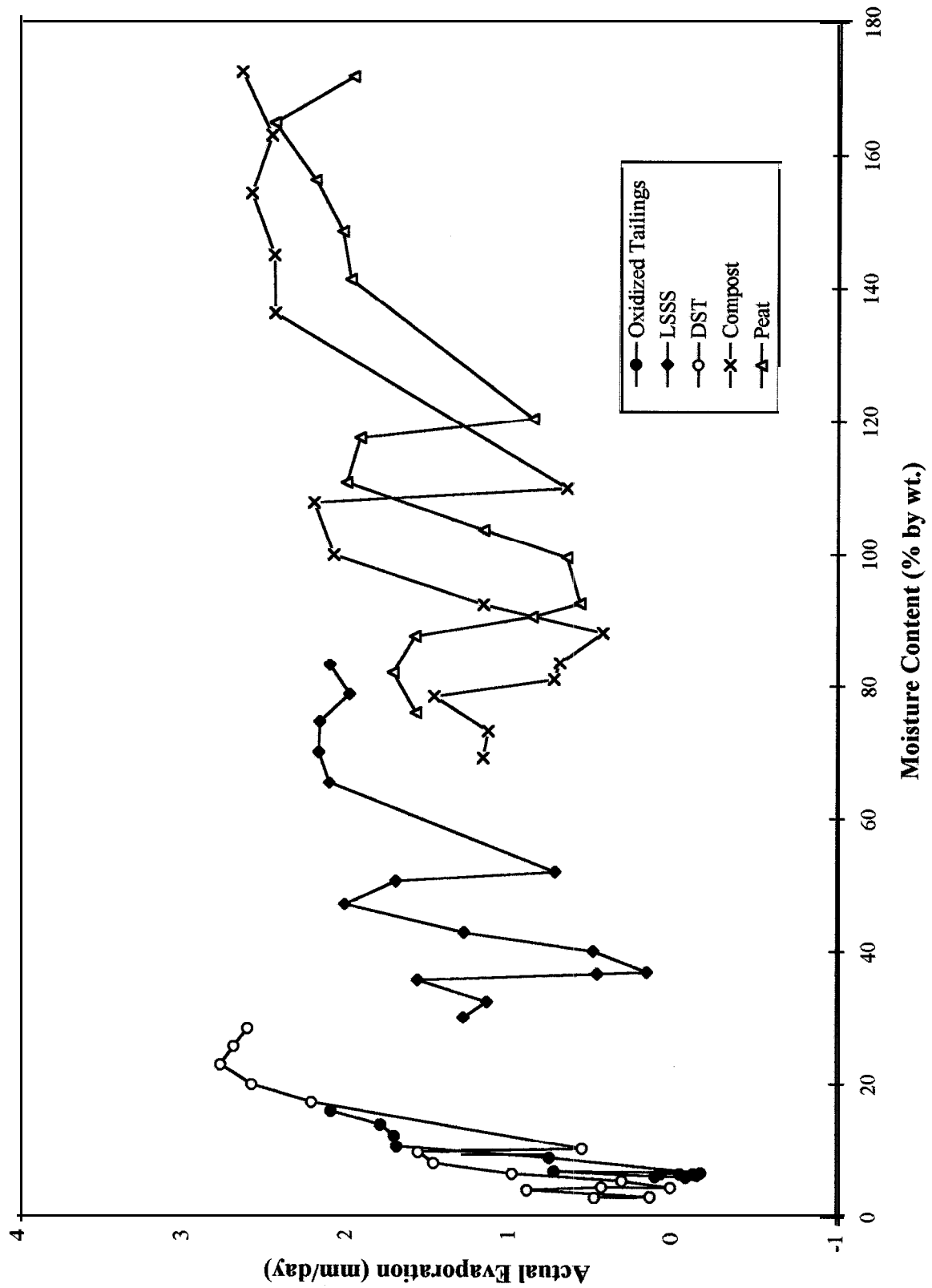
For the determination of decomposition rates in the organic covers, a combination of laboratory analysis and longer term incubation tests and computer modeling were performed. Laboratory analysis included core sampling within the organic cover layer at the beginning and the end of the pilot scale cell test and determination of total organic carbon (TOC) in the solids. The differences in TOC content between the beginning and the end of the test program were used to calculate the decomposition rates of the organic cover materials. The results are presented in Table 11.

Table 11.   The Changes in Total Organic Carbon Content in Organic Cover Materials During One Year Pilot Cell Testing

Cell	Material	Port	Total Organic Carbon (%)		Difference	
			Initial	End	+/- (%)	% of Initial
2	LSSS	1	1.68	1.65	-0.03	-1.8
		3	1.68	1.68	0.00	0.0
		5	1.68	1.48	-0.20	-11.9
4	Compost	1	20.1	6.25	-13.85	-68.9
		3	20.1	14.3	-5.8	-28.9
		5	20.1	21.7	1.6	8.0
5	Peat	1	23.1	22.3	-0.8	-3.5
		3	23.1	19.4	-3.7	-16.0
		5	23.1	24.9	1.8	7.8

The initial TOC contents were 1.68% for the LSSS, 20.1% for the compost and 23.1% for the peat. After one-year pilot cell testing, the TOC contents in the LSSS cover layer at all three ports remained relatively unchanged, whereas the TOC contents of the compost and peat at ports 1 and 3 decreased and at port 5 increased. After one-year of testing, about 69% and 29% of the TOC disappeared at ports 1 and 3 of the compost cover layer, respectively, and about 4% and 16% of the TOC disappeared at ports 1 and 3 of the peat cover layer, respectively. The greater decrease in TOC content noticed in the compost reflects how the compost more readily decomposes than the peat. An increase in TOC at port 5 of both the compost and peat cells indicates the accumulation of TOC due to leaching of organic

compounds from overlying layers. Little or no changes in TOC contents in the LSSS cover cell shows that decomposition was not occurring at easily measurable levels.

The incubation test and computer modeling were performed by Predictive Modeling, Inc., Arkansas, USA. The results of the test and the computer modeling are attached in Appendix H. The main findings of the tests are summarized below.

- The two month incubation tests using various ratios of a different LSSS material from that used in the pilot cell tests with 9.9% TOC blended with DST revealed that there was no evidence of decomposition as carbon dioxide evolution. It is believed that one of two scenarios may have occurred. Either no decomposition occurred because the LSSS and the DST were essentially sterile or evolved carbon dioxide was readsorbed by the LSSS, because of the high pH of the LSSS.
- Determinations of soluble organic carbon and TOC on the initial and final samples suggest that the decomposition was occurring in the LSSS, but that it was not detectable due to readsorption of CO_2 by the lime in the LSSS.
- The first order rate constant for LSSS was 0.00175 d^{-1} which corresponds to values found for the slow fraction of other, similar biosolids.
- Computer modeling predicted that the initial annual decomposition during the warmer months would be 15-16%.
- The minimum amount of decomposition would be depletion of all the soluble organic carbon or about 30% of the organic carbon in the LSSS. If this were to take place, the decomposition would slow markedly after two years.

3.2 Salt Migration Columns

The salt migration program as originally proposed has been completed. A granular cover on desulphurized tailings has also been evaluated to determine the effectiveness of a granular

surface cover placed in reducing the evaporation rate from the desulphurized tailings cover. The final results of the salt migration column tests program follow.

3.2.1 Changes in Surface Evaporation Rate with Cover Depth

Figure 9 illustrates the changes in the evaporation rates with time and cover depth. The evaporation rates were calculated based on the weekly volume of water added into the constant head reservoirs. The evaporation rate in the control cells reached 0 mm/day at day 128 with the 1.0 m cover, day 156 with the 0.5 m cover, and day 93 with the 0.15 m cover. The observed decrease in the evaporation rate in the control columns is interpreted to have been caused by the formation of a salt crust on the surface of the oxidized tailings.

The compost cover exhibited the lowest evaporation rates with time in all three cover depths (Figure 9 and Table 12). In the 1.0 m cover depth, the evaporation rates were noted to decrease over time. Evaporative losses were first noted in the 0.5 m cover after 116 days. The evaporation rates fluctuated between 0.0 and 0.38 mm/day in the 0.15 m cover depth.

When the actual evaporation rates for the surface of the salt migration columns were averaged over the four month test period, the surface evaporation rates were noted to generally decrease with increasing cover depth (Figure 10). This change in evaporation rate was particularly noticeable between cover depths of 0.5 m and 1.0 m for almost all of the cover materials.

For all covers, on average, the evaporation rates were 0.47 mm/day for peat, 0.45 mm/day for the desulphurized tailings + CB, 0.41 mm/day for the desulphurized tailings, 0.22 mm/day for the oxidized tailings, 0.13 mm/day for the LSSS, and 0.12 mm/day for the compost.

Figure 9. **Evaporation Rate vs. Time and Cover Depth for Different Cover Materials**
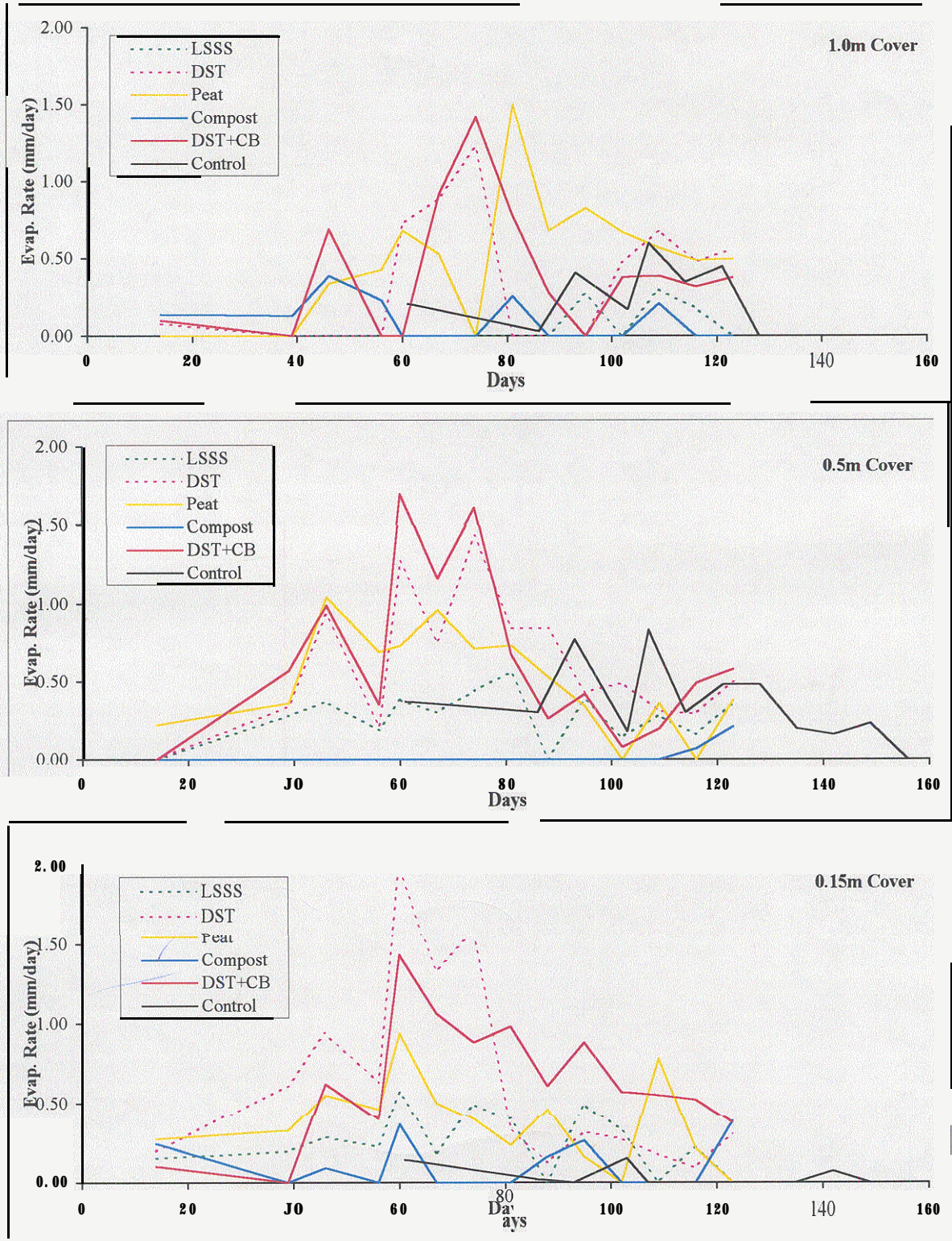
Table 12.   Variation in Evaporation Rate at Varying Cover Depths

Evaporation	Cover Depth (m)		
Rate	**0.15**	0.5	**1.0**
Highest	DST	DST	Peat
	DST + CB	Peat	DST + CB
	Peat	DST + CB	DST
	LSSS	Oxidized Tailings	Oxidized Tailings
I	Compost	LSSS	Compost
Lowest	Oxidized Tailings	Compost	LSSS

Figure 10.   Evaporation Rate vs. Cover Depth for Different Cover Materials
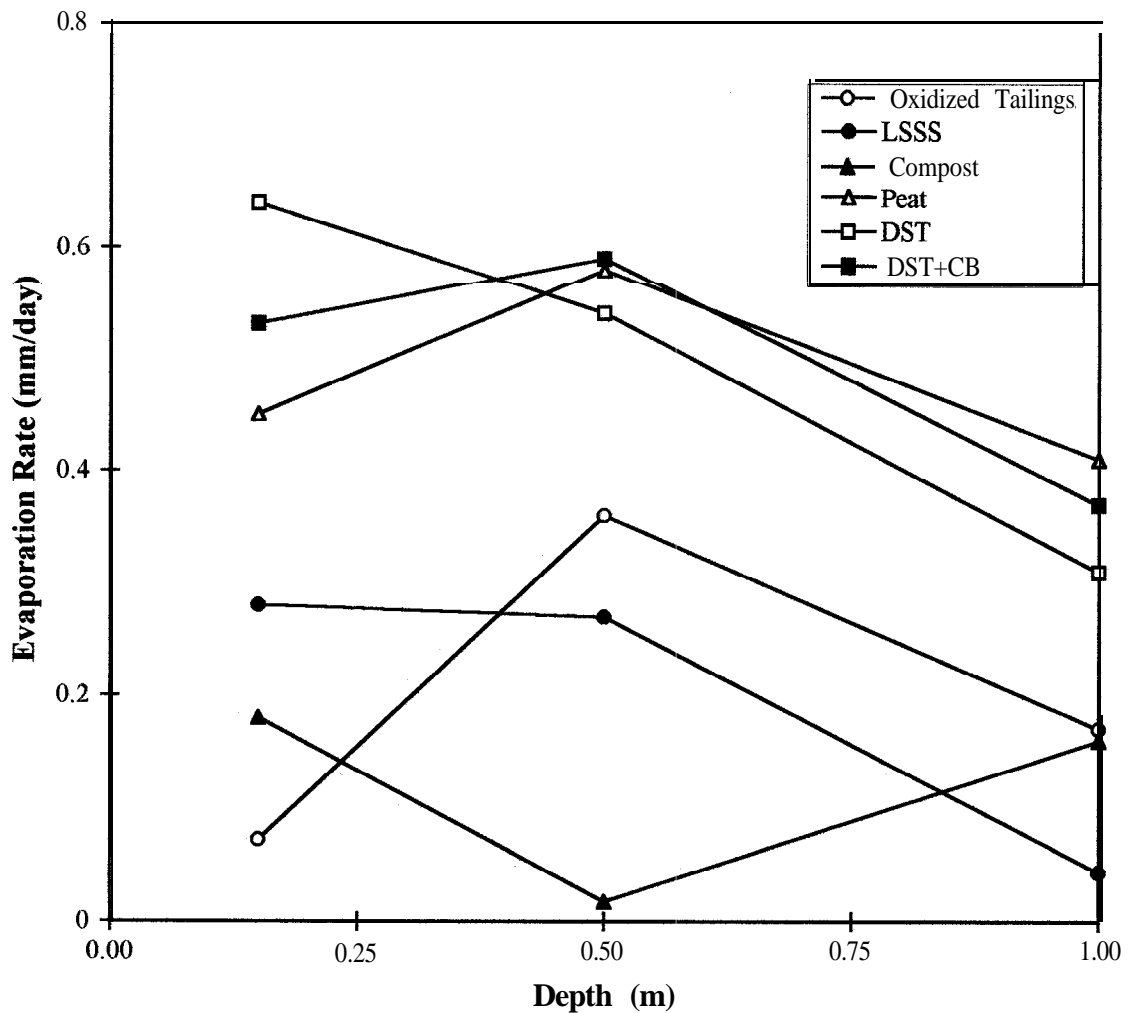
3.2.2 Relationship Between Evaporation Rates, Air Entry Values and Particle Size

The evaporation rates for the different materials averaged over the three different cover depths tested were plotted against the initial air entry values estimated from the drainage curve test work and against the 10% passing size (D_{10}) (Figure 11). On initial review of the data there does not appear to be a direct correlation between the evaporation rates and the air entry values or between the evaporation rates and the D_{10} particle size. The high evaporation rate noted for peat may have been related to the large surface area exposed due to the formation of large cracks in the peat covers. Without the peat results, the highest evaporation rate was associated with high air entry values (Figure 11A) and with low D_{10} particle size (Figure 11B). The high air entry values indicate a higher potential moisture content above the water table. Capillary flow contributed to evaporation losses through permitting the upward movement of water to replace that lost by evaporation losses.

3.2.3 Electrical Conductivity Changes with Cover Depth and Time

Figure 12 shows the relative electrical conductivity ($\frac{C - Co}{Co} \times 100$) at surface over time for the three cover depths. All the cover materials exhibited an increased conductivity at the surface as the drought period increased in duration. This increase in conductivity was noted to be inversely related to the thickness of cover materials. The highest increase in conductivity was noted for the 0.15 m cover depth, a lesser increase in conductivity was noted for the 0.5 m cover depths, and the least increase in conductivity was noted for the 1.0 m cover depth

The relationship between the electrical conductivity changes at the surface and with cover depth was closely connected to the relationship between the evaporation rate and the cover depth. For instance, at a shallow cover depth, both a higher evaporation rate and a greater increase in conductivity were noted at the surface.

Figure 11. Average Evaporation Rates vs. Air Entry values (A) and D_{10} (B)
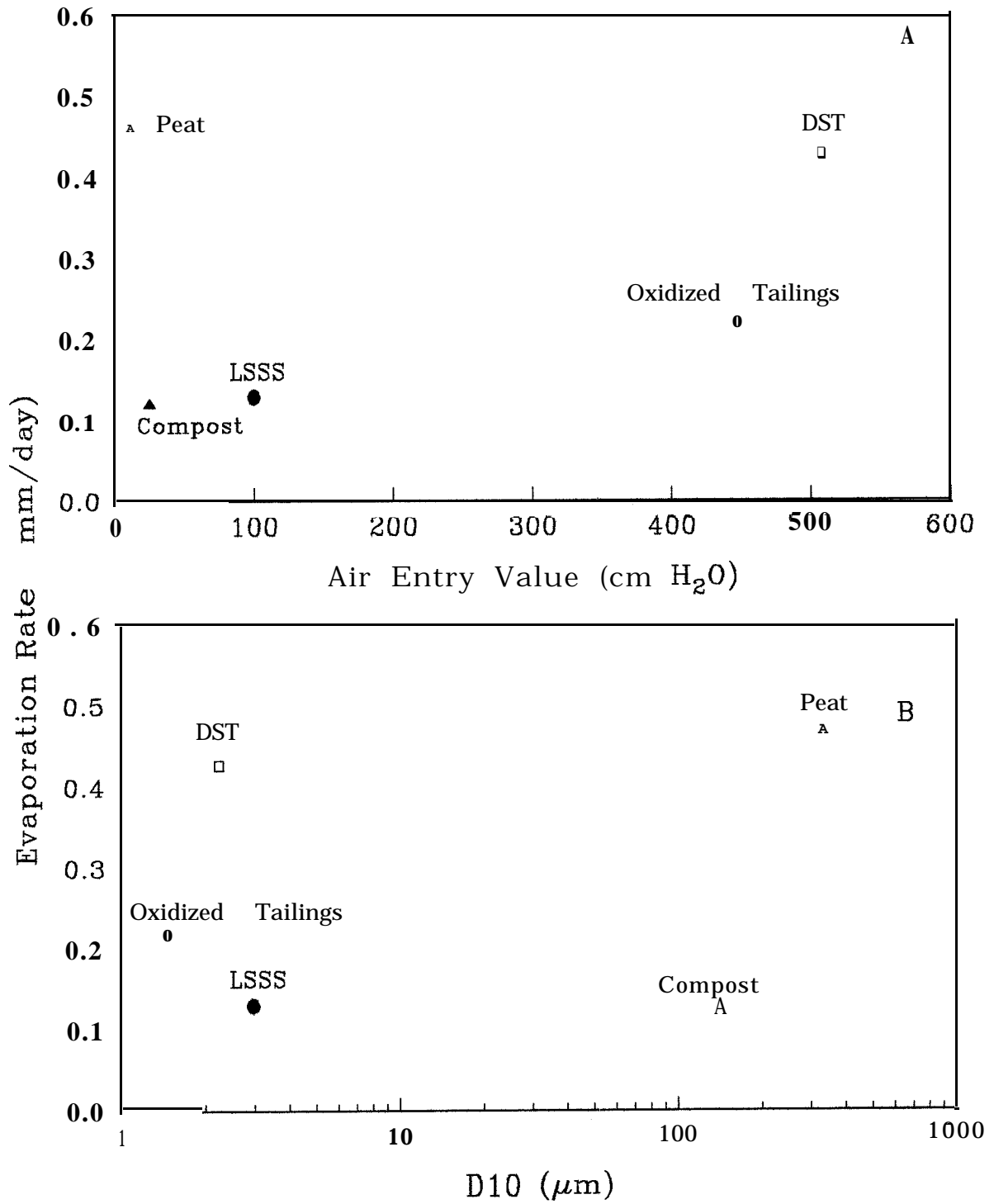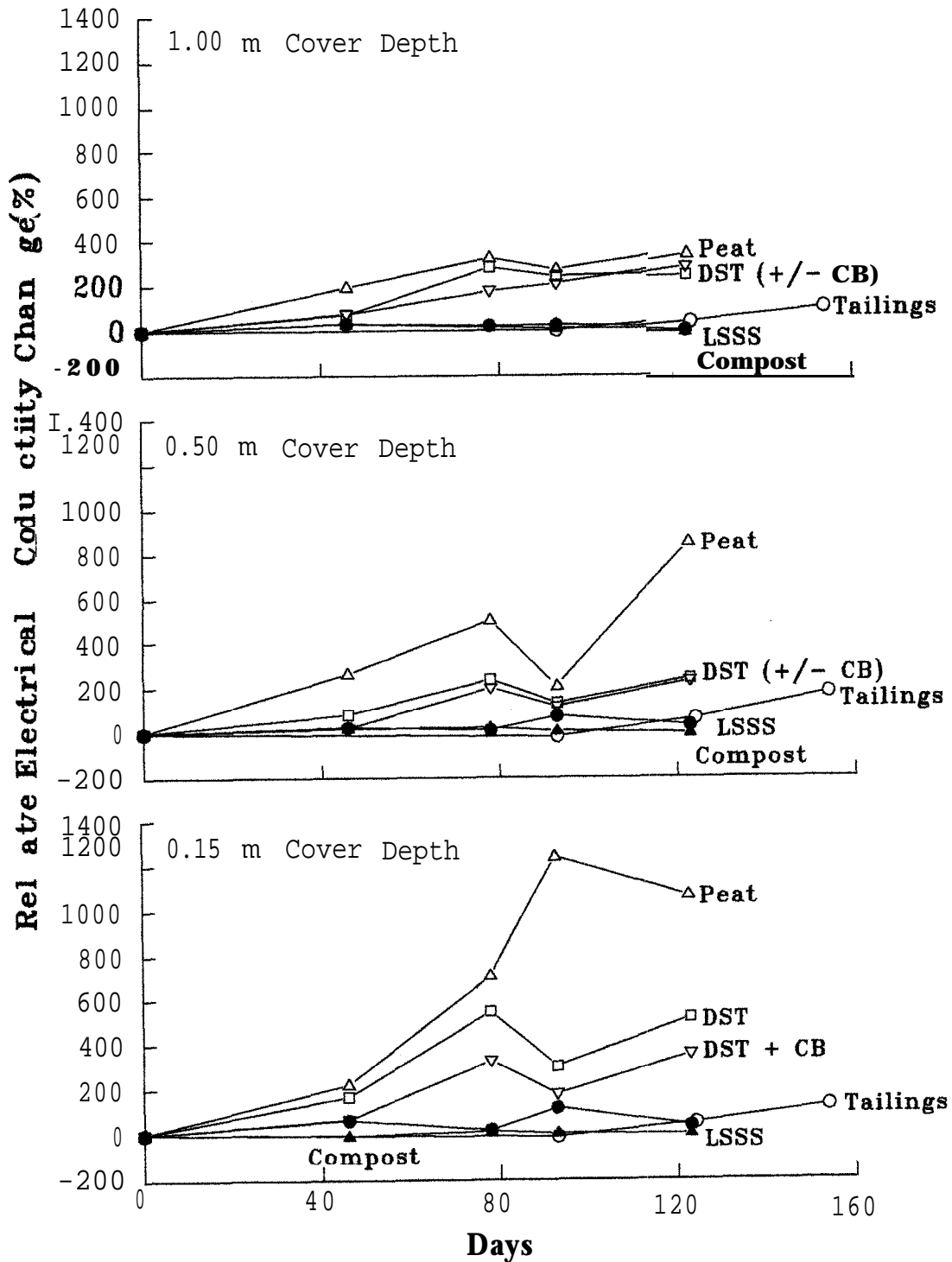
Among the cover materials tested, peat and desulphurized tailings (with or without CB) consistently exhibited the highest percentage increase in electrical conductivity at the surface (Figure 12). The LSSS and compost consistently exhibited the smallest percentage increase in electrical conductivity at the surface. This change in electrical conductivity was closely related to the evaporation rates from the cover surface (Figure 10) (i.e. the high percentage increase in electrical conductivity at the surface of the peat and desulphurized tailings was paralleled by the high evaporation rate observed in the peat and desulphurized tailings columns.

Similar increases in electrical conductivity at the surface were noted for the desulphurized tailings, both with and without the CB at both the 0.5 m and 1.0 m cover depth (Figure 12). However, higher increases in electrical conductivity were observed in the 0.15 m desulphurized tailings cover than those measured in the 0.15 m desulphurized tailings plus CB cover. The differences in electrical conductivity between these two columns were relatively constant over the four month test period (Figure 12). Even though the desulphurized tailings exhibited the highest percentage increases in electrical conductivity, the final electrical conductivity at the surface was still relatively low after four months of drought compared to the other cover materials (Table 13). For compost, the electrical conductivities were similar in all of the cover depths tested and no increases in electrical conductivity occurred over time.

Table 13.   Initial and Final Electrical Conductivity Values (µmhos/cm) at the Surface of the Salt Migration Columns During Four Month Test Period

Cover Material	Electrical Conductivity (µmhos/cm)			
	Initial	Final		
		1.0 m Cover	0.5 m Cover	0.15 m Cover
Oxidized Tailings	1878	3953	5170	4268
Desulphurized Tailings	137	490	464	846
Desulphurized Tailings + CB	137	542	449	625
LSSS	2854	3301	3721	3883
Peat	354	1617	3345	4124

Lakefield Research Limited
Environmental Services

| Compost | 1426 | 1573 | 1364 | 1439 |

The high electrical conductivity noted at the surface of the oxidized tailings for all the cover depths (Table 13) was directly related to the accumulation of salts. A shallow layer of blue yellow crystal salts formed at the surface of the oxidized tailings on the control cells. This layer of salts may exert an osmotic effect on the evaporation rate. A sample of the blue yellow crystals was collected and subjected to X-Ray diffraction analysis and a 24-element ICP-ES scan. The ICP-ES scan indicated that the crystals contained 18.8% Fe, 0.56% Mg, 0.2% Ca, 0.06% Mn, 0.05% Na and 0.04% Al. The X-Ray powder diffraction analysis identified the crystals as rozenite ($FeSO_4.4H_2O$) with possible overlap with starkeyite ($MgSO_4.4H_2O$). Therefore, the crystals consisted primarily of ferrous iron sulphate.

Electrical conductivity changes with cover depth and time at all subsurface sampling points are presented in Figures 13-16. The peat material exhibited the highest percentage increases in electrical conductivity at all the sampling points for all the cover depths. However, there was a decreasing trend in electrical conductivity concentrations noted with an increase in sampling depth in the peat. Compost consistently exhibited the lowest percentage increases in electrical conductivity.

Differences in electrical conductivity between the desulphurized tailings cover and desulphurized tailings plus CB cover were also noted at 0.15 m sampling points of the 0.15 m cover depth (Figure 13). These differences were largest towards the end of the test. Little differences in electrical conductivity were observed at the deeper sampling points or deeper cover depths between these two cover materials (Figures 13-16). In the salt migration column tests, the gravel and sand used as a capillary barrier had a D_{10} value of 0.2-0.3 mm (Figure 5). It has been shown that capillary rise in a porous material is controlled by the D_{10} with smaller grain size resulting in greater capillary rise. Based on the D_{10} value, it is likely that the gravel and sand material would have a capillary rise on the order of about 20 cm or very close to the thickness of the CB layer. Furthermore, greater compaction can lead to greater capillary rise. For this reason, it is probable that the CB layer may have been even

less effective as capillary break under thick covers (1.0 and 0.5 m) than under the thin cover (0.15 m) layer.

Figure 13. Relative Electrical Conductivity Change with Time and Cover Depth at 0.15 m Below the Surface
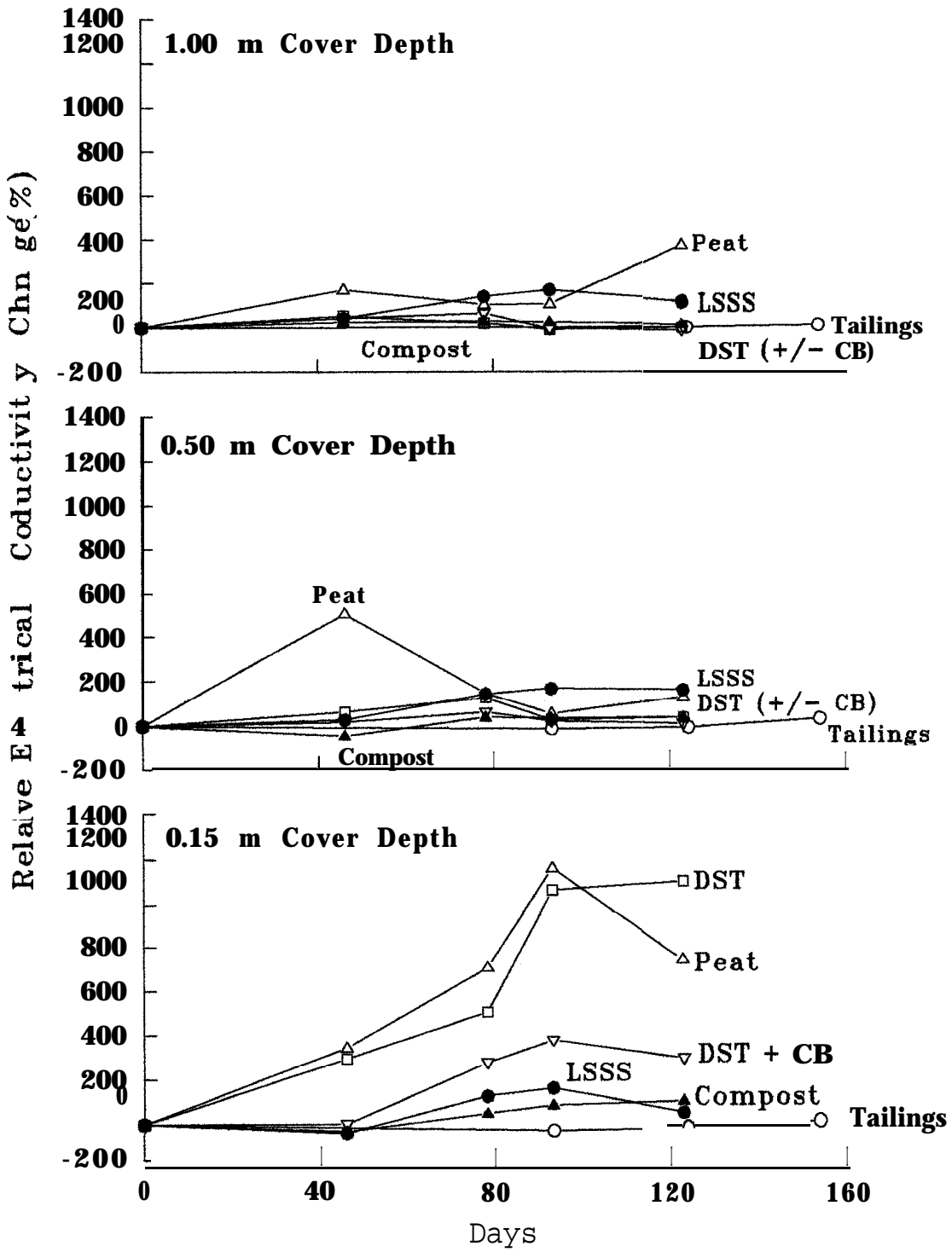
Figure 14. **Relative Electrical Conductivity Change with Time and Cover Depth at**
0.30 **m Below the Surface**
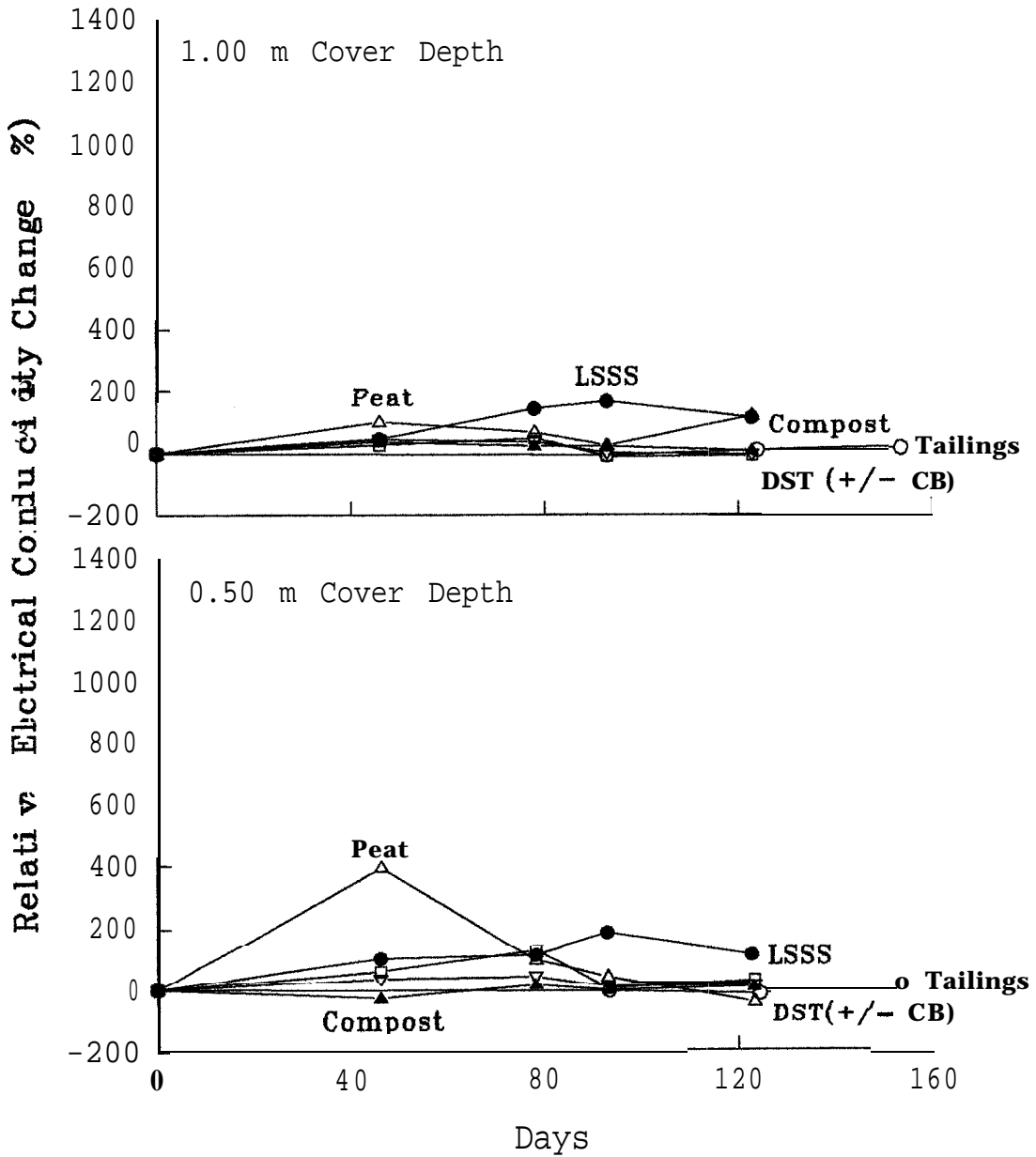
Figure 15. **Relative Electrical Conductivity Change with Time and Cover Depth at** 0.45 **m Below the Surface**
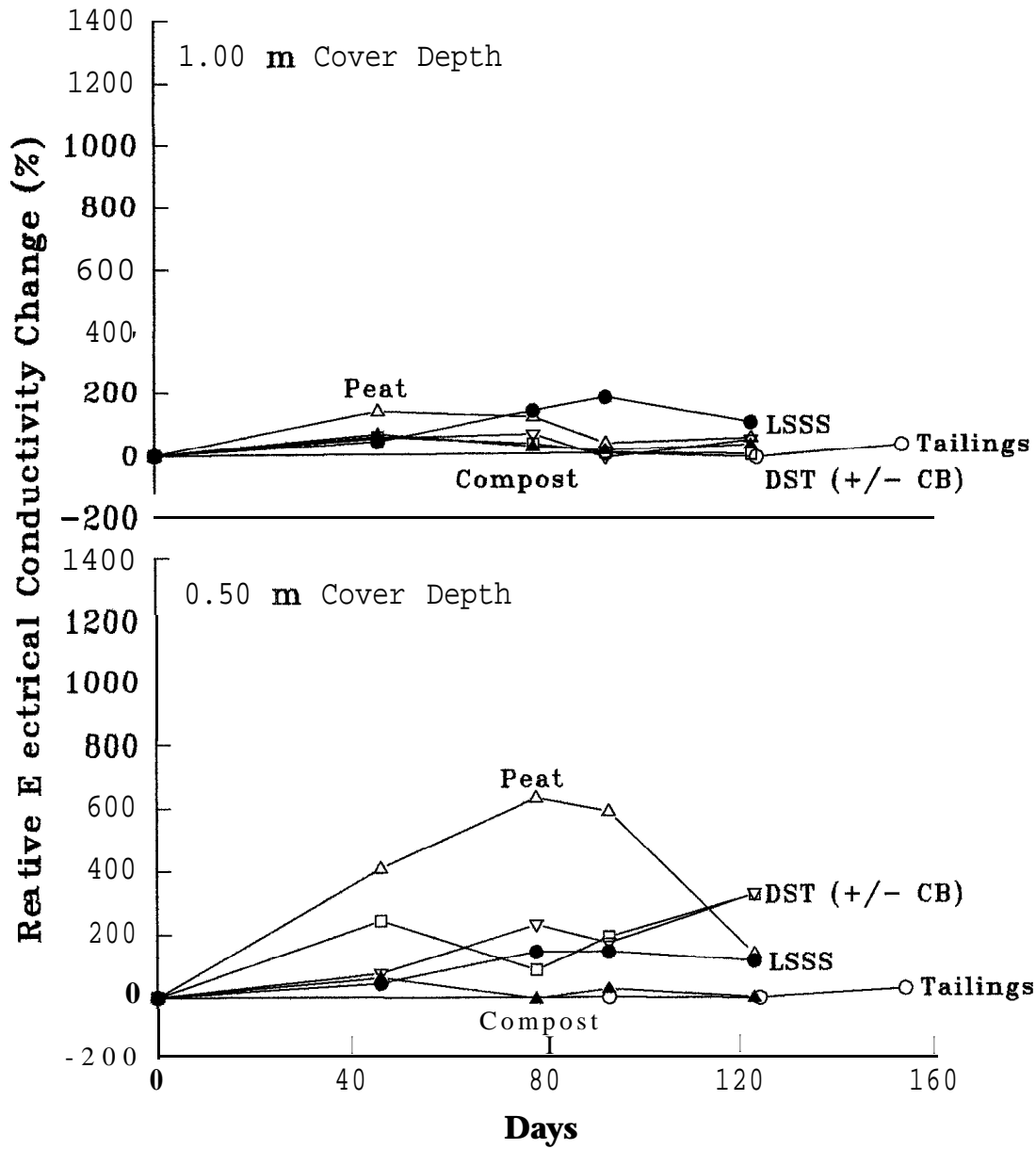
Figure 16.   Relative Electrical Conductivity Change with Time at 0.60 and 0.75 m Below the Surface Under 1.0 m Cover Depth
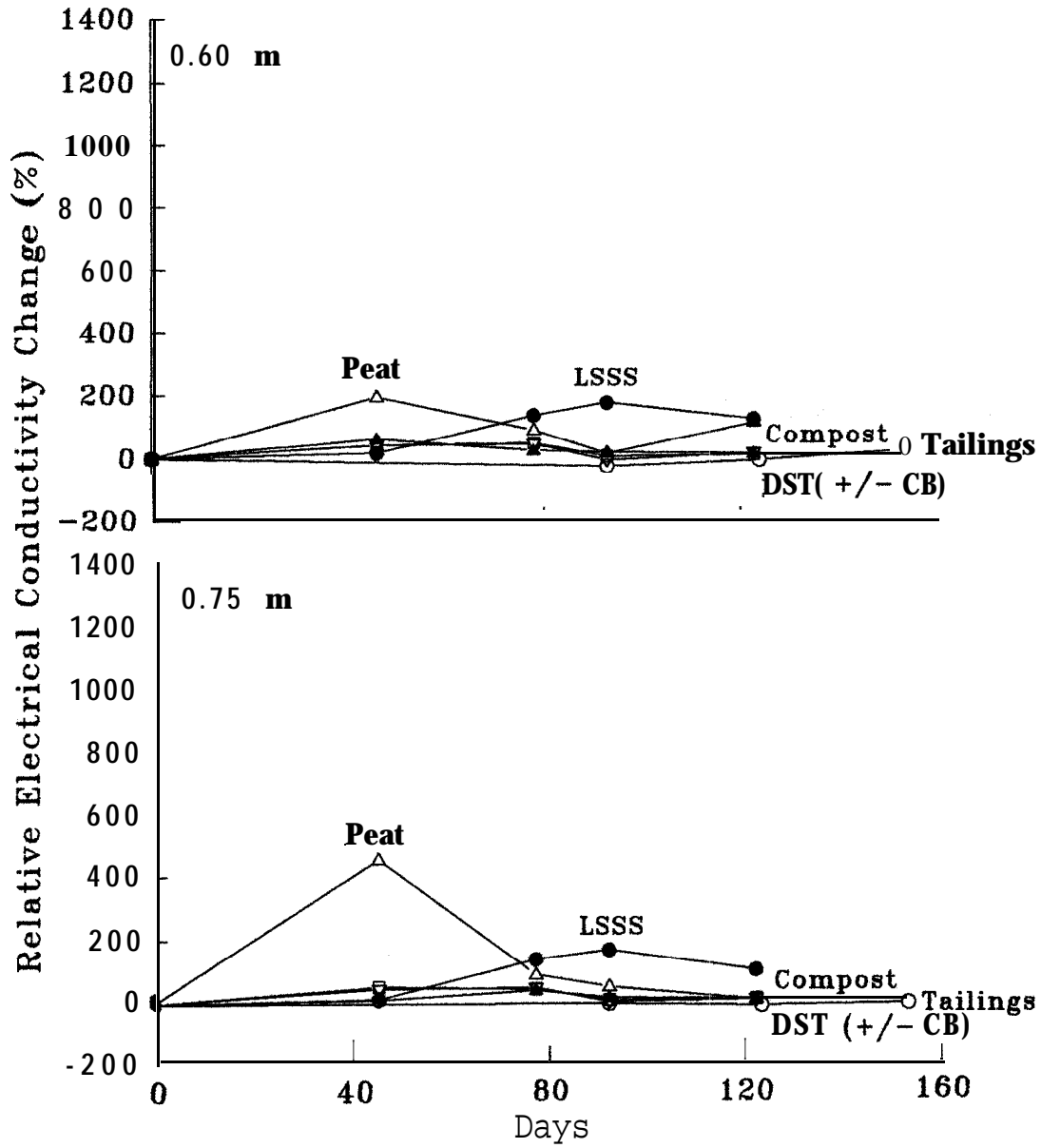
At the 0.15 m sampling point, the LSSS exhibited a large percentage increase in electrical conductivity in all the cover depths tested (Figures 13-16). The electrical conductivity of the LSSS increased from an initial value of 2854 µmhos/cm (Table 13) to 8181 µmhos/cm at the 0.15 m sampling point. Because of the relatively low evaporation rates recorded for the LSSS, this increase was not considered to be attributable to the evaporation rate or the upward migration of salts from the underlying oxidized tailings. It was suggested that the LSSS may have contributed salts to the upward migrating waters, resulting in the high electrical conductivities noted. A shake flask test was performed to determine the contribution of salts to the observed electrical conductivity related directly to the dissolution of the LSSS.

The shake flask test results indicated that the pore water in the LSSS exhibited a naturally high electrical conductivity of 6290 µmhos/cm after the first 24 hour shaking (Table 14). The electrical conductivity decreased to 2960 µmhos/cm after the second 24 hour shaking. The cation salts dissolved in the deionized water were composed mainly of Ca and Mg. The large increase in electrical conductivities noted in the salt columns was, therefore, interpreted to be related to the dissolution of salts in the LSSS and not a direct result of the migration of salts from the underlying tailings.

Table 14.   Shake Flask Test Results for the LSSS

Parameter	First 24 Hours	Second 24 Hours
pH	8.82	8.31
Conductivity (µmhos/cm)	6290	2960
Ca (mg/L)	1140	475
Mg (mg/L)	162	50
Fe (mg/L)	0.20	0.03
Al (mg/L)	0.36	0.23
P (mg/L)	0.63	0.29

Lakefield Research Limited
Environmental Services

The high pH of the LSSS may also have contributed to the greater increase in measured electrical conductivity values. Electrical conductivity is more sensitive to H^+ and OH^- than to SO_4^{2-} and many other common ions that make up the salts in the tailings pore water. The LSSS cover had a pore water pH of greater than 11, indicating a high OH^- concentration. This implies that, if the same increase in concentration, due to evaporation, occurred in the LSSS as in other covers, the LSSS would exhibit a greater increase in electrical conductivity.

3.2.4   Physical and Chemical Characteristics of the Final Destructive Core Samples

Final destructive core sampling was conducted on October 13, 1995, about 11 months after the salt migration column test. Samples were taken from the top, middle and bottom of the cover layer for determination of pH, TDS, electrical conductivity, metal concentrations (Ni, Cu and Fe), SO_4 and volumetric moisture content. The results of the determinations are presented in Tables 15-17. The main findings of the results are summarized below.

- The volumetric moisture contents remained relatively constant at about 50% throughout the cover layers of the oxidized tailings and the desulphurized tailings for all three cover depths, suggesting that the two types of tailings were close to saturation. For the three organic cover materials, the volumetric moisture contents were lower at the top and higher at the bottom of the cover layers, and increased with decreasing cover depths. The high evaporation rates noted at the shallow cover depths and with desulphurized tailings and peat were directly related to the high moisture content near the surface. Even though the oxidized tailings contained a high moisture content, they exhibited low evaporation rates because of the formation of a crust of salts at the surface. The salts formed due to the oxidation of sulphide minerals and precipitation of these at the surface.
- The pH values of the oxidized tailings in the control columns remained relatively constant at about 3.4. The pH values of the LSSS remained above 11 throughout the cover layer for all three cover depths. The pH values for the desulphurized tailings, compost and peat

were higher at the top and lower at the bottom of the cover layer, and decreased with decreasing cover depths. With 0.5 m and 0.15 m cover depths, the pH values at the bottom of the cover layers of the desulphurized tailings, compost and peat were similar to the pH of the oxidized tailings, indicating direct impact on the covers of the underlying oxidized tailings.

- There was a general agreement between the electrical conductivity (EC) measurements and the total dissolved solids (TDS) contents, suggesting that the EC measurements provided a rough estimate of the TDS. The EC and the TDS were higher at the top of the salt migration columns than initial values, indicating the accumulation or concentration of salts through a combined effect of evaporative loss and capillary rise of water.

- The SO_4 concentrations at the top of the covers were higher than the initial values. For the LSSS cover material with 0.5 m and 1.0 m cover depths, the SO_4 concentrations decreased by 50% and 80%, respectively, at the middle and the bottom of the cover layer, suggesting that the high SO_4 concentrations noted at the surface were caused by concentrating SO_4 from underneath the cover layer through the upward movement of water. At the bottom of the cover layer, where the pH was lowered by the oxidized tailings, the SO_4 concentrations were much higher than the initial values.

- The highest concentrations of Fe and Ni were found in the oxidized tailings control columns. High concentrations of Fe and Ni were also observed in the 0.15 m desulphurized tailings cover.

- High concentrations of Cu (71 mg/L) and Ni (8.4 mg/L) were detected at the top of the LSSS cover layer, suggesting the potential of discharge from the runoff water.

- The Ni concentrations were below the detection limit of 0.05 mg/L in the compost and peat cover layer, only with 1.0 m cover depth.

Table 15. **Physical and Chemical Characteristics of Samples Collected from the Salt Migration Columns of 1.0 m Cover on October 13, 1995, as Compared to Their Initial Values**

Material	Sample	M.C. % by vol.	pH unit	EC μmhos/cm	TDS mg/L	SO$_4$ mg/L	Cu mg/L	Fe mg/L	Ni mg/L
Oxidized Tailings	Initial	-	4.12	1878	1070	20951	< 0.03	7760	716
	0-5 cm	50.03	3.23	4140	6320	42052	< 0.02	33590	33.5
	45 cm	48.57	3.36	2070	2410	13702	0.21	9022	27.4
	75 cm	50.86	3.41	1950	2210	34128	< 0.02	16420	18.7
LSSS	Initial	31.61	12.20	2854	3760	5051	15.8	0.09	1.40
	0-5 cm	27.48	9.38	3840	5310	12040	71.4	47.2	8.40
	45 cm	49.31	12.24	5320	3920	2451	44	< 0.03	2.50
	75 cm	43.16	12.26	4990	3870	950	16.2	0.17	1.34
Desulph. Tailings (DST)	Initial	-	7.40	137	116	1135	0.04	0.07	< 0.10
	0-5 cm	49.79	7.89	364	285	2057	0.28	0.59	0.31
	45 cm	46.99	7.63	241	200	1543	0.07	0.40	0.52
	75 cm	47.06	7.71	287	240	1681	0.02	0.40	1.03
Peat	Initial	157.87	7.19	354	600	222	0.07	0.51	< 0.10
	0-5 cm	47.81	6.30	1230	1660	1395	0.08	0.28	< 0.05
	45 cm	61.99	5.89	936	1700	503	0.13	0.53	< 0.05
	75 cm	72.09	5.77	1190	1980	2087	0.11	0.07	< 0.05
Compost	Initial	12.58	8.16	1426	1690	24.5	0.08	1.16	< 0.10
	0-5 cm	5.72	7.37	1790	2250	49	0.19	1.67	< 0.05
	45 cm	29.27	7.25	2130	2580	6701	0.12	0.31	< 0.05
	75 cm	42.38	7.08	2080	2460	499	0.10	0.22	< 0.05
DST+CB	Initial	-	7.40	137	116	1135	0.04	0.07	< 0.10
	0-5 cm	51.88	7.62	254	225	1287	< 0.02	0.32	0.25
	45 cm	47.56	7.70	234	210	685	< 0.02	0.61	< 0.05
	75 cm	47.28	7.71	219	195	1265	0.06	0.48	0.20

Table 16. **Physical and Chemical Characteristics of Samples Collected from the Salt Migration Columns of 0.50 m Cover on October 13, 1995, as Compared to Their Initial Values**

Material	Sample	M.C. % by vol.	pH unit	EC μmhos/cm	TDS mg/L	SO$_4$ mg/L	Cu mg/L	Fe mg/L	Ni mg/L
Oxidized Tailings	Initial	-	4.12	1878	1070	20951	< 0.03	7760	716
	0-5 cm	51.12	3.43	3300	4550	66076	< 0.02	27970	35.1
	15 cm	45.27	3.4	2400	2850	29249	< 0.02	16050	27.2
	45 cm	48.33	3.44	2080	2410	20082	< 0.02	15170	19
LSSS	Initial	31.61	12.20	2854	3760	5051	15.8	0.09	1.40
	0-5 cm	41.94	12.12	6780	6990	5918	18.5	4.85	3.53
	15 cm	48.45	12.14	6130	5100	2666	68.9	2.19	3.23
	45 cm	52.85	12.16	5420	3610	833	24.2	2.64	1.77
Desulph. Tailings (DST)	Initial	-	7.40	137	116	1135	0.04	0.07	< 0.10
	0-5 cm	45.68	7.64	298	200	3133	0.16	0.42	0.65
	15 cm	47.98	7.65	287	170	1604	0.08	0.09	1.44
	45 cm	48.18	3.85	931	835	15876	< 0.02	8488	64.4
Peat	Initial	157.87	7.19	354	600	222	0.07	0.51	< 0.10
	0-5 cm	26.45	5.9	1320	1840	2181	0.03	0.18	0.82
	15 cm	35.78	5.6	1050	1770	326	0.04	0.07	0.19
	45 cm	41.47	3.65	2640	3530	1931	0.03	1.13	0.22
Compost	Initial	12.58	8.16	1426	1690	24.5	0.08	1.16	< 0.10
	0-5 cm	13.90	7.4	2620	3020	119	0.19	1.96	0.19
	15 cm	43.48	6.82	2590	2870	236	0.06	0.21	0.19
	45 cm	52.95	4.1	3200	3960	2470	< 0.02	2.17	0.19
DST+CB	Initial	-	7.40	137	116	1135	0.04	0.07	< 0.10
	0-5 cm	46.05	4.49	422	350	1467	< 0.02	0.68	0.57
	15 cm	49.38	7.62	289	314	1302	< 0.02	0.04	0.66
	45 cm	-	-	-	-	-	-	-	-

Table 17.   **Physical and Chemical Characteristics of Samples Collected from the Salt Migration Columns of 0.15 m Cover on October 13, 1995, as Compared to Their Initial Values.**

Material	Sample	M.C. % by vol.	pH unit	EC µmhos/cm	TDS mg/L	SO$_4$ mg/L	Cu mg/L	Fe mg/L	Ni mg/L
Oxidized Tailings	Initial	-	4.12	1878	1070	20951	< 0.03	7760	716
	0-5 cm	34.68	3.18	5370	9160	24623	< 0.02	12390	210
	15 cm	36.25	3.31	2390	3140	20522	< 0.02	12790	233
LSSS	Initial	31.61	12.20	2854	3760	5051	15.8	0.09	1.40
	0-5 cm	44.43	11.84	5560	5140	4998	34.9	10.4	3.62
	15 cm	46.24	10.91	5710	3300	2427	4.63	0.52	1.28
Desulph. Tailings (DST)	Initial	-	7.40	137	116	1135	0.04	0.07	< 0.10
	0-5 cm	50.19	3.43	1250	1160	17245	< 0.02	7913	62.4
	15 cm	47.46	3.55	1300	1280	17994	< 0.02	12620	43.6
Peat	Initial	157.87	7.19	354	600	222	0.07	0.51	< 0.10
	0-5 cm	22.25	4.42	3480	5040	2542	< 0.02	0.69	0.45
	15 cm	47.07	2.4	5330	6780	10951	0.35	1437	29.9
Compost	Initial	12.58	8.16	1426	1690	24.5	0.08	1.16	< 0.10
	0-5 cm	34.59	6.79	2980	3040	3758	0.11	3.02	0.06
	15 cm	37.09	5.83	3580	4480	2823	0.08	25.7	0.17
DST+CB	Initial	-	7.40	137	116	1135	0.04	0.07	< 0.10
	0-5 cm	47.74	5.66	819	700	8600	< 0.02	2013	46.7
	15 cm	46.20	3.83	1020	900	11208	< 0.02	5446	31.4

3.3   Pilot Test Cell Results

Of the eight pilot cells monitored, seven contained oxidized tailings and the various cover materials tested. The remaining cell contained pyrrhotite tailings with a compost cover. The cells are listed below showing their contents and their pilot cell reference number:

Pilot Cell Reference Number   Contents

          Cell #1   oxidized tailings (control)

          Cell #2   LSSS over oxidized tailings

Cell #3	desulphurized tailings (DST) over oxidized tailings
Cell #4	compost over oxidized tailings
Cell #5	peat over oxidized tailings
Cell #6	desulphurized tailings (DST) and capillary barrier (CB) over oxidized tailings
Cell #7	LSSS plus CB over oxidized tailings
Cell #8	compost over pyrrhotite tailings

Seven sets of monitoring and sampling points were installed in each cell. Ports 1 , 3, 5 and 7 were used to monitor Eh, temperature, and TDR; to sample gases for analysis of O_2, CO_2 and CH_4; and to extract pore water samples for chemical analysis (Figure 3). Ports 1 and 3 were located in the cover layer, Port 5 was in the cover layer but immediately above the interface, and Port 7 was located in the middle of the tailings layer.

3.3.1   Changes in Pore Water pH

The pore water pH in the oxidized tailings control cell fluctuated between 2.7 and 4.4 (Figure 17). The pore water pH of the oxidized tailings layer (i.e. Port 7) in the cells covered with desulphurized tailings with or without CB remained at 3.5. The pore water pH of the oxidized tailings layer in the cells covered with compost and peat increased slightly with time, from 2.9 to 4.0 and from 2.8 to 4.2, respectively. More noticeable pH increases were noted in the pore waters sampled from the oxidized tailings layer underlying the LSSS (Figure 17).

The pore water pH of the underlying oxidized tailings in the cell with LSSS cover without CB gradually increased from 2.8 to 6.1, and in the LSSS cell with a CB the pH increased from 2.7 to 5.9. The pore water pH of the pyrrhotite tailings underlying the compost exhibited a decreasing trend with time, from 7.9 to 6.7.

Figure 17.   Pore Water pH vs. Time at Different Sampling Ports
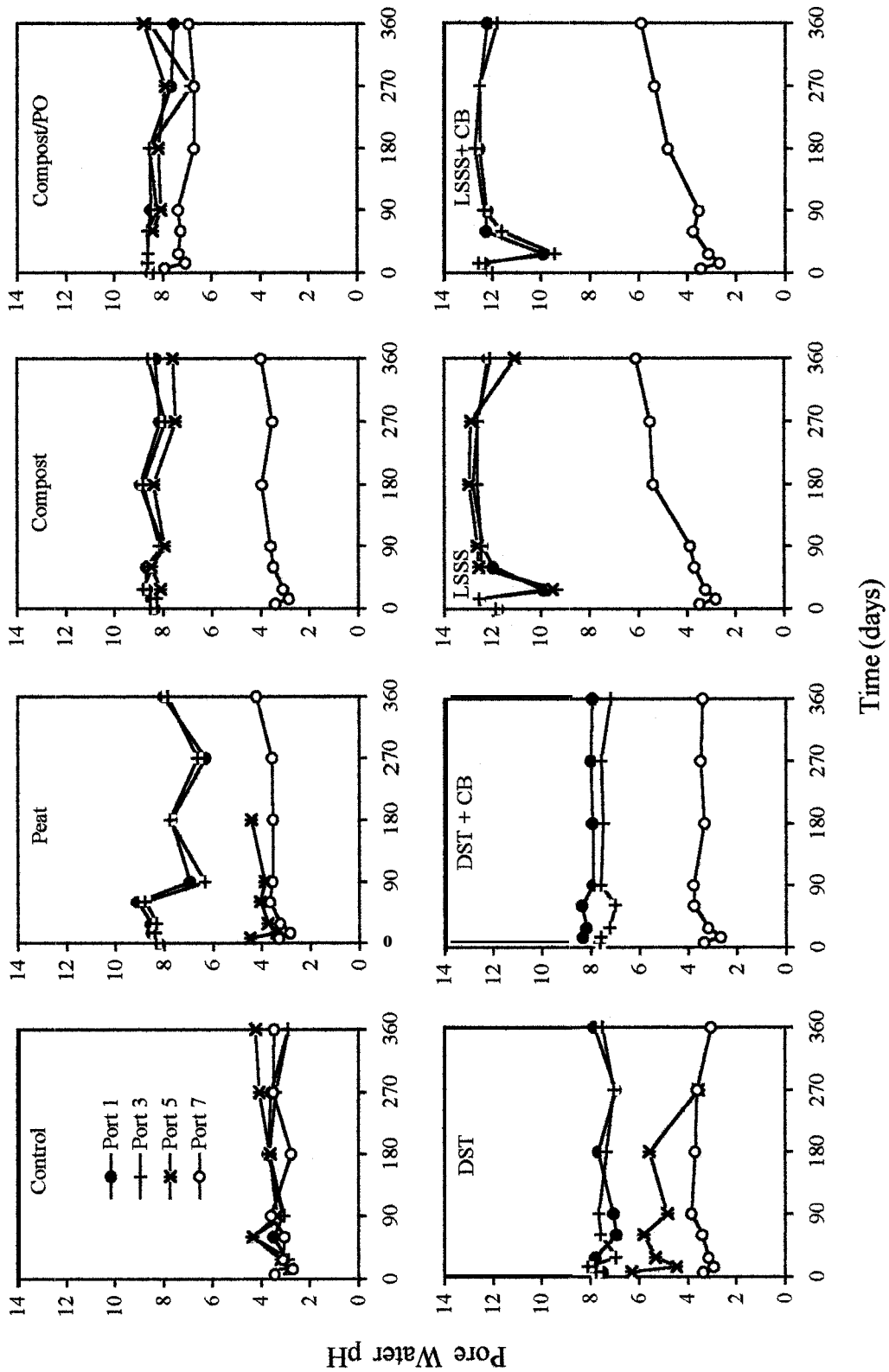
The pH of the water samples collected from the LSSS cover, compost cover and desulphurized tailings cover (ports 1 and 3) remained above 11, 8, and 7, respectively (Figure 17), while the pH of the water samples collected from the peat cover layer fluctuated between 6.3 to 9.1 at Port 1, and between 6.3 and 8.8 at Port 3. The low pH values at Port 5 in both peat and desulphurized tailings cover cells suggest that the water from the underlying oxidized tailings was drawn up during sampling. This may have occurred as Port 5 was located less than 5 cm above the interface between the covers and the oxidized tailings.

3.3.2 Changes in Pore Water Total Dissolved Iron Concentrations

The total dissolved Fe concentrations increased with time to reach the plateau at day 180, and then decreased towards the end of the test in the pore waters sampled from the oxidized tailings (Port 7) in the control cell and in the cells covered with peat, compost and desulphurized tailings, both with and without the CB (Figure 18). The total dissolved Fe concentrations of the pore waters sampled from Port 7 in the oxidized tailings increased from 19,325 to 33,750 mg/L and decreased to 26,700 mg/L in the control cell, increased from 15,015 to 28,313 mg/L and decreased to 14,600 mg/L in the peat cover cell, increased from 18,385 to 27,875 mg/L and decreased to 26,200 mg/L in the compost cover cell, increased from 11,245 to 48,750 mg/L and decreased to 42,700 mg/L at day 270 in the desulphurized tailings cover cell, and increased from 17,340 to 25,375 mg/L in the desulphurized tailings plus CB cover cell. In contrast, the total dissolved Fe concentrations of the oxidized tailings covered with the LSSS alone decreased with time from 17,540 to 1,300 mg/L, and with the LSSS plus CB decreased from 16,836 to 2,170 mg/L.

The high concentrations of dissolved Fe in Port 5 of the peat and desulphurized tailings suggest that the water from the underlying oxidized tailings was drawn up by sampling

process as Port 5 was located less than 5 cm above the interface between the covers and the

oxidized tailings.

Figure 18.   Pore Water Fe Concentrations vs. Time at Different Sampling Ports
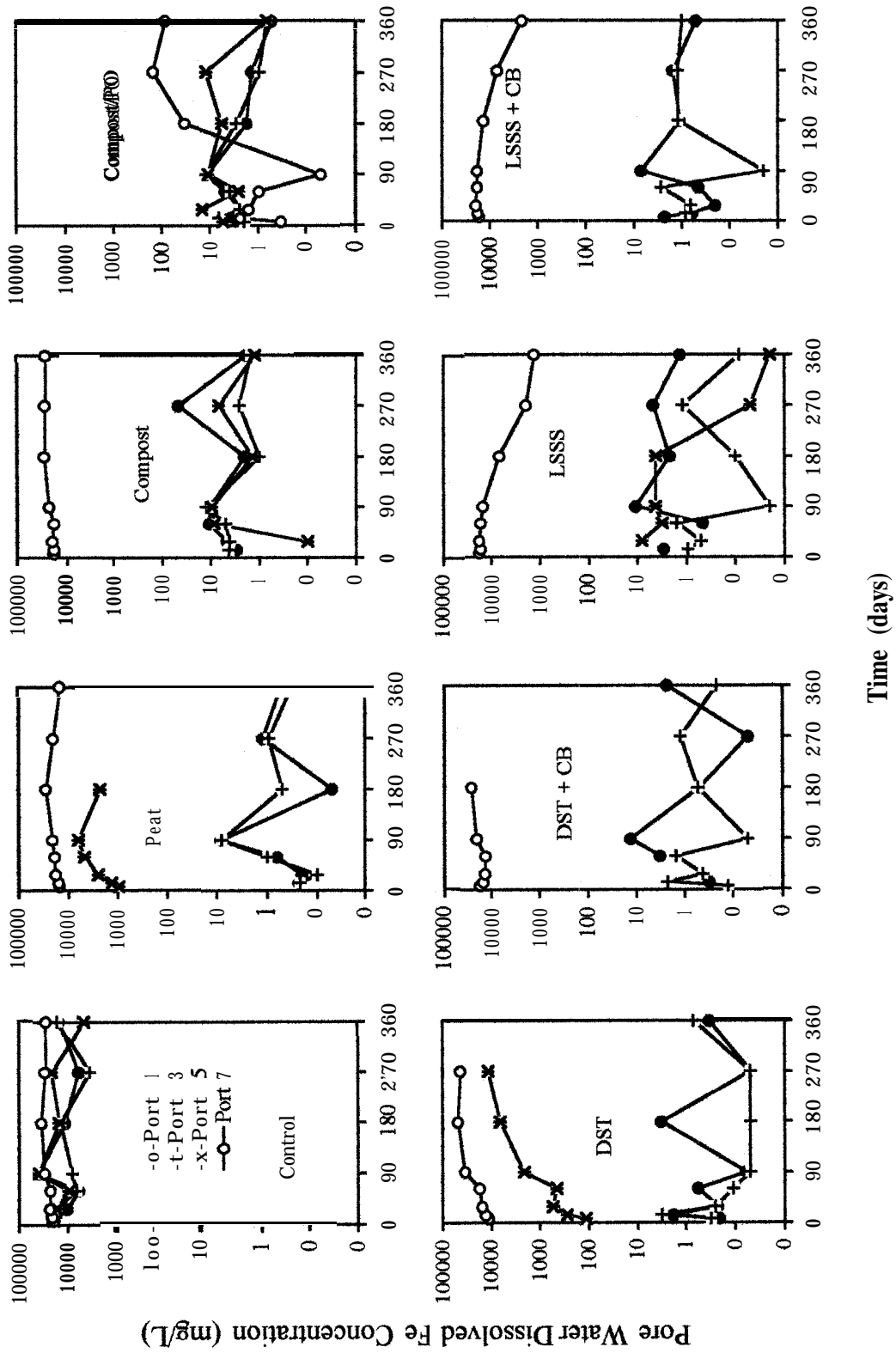
The total dissolved Fe concentrations of the pore water samples from the pyrrhotite tailings at Port 7 underlying the compost cover increased with time from 0.33 to 150 mg/L.

In the first 90 days of the pilot scale cell test, almost all the Fe present in the pore water samples from the oxidized tailings under cover materials was present as Fe^{2+}. Starting at 180 days, the Fe^{3+} concentrations increased to make up more than 50% of the total dissolved Fe concentrations.

3.3.3   Changes in Pore Water Dissolved Organic Carbon and Dissolved Inorganic Carbon Concentrations

From the start to day 270 of the test, the dissolved organic carbon (DOC) concentrations of the pore water samples from the oxidized tailings beneath the covers (Port 7) remained relatively constant at about 10 mg/L in the control cell and in the cells covered with peat, compost and desulphurized tailings (Figure 19). At day 365, slightly higher DOC concentrations at port 7 were noted in these cells. However, the DOC concentrations of the pore water samples from the oxidized tailings underlying the LSSS cover were observed to increase steadily with time from 10 to up to 5592 mg/L in the cell without the CB, and from 8 to 1991 mg/L in the cell with the CB.

The pore water DOC concentrations in all cover layers decreased with time (Figure 19). The DOC concentrations of the pore water sample in the peat cover decreased from 50 to about 20 mg/L at both ports 1 and 3. The DOC concentrations in the compost pore water samples decreased from 1,000 to 100 mg/L at Port 1, to 300 mg/L at Port 3, and to 400 mg/L at Port 5. The DOC concentrations of the pore water samples in the LSSS cover decreased from over 10,000 to 800 mg/L at Port 1 and to 3,500 mg/L at ports 3 and 5.

Figure 19.   Pore Water Dissolved Organic Carbon (Concentrations vs. Time at Different Sampling Ports.
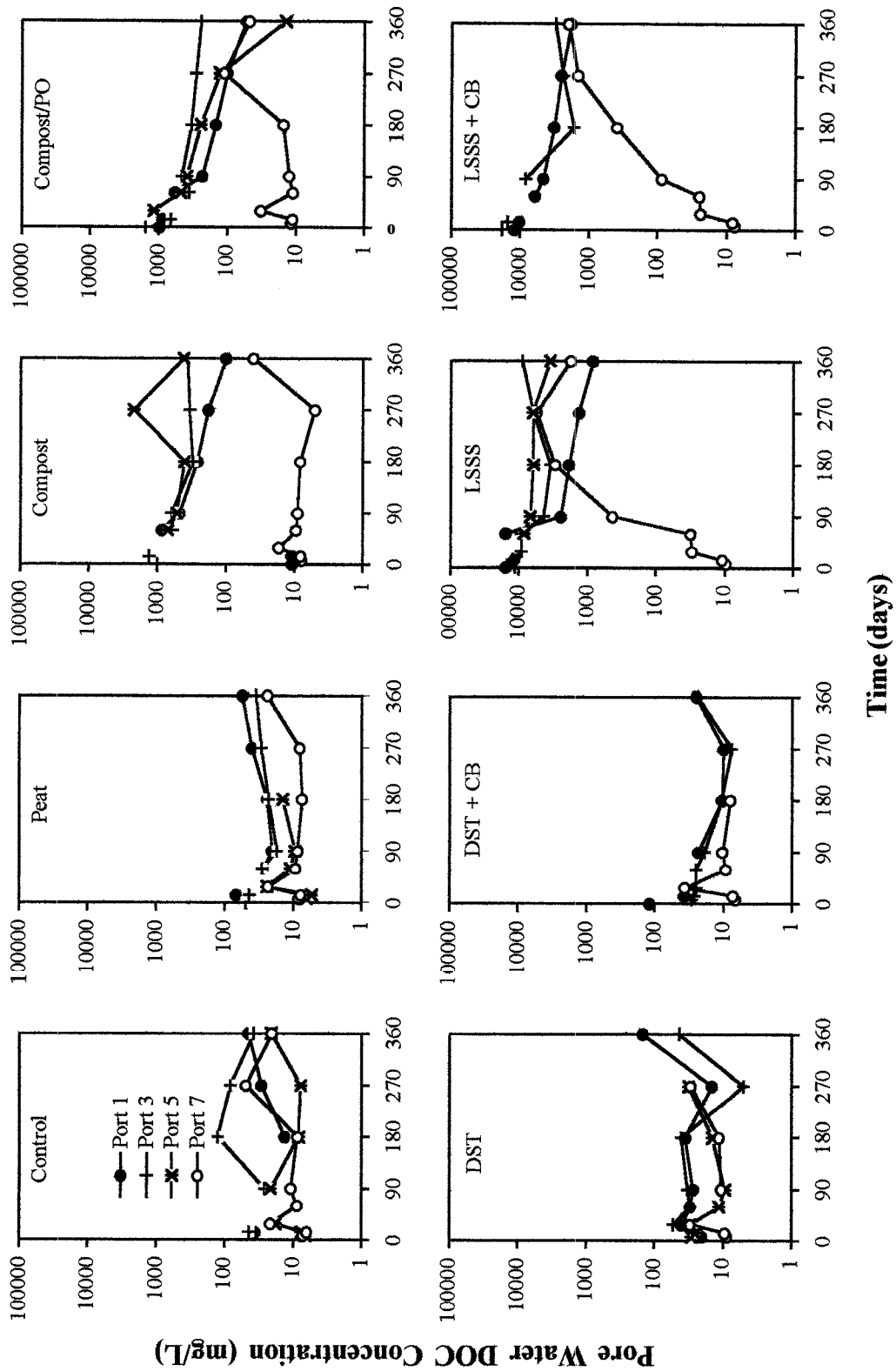
The DOC concentrations of the pore water samples collected from the pyrrhotite tailings under compost cover exhibited an increase at the last two sampling dates from an initial value of 11 at the beginning of the test to as high as 110 mg/L. DOC concentrations in water samples from the overlying compost decreased with time from 1,000 mg/L to 50 mg/L at Port 1, from 1,000 mg/L to 230 mg/L at Port 3, and to 240 mg/L at Port 5. The dissolved inorganic carbon (DIC) concentrations of the pore water samples from the oxidized tailings were generally low (<10 mg/L) in the control cell and in the cells covered with desulphurized tailings, peat and compost (Figure 20). However, the DIC concentrations of the pore water samples from the oxidized tailings underlying the LSSS increased from an initial concentration of < 1 mg/L to 6000 mg/L without the CB. The DIC concentrations in the pore water sample of oxidized tailings under LSSS with CB remained relatively unchanged (<1 mg/L). The increase in pore water DIC concentrations appeared to be related to the high DIC concentrations in the overlying LSSS. The DIC concentrations of the samples collected from the compost were high (up to 1150 mg/L). A high concentration of DIC was also noted in the underlying pyrrhotite tailings (545 mg/L), but not in the underlying oxidized tailings (0 mg/L).

3.3.4 Changes in Pore Water Sulphate and Total Sulphur Concentrations

The pore water sulphate (SO_4) concentrations in all the cells increased with depth. In general, low SO_4 concentrations were noted at Port 1 and high SO_4 concentrations were recorded at Port 7 in all cells (Figure 21).

There was an increasing trend over time in the SO_4 concentrations of the pore water samples from the oxidized tailings (Port 7) in the control cell and in the cells covered with peat, compost and desulphurized tailings (Figure 21). The SO_4 concentrations of the pore waters at Port 7 in the control cell increased over the first 6 months monitoring period from 35,000 to 60,000 mg/L and remained at 48,000 mg/L over the second six months. The SO_4 concentrations of the pore waters at Port 7 in the peat cover cell increased over the first 6 months monitoring period from 35,000 to 60,000 mg/L and decreased to 25,000 mg/L

Figure 20. Pore Water Dissolved Inorganic Carbon Concentrations vs. Time at Different Sampling Ports
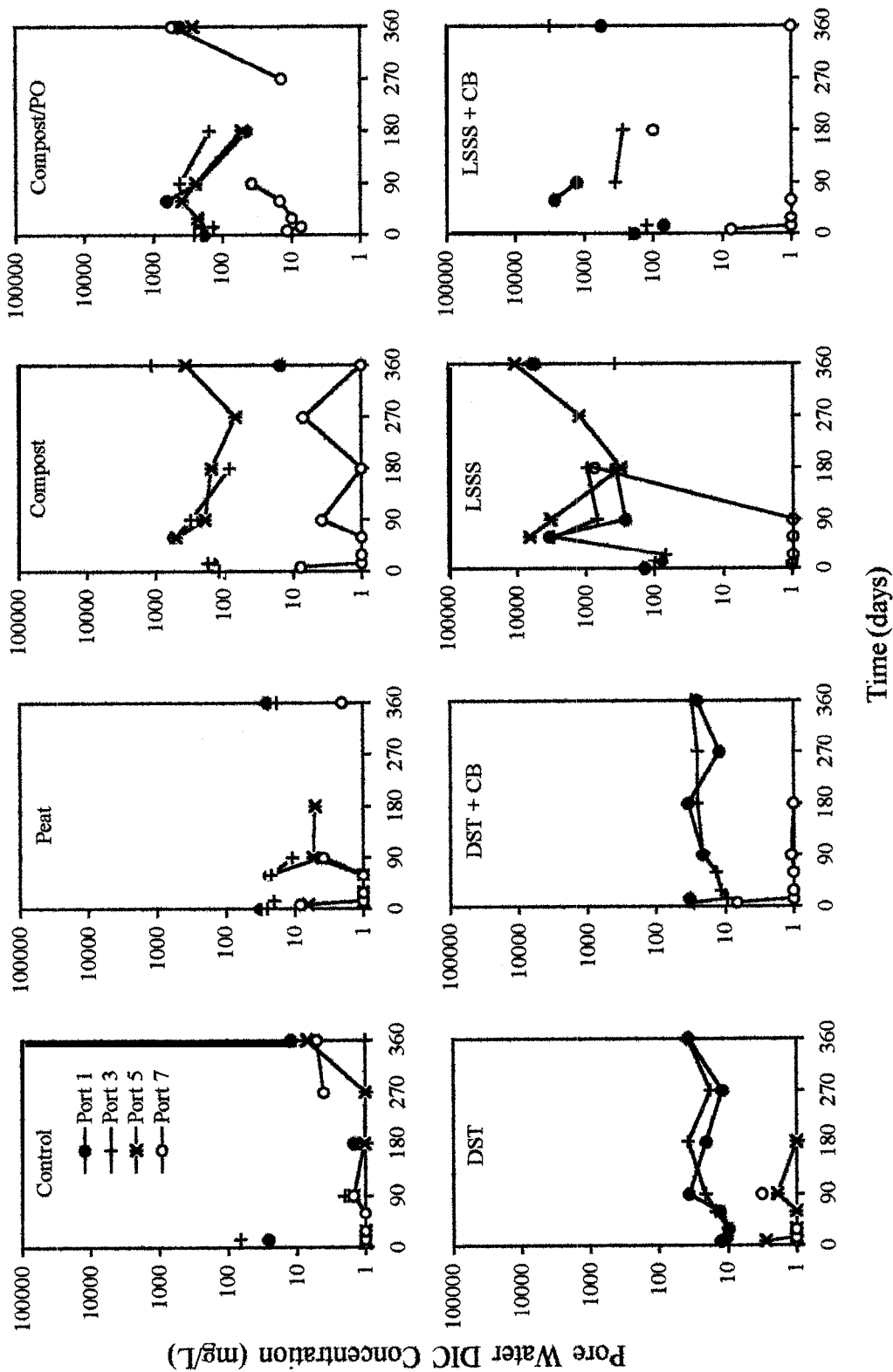
Figure 21. Pore Water SO₄ Concentrations vs. Time at Different Sampling Ports
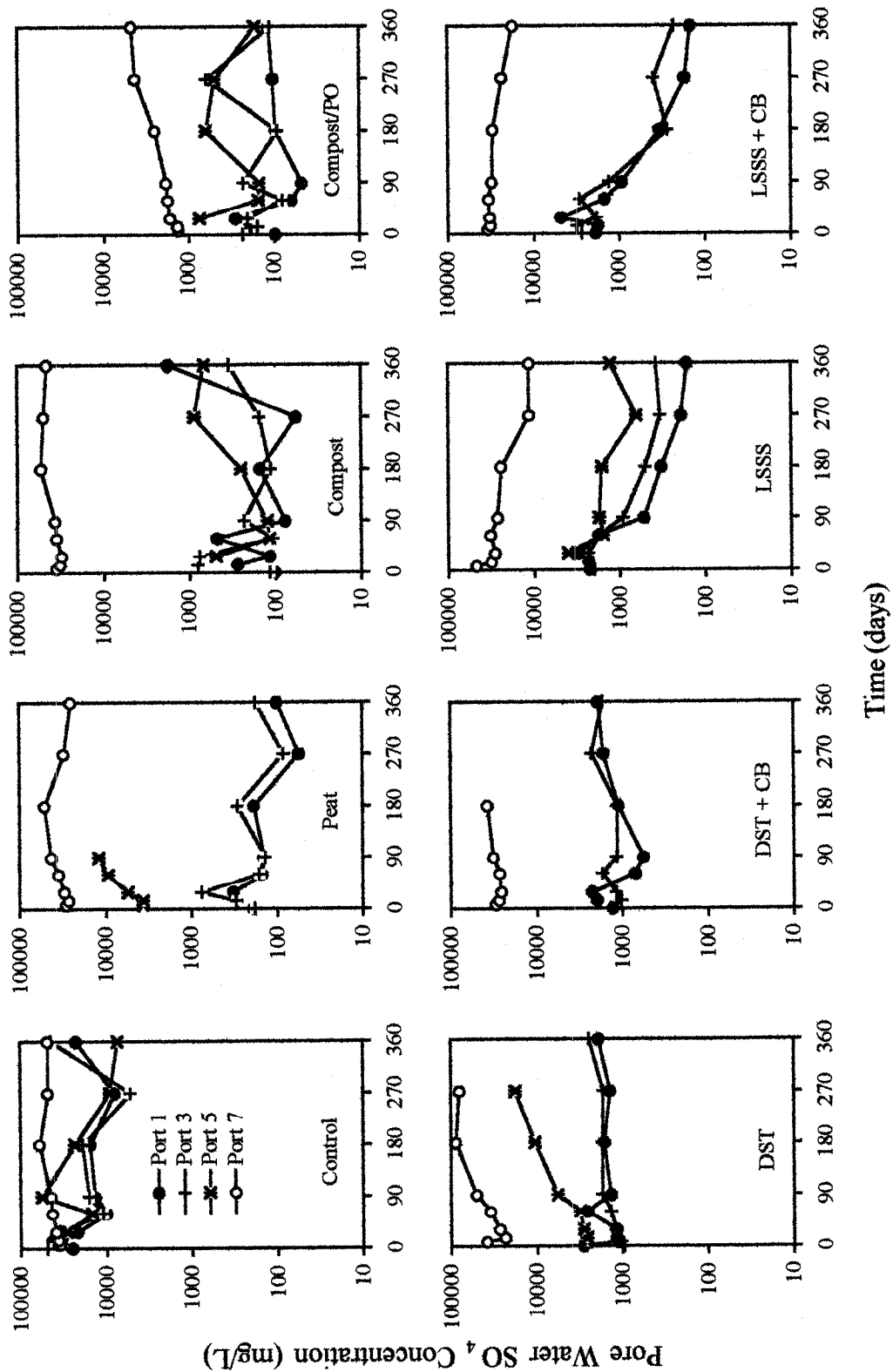
towards the end of the test period. The SO_4 concentrations of the pore waters at Port 7 in the compost cover cell increased over the first 6 months monitoring period from 35,000 to 54,000 mg/L and decreased to 46,000 mg/L towards the end of the test period. In the DST cover cells, the SO_4 concentrations of the pore waters at Port 7 increased from 38,000 to 88,000 mg/L in the cell without CB and from 30,000 to 37,000 mg/L in the cell with CB.

In contrast, the SO_4 concentrations in the pore water samples from the oxidized tailings at Port 7 in the LSSS cover cells decreased with time from 47,000 to 11,000 mg/L in the cell without a CB, and from 34,000 to 17,500 mg/L in the cell with a CB (Figure 21). The SO_4 concentrations of the pore water samples collected from the pyrrhotite tailings under the compost cover increased with time from 1,300 to 4,700 mg/L (Figure 21).

The SO_4 concentrations of the pore water samples collected from the cover layers (ports 1, 3 and 5) exhibited an increasing trend with time in the desulphurized tailings cells (with and without CB) and in the compost cover cell. A decreasing trend was noted in the LSSS cells (with and without CB), and no major trends were noted in the cell where the pyrrhotite tailings were covered by compost (Figure 21). The high SO_4 concentrations observed at Port 5 in both the peat and the desulphurized tailings cover layers were very likely due to the extraction of water from the underlying oxidized tailings layer because the Port 5 was located less than 5 cm above the interface between the cover and the oxidized tailings.

The total S concentrations of the pore waters sampled from all the cells are presented in Figure 22. Because the majority of the total S was present as SO_4, the pore water total S concentrations followed the same pattern as the pore water SO_4 concentrations. This is evident based on the similarity between the Figures 21 and 22.

Figure 22. Pore Water Total S Concentrations vs. Time at Different Sampling Ports

Lakefield Research Limited
Environmental Services
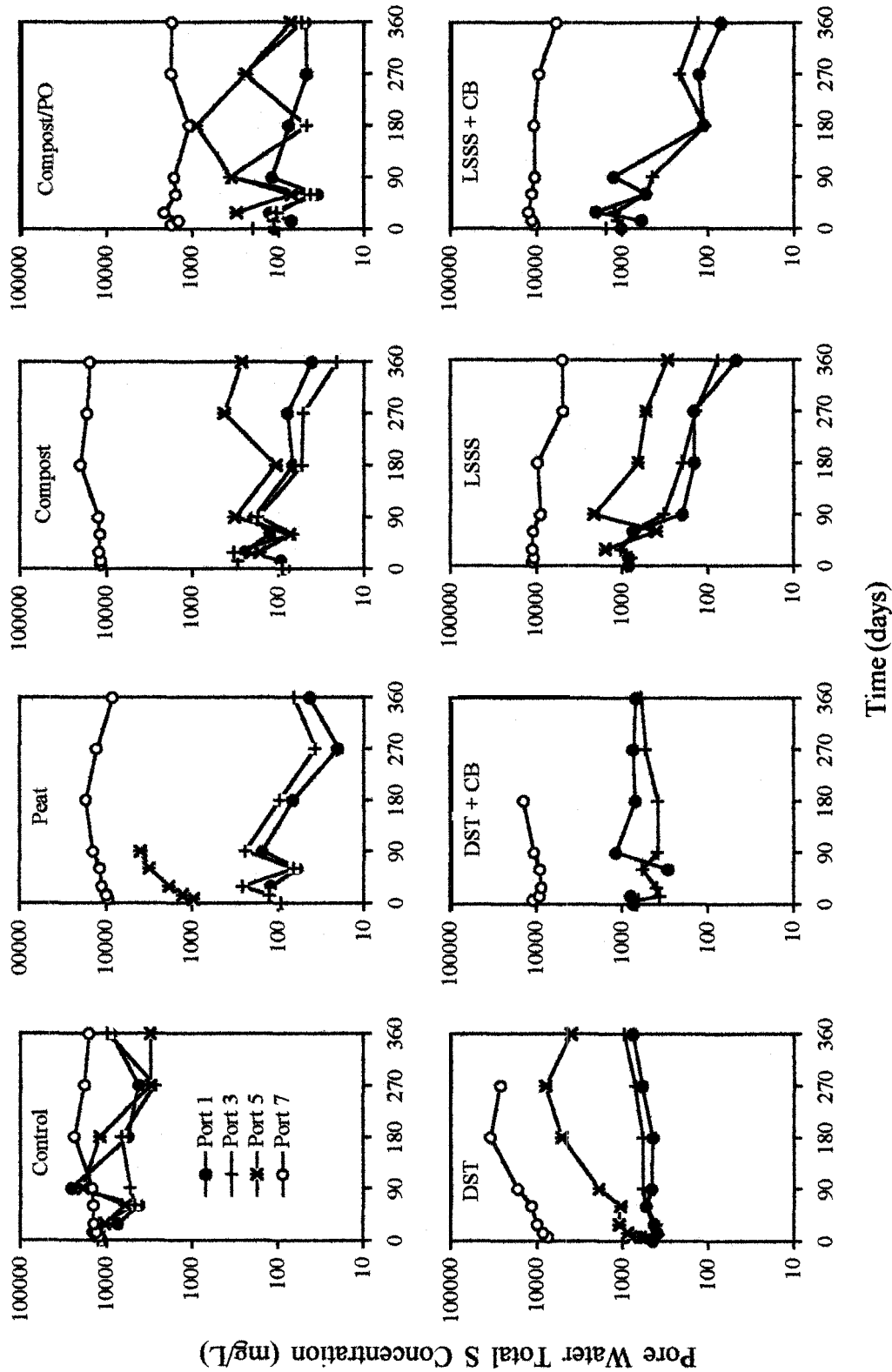
3.3.5 Changes in Pore Water Nickel Concentrations

High Ni concentrations in the pore waters were noted in the control cell (Figure 23). The Ni concentrations of the pore waters at Port 7 in the control cell increased with time from less than the detection limit at the beginning of the test to 32 mg/L after 180 days, and then decreased to 1.1 mg/L. The Ni concentrations in the pore waters sampled from the oxidized tailings under the desulphurized tailings cover (Port 7) exhibited a decreasing trend with time from a high of 230 mg/L to 1.3 mg/L without the CB, and from a high of 66 mg/L to 0.7 mg/L with the CB (Figure 23). The Ni concentrations in the pore water samples from the peat cover cell and compost cover cell were generally low (<0.30 mg/L) or below the detection limit (<0.05 mg/L).

The Ni concentrations in the pore water samples from the LSSS cover cell showed a decreasing trend with time both in the cover layer and in the underlying oxidized tailings layer. In the LSSS cell without a CB, the Ni concentrations of the water samples decreased from 3.0 to <0.05 mg/L at port 1, from 2.5 to 0.62 mg/L at port 3, from 11 mg/L to 1.7 mg/L at Port 5, and from 4 to <0.05 mg/L in the underlying oxidized tailings at Port 7. In the LSSS plus CB cover cell, the Ni concentrations of the water samples decreased from 2.3 to 0.60 mg/L at Port 1, from 3.6 to 1.2 mg/L at Port 3 and from 0.62 to <0.05 mg/L at Port 7.

3.3.6 Changes in Pore Water Copper concentrations

The Cu concentrations in the pore water samples from all the cells, except the LSSS cover cell, were very low (< 0.57 mg/L). This low concentration was especially noticeable at Port 7 where the pore water Cu concentrations sampled from the underlying oxidized tailings or the pyrrhotite tailings were consistently less than 0.02 mg/L (Figure 24). The Cu concentrations in the pore water samples from the LSSS cover layer decreased with time (Figure 24). In the LSSS cell without the CB, the Cu concentrations in the pore water samples decreased from 49 to 1.5 mg/L at Port 1, from 36 to 10.7 mg/L at port 3, and from 125 to 5 mg/L at Port 5. In

Figure 23.   Pore Water Ni Concentrations vs. Time at Different Sampling Ports
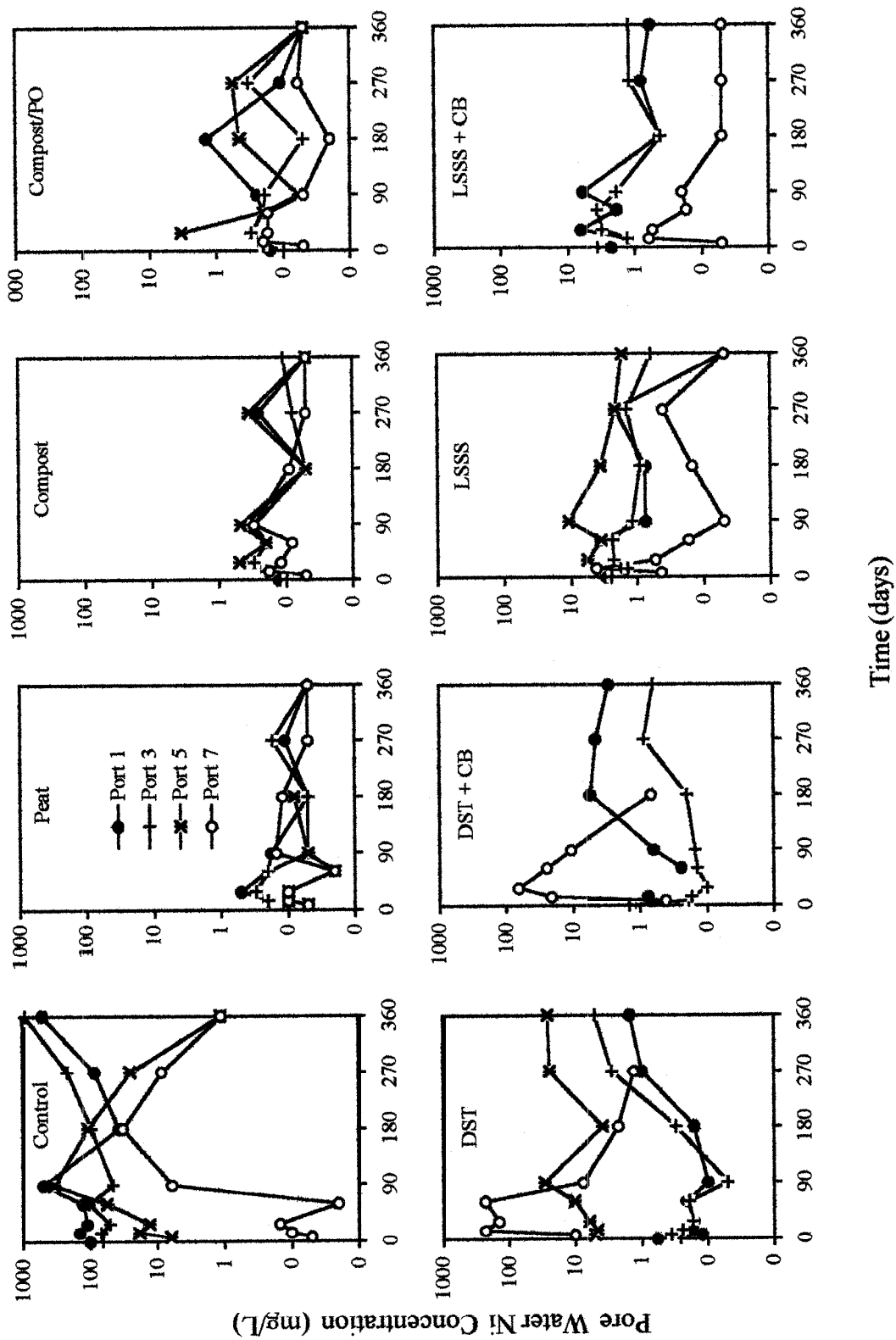
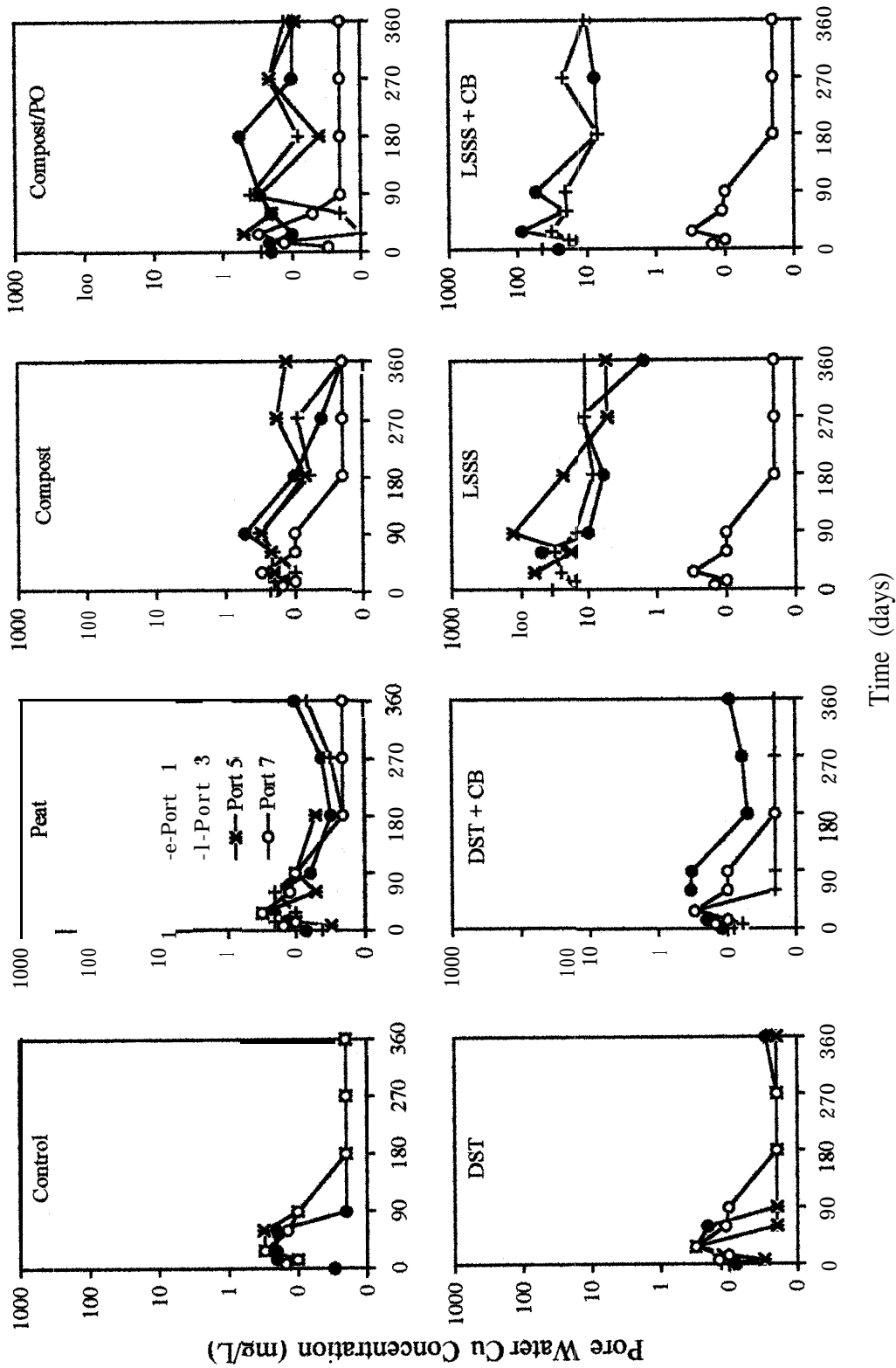**Figure 24.   Pore Water Cu Concentrations vs. Time at Different Sampling Ports**

the cell with the CB, the Cu concentrations decreased from 88 to 10.2 mg/L at Port 1, and from 44 to 1.08 mg/L at Port 3. Although the high Cu concentrations were present in the LSSS cover layer, the Cu concentrations in the pore water samples of the underlying oxidized tailings were present below the method detection limit (<0.02 mg/L). This suggests that the underlying oxidized tailings have acted as a scavenger for Cu.

3.3.7   Changes in Pore Water Lead Concentrations

Figure 25 shows the pore water Pb concentrations only in the control cell and in the oxidized tailings layer (Port 7) under various cover materials. Because the pore water Pb concentrations in all the cover layers were below the detection limit of 0.10 mg/L. The Pb in the pore water samples collected from Port 7 was not detected at concentrations above the method detection limit in the pyrrhotite tailings underlying the compost cover.

The Pb concentrations in the pore water samples from the oxidized tailings (Port 7) in all the cells but the LSSS cover cells increased with time until day 180 and then decreased until the end of the test. The Pb concentrations at Port 7 increased from 1.3 to 4.8 mg/L and then decreased to 2.03 mg/L in the control cell, increased from 1.2 to 4.1 mg/L and then decreased to 0.94 mg/L in the peat cover cell, increased from 1.0 to 3.4 mg/L and then decreased to 1.92 mg/L in the compost cover cell, increased from 0.9 to 5.6 mg/L in the desulphurized tailings cover cell, and from 1.1 to 3.5 mg/L in the desulphurized tailings plus CB cover cell. The Pb concentrations in the pore water samples from Port 7 in the LSSS cover cell were observed to decrease continuously with time from 2.0 to <0.10 mg/L in the cell without CB and from 2.3 to 0.25 mg/L in the cell with CB. Since all of the cover materials showed undetectable Pb concentrations in the pore waters sampled, this increase in Pb concentration in the underlying tailings at Port 7 was not directly related to the overlying cover materials.

Figure 25. Pore Water Pb Concentrations in the Oxidized Tailings Under Various Cover Materials
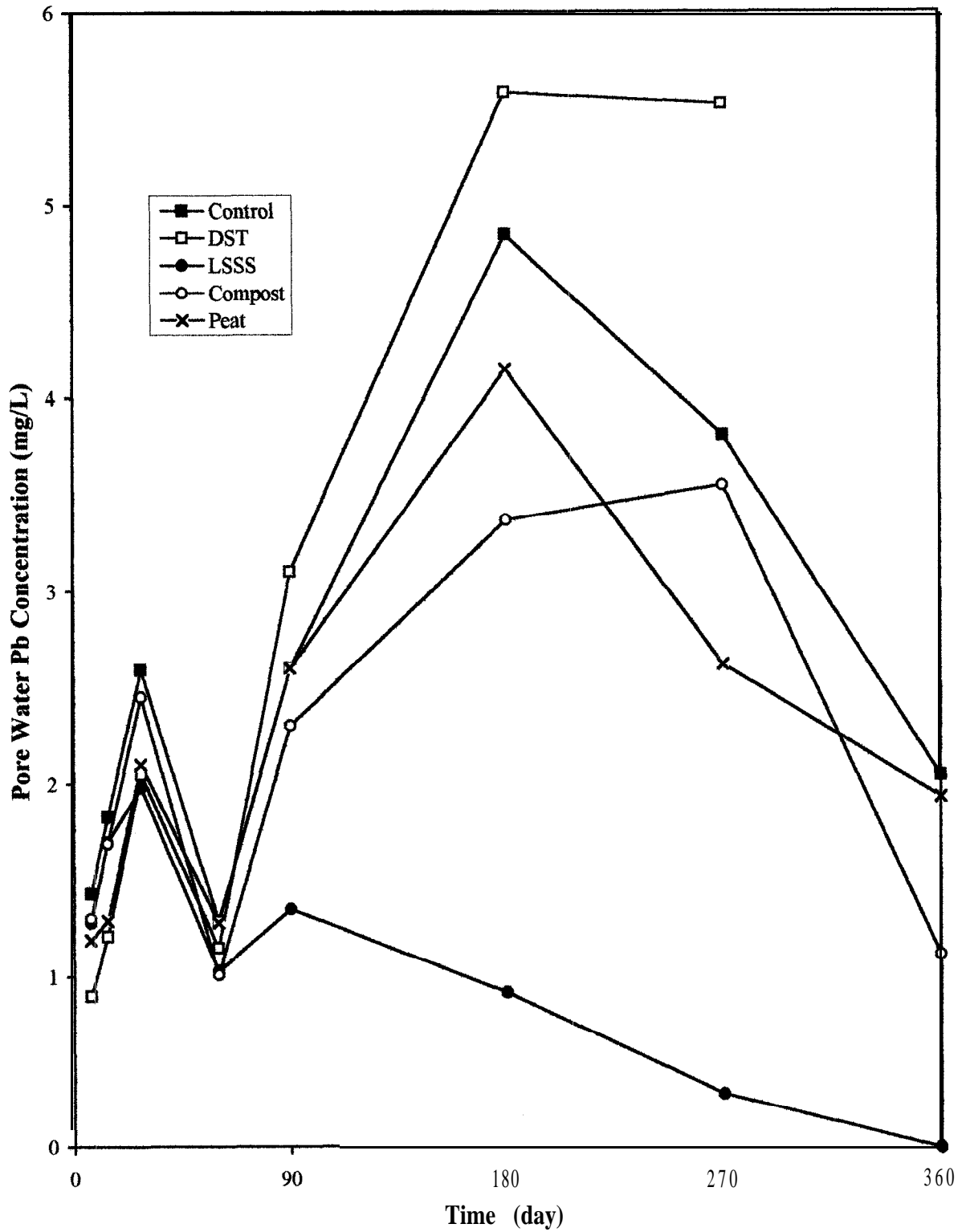
3.3.8 Changes in Pore Water Nitrate Concentrations

High nitrate (NO_3) concentrations, up to 735 mg N/L, were noted in the pore water samples from the compost cover layer and from the peat cover layer (Figure 26). However, the NO_3 concentrations in the underlying oxidized tailings or pyrrhotite tailings were consistently less than 1 mg N/L. This suggests that any NO_3 leached from the cover layers may have been reduced to nitrogen gas in the tailings layer through denitrification processes. The NO_3 concentrations in the pore water samples from the LSSS cover layer were generally below 10 mg N/L.

3.3.9 Changes in Pore Water Total Phosphorous Concentrations

The total phosphorus (P) concentrations of the pore water samples collected from the control cell, the peat cover cell and two desulphurized tailings cover cells, were generally less than 1 mg/L (Figure 27). The total P concentrations of the pore water samples collected from the compost cover layers fluctuated between 1.4 and 28 mg/L. The total P concentrations of the pore water samples in both the underlying oxidized tailings and the pyrrhotite tailings were less than 0.6 mg/L.

The total P concentrations of the water samples from the LSSS cover layers exhibited a decreasing trend with time (Figure 27). In the LSSS cover cell without the CB, the pore water total P concentrations decreased from 64 to 0.36 mg/L at Port 1, from 16 to 1.45 mg/L at Port 3, and from 32 to 4.4 mg/L at Port 5 over the one year monitoring period. In the LSSS cell with the CB, the pore water total P concentrations decreased from 22 to 1.35 mg/L at port 1 and from 9.6 to 3.36 mg/L at Port 3. The pore water total P concentrations in the underlying oxidized tailings were observed to increase from 0.4 to 5.28 mg/L in the LSSS cell and from 0.4 to 2.0 mg/L in the LSSS plus CB cell.
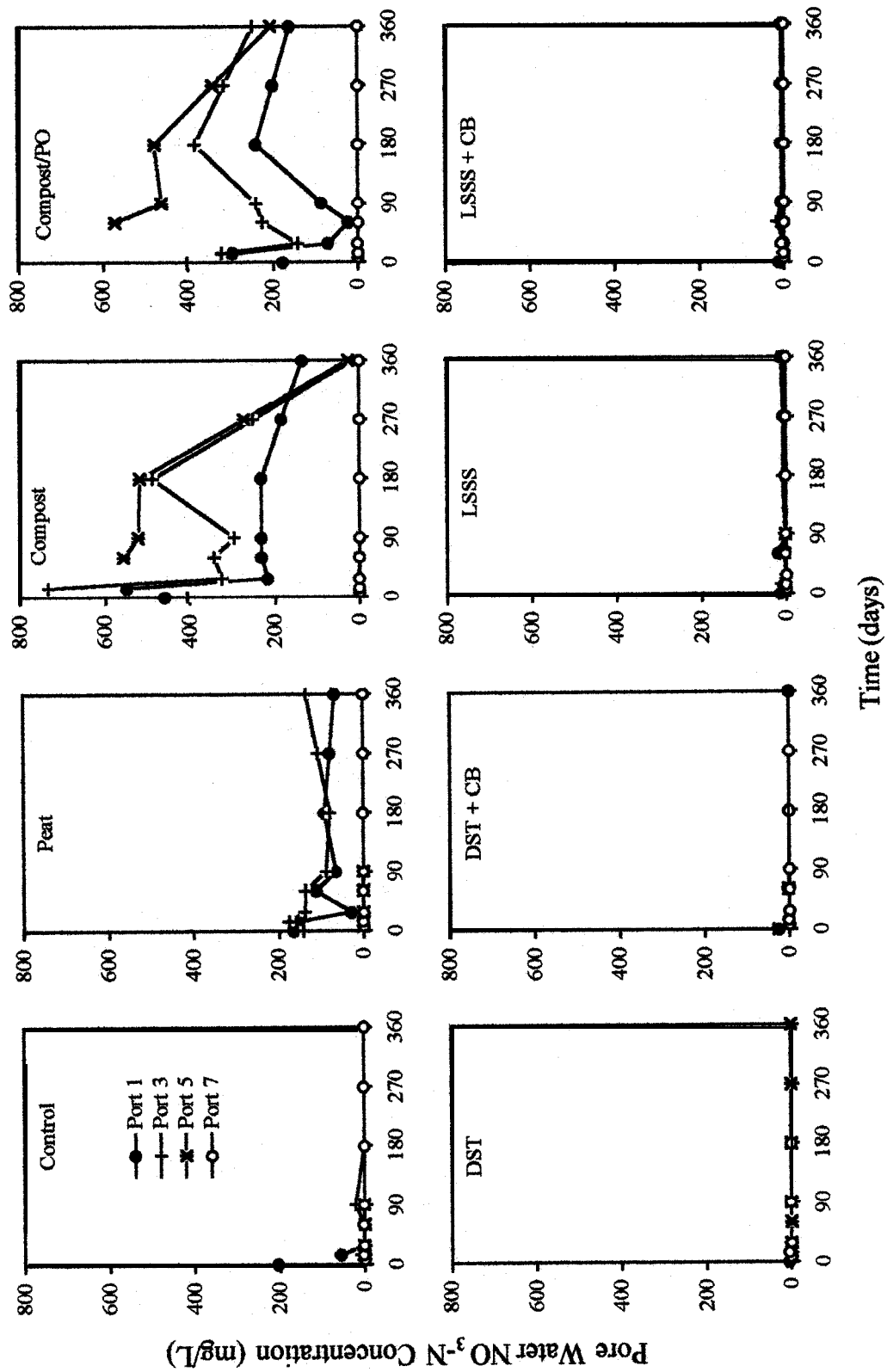
Figure 27.   Pore Water Total P Concentrations vs. Time at Different Sampling Ports
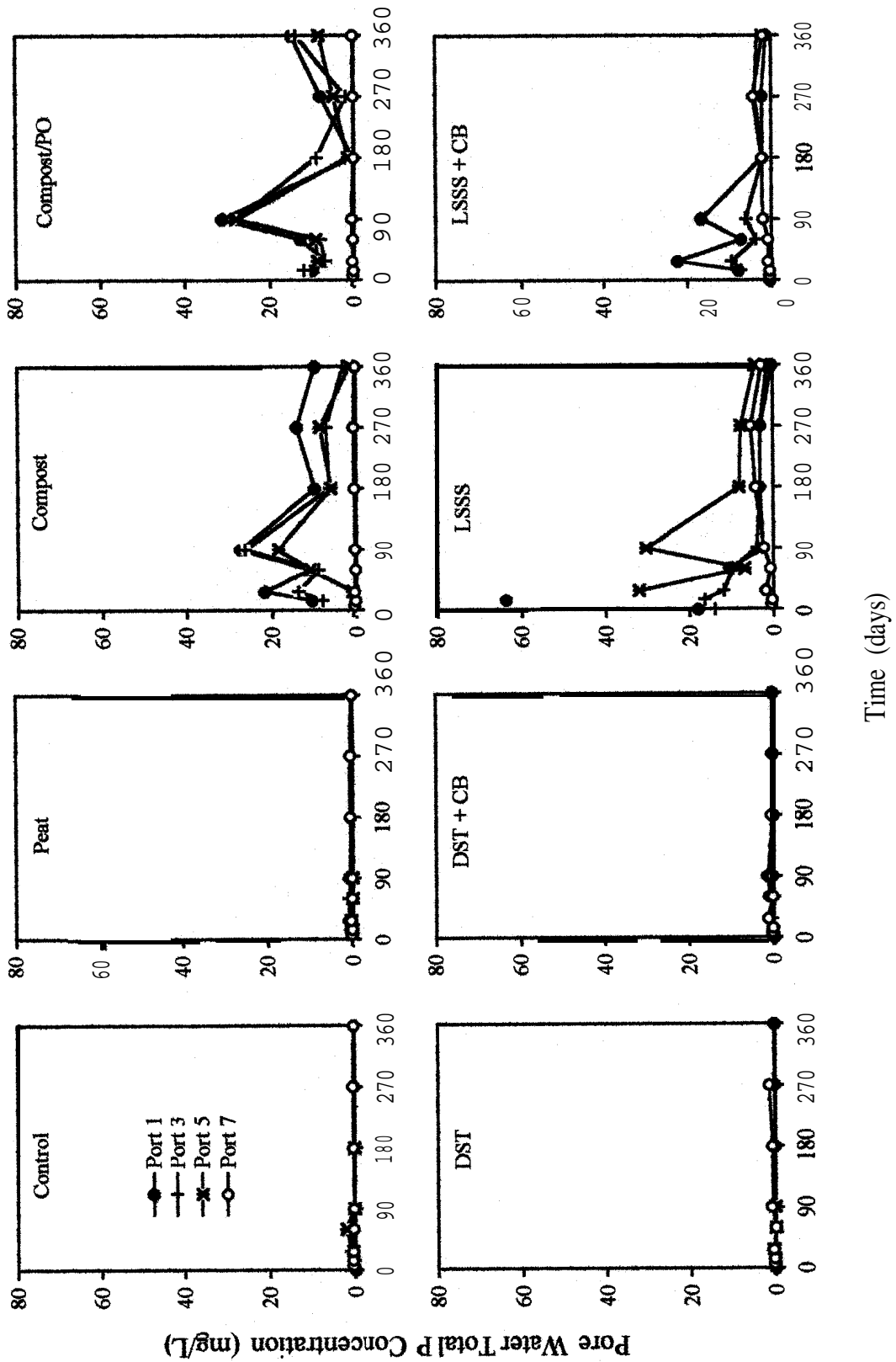
3.3.10 Oxygen Gas Concentration Profile in the Pilot Cells

Figure 28 shows the oxygen (O_2) concentration profiles in the eight pilot cells. The O_2 concentrations were measured on September 26, and November 10, 1995, and January 26, and March 25, 1996. Generally, similar O_2 concentration profiles were noted on these four sampling dates. In most cells no O_2 concentration measurements were recorded for the tailings layers because no gas sample was available due to the high moisture content.

In the control cell, a sharp decrease in the O_2 concentrations was observed between the surface (21%) and 15 cm below the oxidized tailings surface (7.6%). The O_2 concentrations further decreased to a low of 0.2% at 75 cm below the oxidized tailings surface. The steep O_2 gradient existing in the oxidized tailings was produced by either a low O_2 diffusion or a high O_2 consumption due to oxidation of sulphidic minerals present in the oxidized tailings.

In the peat cover cell, the O_2 concentrations decreased slightly from 21% at the surface to >13% at the interface. The O_2 concentration in the tailings immediately below the cover was recorded at >10%. These results suggest that the peat allows O_2 to diffuse from the surface to the tailings. The small change in O_2 with depth (low oxygen gradient) indicates a low resistance to O_2 diffusion in peat (high effective diffusion coefficient).

In the compost cover cells, the O_2 concentrations decreased linearly with cover depth (Figure 28). With compost over the oxidized tailings, the O_2 concentrations were observed to decrease from 21 % at the surface of compost to <5% at the 75 cm depth. In the cell with the compost overlying the pyrrhotite tailings, the O_2 concentrations decreased from 21% at the surface to 4% at the 75 cm depth. At the final sampling date, the O_2 concentrations in the cover layer were higher than at the previous three sampling dates. The O_2 concentrations in the compost cover layer also exhibited a decreasing trend with time. These results show that the compost is better than peat in reducing the O_2 diffusion (or flux) from the surface to the tailings and that the compost may be consuming some of the O_2 for ongoing organic decomposition processes.

Figure 28. O₂ Concentrations vs. Depth for Different Cover Materials
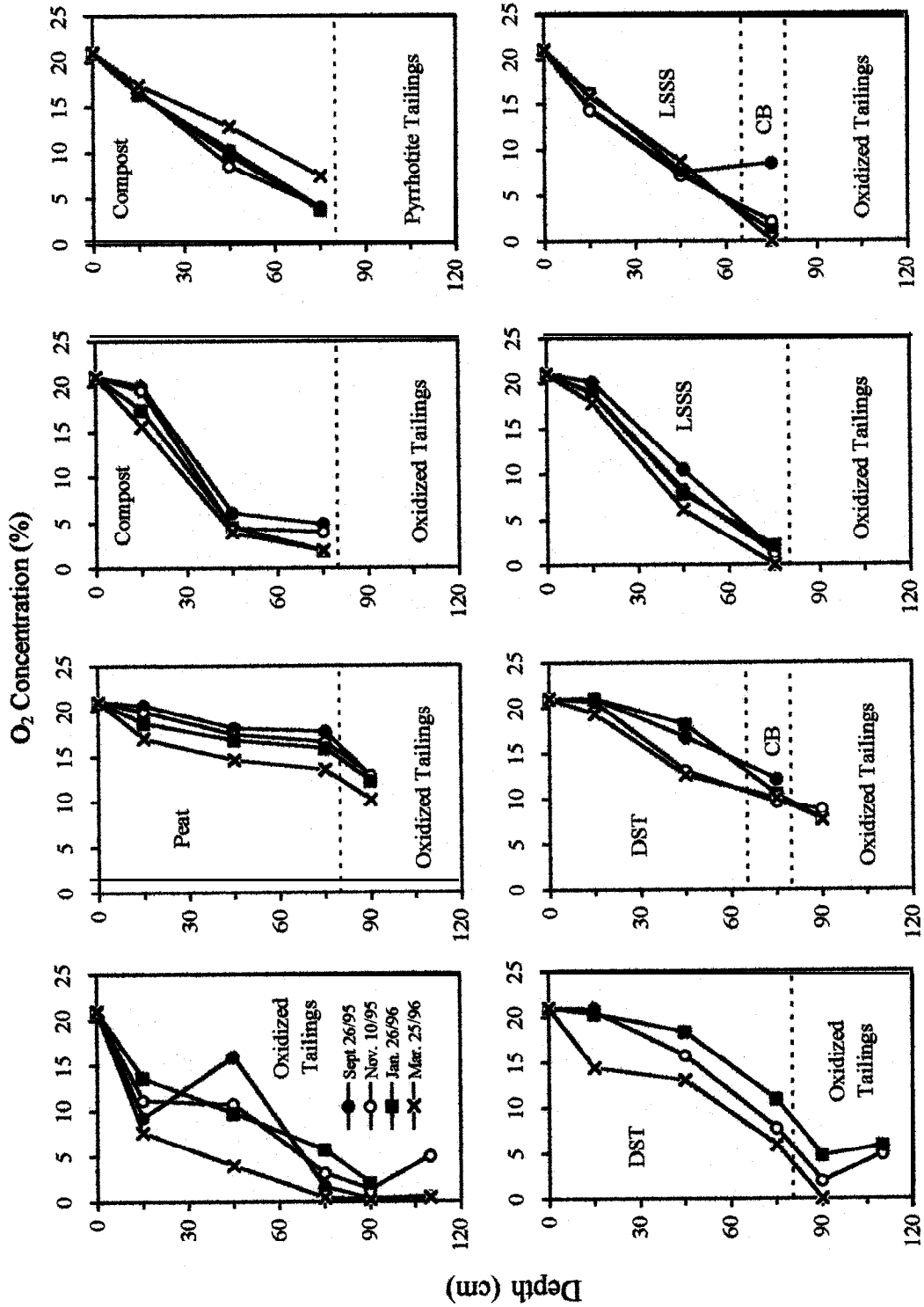
In the desulphurized tailings cover cells, the O_2 concentrations were the same at the surface as at 15 cm below the surface (Figure 28). Without the CB, the O_2 concentrations in the desulphurized tailings cover decreased from 21% at the surface to 6% at the 75 cm depth. A further decrease to <1.9% was recorded in the underlying oxidized tailings layer beneath the desulphurized tailings without the CB. With the CB, the O_2 concentrations in the desulphurized tailings cover decreased from 21% at the surface to 10% at the 75 cm depth, and an O_2 concentration of >8% was recorded in the oxidized tailings under the CB. This suggests that the use of the CB results in increases in the O_2 concentrations in the underlying oxidized tailings. This may be a result of O_2 influx along the CB from the open end of the cells.

In the LSSS cover cells, the O_2 concentrations decreased from 21% at the surface to <1.5% at the 75 cm depth. This indicates that the LSSS is better than the other covers tested for decreasing the flux of O_2 to the tailings surface. The use of the CB resulted in an initial increase in the O_2 concentration to 8.6% at port 5, which was located in the capillary barrier, from 7.6% at port 3. This indicates that the CB may be allowing O_2 to diffuse laterally into the tailings from the drainage end of the pilot cells where it is exposed to the atmosphere. However, the O_2 concentrations at port 5 decreased with time from 8.6% to 0% at the end of the test, a result similar to LSSS cover without CB. The blackening of the CB under the LSSS was evident during O_2 measurement, suggesting the existence of an anoxic environment within the CB.

On March 25, 1996, carbon dioxide (CO_2) and methane (CH_4) were simultaneously measured with O_2 using a GeoGroup GA-90 Methane-O_2-CO_2 Analyzer and the concentrations are presented in Table 18.

Lakefield Research Limited
Environmental Services

Table 18.   Carbon Dioxide and Methane Concentrations Measured in Pilot Scale Test Cells on March 25, 1996

Cell	Material	Port	CO_2 (%)	CH_4 (%)
1	Control	1	0	0
		3	0	0
		5	0	0
		6	0	0
		7	0	0
2	LSSS	1	0	0
		3	0	0
		5	0	0
3	DST	1	0.5	0
		3	2.6	0
		5	9.2	0
		6	6.4	0
4	Compost	1	5.2	0
		3	19.1	0
		5	22.7	0
5	Peat	1	3.2	0
		3	6.1	0
		5	7.2	0
		6	4.3	0
6	DST+CB	1	0	0
		3	1.2	0
		5	0.4	0
		6	0.2	0
7	LSSS+CB	1	0	0
		3	0	0
		5	21.8	0.1
8	Compost/ Pyrrhotite Tailings	1	3.4	0
		3	8.9	0
		5	15.5	0

Higher CO_2 concentrations were detected in the compost cover layer than in the peat cover layer, suggesting higher decomposition rate for compost than for peat. Higher CO_2 concentrations were observed at the bottom cover layer of the compost and peat, indicating that the CO_2 produced from the decomposition is not released into the atmosphere, but occupies the pore space.

Virtually no CO_2 was detected in the LSSS cover layer. Any CO_2 evolved from the decomposition of LSSS may have been readsorbed by the lime in the LSSS due to high pH (>11) as suggested previously in the incubation test. This does not mean that the decomposition of the LSSS is not occurring. A high CO_2 concentration (21.8%) and a trace amount of CH_4 (0.1%) were detected in the capillary break under the LSSS. The storage of CO_2, CH_4 and possibly H_2S, a product of sulphate reduction, in the CB prevents the influx of O_2 from the drainage end of the pilot cell, thereby maintaining a reducing environment.

3.3.11 Moisture Content and Degree of Saturation in the Cells

The TDR was used to measure the moisture contents in the pilot cells and the moisture contents were expressed as % dry weight (weight of water/weight of dry solid). A calibration box was constructed at the beginning of the test program and used to provide a calibration curve for the TDR readings collected over varying moisture contents. In-situ core sampling of the pilot cells was conducted on November 17, 1995 and April 11, 1996, to provide data for the calculation of the gravimetric and volumetric moisture contents, and to relate the in-situ moisture content measurements to the TDR moisture contents.

For both the oxidized tailings and the LSSS cells, the TDR moisture content measurements did not correlate well with the in-situ moisture content measurements. This is believed to be due to the highly conductive nature of these materials. However, a very good correlation was found to exist between the TDR moisture content measurements and the in-situ volumetric moisture content measurements for peat, compost and the desulphurized tailings. Therefore,

the TDR moisture content measurements have been corrected through the application of this calibration/correction factor and is expressed as % volumetric moisture content.

Figure 29 shows the changes of the volumetric moisture content in the cover layers of the peat, compost and desulphurized tailings over time. The volumetric moisture contents remained at above 50% for peat and compost and at 40% for desulphurized tailings. The volumetric moisture contents were higher at the deeper cover layer (port 5) than at the shallower cover layer (ports 1 and 3). Towards the end of one year testing, the volumetric moisture contents increased at port 5 for the peat, compost and desulphurized tailings (Figure 29). The volumetric moisture contents at ports 1 and 3 remained relatively constant over the entire testing period for peat, compost and desulphurized tailings over the oxidized tailings. The volumetric moisture contents at port 1 decreased with time for the compost covering the pyrrhotite tailings.

A vacuum system was installed in the cells to remove excess water and assist in consolidation of the tailings. The vacuum was started on March 31, 1995 and shut off 112 days after the pilot test began. It appears from the results shown in Figure 29 that the operation of the vacuum system had a slight influence on the moisture content of the cover materials at port 5 but not at ports 1 and 3. The decrease in moisture content of compost at port 1 in the compost/pyrrhotite cell was due to evaporative loss of water.

The in-situ volumetric moisture contents were measured on November 17, 1995 and April 11, 1996, and are presented in Figure 30. In the peat cover layer, the volumetric moisture contents increased from 53% at port 1 to 69% at port 5. In the compost cover layer, the volumetric moisture contents increased from 50% at port 1 to 63% at port 5 in the compost over the oxidized tailings, and from 49% at port 1 to 68% at port 5 in the compost over the pyrrhotite tailings. The desulphurized tailings and the LSSS maintained a relatively constant moisture content at about 40% and 50%, respectively, throughout the cover layer thickness.

Figure 29. Volumetric Moisture Content by TDR vs. Time for Different Cover Materials
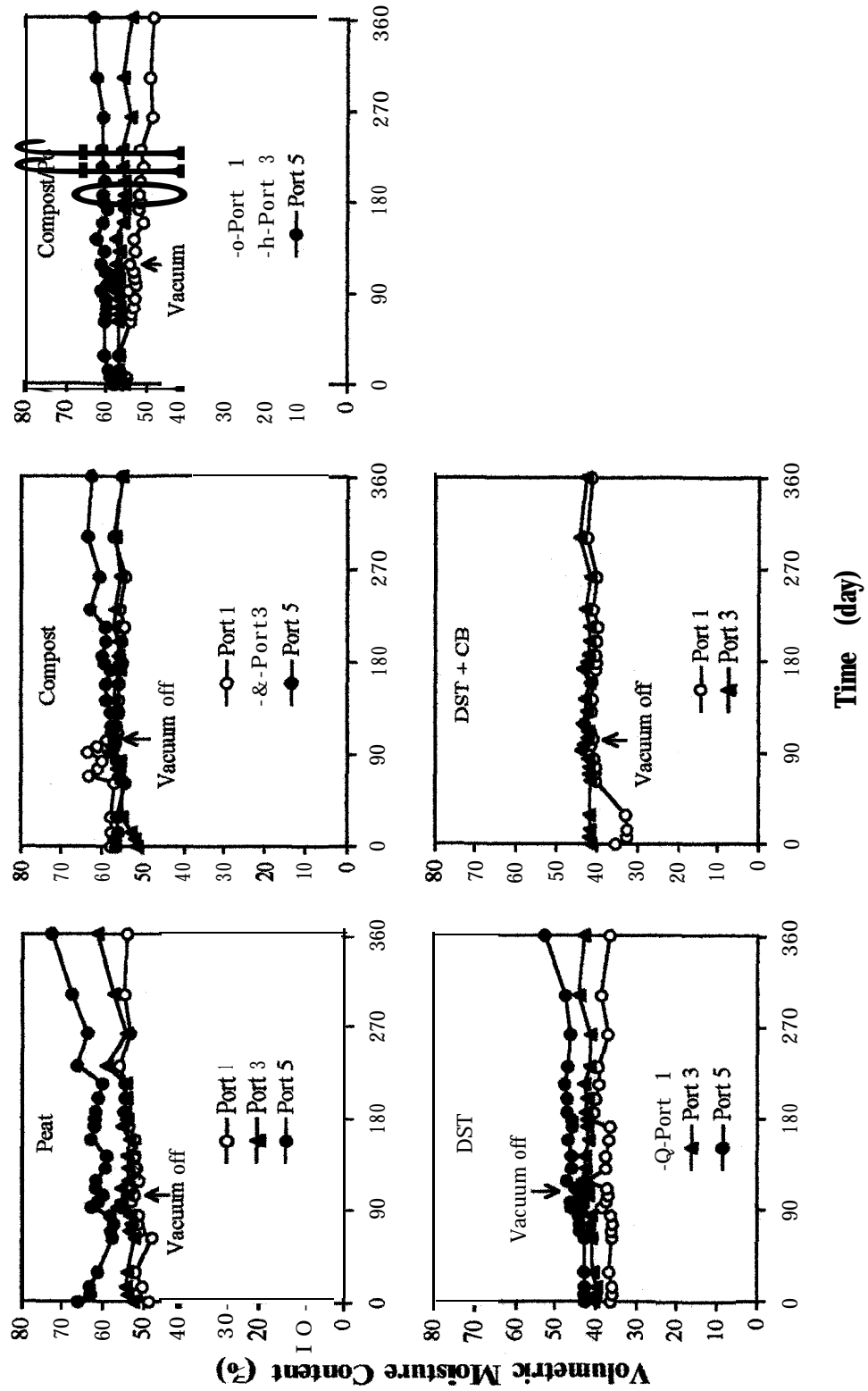
The volumetric moisture contents at ports 6 and 7, in the underlying oxidized tailings, were about 40% in the control cell and in the cells covered with peat and desulphurized tailings. In the remaining cells, the volumetric moisture contents of the underlying oxidized tailings were variable between 30-40% in the compost cover cell and in the LSSS cover cell (Figure 30).

The degree of saturation in the cell material was calculated using the in-situ volumetric moisture contents measured on November 17, 1995 and April 11, 1996. The degree of saturation is defined as the water content normalized to the porosity. It is more meaningful to express the moisture content as degree of saturation because it is the degree of saturation that controls the oxygen diffusion rate and not the volumetric moisture content. The degree of saturation for each material is plotted in Figure 31. The data in Figure 31 clearly show that only the LSSS and the desulphurized tailings were able to maintain about 90% saturation throughout their cover depth. Peat and compost materials had about 60% saturation at the shallower cover depth and about 90% saturation at the deeper cover depth.

The volumetric moisture content was also measured over a short time scale using the TDR system before and after weekly application of simulated rainfall. Figures 32 and 33, and 34 and 35 show the changes of the volumetric moisture content in the compost and desulphurized tailings cover layers. Generally, increases in the moisture content occurred within 5 hours after the rainfall application and the moisture contents were then observed to decrease to similar levels before the rainfall application.

Figure 30. **In-situ Volumetric Moisture Content vs. Depth for Different Cover Materials**
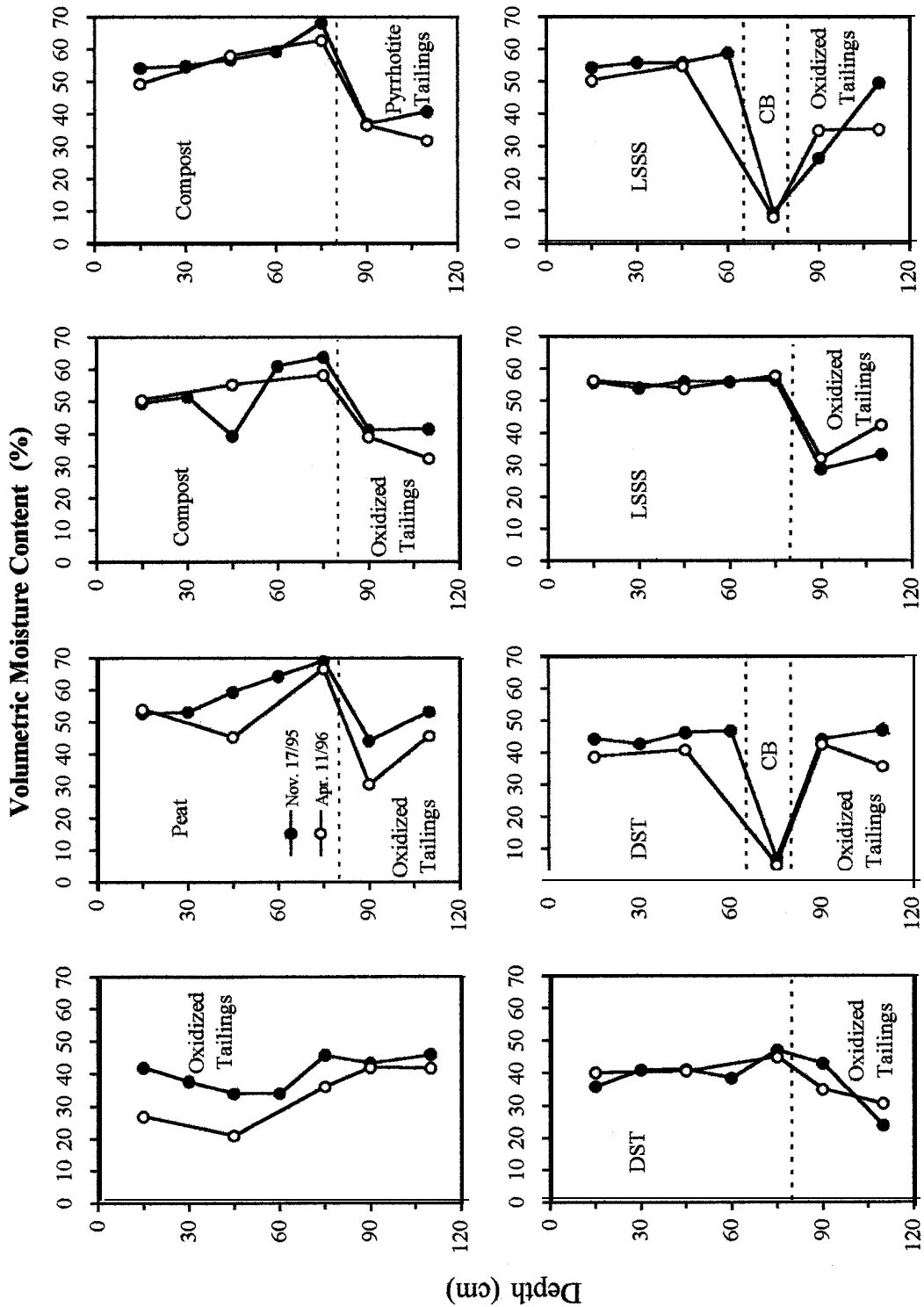
Figure 31. **Degree of Saturation vs. Depth for Different Cover Materials**
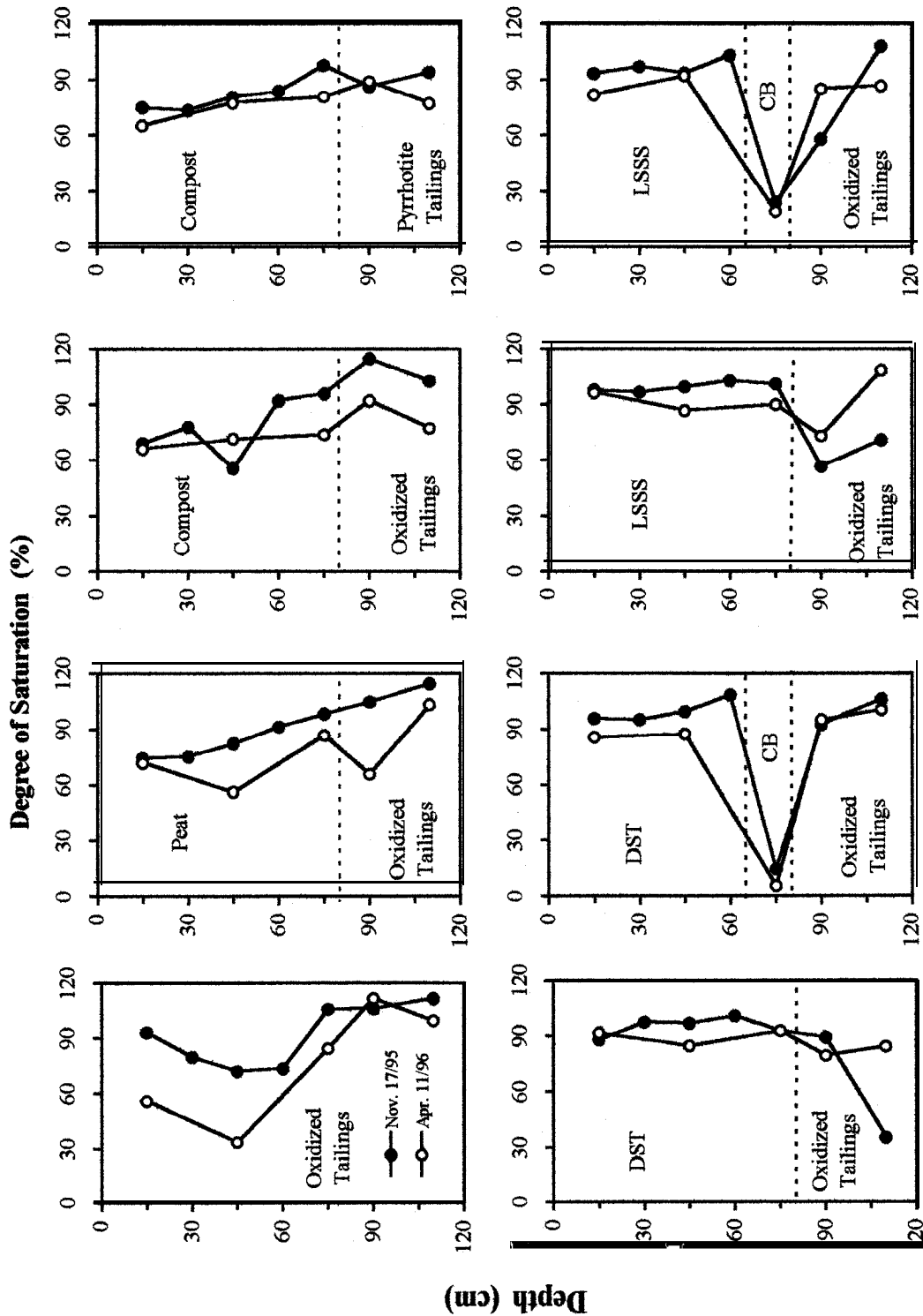
Figure 32. Volumetric Moisture Content Before and After Rainfall at Different Sample Ports in Strathcona Pilot Cell #3 (DST over Oxidized Tailings)
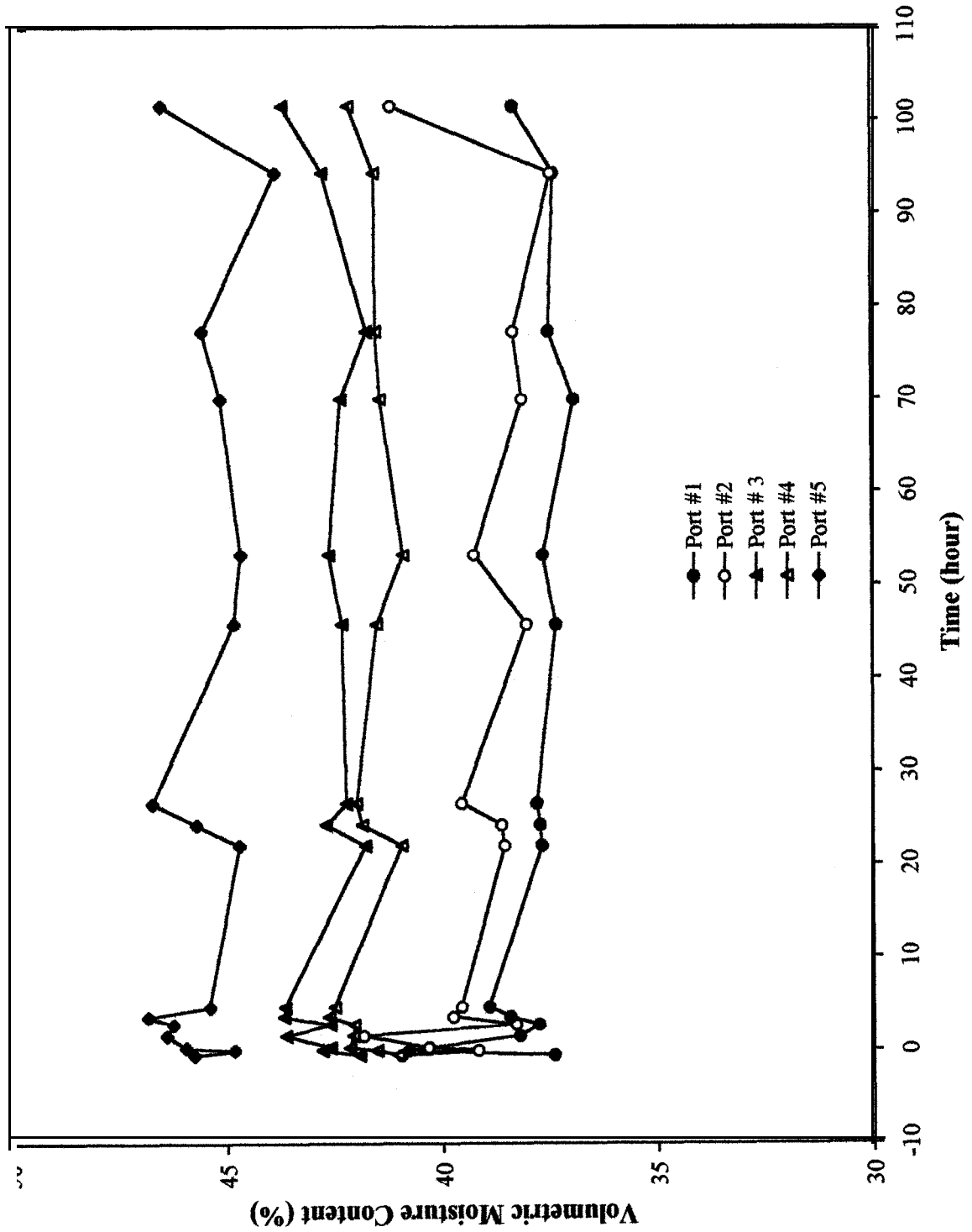
Figure 33. **Volumetric Moisture Content Before and After Rainfall at Different Sample Ports in Strathcona Pilot Cell #6 (DST+CB over Oxidized Tailings)**

Lakefield Research Limited
Environmental Services
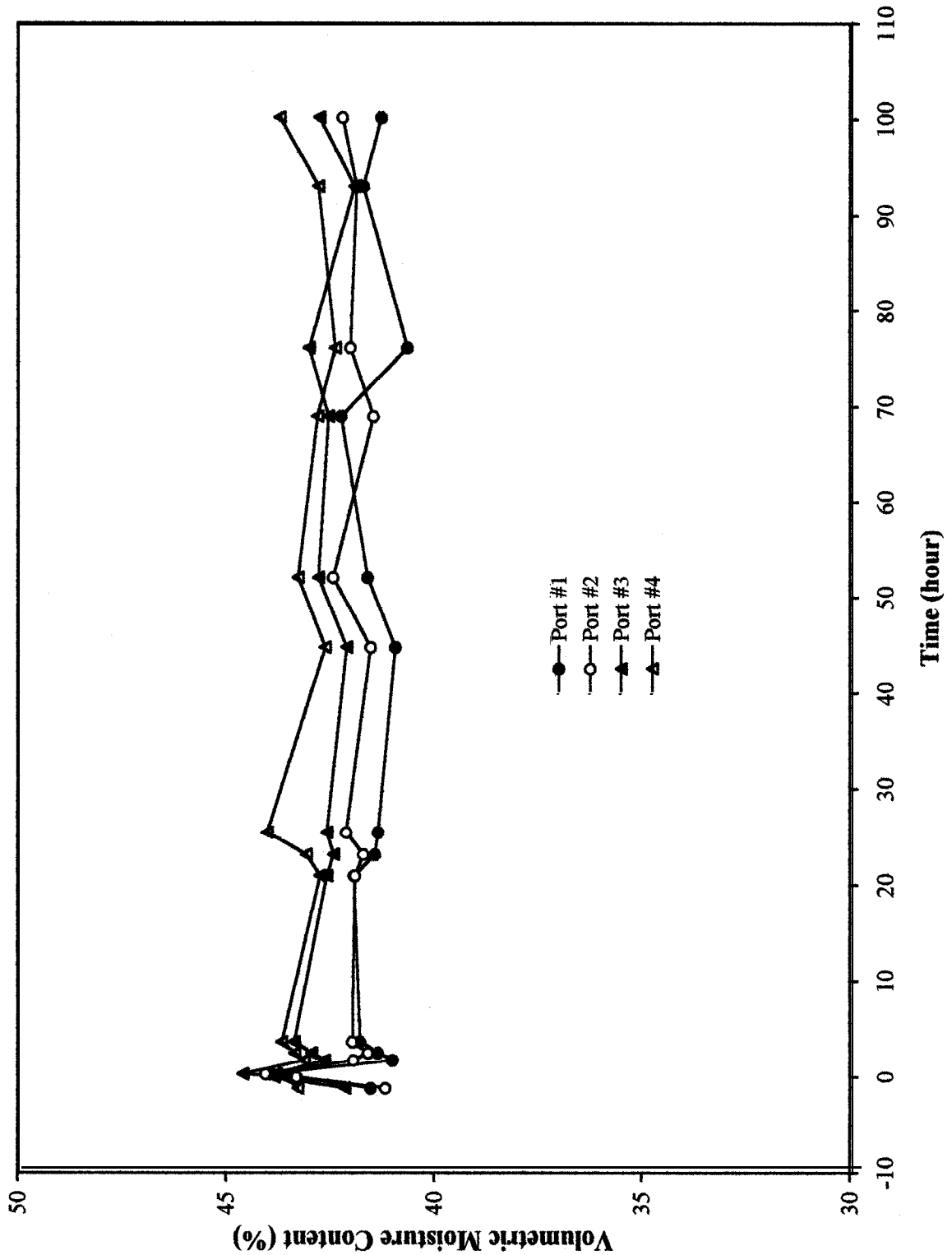
Figure 34. **Volumetric Moisture Content Before and After Rainfall at Different Sample Ports in Strathcona Pilot Cell #4 (Compost over Oxidized Tailings)**
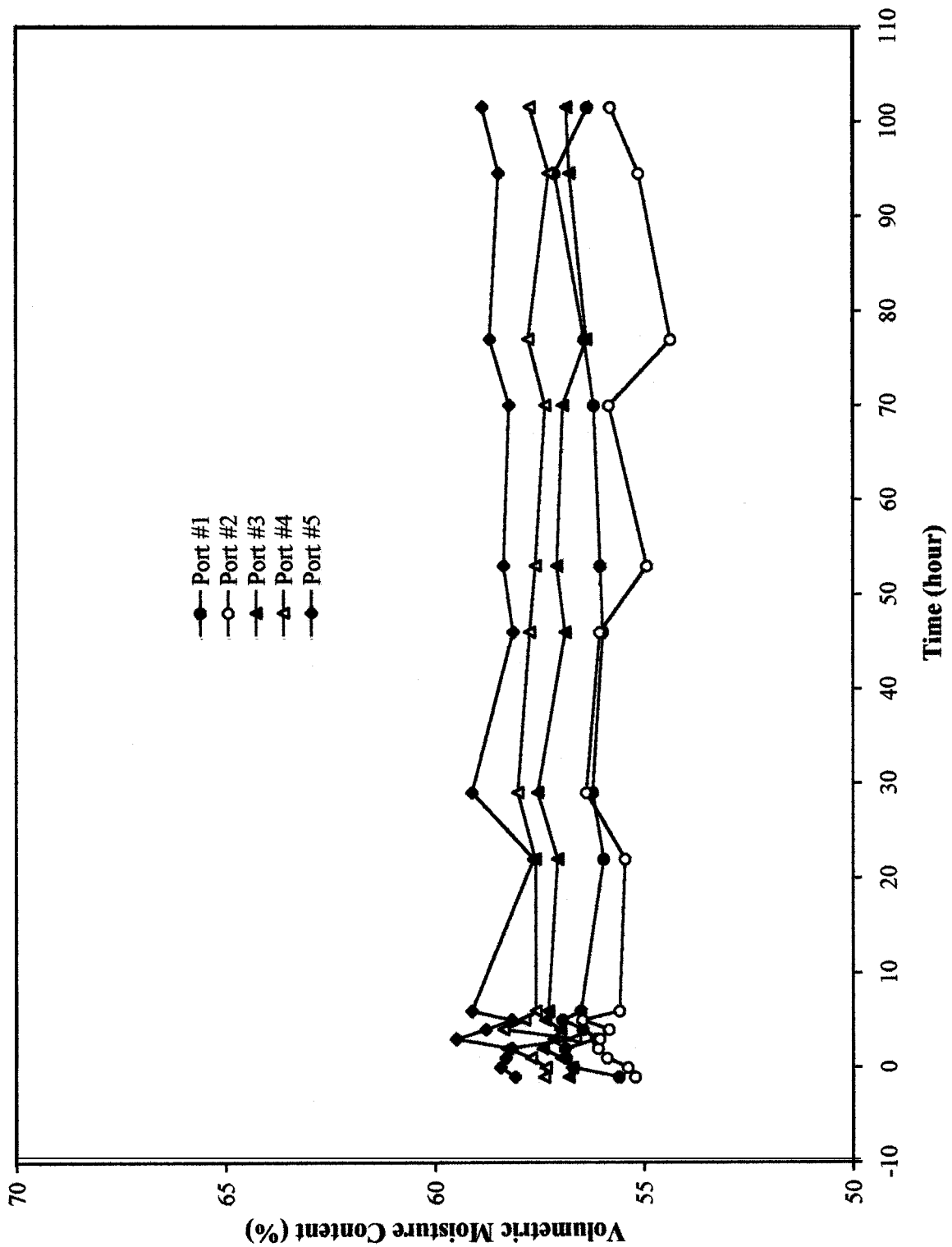
Figure 35, **Volumetric Moisture Content Before and After Rainfall at Different Sample Ports in Strathcona Pilot Cell #8 (Compost over Pyrrhotite Tailings)**
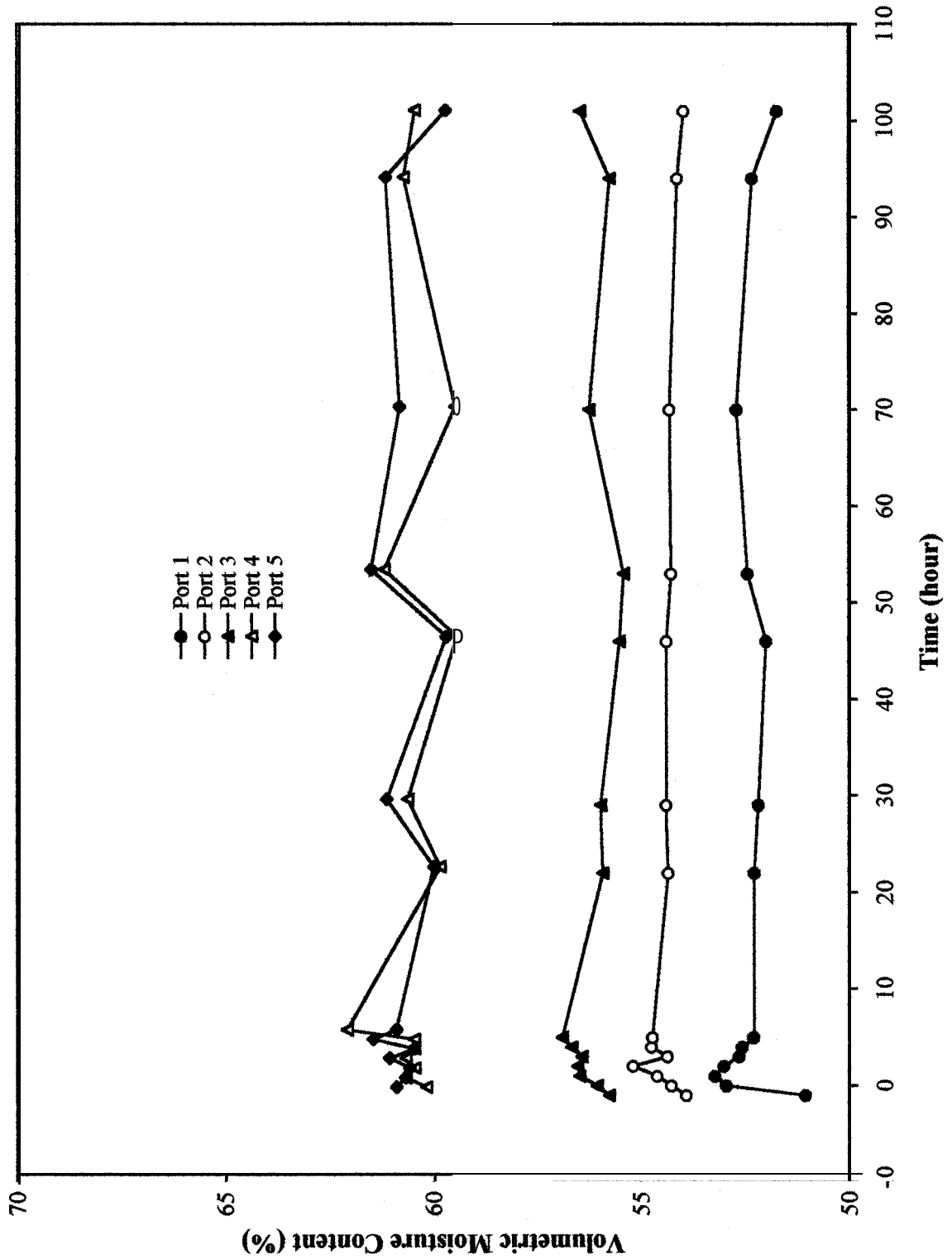
3.3.12 Water Balance Calculation in the Cells

The volumes of various flows in and out of the pilot cells were recorded for water balance calculations. These flows included: rainfall application, pan evaporation, free drainage from the cells (leachate) at different levels and the vacuum drain water (leachate). Evaporative flux tests were conducted to determine the ratio of actual evaporation (AE) to potential evaporation (PE). AE was determined with saturated cover materials. PE was determined with simulated acidic water (pH 4.2) which was applied to the pilot cells. From the material characterization test work, the average ratio of AE/PE for the first 7 days was 0.750 for the oxidized tailings, 0.893 for the desulphurized tailings, 0.831 for the LSSS, 0.869 for compost and 0.843 for peat. These ratios were used to calculate the actual evaporation from the daily pan evaporation in the pilot cell test area. Table 19 presents the balance sheet for the eight pilot test cells from March 30, 1995 to April 1, 1996.

Table 19 shows that, over one year period, seven out of eight pilot cells had a water surplus (i.e., more water input than output). A water deficit was estimated to exist in the desulphurized tailings cover cells without CB. The total input in the form of simulated rainfall was 1030.8 litres for each cell, which is equivalent to about 20 litres per week per cell, or 13.3 mm rainfall. The actual evaporation loss from the surface varied from 463.8 to 552.3 litres, which corresponds to 8.9-10.6 litres per week per cell or 5.9-7.1 mm. The actual evaporation loss represented 45-53% of the water input. The total discharge from the cell due to free drainage varied from 359.1 to 500.8 litres, which corresponded to 6.9-9.6 litres per week per cell. The total discharge represented 35-49% of the water input.

Over 90% of the total discharge from the cells was collected at the bottom of the oxidized tailings layer when organic materials such as LSSS, peat and compost were used as covers (Table 19). The discharge from the bottom of the oxidized tailings layer was 95% under the LSSS, 90-91% under compost and almost 100% under peat. The discharge from the interface accounted for 2.4% under the LSSS, 8-10% under compost and 0.1% under peat. When

inorganic materials such as desulphurized tailings were used as a cover, about 90% of the discharge was collected from above

Table 19.   Water Balance Sheet for the Eight Pilot Cells During One Year Testing

Cell	Level	Discharge			Actual Evaporation		Input	Balance
		mL	% of Total	% of Input	mL	% of Input	(mL)	(mL)
Control	Cover	98650	19.65					
	Tailings	403361	80.35					
	Total	502011	100.00	48.70	463831	45.00	1030824	64982
LSSS	Cover	13420	3.01					
	Interface	10614	2.38					
	Tailings	421472	94.61					
	Total	445506	100.00	43.22	513924	49.86	1030824	71394
Desulph. Tailings	Cover	13102	2.62					
	Interface	440806	88.02					
	Tailings	46908	9.37					
	Total	500816	100.00	48.58	552268	53.58	1030824	-22260
Compost	Cover	172	0.04					
	Interface	34489	8.75					
	Tailings	359610	91.21					
	Total	394271	100.00	38.25	537425	52.14	1030824	99128
Peat	Cover	502	0.13					
	Interface	406	0.10					
	Tailings	390268	99.77					
	Total	391176	100.00	37.95	521346	50.58	1030824	118302
DST with CB	Cover	53249	12.17					
	Interface1	237938	54.39					
	Interface2	47347	10.82					
	Tailings	98969	22.62					
	Total	437503	100.00	42.44	552268	53.58	1030824	41053
LSSS with CB	Cover	5	0.00					
	Interface1	3960	0.82					
	Interface2	21200	4.40					
	Tailings	456690	94.78					
	Total	481855	100.00	46.74	513924	49.86	1030824	35045
Compost/	Cover	0	0.00					
	Interface	36142	10.06					

Pyrrhotite	Tailings	322960	89.94					
	Total	359102	100.00	34.84	537425	52.14	1030824	134297

the interface without CB, and above 70% in the cells with CB. This suggests that the desulphurized tailings used as a cover generate less leachate from the oxidized tailings.

3.3.13 Leachate Characteristics

Leachate of free drainage was collected from the bottom oxidized tailings layer for analysis during the week of October 13, 1995, October 31, 1995, November 29, 1995, January 8, 1996, January 29, 1996, February 19, 1996, and March 11, 1996. During the week of March 11, 1996, discharge from the runoff and interface was also collected for analysis. Analyses conducted on the leachate samples included pH, electrical conductivity, SO_4 and dissolved 24-elemental ICP scan. The detailed analytical results are attached in Appendix H.

The following paragraphs focus on the changes in pH and SO_4 and dissolved Fe concentrations in the leachate collected from the bottom oxidized tailings layer in the control cell and in the cells covered with LSSS, compost and peat. In the cell covered with the desulphurized tailings without CB, virtually no discharge was collected from the underlying oxidized tailings during the last six months of the program, therefore, the desulphurized tailings have not been included in the following comparisons. However, in the cell covered with the desulphurized tailings with CB, the underlying oxidized tailings started discharging leachate on December 20, 1995, at a pH of <2.7 and with very high concentrations of Fe, Ni, Pb, Zn and SO_4.

Figure 36 shows the leachate pH changes in the control cell and in the cells covered with LSSS, compost and peat. The leachate pH in the LSSS cover cell increased continuously with time from 4.1 at the beginning to 6.2 at the end of one year of testing. The leachate pH in the compost cover cell increased from 2.7 to 4.2 and then decreased to 3.4 towards the end of the test. Similar leachate pH values were recorded for the control cell and the peat cover cell, with pH fluctuating between 2.1 and 3.0.

Figure 36. Leachate pH Changes in the Control Cell and in the Cover Cells

Leachate pH vs. Sampling Date

Legend:
- Control
- LSSS
- Compost
- Peat

X-axis (Sampling Date): 10/13/95, 10/31/95, 11/29/95, 1/8/96, 1/29/96, 2/19/96, 3/11/96
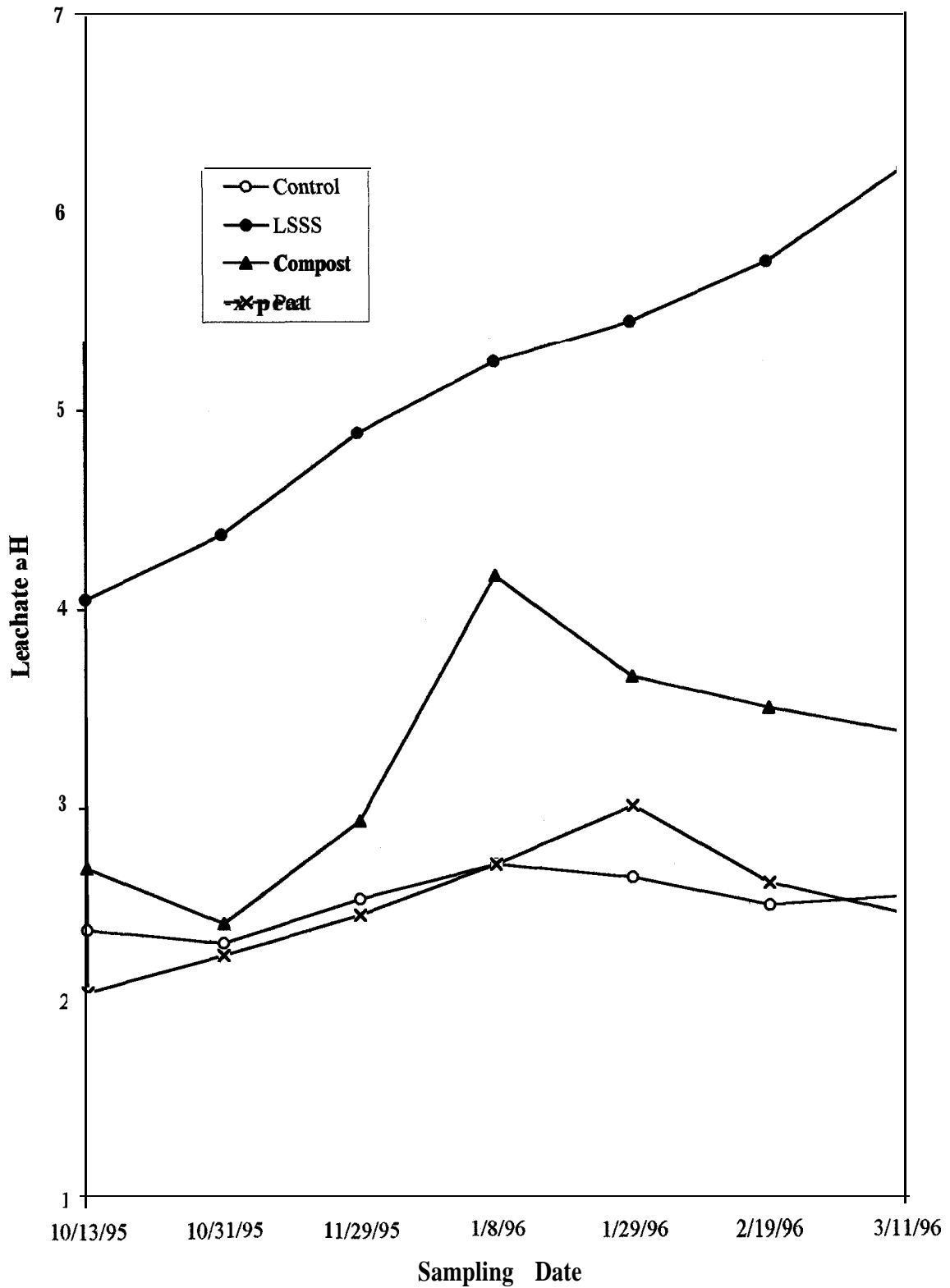
Figure 37 shows the SO_4 concentration changes in the leachate samples collected from the control cell and the cells covered with LSSS, compost and peat. The highest SO_4 concentrations were found in the leachate samples collected from the control cell, which fluctuated between 27,000 mg/L and 71,000 mg/L. The lowest SO_4 concentrations were found in the leachate from the LSSS cover cell, which decreased with time from a high of 37,000 mg/L at the beginning to 12,000 mg/L at the end of the test. The leachate SO_4 concentrations from the peat cover cell also decreased with time from 45,000 mg/L to 25,000 mg/L. The leachate SO_4 concentrations from the compost cover cell fluctuated between 19,000 mg/L and 35,000 mg/L.

Figure 38 shows the changes in dissolved Fe concentrations in the leachate samples collected from the control cell and in the cells covered with LSSS, compost and peat. Similar changes were observed in leachate dissolved Fe concentrations as were observed in the leachate SO_4 concentrations. The dissolved Fe concentrations in the leachate samples collected from the compost cover cell fluctuated between 22,000 mg/L and 36,000 mg/L. The dissolved Fe concentration in the leachate samples collected from the peat cover cell decreased slightly with time from 22,000 mg/L to 16,000 mg/L. A dramatic decrease in leachate dissolved Fe concentrations was observed in the LSSS cover cell (from 36,600 to 12,400).

Although the LSSS cover cell showed improvements in leachate quality (e.g. increase in pH and decrease in SO_4 and dissolved Fe, Pb, Ni and Zn), the dissolved total P concentrations remained high in the leachate, varying from 3.1 to 4.3 mg/L. In addition, the leachate samples collected from the LSSS cover cell contained very high concentrations of phenolic compounds. The leachate phenol concentration was 60,000 µg/L in the samples collected from the LSSS cover cell without CB and 55,000 µg/L in the LSSS cover cell with CB. In contrast, the phenol concentrations in the leachate samples collected from both the compost and peat cover cells were between 12 and 24 µg/L.

Figure 37. **Leachate SO_4 Changes in the Control Cell and in the Cover Cells**

Lakefield Research Limited
Environmental Services
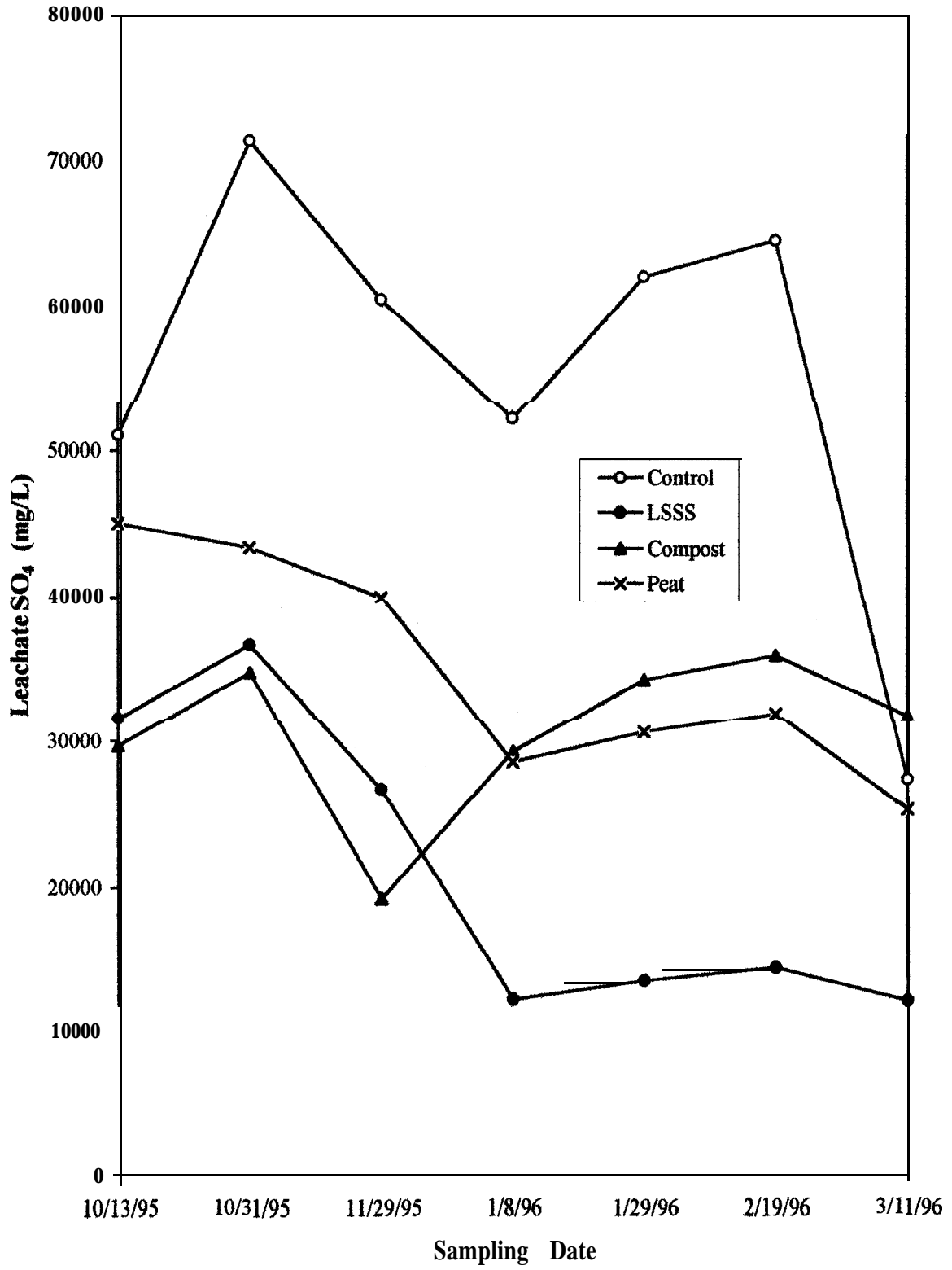
Figure 38. Changes in Leachate Dissolved Fe Concentrations in the Control Cell and in the Cover Cells
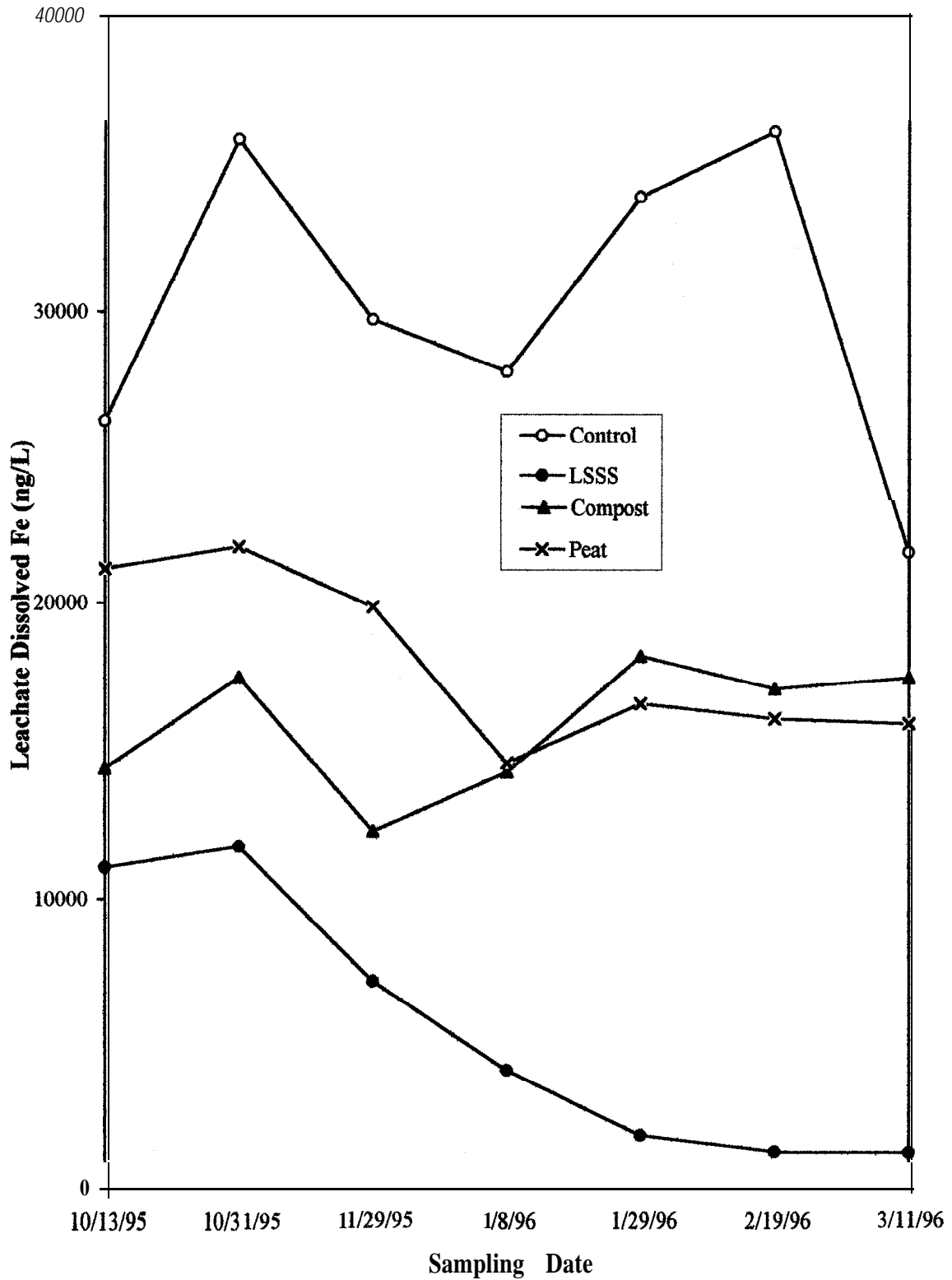
The concentrations of polycyclic aromatic hydrocarbons (PAHs) were below 1 mg/L in the leachate samples collected from the organic cover cells (LSSS, compost and peat).

3.3.14 Cell Loading Calculations

Measurements of the volume of surface runoff, interface discharge and basal leachate and their respective water quality analyses were used to calculate the total cell loading for sulphate, iron and nickel in the control cell and in the cells covered with desulphurized tailings, LSSS, compost and peat. As the leachate analyses were introduced at the later stage of the test program, the pore water analyses from scheduled sampling dates were used to estimate the cell loading at the early stage of the test program. Therefore, the loading for the desulphurized tailings cover cell may have been overestimated because higher concentrations of the analytes would be expected in the pore water than in the leachate.

Figure 39 compares the loading of SO_4, Fe and Ni in the cells covered with desulphurized tailings, LSSS, compost and peat with the control, which is represented by 100%. Figure 39 clearly shows that the desulphurized tailings and LSSS covers resulted in a lower release of total metals and salts to the environment than the compost and peat. Compared to the control, the SO_4 loading was 33% for the desulphurized tailings cell, 46% for the LSSS cell, 78% for the peat cell, and 85% for the compost cell. The Fe loading was 22% for the LSSS cell, 30% for the desulphurized tailings cell, 71% for the compost cell and 72% for the peat cell. Almost all the SO_4 and Fe loading were from the tailings layer under the organic cover materials, whereas slightly less than half of the SO_4 and Fe loading were from the tailings layer under the desulphurized tailings cover.

The Ni loading to the environment was generally low under the organic cover materials, and accounted for <1.6% of the control. A high Ni loading (70%) was observed under the desulphurized tailings cover.

Figure 39.   Sulphate, Iron and Nickel Loading Relative to the Control Cell
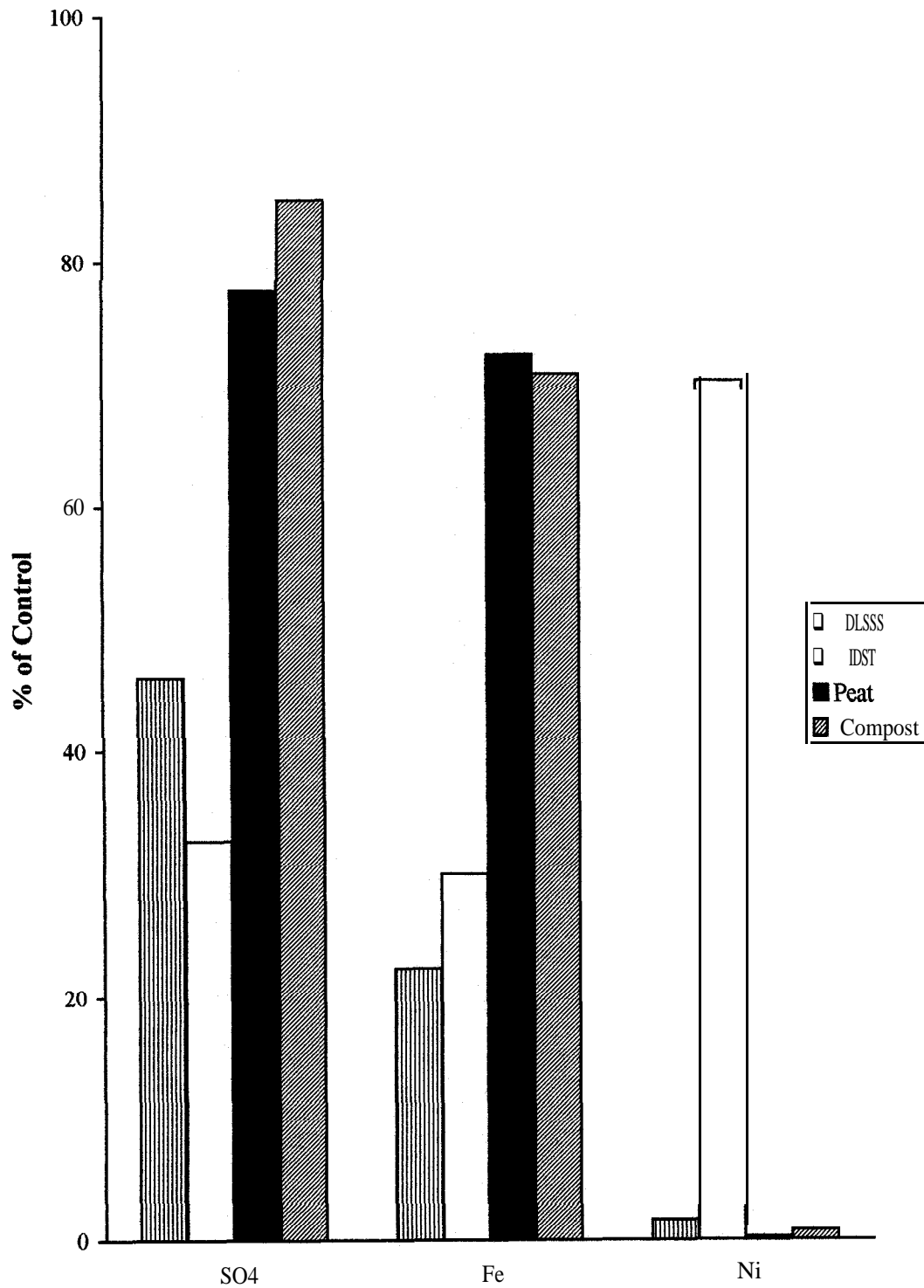
4.0 DISCUSSION

4.1 Effects of Evaporation on Salt Migration

The highest evaporation rates were observed at the surface of the peat and desulphurized tailings Salt Migration Columns (SMC). The highest percentage increases in electrical conductivity were also noted at the surface of peat and desulphurized tailings covers. This suggests that there is a direct relationship between the evaporation rate and the salt accumulation at the surface. The high evaporation rate at the surface of peat may have been due to a high initial moisture content, a high rate of capillary water flow from the deeper layer and the large surface area exposed for evaporation due to the formation of cracks. The high evaporation noted in the desulphurized tailings columns may have been due to high moisture content available for evaporation.

The lowest evaporation rates and, correspondingly, the lowest percentage increases in electrical conductivity were observed at the surface of the compost and the LSSS SMC . The low evaporation rate of the compost may have been related to the low initial moisture content and a low degree of interconnection between the particles of the compost. The low evaporation of the LSSS may have been due to the osmotic effect of the high salt concentrations in the LSSS and to the compaction of the dried material.

When the SMC with 0.15 m covers of peat and compost were decommissioned, a hardpan was found at the interface between both covers and the underlying oxidized tailings. As the hardpan could reduce the movement of water and salts from the underlying tailings, this may have contributed to the very low evaporation rate noted (close to 0 mm/day) for the compost and the peat near the end of the program. The reduced movement of water from the underlying oxidized tailings may have also caused the formation of cracks in the peat cover.

A salt crust formed at the surface of all the control cells. The formation of the salt crust drastically decreased the evaporation rate from the oxidized tailings to 0 mm/day in all

control cells. This occurred even though the tailings surface contained a high moisture content which was available for evaporation. The decrease in the evaporation rate may also have been caused by the osmotic effects of salts in the oxidized tailings.

Even though the desulphurized tailings cover showed a high percentage increase in electrical conductivity, the final conductivity of the desulphurized tailings after the 4 month test period was less than 1000 µmhos/cm with 0.15 m cover depth and less than 500 µmhos/cm with >0.5 m cover depth. These conductivity values were lower than the initial conductivity of the compost and LSSS.

The method developed at Lakefield Research for the measurement of electrical conductivity determines the soluble salt conductivity in a more diluted way than the saturated paste method. On average, the electrical conductivity measured by the saturated paste method was 10 times the electrical conductivity measured by the Lakefield method. In the SMC test, the desulphurized tailings with 0.15 m and 0.5 m cover depths had electrical conductivities of 846 and 464 µmhos/cm at the surface, respectively. These corresponded to electrical conductivities of 8460 and 4640 µmhos/cm if the electrical conductivity had been measured by the saturated paste method. According to the saturated paste method, electrical conductivities of 0-2000 µmhos/cm are classified as non-saline, 2100-4000 µmhos/cm as slightly saline, 4100-8000 µmhos/cm as moderately saline, 8100-16000 µmhos/cm as strong saline and >16000 µmhos/cm as very strongly saline. Therefore, an electrical conductivity of 8460 µmhos/cm at the surface of the desulphurized tailings with 0.15 m cover depth would be classified as strong saline, and an electrical conductivity of 4640 µmhos/cm at the surface of the desulphurized tailings with 0.5 m cover depth would be classified as moderately saline. In terms of electrical conductivity alone, some influence on plant growth may occur for the 0.15 m cover depth. This should be verified with growth tests. The influence of certain level of soluble salts on plant growth depends on several factors such as climatic conditions, soil texture, salt distribution in the profile, salt composition and plant species. It also must be pointed out that the electrical conductivity values in the salt migration column test are

obtained under four month consecutive drought conditions, which represents the worst case scenario.

Although the LSSS exhibited a low percentage increase in electrical conductivity at the surface due to a low evaporation rate, the initial electrical conductivity was much higher than the other cover materials. The high electrical conductivity of the LSSS was caused by the dissolution of salts and high pH present in the LSSS and was not directly related to the migration of salts from the underlying tailings. The dissolved salts were mainly composed of cations such as Ca^{2+} and Mg^{2+} and anions such as SO_4^{2-} and HCO_3^-. The high salt content and high alkalinity (pH>12) present in the LSSS would make it difficult to grow vegetation.

The compost material maintained a relatively constant electrical conductivity at 1400 µmhos/cm throughout the 4 month test period and through all the cover depths tested. This indicates that the compost is very resistant to upward salt migration.

The use of a 0.15 cm thick capillary barrier in conjunction with the desulphurized tailings appeared to reduce the migration of salts only in the 0.15 m cover depth, although the evaporation rate was not affected. The ineffectiveness of the CB was believed to be due to the presence of medium to fine grained fraction (D_{10}=0.2-0.3 mm), which caused a capillary rise on the order of about 20 cm which was very close to the thickness of the CB layer. Compaction of the CB may have also caused a greater capillary rise. Therefore, the CB layer may be less effective as capillary break under the thick cover layers (0.5 m and 1.0 m) than under the thin cover (0.15 m) layer.

The result of the column tests have shown that fine-grained material, such as desulphurized tailings, at ground surface can cause salt accumulation. These salts can then be washed away with surface run off during rainfall events. This is not acceptable if long-term surface water quality impacts are to be avoided. A capillary barrier or a surface evaporation barrier may be used to reduce or eliminate surface salt accumulation. It is also likely that fine-grained

materials at the surface will require erosion protection to maintain the physical integrity of the cover system and this may be designed to be complementary with an evaporation barrier.

4.2   Pilot Test Cells

4.2.1   Sulphate and Iron Concentrations in Pore Water

High concentrations of SO_4 and Fe were initially observed in the pore water of the oxidized tailings. These concentrations were due to the oxidized nature of the Strathcona tailings used in these tests. Small changes may, therefore, be difficult to interpret over a short period.

Results to date show that only the LSSS test cells caused relative decreases in the concentrations of SO_4 and Fe in the underlying oxidized tailings over the testing period. The chemicals from the LSSS material (high pH, high Ca^{2+}) may have contributed to the observed decreases in SO_4 and Fe. It is not known whether the observed decreases in SO_4 and Fe concentrations were solely due to decreases in the amount of oxidation in the oxidized tailings or due to the precipitation of existing iron and sulphate as $Fe(OH)_3$ and gypsum ($CaSO_4^.2H_2O$) as the water from the LSSS cover infiltrated the underlying oxidized tailings layer.

An increase in pH and increase in DOC in the oxidized tailings pore water were noted under the LSSS cover. The high alkalinity present in the LSSS may have contributed to the pH increase in the oxidized tailings layer. The decomposition of the organic material in the LSSS may be related to the observed DOC increase in the oxidized tailings. These findings indicate that the leachate from the LSSS cover was transported to the underlying oxidized tailings through the infiltration of rainwater. The increases in pH and DOC may favor the increased activity of sulphate-reducing bacteria (SRB), resulting in decreased concentrations of Fe and SO_4 due to the reduction of sulphate to sulphide and subsequent precipitation of insoluble metal sulphides. The black precipitate noted in the cells may have been the

amorphous form of ferrous sulphide (FeS). A wide black band has formed at the interface between the LSSS and the oxidized tailings (refer to Plate No. 12). This was further indication of the presence of active sulphate-reducing bacteria populations.

The sulphate reduction that continued at the base of the LSSS cover was possibly because of the following three conditions: 1) pH was >4.5; 2) the cover was blocking oxygen migration to this zone (0% O_2 at the interface), creating a reducing environment; and 3) the organic matter being leached from the LSSS provided a source of carbon for the SRB. However, it is possible that when the organic carbon is completely decomposed or leached from the cover, sulphate reduction will cease and oxygen diffusion will cause the oxidation of recently formed metal sulphides. The oxidation of the newly formed metal sulphides could be prevented by maintaining a high degree of saturation in the cover layer or by providing additional carbon source for the SRB. The LSSS has been able to maintain >90% degree of saturation over the entire cover depth. This ability provides a benefit to the underlying oxidized tailings by limiting the rate of O_2 infiltration to approximately the rate of diffusion through water. The decrease in O_2 infiltration will serve to decrease the rate of tailings oxidation and increase the life of the cover.

The increasing immobilization of metals by complexation to organic compounds and the formation of metal sulphide precipitates were mediated primarily by the soluble humic acids and by the SRB that are found in anoxic environments. These anaerobic microbes require organic compounds, particularly simple organic acids, for their metabolism and thereby consume acidity. This consumption of organic acids results in an increase in pH which would further enhance the SRB activity. SRB and other bacteria also cause an increase in pH through an acid consuming process, which results in the formation of methane or hydrogen gas. Increasing pH and certain organic compounds also suppress the acid-generating process by inhibiting the growth and activity of the autotrophic iron oxidizing bacteria *Thiobacillus ferrooxidans* that thrive at the low pH range of 1.5 to 3.5. Through this interactive system, a reversal of the acid rock drainage (ARD) process was seen to be occurring beneath the LSSS cover.

All other cover materials tested exhibited increasing concentrations of SO_4 and Fe in the pore water of the underlying tailings. The increases in SO_4 and Fe may have not been due to the reductive dissolution of Fe in the tailings since the pore water DOC concentrations in the oxidized tailings remained relatively constant (at about 10 mg/L) over the testing period. The increases in Fe and SO_4 was possibly a result of the ongoing oxidation process occurring in the test cells.

The use of a capillary barrier layer was observed to produce different results under the LSSS than under the desulphurized tailings. Under the LSSS, the pore water pH and DOC increased and the SO_4 and dissolved Fe concentrations decreased with time, while under the desulphurized tailings, the pore water pH and DOC remained unchanged and the SO_4 and dissolved Fe increased over time. These results were similar to those observed in the pore water under the DST without the CB. A black band was also formed at the interface between the CB and the oxidized tailings under the LSSS cover, but the intensity was noted to decrease towards the drainage end of the pilot cell (Plate #13). This suggested that a reducing environment existed in the CB layer under the LSSS. Under the desulphurized tailings cover, the CB layer could easily be a conduit for lateral O_2 diffusion from the open end of the pilot cell. This conclusion is supported by the O_2 profile data.

4.2.2   Effect of Vacuum Application in the Oxidized Tailings

Based on the initial experimental configuration, it was anticipated that the oxidized tailings would remain saturated for the duration of the test. It was recommended during a peer review meeting held at Lakefield Research Limited, on November 24, 1994, that a vacuum system be installed at the bottom of the oxidized tailings layer to simulate an unsaturated tailings zone. Without vertical drainage, the capillary barrier would serve no purpose, and little drainage would occur. Therefore, leachate produced in the covers would not be able to interact with the oxidized tailings. Subsequent computer modeling of the cells by Lee Barbour of the University of Saskatchewan confirmed that the oxidized tailings would remain saturated and

little interaction would occur between the oxidized tailings and covers without structural modification to the cells.

The vacuum system was installed in order to provide a realistic physical model of drained tailings and covers. Generally, the water table existed at the location of the lowest drain. In this experiment the lowest drain, and therefore the water table, was located 1.5 m below ground surface. Suction was applied at a pressure below the air entry values determined for the oxidized tailings from the drainage curve test work by Noranda Technology Centre (NTC). The system was set up in parallel so that equal suction was applied at all cells.

The vacuum system used was able to remove air as well as water. It was suggested that air could be drawn through the covers in the process of vacuum application. This could negatively influence the possible cover effects because the covers would no longer be diffusion limited, as would be expected in a field situation. Therefore, vacuum application was terminated after 112 days into the test program to avoid the possibility of drawing oxygen into the cell. Tensiometers were installed in the cells to permit analysis of the vacuum effects and modify the vacuum application process to avoid the possibility of air diffusion. It was anticipated that short intermittent vacuum application would avoid any potential negative effects while providing drainage of the oxidized tailings to simulate a deeper water table condition.

There are no data to suggest that the infiltration of oxygen into the covers occurred as a direct result of the vacuum application. The possibility of the influence of induced oxygen migration into the covers on the data for the early portion of the test program, however, will continue to be considered in the evaluation of data collected from the pilot cell studies.

4.2.3 Oxygen Gas Profile in Covers and Tailings

The oxygen profiles in the pilot cells were measured to determine the depth of oxygen penetration and estimate oxygen flux through the covers and tailings. These measurements were made on days 180, 224, 300 and 360 of the test.

The oxygen gradients indicated that compost and LSSS covers were relatively resistant to oxygen migration. The desulphurized tailings also exhibited a steep oxygen concentration gradient, which resulted from a combination of high O_2 demand for oxidation of residual S present in the desulphurized tailings and low O_2 diffusion in the desulphurized tailings due to high degree of saturation (>90%). The gas samples collected from the desulphurized tailings plus capillary barrier cell may have been contaminated by oxygen that had migrated laterally through the capillary barrier. No oxygen gradient existed in the peat cover layer, indicating that the peat was very susceptible to oxygen penetration due to its low degree of saturation (about 60%).

4.2.4 Decomposition of Organic Cover Materials

The total organic carbon (TOC) concentrations were measured before and after one year pilot cell test, and the difference was used to show the net gain or loss of carbon in the cover layer during the one year period. The analytical results show that there was little change in TOC in the LSSS cover layer and a net loss of TOC in the compost and peat cover layers.

The TOC data indicated that the LSSS did not decompose. This observation was contrary to the results of the DOC analyses in the pore water of LSSS cover layer and the underlying oxidized tailings and to the phenol concentrations noted in the leachate samples collected at the bottom of the LSSS cover cell. The decrease in pore water DOC in the LSSS cover layer and increase in pore water DOC in the underlying oxidized tailings with time show that the LSSS decomposed and provided a carbon source for the SRB to reduce sulphate and form metal sulphides. In a short-term (60 days) incubation test using a different type of LSSS

(TOC 9.9% and pH>11), there was also no evidence of decomposition based on CO_2 evolution data, however, the TOC and DOC concentrations decreased during the test. The CO_2 evolved during decomposition may have been readsorbed by the lime materials in the LSSS.

$$\text{Organic C} \Rightarrow \text{soluble Organic C} \Rightarrow CO_2 + Ca(OH)_2 \Rightarrow CaCO_3$$

Using the incubation results as input data, the computer modeling exercise predicted an annual 15-16% of decomposition rate during the first two years under the weather conditions where it will be applied. The decomposition rate would be much slower after the soluble and readily decomposable organic carbon have been depleted. It is roughly estimated that after 10 years about 80% of organic carbon would be lost as CO_2.

The compost cover showed the highest organic carbon decomposition in the pilot cells tested. During the one-year testing, about 69% of organic carbon was lost from top 15 cm and about 30% from the 45 cm cover depth. Therefore, approximately one third of the top 15 cm and two thirds of the middle 15 cm remained for further decomposition. The leaching of the organic compounds from the top cover layer resulted in a slight increase in TOC at the 75 cm cover depth. The DOC concentrations in the pore water of the underlying oxidized tailings was not affected by the decomposition of the compost cover layer.

Peat exhibited much lower decomposition than compost, largely due to the presence of humified material. In the peat cover layer, about 4% of the organic carbon was lost at the top 15 cm cover depth, and 16% at the 45 cm cover depth. A slight increase in TOC at the 75 cm cover depth was also noted. The DOC concentrations in the pore water of the underlying oxidized tailings were not affected by the decomposition of peat cover layer.

4.2.5   Hydrology of the Cover-Tailings System

The average rain water applied to the pilot cell was equivalent to approximately 20 L/week over an area of 1.5 m^2 or 0.013 m /week. The average actual evaporation was equivalent to 0.0065 m/week. Therefore, the net infiltration was 0.0065 m/week. In a material containing volumetric moisture content of 32%, such as oxidized tailings, the infiltration rate (or replacement rate) of the water would be 0.020 m/week or 2.9 mm/day. Over the 360 day period, this represented a depth of replacement of 1.04 m. Some of the covers, such as compost, had a volumetric moisture content of about 50%. Therefore, the replacement rate would be lower, at approximately 0.013 m/week or 1.9 mm/day. Over 360 days the replacement depth would be 0.67 m for compost.

Due to the presence of previously oxidized material in the tailings and related metals concentrations in the pore water, it was necessary to permit sufficient time to allow for flushing of the pores by replacement infiltrating waters before determining whether only new oxidation was occurring.

The discharge from the cells as surface runoff and at interface was negligible for the organic cover materials such as LSSS, compost and peat, and the loading of salts into the environment was exclusively from the bottom of the underlying oxidized tailings. Over 90% of the discharge was collected above the interface from the desulphurized tailings. This indicates that a small volume of leachate was generated from the bottom of the oxidized tailings under the desulphurized tailings. However, the pore water of the oxidized tailings exhibited concentrations of sulphate and metals higher than the control. This suggested that either the previously oxidized products were not flushed out or oxidation of the sulphides was ongoing. This further presents a potential for leaching of metals.

In comparison with DST cover cell, the oxidized tailings control cell had a higher percentage of discharge as runoff from the surface. The formation of an oxidized layer (hardpan) at 15 cm below the surface may have contributed to the high volumes of runoff from the surface of

the oxidized tailings control cell. The control cell also had a higher percentage of discharge at the tailings base. In the control cell, only two collection trays were installed, one at the surface and one at the base, whereas in the DST cover cell, three collection trays were installed, one at the surface, one at the interface between the DST and the oxidized tailings and one at the base. Therefore, in the control cell, discharge collected from the tailings base consisted of two components, one from the bottom tailings layer and one from the location equivalent to the interface between the cover and the oxidized tailings.

5.0   SUMMARY

The following preliminary findings are based on the characterization of the materials, salt migration column tests and the pilot scale test cells.

5.1   Characterization of Tailings and Cover Materials

- The ICP-ES scan revealed that the oxidized tailings were higher in Al, Ca, Mg and Na, lower in Ni and Zn, and similar in Cd, Co, Cr, Cu, Mn and Pb than the pyrrhotite tailings.
- The oxidized tailings contained 38% Fe and 19% S, while the pyrrhotite tailings contained 53% Fe and 30% S.
- Pyrrhotite was the major sulphide mineral phase for both tailings types.
- The peat, compost and gravel had coarse grain size distributions. The oxidized tailings, pyrrhotite tailings, desulphurized tailings and LSSS had fine grain size distributions.
- The oxidized tailings, desulphurized tailings and pyrrhotite tailings had air entry values of >200 cm H_2O and hydraulic conductivity in the range of 10^{-5}-10^{-6} cm/s, while the peat, compost and LSSS had air entry values of <100 cm H_2O and hydraulic conductivity in the range of 10^{-1}-10^{-3} cm/s.
- During the evaporative flux tests all the materials tested were initially saturated. The average actual evaporation to potential evaporation ratio for the first seven days was 0.75

for the oxidized tailings, 0.893 for the desulphurized tailings, 0.831 for the LSSS, 0.869 for the compost and 0.843 for the peat.

5.2   Salt Migration Columns

- Peat and desulphurized tailings yielded the highest evaporation rate in the salt migration column tests and correspondingly, also yielded the highest percentage increase in electrical conductivity near the surface.
- Compost exhibited the lowest evaporation rate. The electrical conductivity in the compost cover layer remained relatively constant with time and throughout all the sampling depths.
- The LSSS had a very low evaporation rate and a high initial electrical conductivity. The dissolution of salts in the water was likely responsible for the elevated electrical conductivity. The salts dissolved in the water consisted mainly of Ca and Mg, and possibly SO_4 salts.
- The capillary barrier used in the salt migration columns appeared to reduce the salt accumulation only in the shallow cover depth (0.15 m), although it did not reduce the evaporation rate. The capillary barrier had no effect in reducing the salt migration in the thicker cover layers tested (0.5 and 1.0 m) due to capillary rise by compaction and presence of medium and fine grained fractions.

5.3   Pilot Scale Test Cells

- The Fe and SO_4 concentrations of the oxidized tailings pore waters showed a slight increase over time with peat, compost and desulphurized tailings covers.
- With the LSSS as a cover, a decrease in the Fe and SO_4 concentrations of the pore waters in the underlying oxidized tailings was accompanied by an increase in pH and dissolved organic carbon in the oxidized tailings.

- A large oxygen concentration gradient was observed in the compost and LSSS cover cells. A steep oxygen concentration gradient was also observed in the desulphurized tailings cover layer. The oxygen concentrations in the peat cover cell remained relatively high at 17 % through the cover layer. The capillary barrier used in the pilot scale tests allowed the lateral migration of O_2 into the oxidized tailings under the DST, but not under the LSSS.

- The desulphurized tailings and the LSSS maintained >90% degree of saturation, which reduced the O_2 diffusion.

- Cu was not detected above the detection limit in the tailings pore water collected from all the cells.

- The pore water Ni concentrations in the oxidized tailings under cover materials decreased but those in the control cell remained high.

- The pore water NO_3 concentrations in the oxidized tailings were below the permissible level of 10 mg N/L.

- The total P concentrations in pore water of the oxidized tailings were above 2 mg/L under LSSS, but <0.5 mg/L under other the cover materials.

- The LSSS and desulphurized tailings cover reduced the loading of salts into the environment.

6.0   CONCLUSION

The main objective of this test program was to comparatively evaluate the effectiveness of various organic cover materials at limiting or reducing the impacts of acid generation on the environment from acid generating tailings. An inorganic cover material was also included in the study, both for comparative purposes and due to the potential economic availability of large volumes of this material at operating mining properties.

The primary property of a good cover material is to restrict oxygen entry or diffusion into the underlying tailings. Organic cover materials were believed to potentially exhibit this property by providing the following: a physical barrier to oxygen migration as a result of naturally high moisture contents; an oxygen consuming barrier through the natural decomposition of the organic material; a decreasing hydraulic conductivity associated with a decomposing, compacting organic cover; and the provision of a carbon substrate for sulphate reducing bacteria growth.

The organic cover materials tested demonstrated that there were significant differences in the ability of each material to provide a beneficial tailings cover. In addition, similarities in some of the characteristic properties of the organic materials did not directly influence their ability to provide desirable cover properties. For example, each of the peat, compost and LSSS exhibited air entry values of <100 cm H_2O and hydraulic conductivity in the range of 10^{-1}-10^{-3} cm/s. Based on these results, these materials would not be expected to perform as good covers. The compost and LSSS, however, were found to be a very good oxygen barrier as they acted as oxygen sinks. In contrast, the peat cover, which had a high humus content and was therefore resistant to further decomposition, was observed to be very susceptible to oxygen diffusion.

The results to date from the pilot scale test cells show that, of all the materials tested, the LSSS appears to perform better as a tailings cover. The LSSS contained a naturally high alkalinity for neutralizing acidity and high concentrations of dissolved organic carbon for biological use. It also exhibited a high O_2 consuming ability, maintained >90% degree of saturation throughout it's depth, had a low surface evaporative flux, and maintained relatively low rates of evaporative loss even under drought conditions. The LSSS cover materials also affected the pore water chemistry of the underlying tailings by causing an increase in pore water pH and DOC concentrations and a decrease in the total iron and sulphate concentrations. The decrease in Fe and SO_4 in the underlying oxidized tailings may have been due to:
1. precipitation of Fe as $Fe(OH)_3$ and SO_4 as $CaSO_4.2H_2O$ and/or,

2. reduction of SO_4 to sulphide by SRB and the subsequent precipitation of sulphides.

In addition, a wide black band, interpreted to be evidence of the reduction and precipitation of sulphide minerals, appeared at the interface of the tailings and the LSSS. The net result was an increase in leachate pH and decreases in leachate sulphate and metal concentrations. While the results for the LSSS are positive in most areas, there are also some negative properties or effects noticed which are specifically related to the LSSS. These include: the very high pH of the material and its potential impact on vegetative growth; the appearance of elevated copper concentrations in the pore water of the cover material; high concentrations of total P in the leachate; the high salt content in the LSSS pore water resulting from the dissolution of salts in the LSSS under drought conditions; and the very high electrical conductivity of the leachate from the tailings-cover system. Although the data to date show no evidence of the dissolution of metals caused by the migration of organic acids into the underlying tailings, concern still exists that this and the effect of reductive dissolution may cause an increase in metals concentrations in the effluent from the oxidized tailings. Due to the many favorable results for this cover material, it is suggested that continued monitoring of this cover system would be a worthwhile effort in providing data on the longer term effects of the cover on the underlying tailings. A parallel bench scale test program using a different LSSS material is ongoing and should provide additional useful information on this material.

The desulphurized tailings exhibited both an air entry value of >200 cm H_2O and a hydraulic conductivity on the order of 10^{-5} cm/s, and contained low salt concentrations. These characteristics are considered to be favorable tailings cover characteristics since they will result in high degree of saturation (>90%), low influent flows and minimal impact on seepage and runoff from the cover. Desulphurized tailings are considered unsuitable for use as a cover material alone, however, due to the high evaporation losses and resultant formation of cracks in the cover that permit oxygen to migrate directly to the underlying tailings. This resulted in an observed increase in the Fe and SO_4 concentrations in the underlying tailings. The high evaporative losses from the surface of the desulphurized tailings also resulted in an

increase in salt concentrations after exposure to drought conditions, although the increase in electrical conductivity at the surface of the desulphurized tailings would not likely pose a threat to plant growth. Growth tests would need to be conducted to confirm this.

It is possible that the application of an evaporation barrier over the desulphurized tailings (to limit evaporative losses), and/or the blending of the desulphurized tailings with an organic material (to provide organic substrate for oxygen consumption) may improve the effectiveness of the desulphurized tailings as a cover material. It is clearly evident that evaporation and salt migration to the surface is an important issue for fine-grained cover materials. This implies that action is required to reduce this effect, such as the construction of an evaporation barrier that would decrease the driving force for upward salt migration. This concept can also be used as erosion control, which may be required to protect fine-grained covers. If the evaporation can be significantly reduced, then the potential for the washing of oxidation products after intervals of net evaporation can also be significantly reduced. The additional benefit of evaporation barrier would be reducing the formation of cracks which act as a conduit for O_2 diffusion.

Under drought conditions, the lowest evaporation rates were noted at the surface of the compost and LSSS covers. The electrical conductivities measured in the compost cover remained constant at 1400 μmhos/cm throughout the drought period for all cover depths, suggesting that the compost was very resistant to evaporative loss and salt migration. The formation of a hardpan, noted at the interface of the compost and the oxidized tailings, may have contributed to the low evaporation and salt migration rates noted. The compost cover also exhibited a high oxygen consumption ability and an alkaline pH. Negative properties of the compost included high NO_3 concentrations in the compost pore water. The DOC concentrations in the underlying tailings pore water indicate that the compost has not interacted with the underlying tailings. The concentrations of Fe and SO_4 in the underlying tailings pore waters continued to show an increasing trend. It is possible that, with time, additional information would come available concerning the effectiveness of this material as a cover material. However, the compost degrades rapidly and would likely not be suitable as a long-term cover material.

Of the organic cover materials tested, peat appears to show the least favorable cover characteristics. The peat exhibited high evaporation rates at the cover surface, and correspondingly, a high percentage increase in salt accumulation at the surface under drought conditions. In addition, the peat did not have any effect on oxygen migration due to a combined inability to consume the incident oxygen and maintain a level of saturation sufficient to reduce the oxygen infiltration rates. Similar to the desulphurized tailings and the compost covers, the Fe and SO_4 concentrations in the underlying oxidized tailings exhibited an increasing trend with time, and the pH in the tailings pore waters remained below 4.0. The DOC concentrations in the underlying oxidized tailings pore water remained at 10 mg/L throughout the test period, indicating that the observed increase in Fe and SO_4 was not due to reductive dissolution processes.

In conclusion, based on the results to date, lime stabilized sewage sludge (LSSS) and desulphurized tailings appear to offer the greatest potential for reducing sulphate and metal loading in water migrating from oxidized tailings to the environment. The reasons for this effect are different for each cover. The LSSS is actively changing the underlying oxidized tailings environment by reversing the ARD processes with an increase in pH, decrease in dissolved metals concentrations and formation of a reducing environment at the cover-tailings interface. The desulphurized tailings have a low hydraulic conductivity and a high degree of saturation, which are two favorable characteristics of the cover. However, the oxidation process is ongoing in the underlying oxidized tailings due to the presence of cracks.

7.0   RECOMMENDATIONS

Due to the nature of the oxidized tailings, sufficient time is required to flush the pores by the replacement of infiltrating waters before determining if only new oxidation is occurring. More time is also required to assess the relative effectiveness of the cover materials at reducing acid generation.

It is recommended that well-designed field scale tests be conducted to provide a more thorough evaluation of cover performance complementary to the laboratory studies described in this report. It is also recommended that the decomposition rate of the organic cover be conducted in situ under the field conditions.

It is also recommended that further investigation be conducted into the use of evaporative barriers for reducing cracking due to drying and maintaining saturation in the fine grained cover layers.

Investigation into the use of blends of LSSS and DST is recommended to improve the performance of the covers by making use of the good properties of both materials, and to improve economics.

8.0   ACKNOWLEDGMENTS

Lakefield Research Limited would like to thank the following contributors to the Covers Evaluation Project.

Mr. Mike Sudbury	Falconbridge Ltd., Toronto, Ontario
Mr. Mark Wiseman	Falconbridge Ltd., Santiago, Chile
Mr. Glen Hall	Falconbridge Ltd., Sudbury Operations, Ontario
Mr. Joe Fyfe	Falconbridge Ltd., Sudbury Operations, Ontario
Mr. Luc St. Arnaud	Noranda Technology Centre, Pointe Claire, Quebec
Dr. S. Lee Barbour	University of Saskatchewan, Saskatoon, Saskatchewan
Dr. Ward Wilson	University of Saskatchewan, Saskatoon, Saskatchewan
Dr. Ron Nicholson	University of Waterloo, Waterloo, Ontario
Dr. Glenn Pierce	Ottawa, Ontario
Mr. Randy Knapp	Senes Consulting, Richmond Hill, Ontario

The following group of technical experts were also consulted and participated in the development of the test program. The technical experts included:

- Mr. Bill Hook   Gabel Corporation, Victoria, British Columbia,
- Mr. Gene Shelp   University of Guelph, Guelph, Ontario,
- Mr. Ward Chesworth   University of Guelph, and
- Mr. Graeme Spiers   University of Guelph

Respectfully Submitted

LAKEFIELD RESEARCH LIMITED

L. Liu, Ph.D.   Linda C.M. Elliott, M.Eng.
Research Scientist   Project Manager

Richard H.O. Wagner, P.Eng   S. Wade Stogran
Project Engineer   Manager - Environmental Services
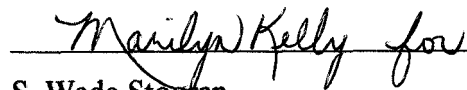
LIST OF PLATES

Plate #1. Hygrothermograph and Potential Evaporation Pan

Plate #2. Strathcona Salt Migration Columns (#1 - #6) January 1995

Plate #3. Strathcona Salt Migration Columns (#7 - #12) January 1995

Plate #4. Strathcona Salt Migration Columns (#13 - #18) January 1995

Plate #5. Interior View of Pilot Cell Showing Probes

Plate #6. Filling Pilot Cell with Tailings

Plate #7. Strathcona Control Cell after Topping Up

Plate #8. Surface Crack in Control Pilot Cell, July 1995

Plate #9. Surface Crack in Desulphurized Tailings, July 1995

Plate #10. Interface Between Mature Compost Cover and Oxidized Tailings, November 1995

Plate #11. Interface Between Peat Cover and Oxidized Tailings November 1995

Plate #12. Interface Between Lime Stabilized Sewage Sludge Cover and Oxidized Tailings,
                November 1995

Plate #13. Interface Between Lime Stabilized Sewage Sludge with Capillary Barrier Cover
                and Oxidized Tailings, November 1995

Lakefield Research Limited
Environmental Services
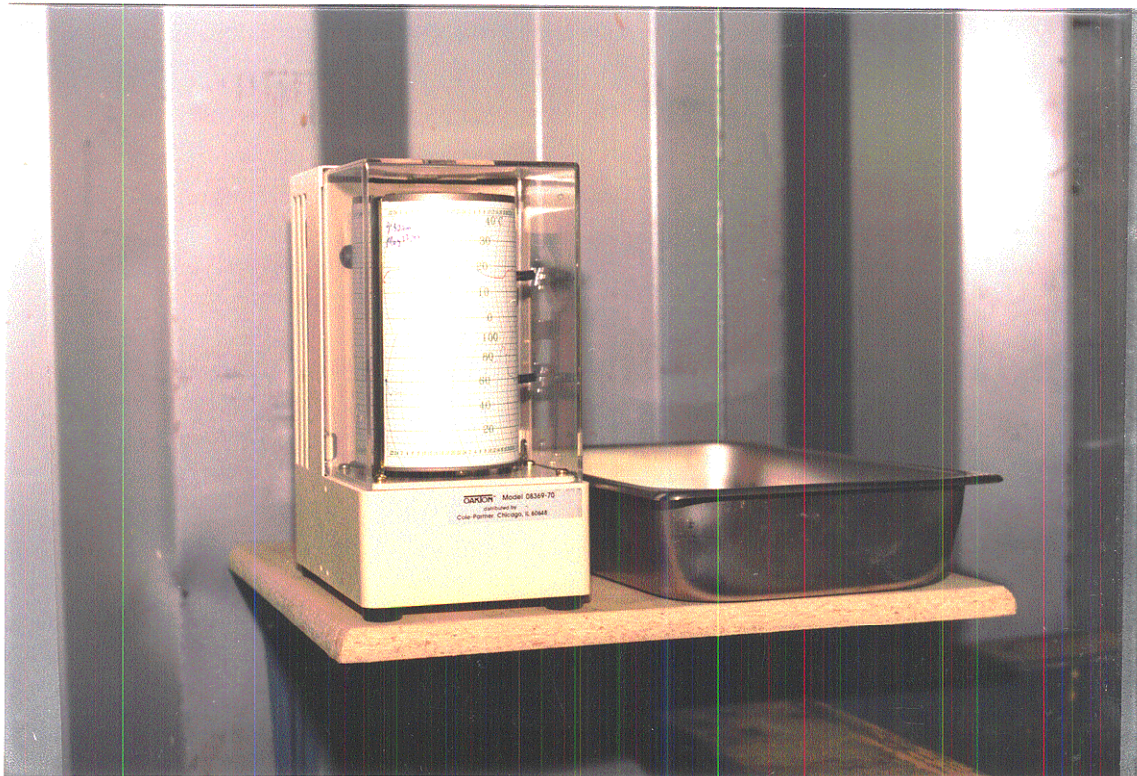
Plate #1:   Hygrothermograph & Pan Evaporation Set-up

Plate #2:   Strathcona Salt Migration Columns
(#1 - #6) January 1995)

Plate #3:   Strathcona Salt Migration Columns
                   (#7 - #12) January 1995)

Plate #4:   Strathcona Salt Migration Columns
                   (#13 - #18) January 1995)
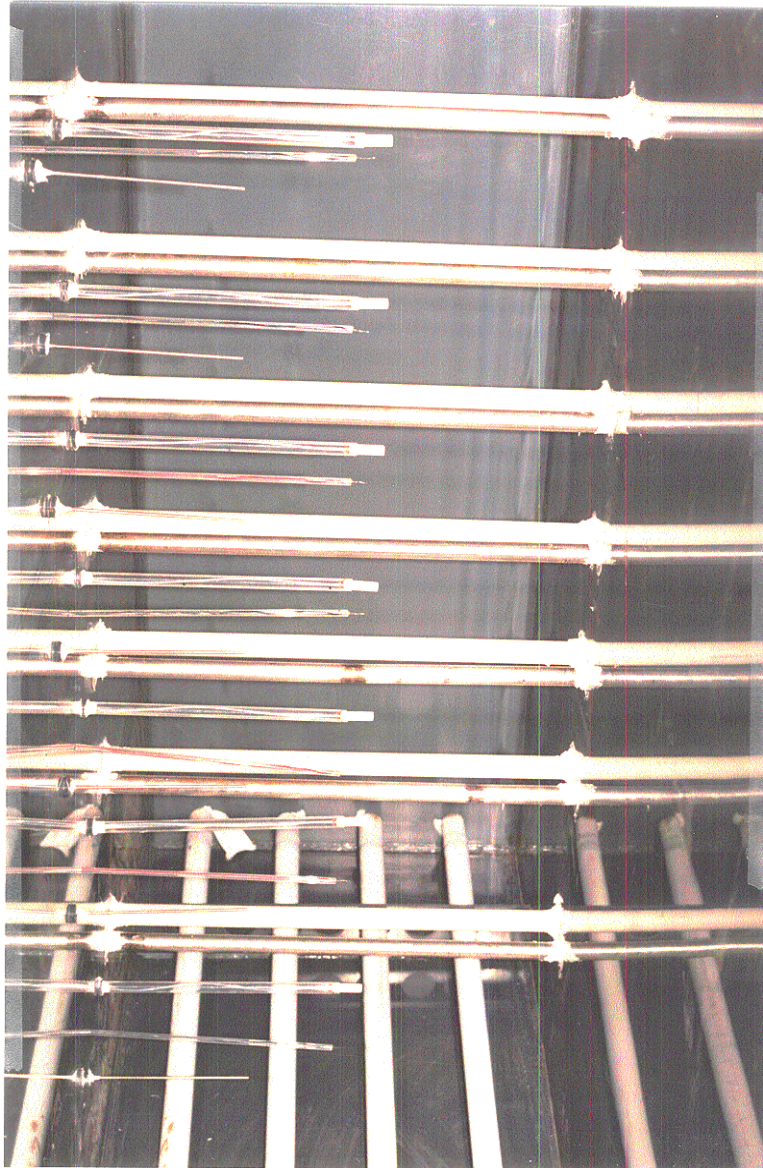
Plate #5:   **Interior View of Pilot Cell Before Filling**

Plate #6:   Filling Pilot Cell with Tailings
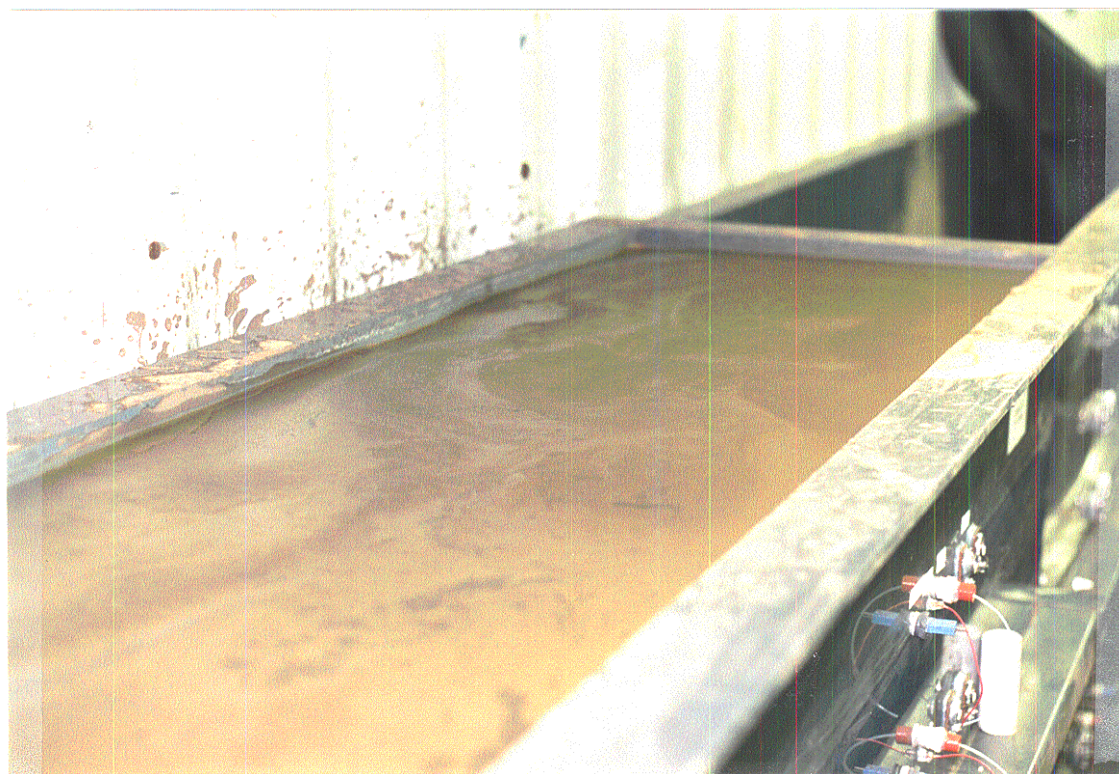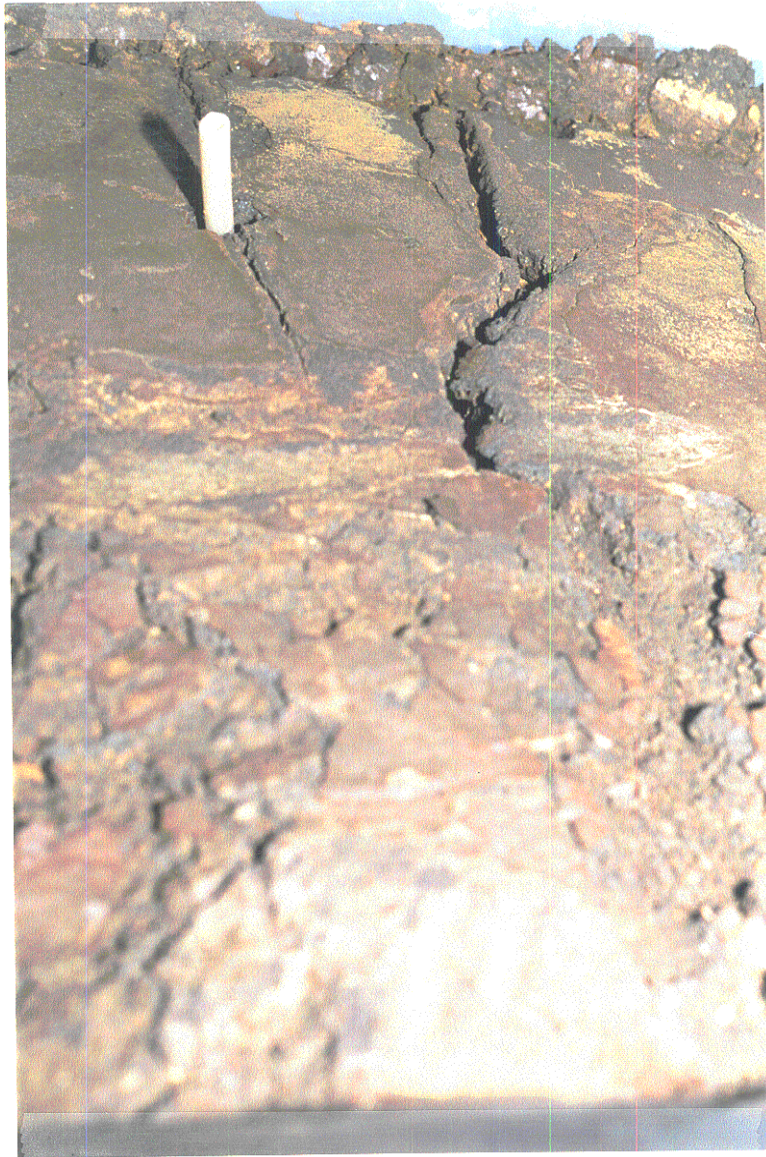
Plate #7:   Strathcona Control Cell After Topping Up

Plate #8:   **Surface Crack in Control Pilot Cell, July 1995**

Plate #9:   **Surface Crack in Desulphurized Tailings Cover, July 95**
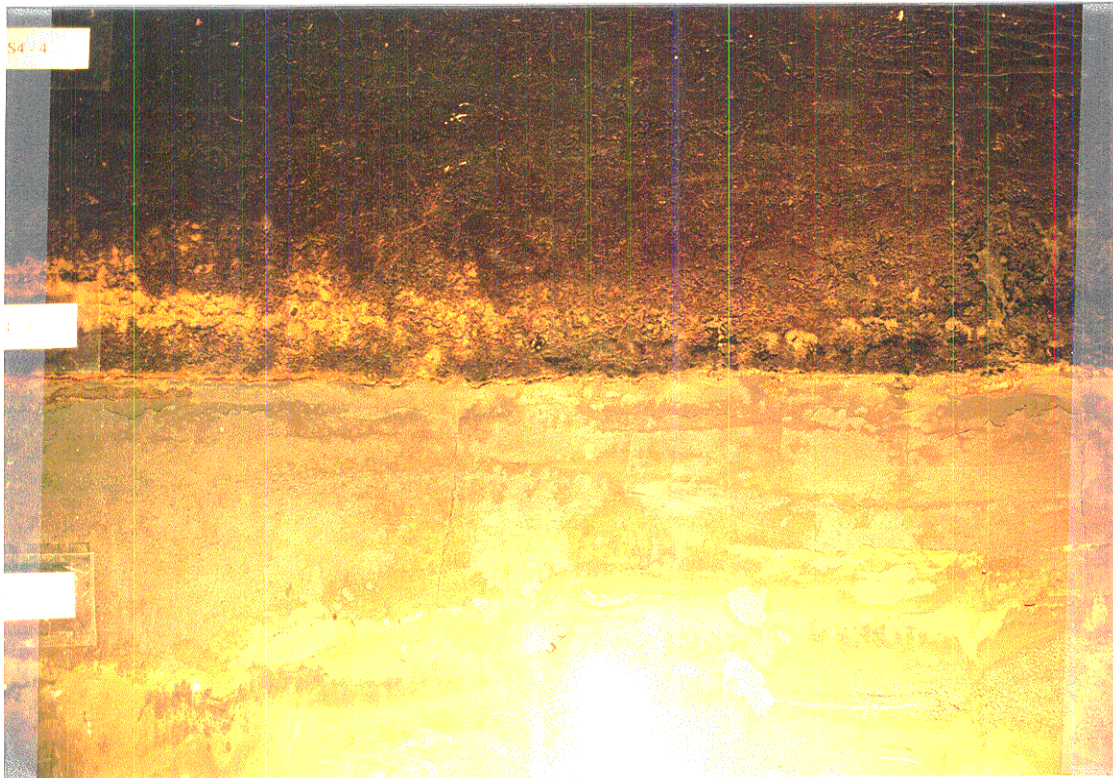
Plate #10:   Interface Between Mature Compost Cover and Oxidized Tailings November 1995
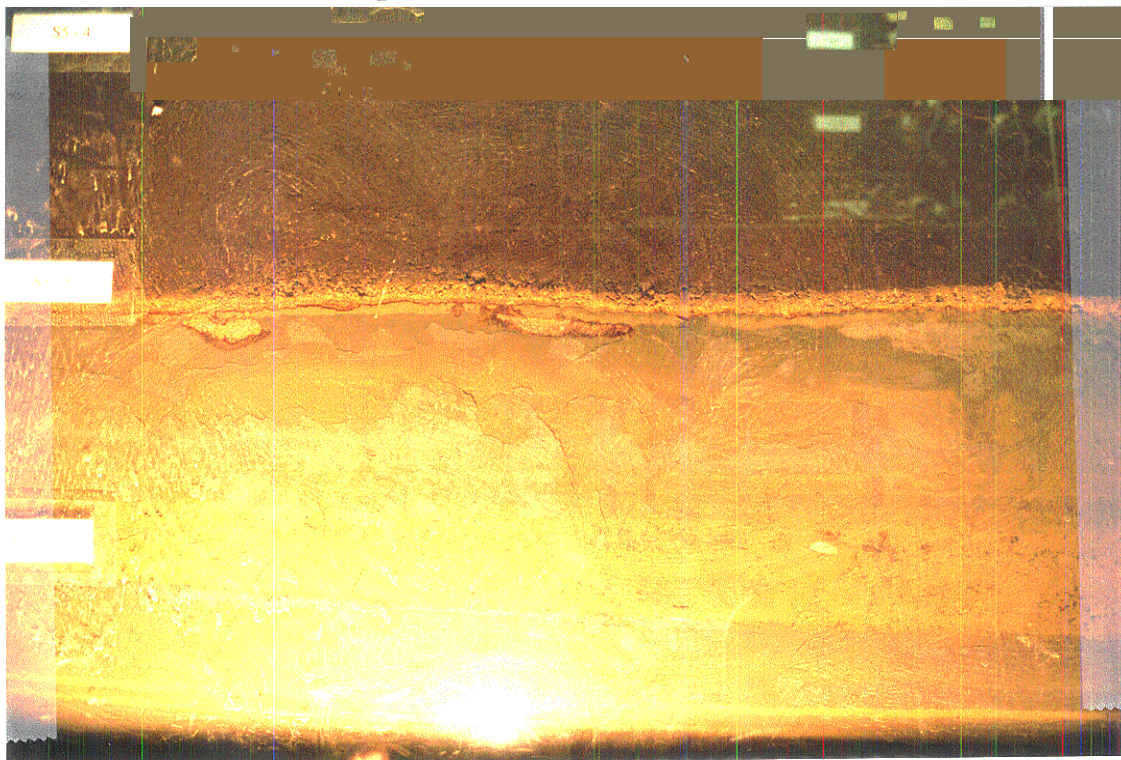
Plate #11:   Interface Between Peat Cover and Oxidized Tailings November 1995
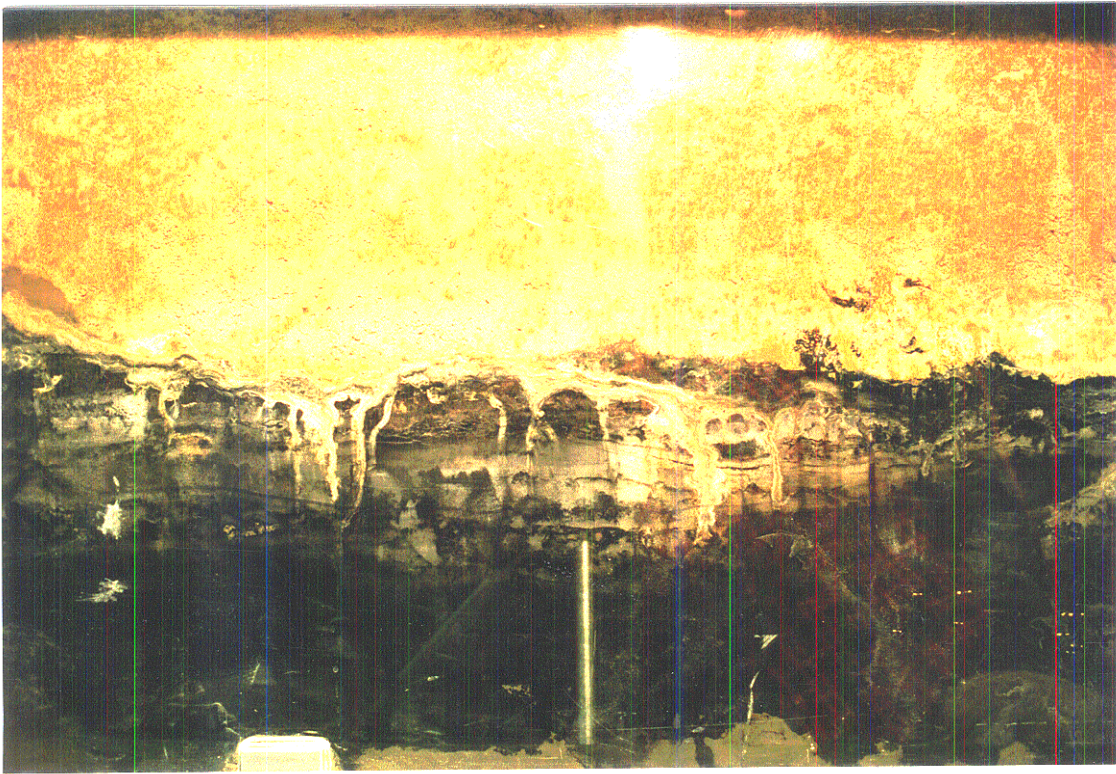
Plate #12: Interface Between Lime Stabilized Sewage Sludge Cover and Oxidized Tailings,November 1995
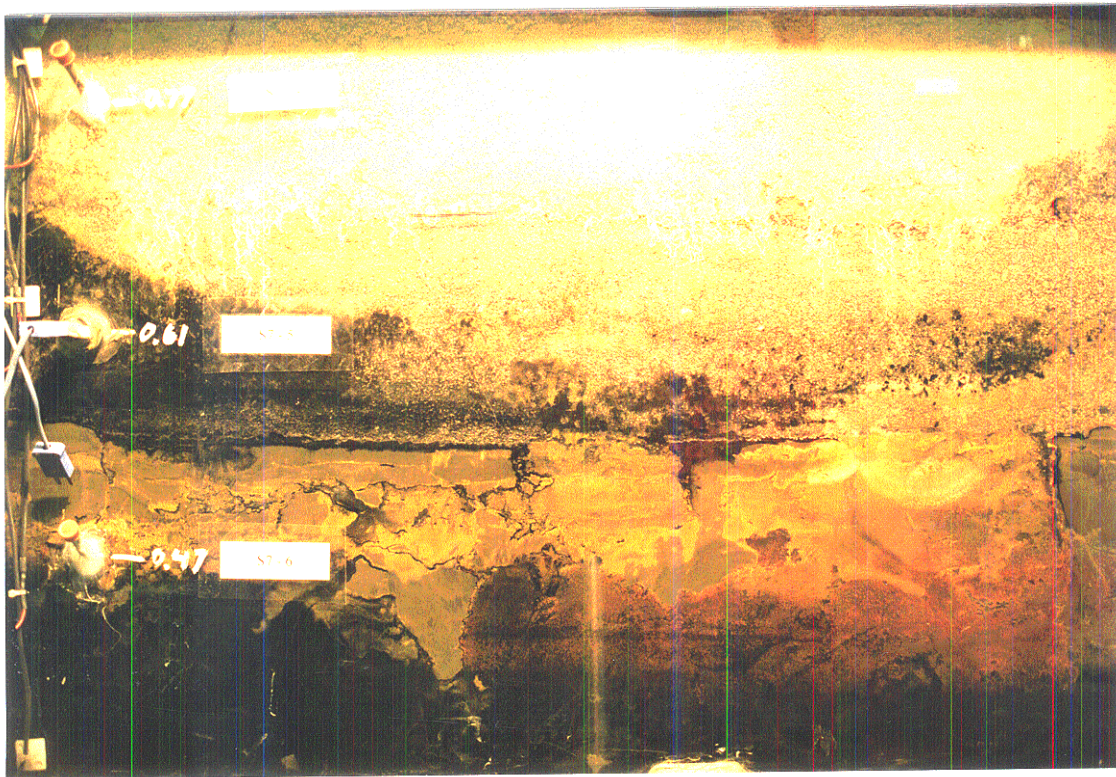
Plate #13: Interface Between Lime Stabilized Sewage Sludge with Capillary Barrier Cover and Oxidized Tailings November 1995

APPENDIX A

**ANALYTICAL RESULTS FOR NEPHELINE SYENITE
AS A FILTER MATERIAL**

LAKEFIELD RESEARCH

A Division of Falconbridge Limited

P.O. Box 4300. 185 Conoession St., Lakefield, Ontario, KOL 2H0

Phone : **705-652-2000** • FAX : **705-652-6365**

Environmental Services

Attn : L. Elliott

Lakefield, October **25**, 1994

Date Rec. : **October** 11, 1994
LR. Ref. : **OCT6196.C94**
Reference : —
Project : **9447511 (7-111)**

CERTIFICATE OF ANALYSIS

Element	Filter Sand**	Duplicate **
C [---]	0.9975	0.9975
N [HCL]	0.0973	0.0973
HCL added [mL]	20	'40
NaOH [added mL]	9.7	25.7
HCL (mL) [consumed]	10	14
NP [*]	24	34
MPA [*]	0.31	0.31
CNNP [*]	24	34
NP/MPA [*]	77	110
S [%]	< 0.01	< 0.01
S= [%]	< 0.01	< 0.01
Paste pH (units]	10.2	--

Constant (C) = (mL acid in blank) / (mL base in blank)
mL acid consumed = (mL acid added) - (mL base added x C)

*NP (Neutralization Potential)
 = (mL acid consumed) x (25) x (N of acid)
*MPA (Maximum Potential Acidity)
 = % Sulphur x 31.25
*CNNP (Common Net Neutralization Potential)
 = NP-MPA

*Results 'expresses as tonnes CaC03 **eq/1000** tonnes material

Note: ** MPA based on 0.01% total sulphur **value.**

Dave Hevenor

A MEMBER OF IAETL **CANADA**

Accredited by CAEAL for specific tests registered with the Association

LAKEFIELD RESEARCH

A Division of Falconbridge Limited

P.O. Box 4300, 185 Concession St., **Lakefield,** Ontario, **KOL 2HO**

Phone : 705-652-2000 • **FAX : 705-652-6365**

Environmental **Services**
- -

Lakefield, October 25, 1994

Attn : L. Elliott

CERTIFICATE OF ANALYSIS

Element.	Filter Sand
Leachate [solution]	1
Vol. Soln [mLs]	2000
Moisture [%]	< 0.1
Init. **pH** [units]	4.87
Final **pH** [units]	**8.82**
Al [mg/L]	0.62
As [mg/L]	< 0.05
Ba [mg/L]	< 0.02
Be [mg/L]	< 0.005
Ca [mg/L]	2.48
Cd [mg/L]	< 0.01
Co [mg/L]	< 0.02
Cr [mg/L]	< 0.02
Cu [mg/L]	< 0.02
Fe [mg/L]	0.02
Mg [mg/L]	0.07
Mn [mg/L]	0.01
Mo [mg/L]	< 0.05
Na [mg/L]	1.88
Ni [mg/L]	< 0.02
P [mg/L]	< 0.10
Pb [mg/L]	< 0.05
S [mg/L]	0.60
Sb [mg/L]	< 0.05
Se [mg/L]	< 0.01
Si [mg/L]	0.86
Sn [mg/L]	c 0.10
Te [mg/L]	< 0.05
Zn [mg/L]	< 0.01
Hg [mg/L]	< 0.001

Extraction Fluid # 1

ASTM EPA + ICP SCAN

OD trace . Te risn
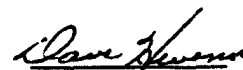
Russ Calow

A MEMBER **OF IAETL** CANADA

Accredited by CAEAL for specific tests registered with the Association

Environmental   Services

Lakefield, October 25, 1994

Date Rec. : October 11, 1994
LR. Ref.   : **OCT6197.C94**
Reference : ---
Project   : 9447511

Attn : L. Elliott

CERTIFICATE OF ANALYSIS

Modified ASTM D3987 Shake Extraction

Element	Filter Sand
moisture **[%]**	< 0.1
InitialpH [units]	7.16
Final **pH** [units]	9.04
As **[mg/L]**	< *0.05*
Ag **[mg/L]**	< *0.02*
Ba **[mg/L]**	< *0.02*
B **[mg/L]** .	< *0.02*
Cd **[mg/L]**	< 0.01
Cr **[mg/L]**	< *0.02*
Pb **[mg/L]**	< *0.05*
Hg **[mg/L]**	< *0.001*
Se **[mg/L]**	< 0.01
NO2 as N **[mg/L]**	< *0.006*
NO3 as N **[mg/L]**	< *0.005*
F **[mg/L]**	*0.07*
CN− **[mg/L]**	< 0.01
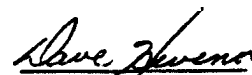
Dave Hevenor

A MEMBER OF **IAETL** CANADA

Accredited by CAEAL for specific tests registered with the Association

Cost 225 - 100 Leach + 125 Test

APPENDIX B

**RESULTS OF UNIVERSITY OF SASKATCHEWAN
COMPUTER MODELING OF CELL**

MEMORANDUM

To: Lee Barbour

From: Darren Swanson

Date: December 21, 1994

Re: **Additional preliminary modelling for the Faiconbridge Research and Development Tailings Cover Project**

Included are the results of additional generic modelling for the Falconbridge cover physical model as requested.   Please review and get back to me if modifications or additional simulations are required.

Objective

The objective of the generic modelling exercise is to illustrate possible performance scenarios of the proposed physical model for the following conditions:

- a no flow lower boundary
- a lower drainage boundary
- various capillary barrier lengths.

Methodology

Generic soil properties were specifically designed to so that a capillary break could be effectively illustrated. The generic properties requested for the additional modelling would not illustrate the capillary break effect due to the similarity of air entry values between the cover and the capillary barrier materials. The properties selected for the generic modelling are attached.   The air entry value of the cover material is approximately three times the air entry value of the capillary barrier.

The simulation of three boundary condition scenarios was requested For each boundary condition scenario three capillary barrier lengths were requested. The requested simulations are summarized as follows:

	top boundary	lower boundary	right -boundary	capillary barrier	length
la	flux	drainage	no flow	Partial	
lb	flux	drainage	no flow	full	
1 c	flux .	drainage	no flow	none	
2a	flux	drainage	drainage	Partial	
2 b	flux	drainage	drainage	full	
2c	flux	drainage	drainage	none	
3a	flux	no flow	drainage	Partial	
3 b	flux	no flow	drainage	m l	
3c	flux	no flow	. drainage	none	

Scenarios 2a, 2b, and 2c were not simulated. With a lower suction boundary present there is no possibility of lateral drainage from the physical model Scenarios 1 and *2* would give the same results. Scenarios 1 and 3, were performed for a total of six simulations. All results are for steady state conditions. The surface flux is equivalent to 400 mm/year. A lower head boundary of -2.5 m (approx. 25 kPa negative pore-water pressure) was used for the lower drainage boundary scenarios.

Summary of Results

The simulation results for scenarios la-c, and 3a-c, are attached. For each simulation a contour plot of total head (m) is provided along with vertical cross-section profiles of pore-water pressure (kPa) and vohunetric water content.

- The capillary break effect was evident in the lower drainage boundary scenarios #la and #lb. A capillary break was not produced in the no flow lower boundary scenarios #3a and #3b. Appreciable negative pore-water pressures could not develop in the tailings for the no flow lower boundary scenarios due to the water ponding. A capillary break is not produced for the no flow lower boundary scenarios because the capillary barrier can sustain the low pore-water pressures that developed in the tailings. The capillary barrier only becomes effective when the negative pore-water pressures in the underlying tailings become greater thau the negative pore-water pressure corresponding to the residual water content of the capillary barrier. The air entry value of the cover must be higher than this negative pore-water pressure for the cover to remain saturated.

- The extent of the capillary break depended on the length of the capillary barrier. A full capillary break was seen in the full capillary barrier scenario #lb. No capillary -break was seen in the no capillary barrier scenario #1c. It follows that a partial capillary 'break was seen for the partial capillary barrier scenario #la. The high suctions that build up in the tailings are transferred to the overlying cover at locations where there is no capillary barrier present. The flow pattern that developed for scenario #la is a classic example of unsaturated flow. The hydraulic conductivity of the capillary barrier is significantly lower than the cover material for the negative pore-water pressures that developed at the interface between the two materials. This resulted in the Lateral flow patterns seen in the total head plots.

- A water table developed halfway through the tailings for the no flow lower boundary scenarios. The height of the' water table depends on the relative difference between the surface flux applied and the saturated hydraulic conductivity (Ksat) of the tailings material. For these simulations, the Ksat of the tailings is approximately 10 times greater than the applied surface flux (it should be noted that the original generic modelling dated Nov. 28, the Ksat of the tailings was an order of magnitude lower than the silt tailings Ksat used in this report).

Keynote Observations

- A capillary break does not develop for a lower no flow boundary.

- A capillary break will develop for a lower drainage boundary when a negative pore-water pressure is maintained at the base which is greater than the negative pore-water pressure corresponding to the residual water content of the capillary baker. This is provided the cover material has a higher air entry value than the capillary barrier.

- A full capillary break is not achieved for a capillary barrier that extends only part way across the length of the model. Lateral flow develops around the partial capillary barrier for a lower drainage boundary.

- The extent of water ponding, for a no flow lower boundary, depends on the relative difference between the applied surface flux and the saturated hydraulic conductivity of the tailings.

3

Upper graph:

Y-axis (right): Volumetric Water Content — 5.00E-01, 4.50E-01, 4.00E-01, 3.50E-01, 3.00E-01, 2.50E-01, 2.00E-01, 1.50E-01, 1.00E-01, 5.00E-02, 0.00E+00

X-axis: Pore-Water Pressure (kPa) — -100, -80, -60, -40, -20, 0

Curve labels: tailings, cover, capillary barrier

Lower graph:

Y-axis (right): Hydraulic Conductivity (m/s) — 1.00E+00, 1.00E-02, 1.00E-04, 1.00E-06, 1.00E-08, 1.00E-10, 1.00E-12, 1.00E-14

X-axis: Pore-Water Pressure (kPa) — -100, -80, -60, -40, -20, 0

Curve labels: tailings, cover, capillary barrier
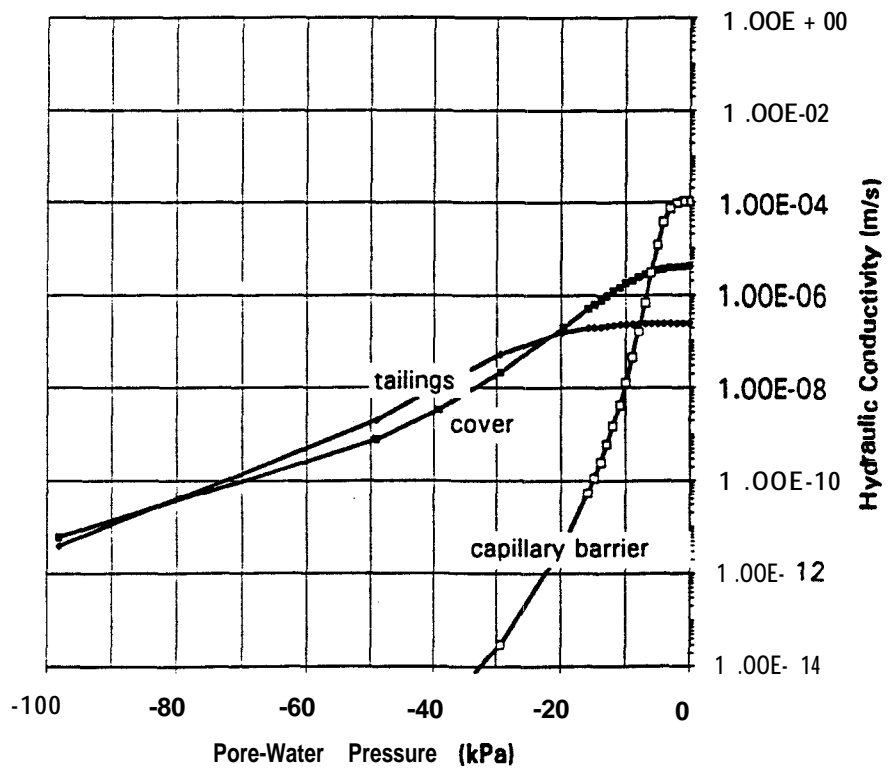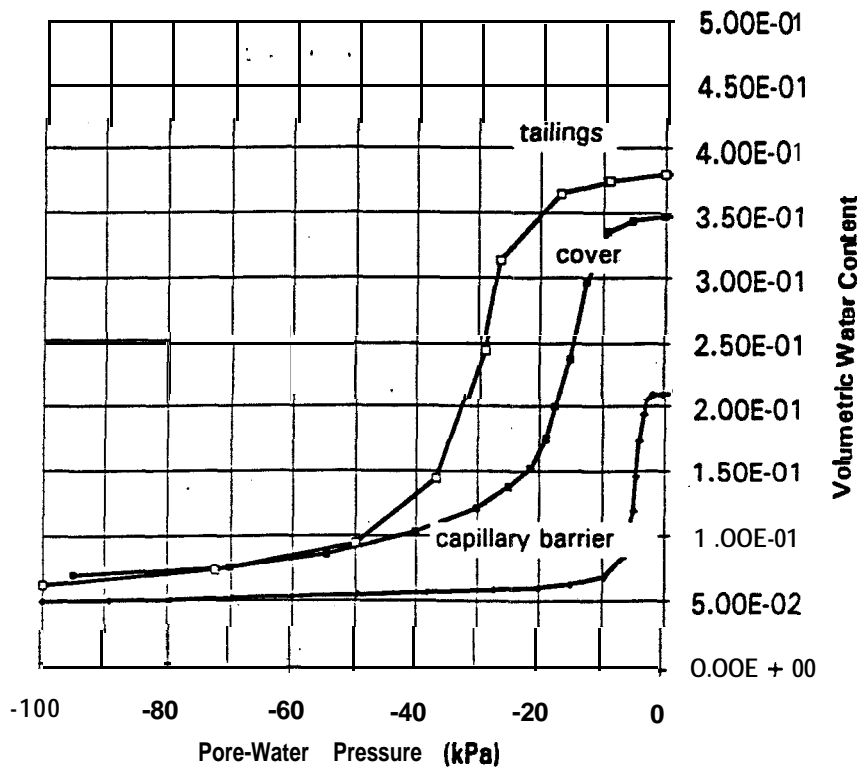
Material Properties
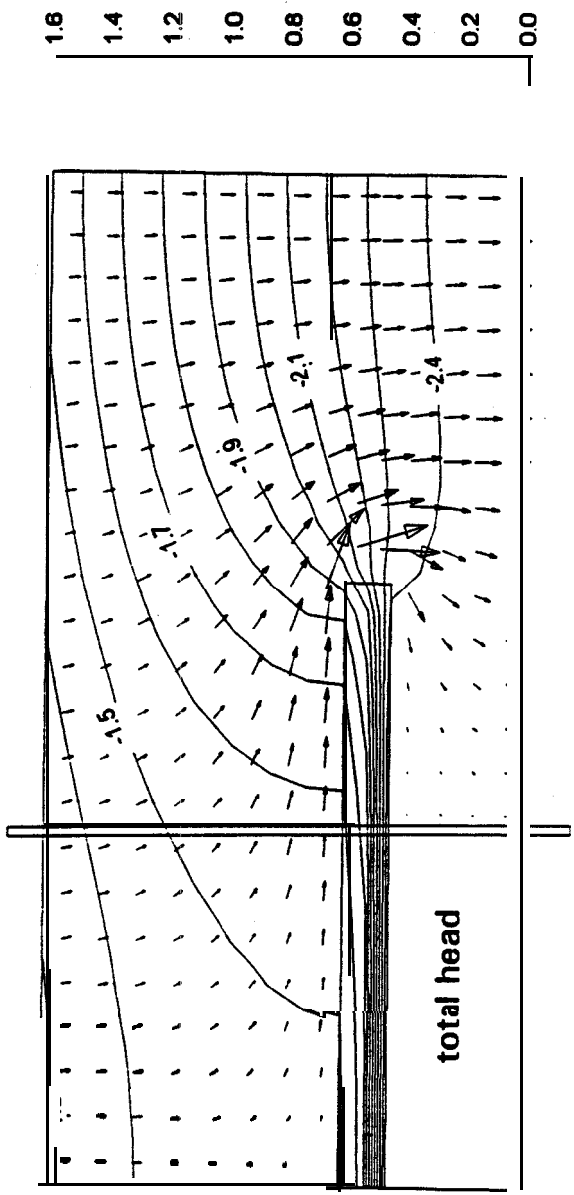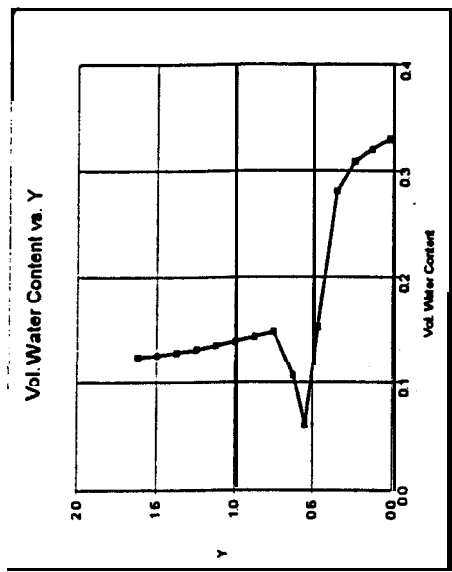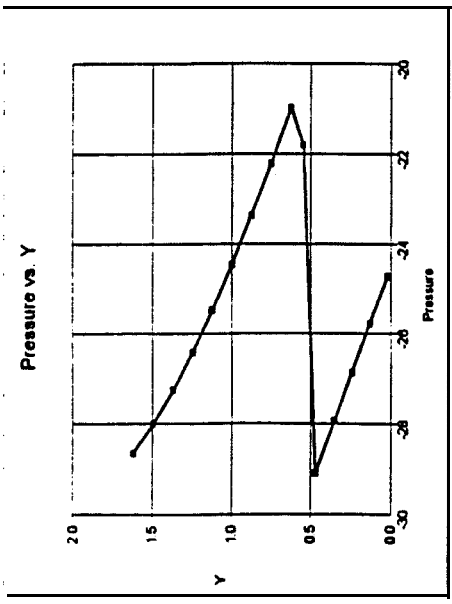
Scenario #1a (lower suction boundary of -2.5 m, partial capillary barrier)
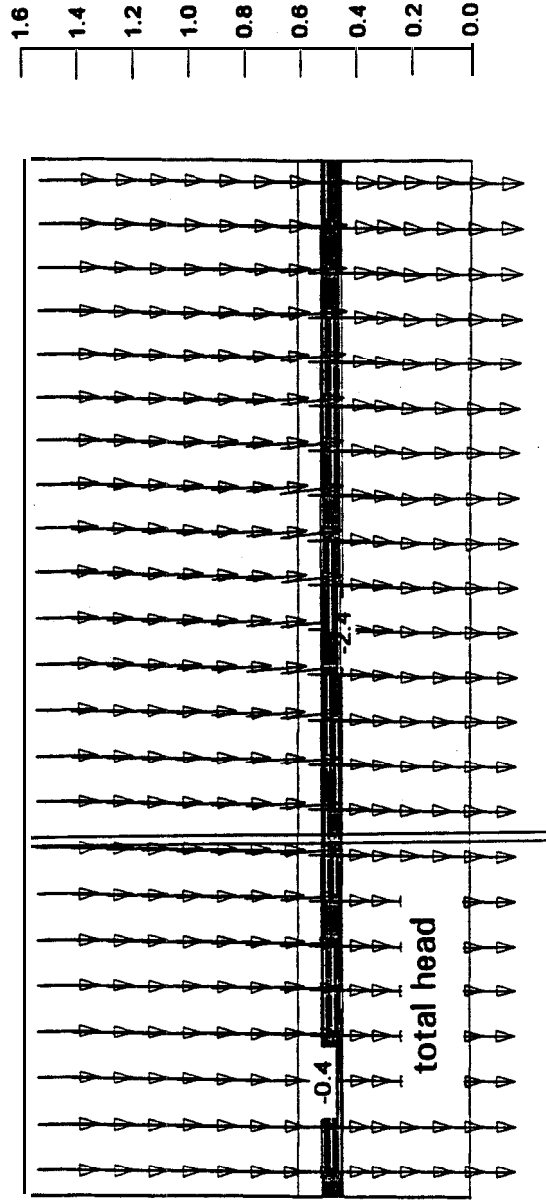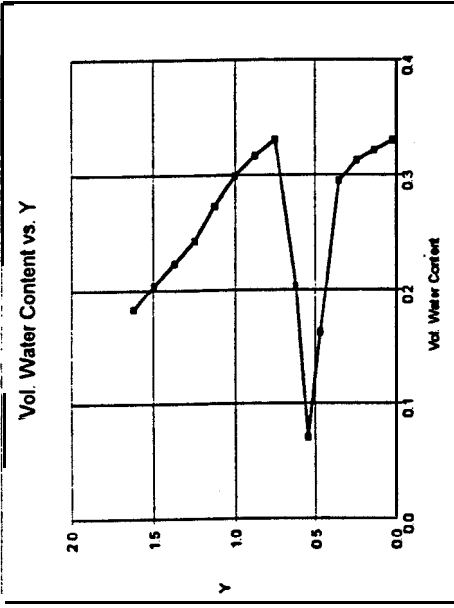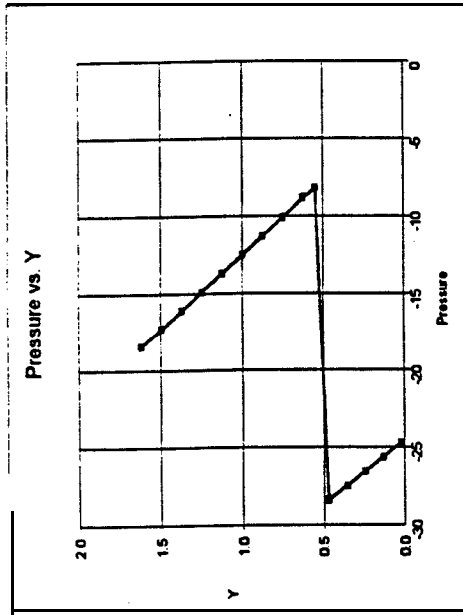
Scenario #1b (lower suction boundary of -2.5 m, full capillary barrier)
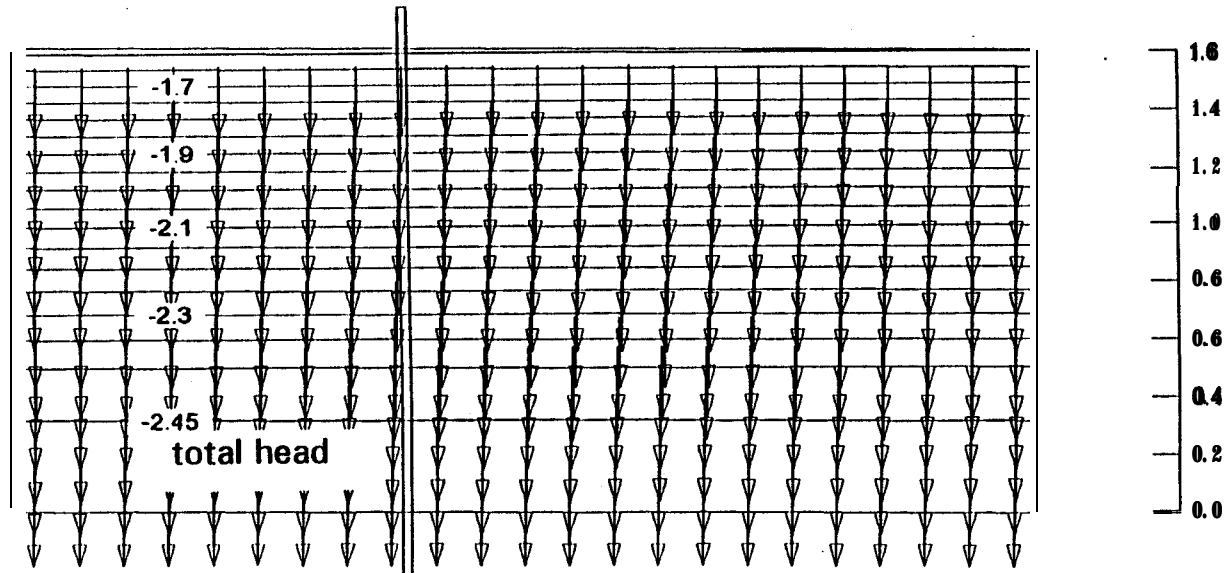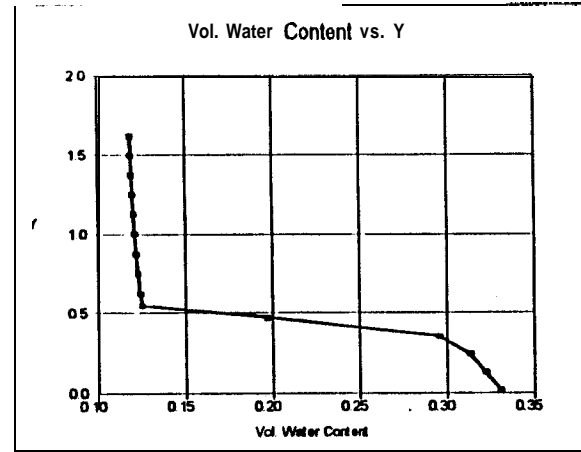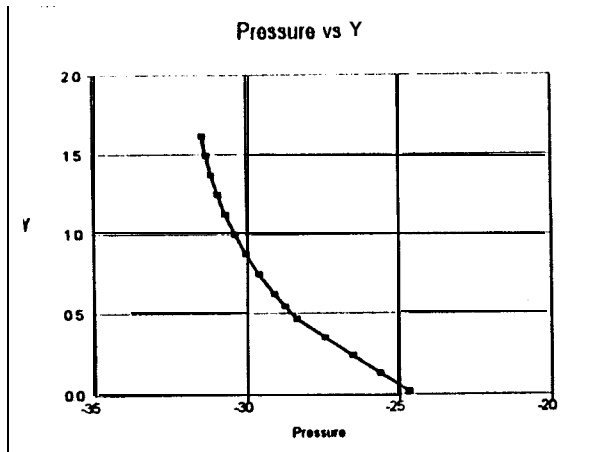
Scenario #1c (lower suction boundary of -2.5 m, no capillary barrier)

Vol. Water Content vs. Y

Pressure vs. Y
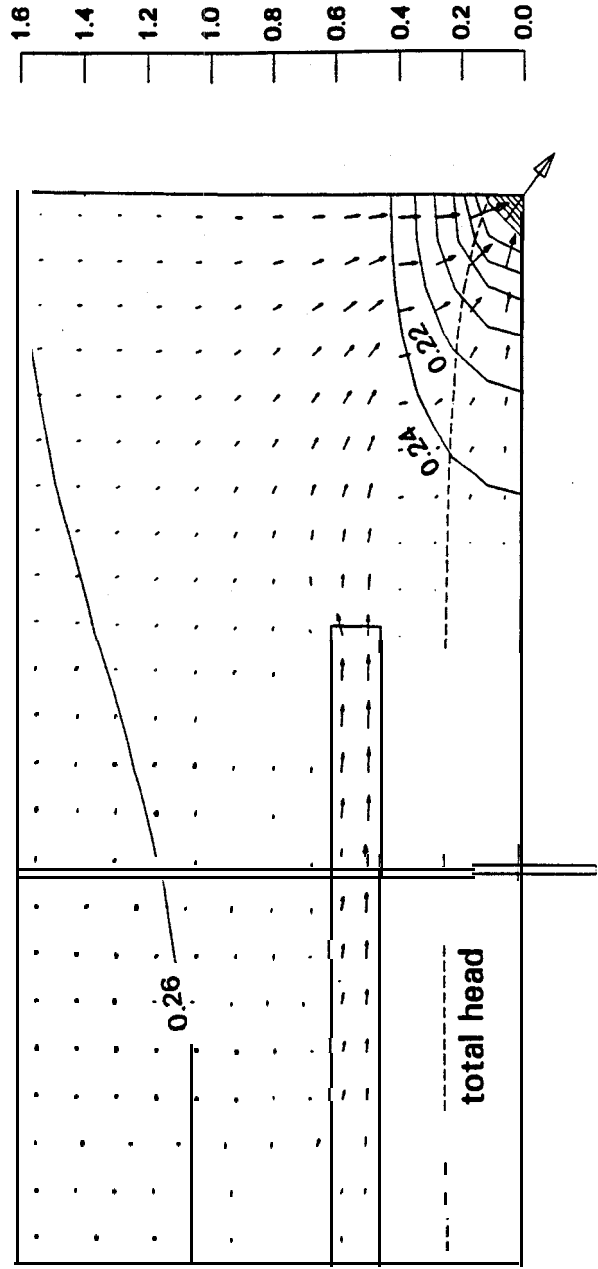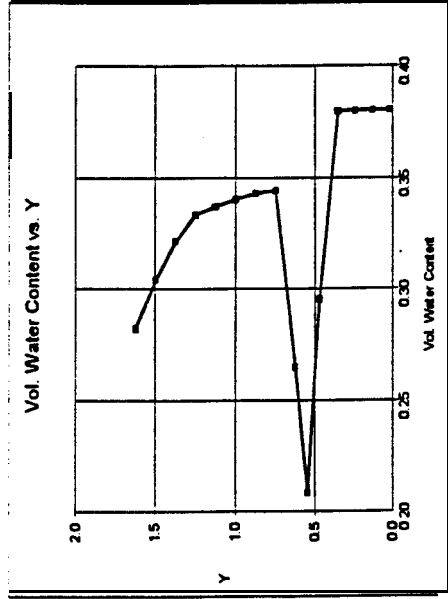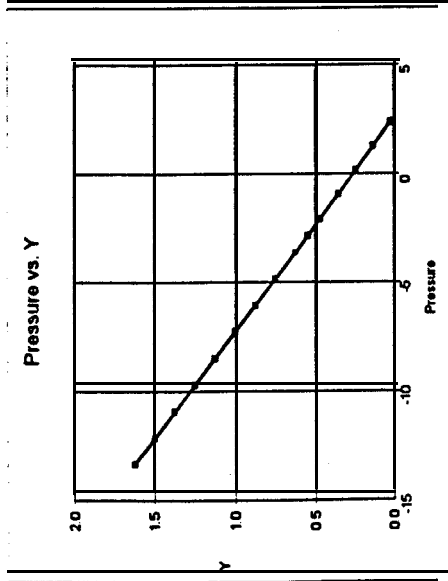
Scenario #3a   (lower no flow boundary, partial capillary barrier)

Vol. Water Content vs. Y

Vol Water Content

Y

2.0 1.5 1.0 0.5 0.0

0.20 0.25 0.30 0.35 0.40

Pressure vs. Y

Pressure

2.0 1.5 1.0 0.5 0.0

-15 -10 -5 0 5

1.6
1.4
1.2
1.0
0.8
0.6
0.4
0.2
0.0

0.24

total head
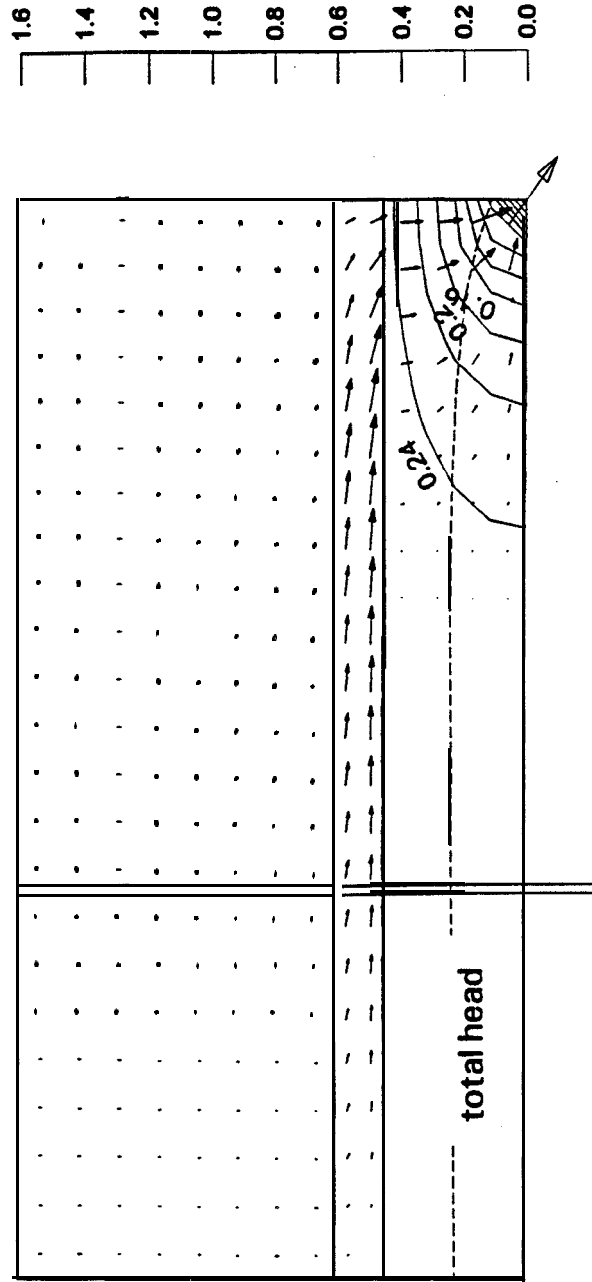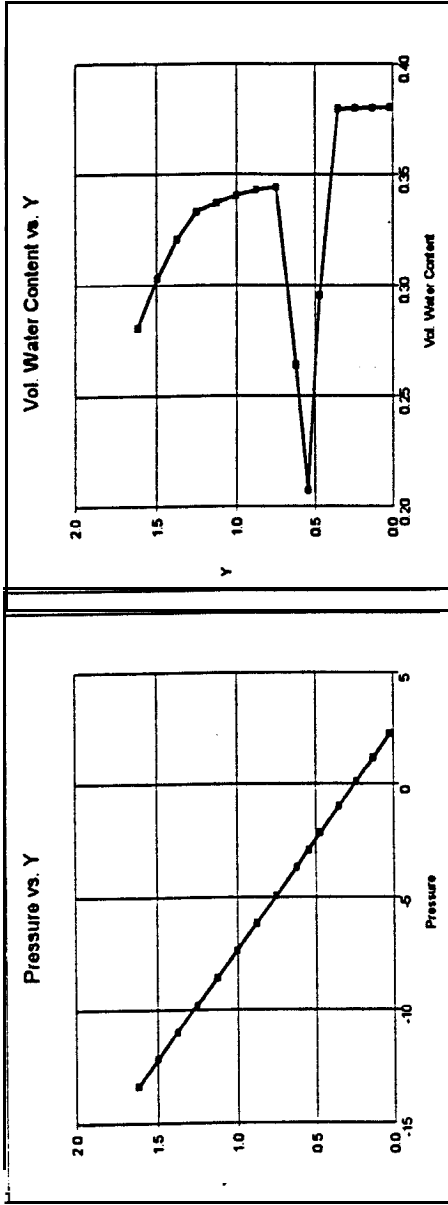
Scenario #3b   (lower no flow boundary, full capillary barrier)
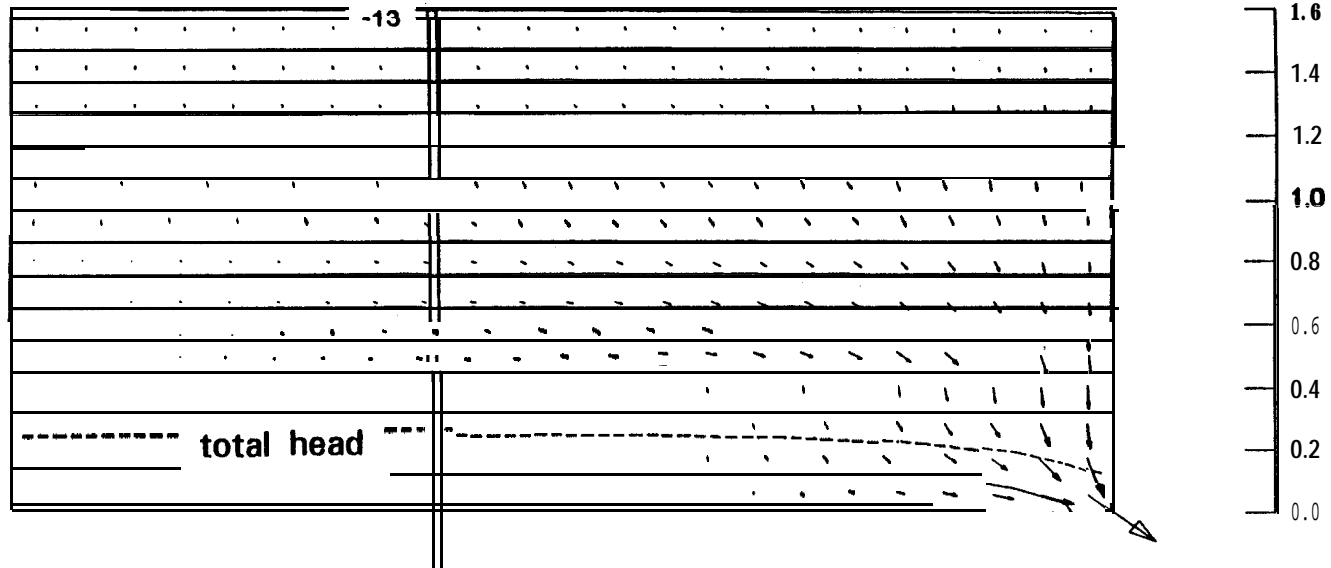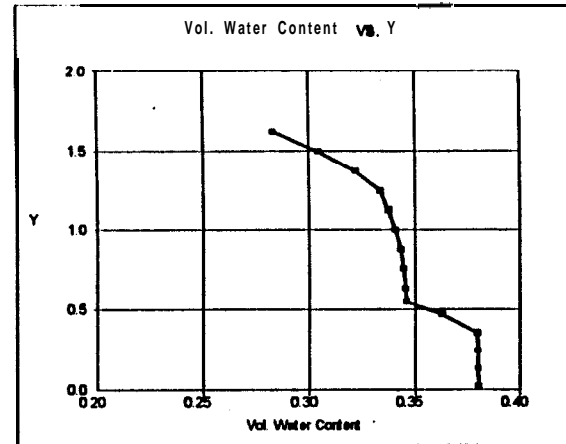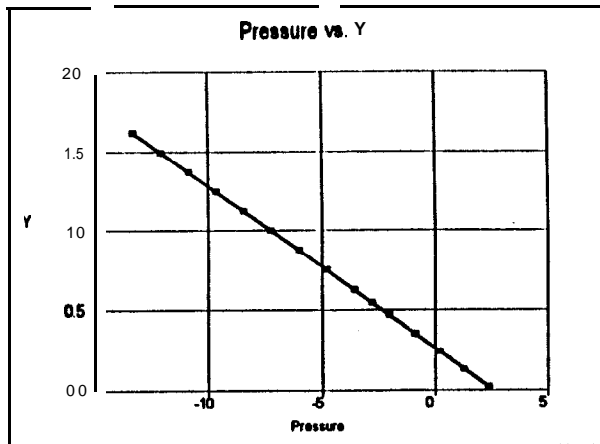
Scenario #3c (lower no flow boundary, no capillary barrier)

APPENDIX C

PILOT CELL SATURATION PROCEDURE

STRATHCONA PILOT CELL SATURATION PROCEDURE

Objective: Add rainfall until cells are saturated, then allow to drain to field capacity by applying vacuum at 3.75" Hg until no further water flows from the cells.

Saturation procedure:

1.   Fill plastic container with tap water from garden hose.
2.   put pump/mixer in water to aerate and leave running overnight (minimum 12 hours aeration). Record the time of aeration and maintain this as a constant during the life of the program.
3.   Add 60:40 sulfuric acidnitric acid and adjust to pH 4.2, continue to stir while preparing acid and taking reading. Record pH.
4.   Collect a sample for analysis at the lab for the first batch made and submit to the lab for analysis of a number of parameters.
5.   Turn Vacuum off.
6.   Add 22 liters of acid rain (600 mL/min) per hour per cell every two days. This will need to be applied over the entire cell relatively consistently. Our current system consists of manually spraying the acid rain through a garden hose attachment to the sump which would be placed in the bottom of the acid rain tank. One tank will provide sufficient water to wet 20 Strathcona cells at the above application rate.
7.   Record the date, start time, volume and duration of the ram application for each cell.

Collect water from drainage trays at the end of the cells and record water volumes collected. Keep a close eye on this to ensure all water is captured and measured.

Continue this process until the cells appear saturated (free water visible at surface). Check the TDR results against the calibration curves. Saturation is approximately 40% moisture content by weight for most of the materials involved.

APPENDIX   D

RAINFALL   APPLICATION   FOR   STRATHCONA   PILOT   CELLS

RAINFALL APPLICATION-STRATHCONA CELLS

Rainfall is to be applied to the cells once per week. Rates of application are calculated on the following basis.

R = Strathcona rainfall/application x area of application x lab PE/ Strathcona PE

Strathcona mean annual rainfall: 872 mm/yr*

Strathcona Pan Evaporation Rates: 550 mm/yr*

*(from Environment Canada, Average 20 year rainfall data for the Sudbury Airport, and pre- 1965 pan evaporation averages for the Sudbury Basin)

Therefore:

R = rainfall x application rate x area of application (cell) x lab PE ÷ Sudbury PE

R = 0.872 m/yr ÷ 52 weeks/yr x 1.5 m2 x 340 mm/yr ÷ 550 mm/yr

= 15.5 litres per application per cell (for weekly application)

Monitor and record discharges from each drainage tray at each cell. Check collection bottles daily to ensure all water is captured.

Note: Pan evaporation rates for the lab are preliminary and may require modification in future. On-going analysis is being performed for the Strathcona container.

APPENDIX E

TDR CALIBRATION TEST RESULTS

Compost

Moisture Content	Time Delay (ns)	
(% By Weight)	2"	4.75"
1	9.63	11.07
34	14.66	17.24
45	14.93	18.08
56	17.96	

Peat

Moisture Content	Time Delay (ns)	
(% By Weight)	2"	4.75"
43	12.52	14.95
50	15.23	19.15
54	18.53	20.1

STRATHCONA COVERS EVALUATION
COMPOST
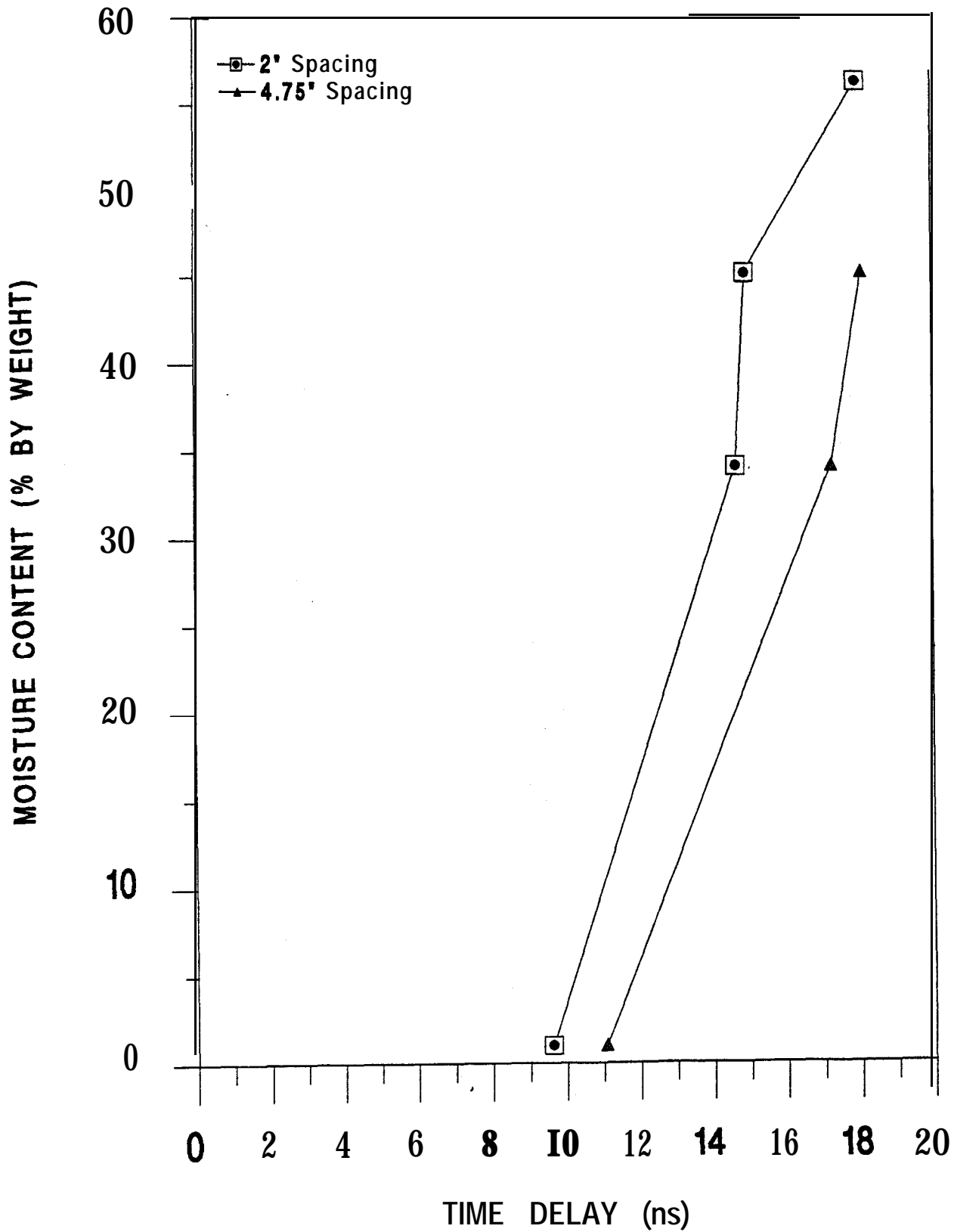
STRATHCONA TAILINGS COVER EVALUATION
PEAT

Chart showing MOISTURE CONTENT (% BY WEIGHT) on the vertical axis (40 to 60) versus TIME DECAY (ns) on the horizontal axis (10 to 30).

Legend:
- 2' Spacing
- 4.75' Spacing
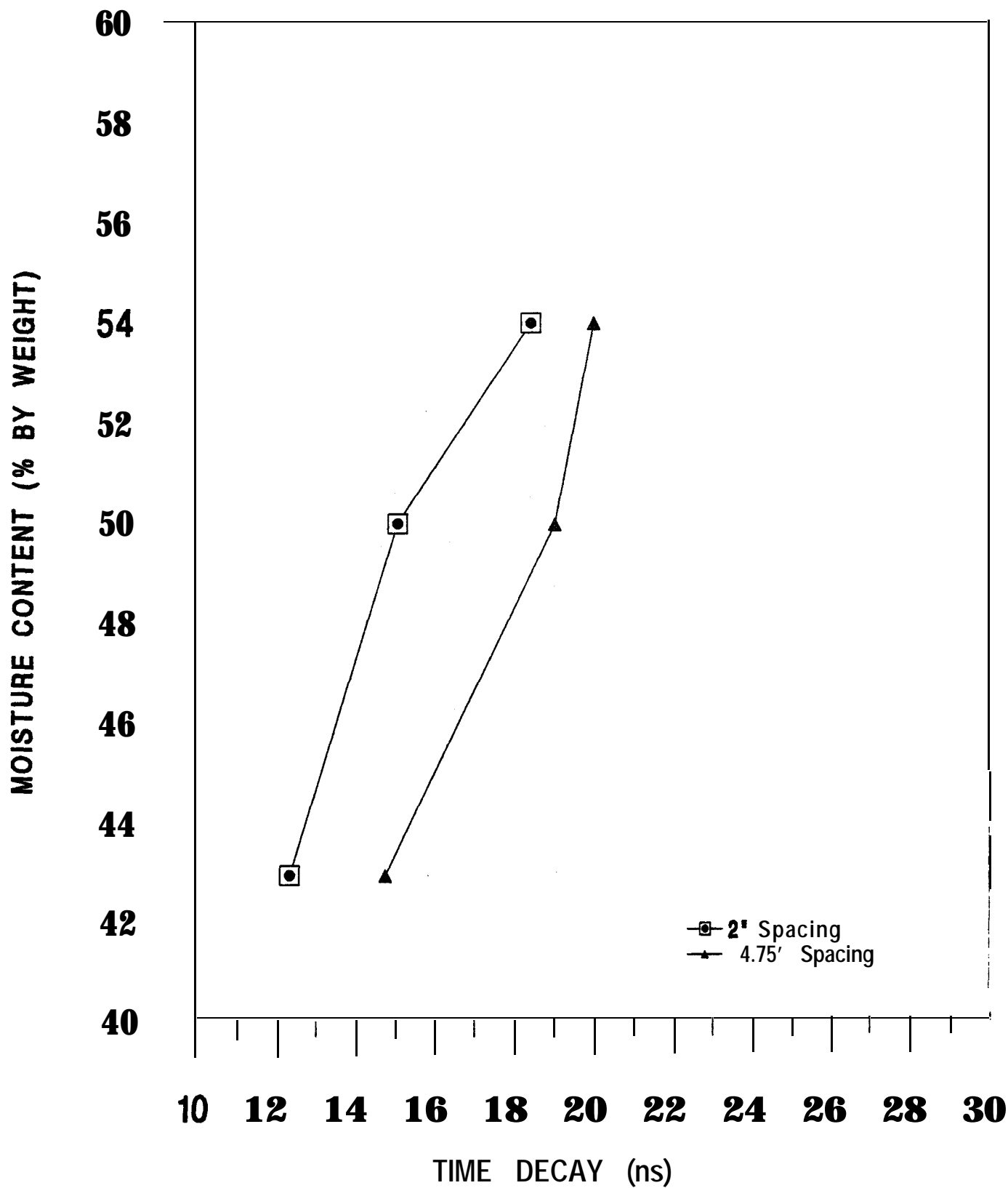
APPENDIX F

SATURATED EXTRACTION PROCEDURE

Procedure for Extracting Pore Water From Dry Pilot Cells

Objective: To extract solution sample from solids sample taken from the pilot cells. This procedure is only used when adequate pore water cannot be extracted in situ.

Theory: The analysis of the pore water in the pilot cells provides important chemical and physical data which is integral to the understanding of the internal processes in a covered tailings situation. Often the pore water cannot be extracted through in situ means. This may be due to capillary suction forces, blocked porous cap on the solution sampler, or the presence of cracking. In such a situation an alternative sampling procedure has been devised to extract pore water. It involves taking a solid soil sample from the pilot cell at the affected level and extracting the pore water later through saturated paste method.

Health, Safety, and Environmental Implications:
Latex gloves, eye protection, and steel toed boots should be worn at all times while sampling the pilot cells and working in the lab in the extraction procedure.

Equipment List:
- utility knife
- latex gloves
- core sampler
- eye protection
- distilled water
- sample containers (60 mL)
- spatula
- filter funnel lined with a 0.45 μm filter paper
- vacuum source

Procedure: Use a core sampler to sample the soil at the locations illustrated on the attached page. See the appropriate procedure for using the core sampler. Extract the core from the sampler and split it in half using the utility knife. The two halves must be placed in separate labeled sample containers (60 mL) immediately after extraction in order to prevent moisture loss. One of the two halves must be placed in the freezer for storage. Send the remaining half to the Environmental Lab at Lakefield Research Limited. The amount of sample used depends on the number of measurements being made on the extract. A 250-g sample provides sufficient extract for most purposes.
In the lab, add distilled water to the sample while stirring it with a spatula. At saturation the paste will glisten as it reflects light, flow slightly when the

container is tipped, and the paste slides freely and cleanly off the spatula. After the mixing allow the sample to stand for at least 1 hour and then recheck for saturation. Free water should not collect on the surface. If the paste **stiffens,** or loses its glisten, add more water and remix. If **free** water exists on the surface after standing, add more sample and remix. Transfer the paste to the filter funnel lined with a 0.45 pm filter paper and apply vacuum. Save the filtrate for metals and other analysis.

Note: Two extreme situations may exist in this procedure.

1. Large amounts of water soluble material is present. Thus pore water is saturated with salt. Addition of more water will dissolve more salts, may be to saturation ?

2. Pore water present may have dissolved all soluble salts. Thus the addition of more water will only dilute existing pore water.

Will this procedure tell you what you want to know considering the 2 above situations ? In reality most samples will probably fall between these two conditions.

APPENDIX G

MINERALOGICAL EXAMINATION OF STRATHCONA
SULPHIDE TAILINGS AFTER ONE YEAR PILOT CELL TESTING

**Mineralogical Examination
of Strathcona Sulphide Tailings
After One Year Pilot Cell Testing**

Project No: 7777-112

NOTE: This report refers to the samples as received.
The practice of this Company in issuing reports of this nature is to require the
recipient not to publish the report or any part thereof without the written consent of
Lakefield Research Limited.

6

Mineralogical Examination of
Strathcona Sulphide Tailings

Summary

Nine samples (l-0, 1-6, 2-6, 3-6, 4-6, 5-6, 6-6, 7-6, 8-6) were submitted to the mineralogy laboratory for general mineral identification, and chemical and textural characterization, with special emphasis on the presence or absence of textures indicative of sulphide oxidation. The aim of the study was to determine the comparative stability of the sulphide tailings, which had previously been covered with different materials (i.e. lime-stabilized sewage sludge (LSSS), de-sulpherized tailings (DST), peat, and compost).

Nine polished thin sections, and nine polished sections of each sample were prepared and examined under transmitted and incident light, using an ore microscope at 100x to 1000x magnification.

Microscopic results indicate that all nine samples are sulphide-rich tailings of basically the same mineralogical composition, consisting of variable proportions of pyrrhotite, (with trace chalcopyrite), limonite cements, silicates (dominantly quartz, with lesser plagioclase, and hornblende), and magnetite. The sulphide component of the samples varies from 15% (sample 3-6), up to 85% (sample 8-6).

Pyrrhotite typically occurs as liberated grains or enclosed within limonite cements. The majority of pyrrhotite grains have a relatively fresh appearance, or only show incipient oxidation in the form of ragged and fractured margins. Sample 8-6 shows the lowest level of pyrrhotite oxidation. Samples l-6,2-6,4-6 and 5-6 show minor amounts of pyrrhotite oxidation, while in samples l-0, 3-6, 6-6 and 7-6 a higher proportion of pyrrhotite grains show fairly extensive to complete oxidation, with corroded rims and alteration to limonite/Fe-oxyhydroxide. Pyrrhotite encased within limonite cements in these samples (l-0,3-6,6-6, 7-6) exhibits irregular, leached margins.

All samples (except 8-6) show various degrees of limonite cementation around both the sulphide and non-sulphide mineral components (varying from 5 to 35% of an individual sample). These cements may represent limonite which precipitated in-situ from pyrrhotite oxidation, and/or Fe-oxyhydroxides (limonite) precipitated from circulating Fe-rich solutions. The highest proportion of limonite cementation occurs in samples l-0, 6-6, and 7-6, where limonite contributes more than 20% of the total sample. These samples also contain the most highly oxidized pyrrhotite. Sample 8-6 is unique, and only shows trace abundance of limonite (< 1% of total sample).

Carbonates (particularly calcite ($CaCO_3$)) act to buffer potential acid generation from sulphide oxidation in a tailings sample, or increase the neutralization potential of the sample. However, only trace calcite was identified in samples 2-6 and 3-6. The presence of gypsum in samples l-0, l-6, 2-6, 3-6 and 4-6 suggests the presence of original calcite, as gypsum typically forms as a secondary mineral phase.

Table 1: Summary of estimated volume % of pyrrhotite, limonite, carbonates, and gypsum.

Sample / Cover		Pyrrhotite (est. vol. %)	Extent of Pyrrhotite Oxidation	Limonite (est. vol. %)	Calcite (est. vol. %)	Gypsum (est. vol. %)
1-0	Control (surface)	20 - 25	moderate	30 - 35	---	trace
1-6	Control (deeper)	50 - 55	minor to moderate	5 - 10	---	trace
2-6	LSSS	35 - 40	minor	15 -20	trace	trace
3-6	DST	15 - 18	moderate	8 - 10	trace	trace
4-6	Compost	50 - 55	minor	6 - 8	---	trace
5-6	Peat	35 - 40	minor	10 - 12	---	---
6-6	DST+CB	35-40	minor to moderate	15 -20	---	---
7-6	LSSS + CB	30 - 35	minor to moderate	25 - 30	---	---
8-6	Compost/Fresh Po	80 - 85	trace	< 1	---	---

Control: oxidized tailings
LSSS: lime-stabilized sewage sludge
DST: de-sulpherized tailings
CB: capillary barrier
Po: pyrrhotite

Regards
LAKEFIELD   RESEARCH   LIMITED
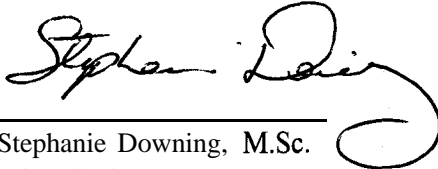
Stephanie Downing, M.Sc.
Mineralogist

**Sample (1-O): Control (oxidized tailings) at the surface
PS 5759 and PTS 2732**

The (1-O) tailings sample is dark-orange to brown in colour, and is composed dominantly of
oxides,   silicates,   and   sulphides.

Mineralogy	Est. Vol. %	Typical Grain Size
Limonite	30 to 35	aggregates up to 0.60 mm
Pyrrhotite	20 to 25	15 to 120 pm
Quartz	10 to 12	40 to 115 μm
Plagioclase	10 to 12	60 to 150 μm
Magnetite	5 to 8	15 to60 μm
Amphibole	2 to 4	aggregates up to 300 μm
Chlorite	2 to 4	30 to 150 μm
Epidote	1 to 2	up to 120 pm
Biotite	< 1	< 40 μm
Chalcopyrite	0.5	10 to 70 μm
Gypsum	0.5	75 to 120 μm
Pyrite	trace	70 to 120 μm

This pyrrhotite-rich tailings sample (1-O) shows moderate to extensive effects of oxidation. It
consists primarily of discrete grains, and limonite cemented 'clumps' or aggregates composed
dominantly of pyrrhotite, quartz, and plagioclase. Minor magnetite, amphibole, and
phyllosilicates also occur within limonite cements, or occur as discrete grains throughout the
sample.

Oxides consist dominantly of limonite, with minor magnetite. Limonite cements are
volumetrically more abundant than pyrrhotite and occur as variably sized particles, ranging from
earthy to compact in nature. They commonly enclose mixtures of sulphides, silicates, and
magnetite. The cements host abundant voids or cavities, which may represent either plucked
pyrrhotite (during section preparation), dissolved pyrrhotite, or earthy limonite. Magnetite
typically occurs as discrete grains, or encased by limonite cements.

Sulphides consist almost entirely of pyrrhotite, with only trace amounts of chalcopyrite and pyrite. Pyrrhotite typically occurs as discrete grains dispersed throughout the sample, and a minor proportion occurs within limonite cements. It commonly shows peripheral effects of incipient to moderate oxidation (in the form of ragged or corroded grain margins, and/or replacement rims of secondary Fe-oxyhydroxide or limonite). A few pyrrhotite grains within limonite cemented 'clumps' show alteration to marcasite, while others appear leached. A minor proportion are unaltered or relatively fresh in appearance. Chalcopyrite and pyrite occur as rare discrete grains throughout the sample, and chalcopyrite also forms inclusions in non-opaque. Unless otherwise noted, pentlandite invariably occurs as rare flame structures in pyrrhotite, in this sample, and following samples.

Silicates (30 to 35% of total sample) consist primarily of quartz, plagioclase, and amphibole, with minor phyllosilicates (chlorite and biotite) and trace epidote. They occur as discrete grains, form aggregated particles, and are commonly enclosed within limonite cements.

Rare discrete grains of gypsum are present throughout the sample.
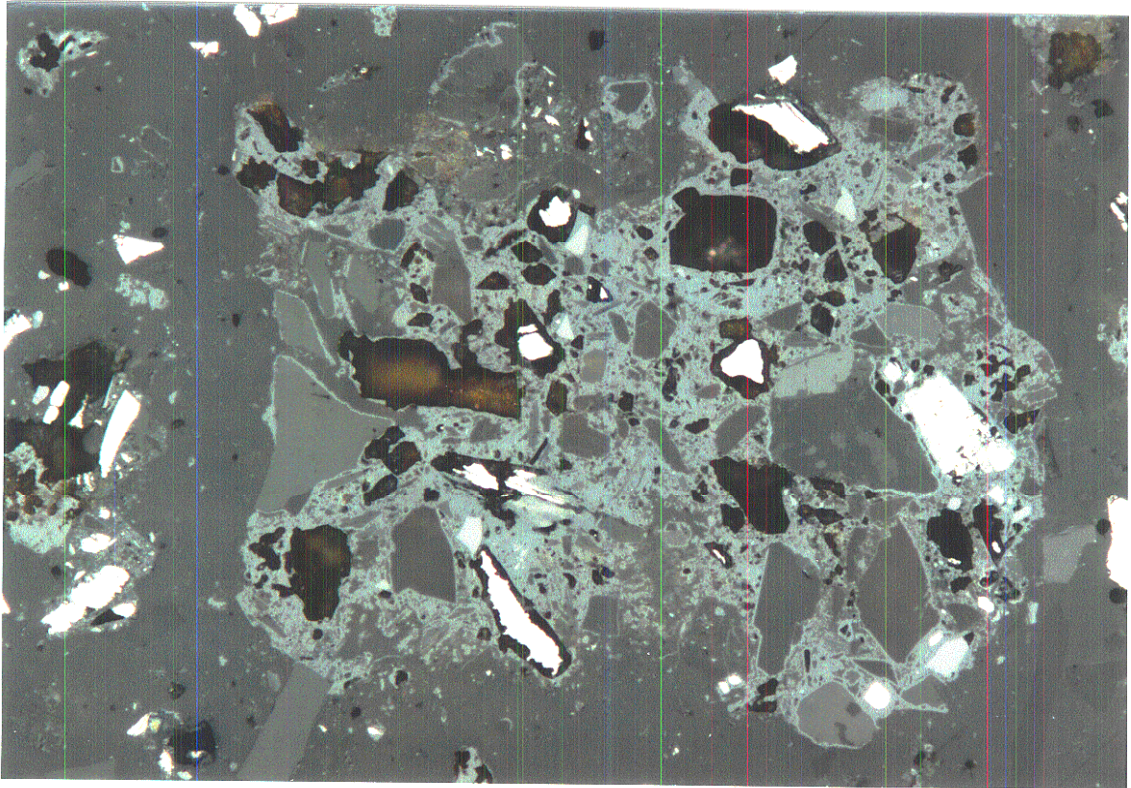
| Illustration #1 | Magnification 200x | Incident Light | 125 µm |
| Sample 1-0 | | PS 5759 | |

Photomicrograph of a representative limonite cemented 'clump' or aggregate. Limonite cementation is fairly compact, and occurs around both pyrrhotite (white) and silicates (dark-grey) alike. The occurrence of limonite around both sulphide and non-sulphide mineral components suggests local re-mobilization and precipitation of Fe-rich circulating fluids produced from active sulphide oxidation. Pyrrhotite within this cemented aggregate appears highly corroded and leached, and abundant cavities remain in the limonite (black holes).
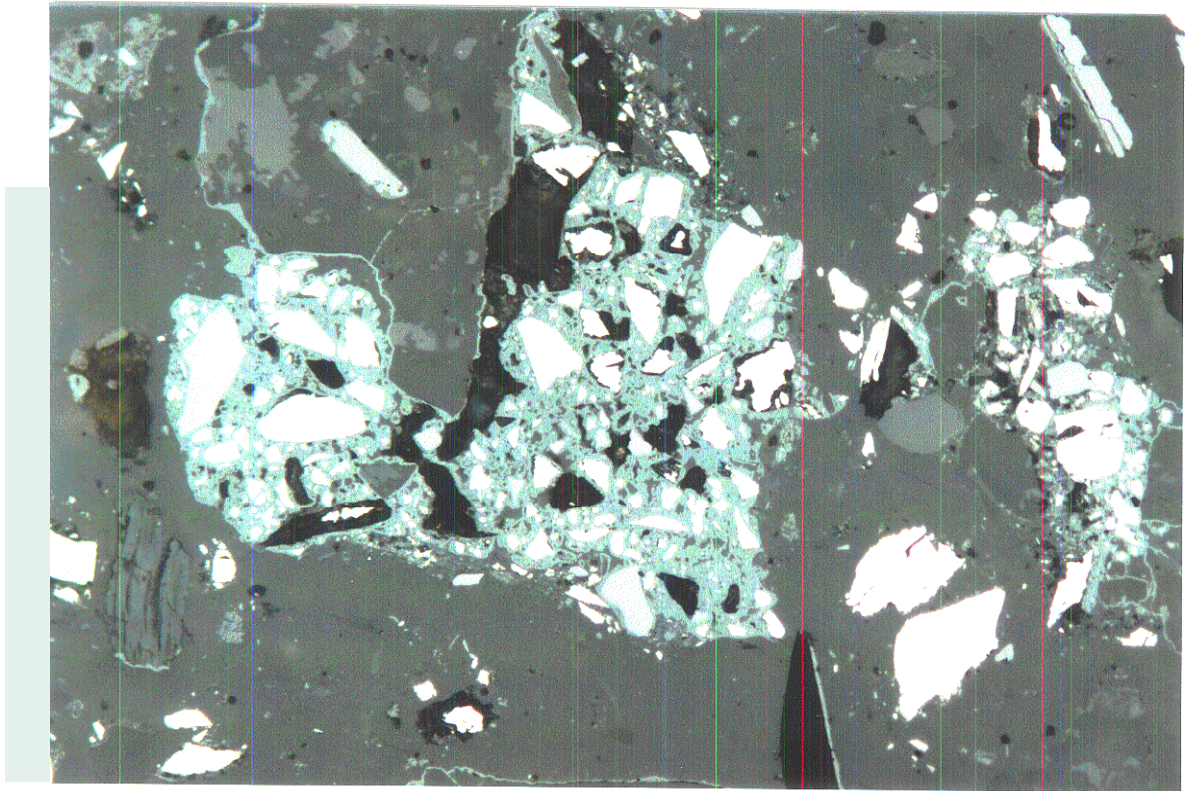
| Illustration #2 | Magnification 200x | Incident Light | 125 µm |
| Sample 1-0 | | PS 5759 | |

Photomicrograph of a representative highly compact limonite cemented aggregate. Note the pyrrhotite grains, ranging from relatively fresh (sharp grain boundaries) in appearance, to slightly oxidized (ragged margins), to highly corroded (leached grains within limonite 'clump'). Magnetite (light-grey) is also present within the limonite cements, and cements commonly form coatings around silicates.
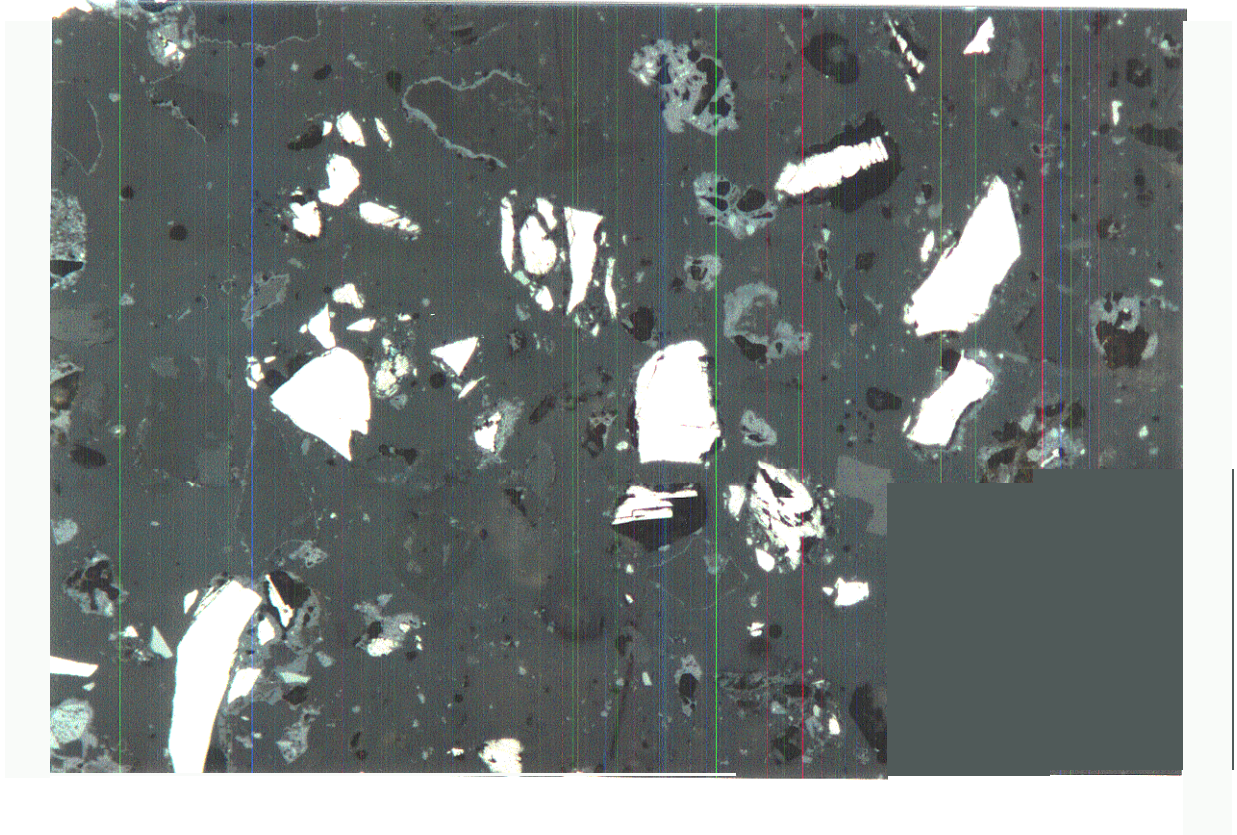
Illustration #3   Magnification 200x   Incident Light   125 μm
Sample 1-U   **PS 5759**

Photomicrograph of representative liberated pyrrhotite, showing moderate to extensive effects of oxidation. with ragged grain boundaries. and oxidation to an Fe-oxyhydroxide.

Sample (l-6): Control (oxidized tailings) 90 cm from the surface
PS 5760 and PTS 2733

The (l-6) tailings sample is dark-brown to black in colour, and is composed dominantly of sulphides, silicates, and oxides respectively.

Mineralogy	Est. Vol. %	Typical Grain Size
Pyrrhotite	50 to 55	up to 120 pm
Quartz	10 to 12	30 to 120 μm
Magnetite	8 to 10	30 to 60 μm
Limonite	5 to 10	aggregates up to 150 μm
Plagioclase	6 to 8	50 to 150 μm
Amphibole	2 to 4	50 to 80 μm
Chlorite	1 to 2	20 to 50 μm
Biotite	1 to 2	30 to 50 μm
Epidote	1 to 2	50 to 85 μm
Chalcopyrite	trace	up to 80 μm
Pentlandite	trace	< 30 μm
Gypsum	trace	~ 40 μm

This sample (l-6) contains a higher proportion of pyrrhotite, compared to the previous surface sample (1-0), and a lower proportion of limonite cementation, and thus is not as highly oxidized. It consists primarily of pyrrhotite, with lesser silicates (quartz and plagioclase), and oxides (limonite and magnetite). Minor amphibole and phyllosilicates are also present. •

Pyrrhotite typically occurs as discrete, liberated grains. Pyrrhotite textures range from relatively fresh, to altered or corroded along grain boundaries. Some pyrrhotite grains contain micro-fractures, and exhibit small pyrrhotite shards around their periphery, indicative of incipient oxidation. A relatively small proportion of pyrrhotite is found within limonite cements. Pyrrhotite within a few cemented 'clumps' appears leached and holes or cavities remain in the section. There is an overall increase in the proportion of pyrrhotite fines in this sample, which commonly show alteration to an Fe-oxyhydroxide (limonite). Other sulphides include trace chalcopyrite, which occurs as discrete grains, or forms inclusions in silicates.

9

Silicates (25 to 30% of total sample) consist primarily of quartz, plagioclase, and amphibole, with minor phyllosilicates and epidote. Silicate textures and occurrences are as described for the previous sample (1-O).

Oxides consist entirely of limonite and magnetite. Occasional limonite cemented 'clumps' are compact in nature, whereas, the majority are non-compact. Magnetite typically occurs as liberated grains, and a smaller proportion of grains are included within limonite cements.

A few rare grains of gypsum are present.
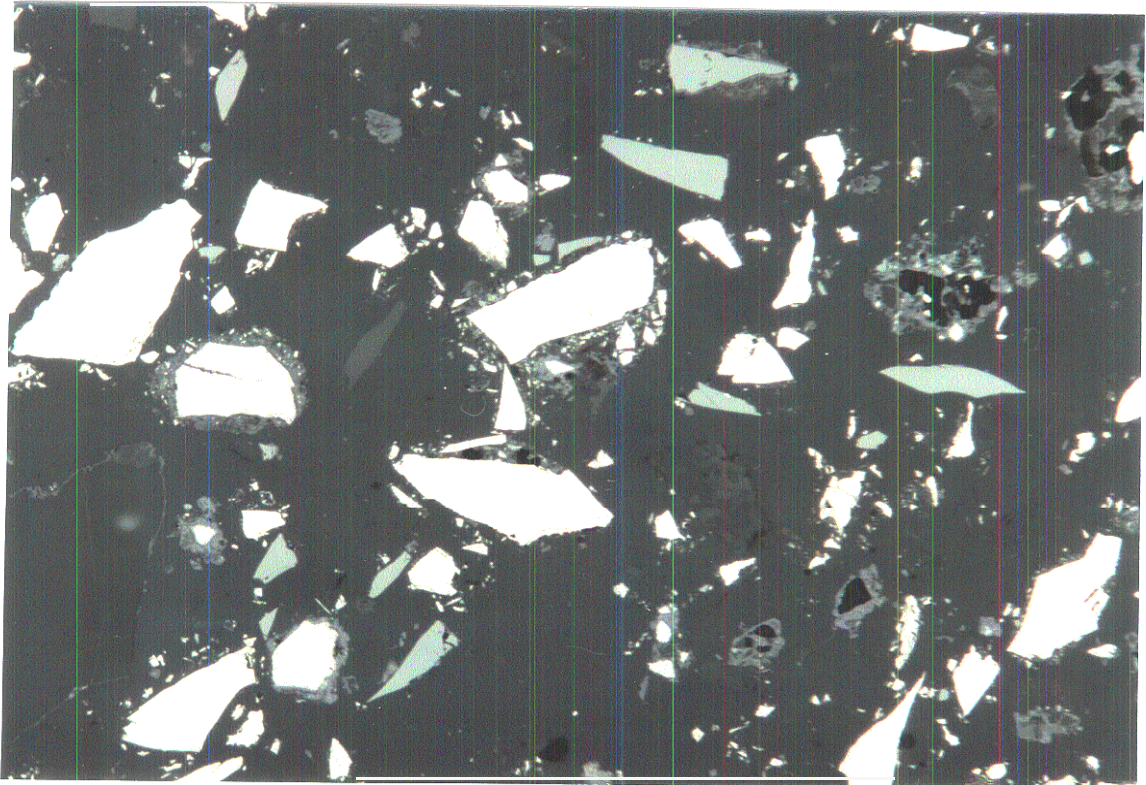
Illustration #4   Magnification   200s   **Incident Light**   125 μm
Sample 1-6   **PS 5760**

Photomicrograph **of representative pyrrhotite grains. showing initial** breakdown along the crystallographic **grain boundaries, indicative** of **incipient osidatinn** Note **abundant finer surrounding a** few **pyrrhotite grains. and** limonite (bluish-grey) **rims.**
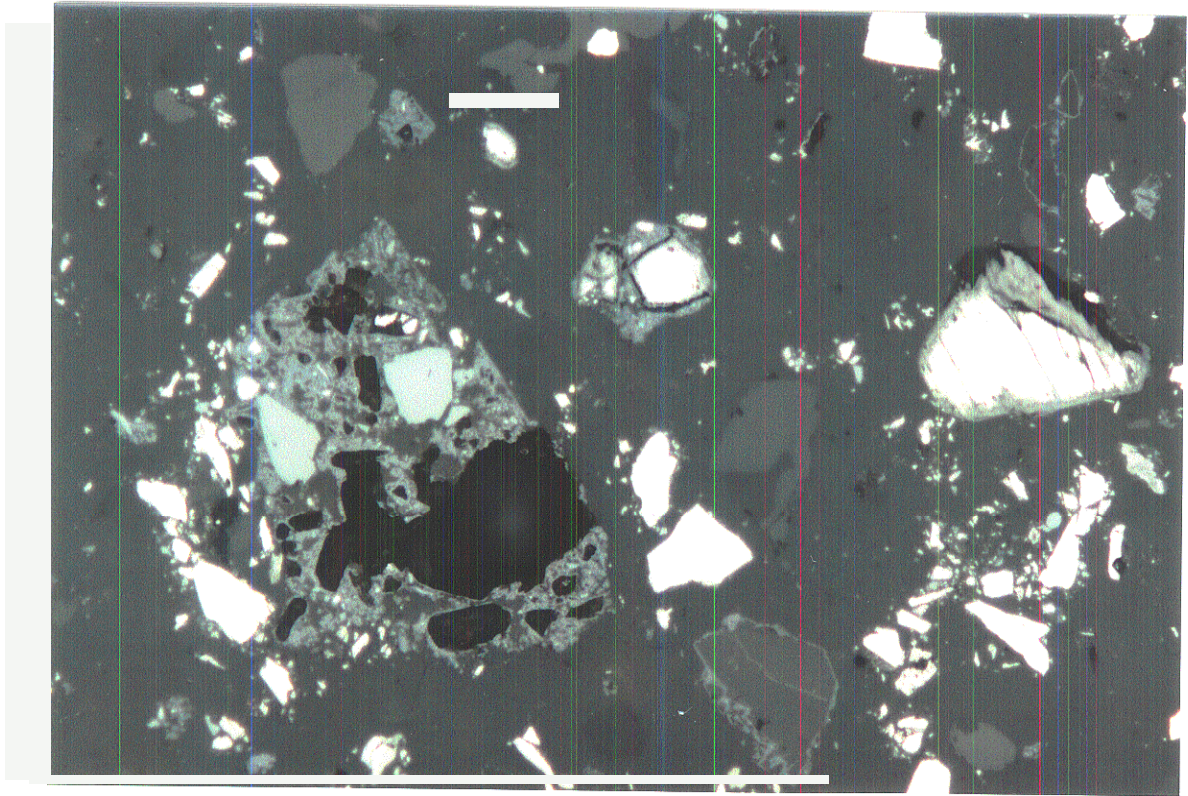
Illustration **#5**   Magnification 200x   Incident Light   *125* μm
Sample 1-6   **PS** 5760

Photomicrograph of a representative highly oxidized pyrrhotite grain (centre-right), showing alteration to marcasite. A loosely cemented limonite 'clump' contains magnetite (grey) and pyrrhotite (white) grains.

Sample (Z-6): Oxidized tailings covered with LSSS
PS 5761 and PTS 2734

The (2-6) tailings sample is dark-brown to black in colour, and is composed dominantly of sulphides, silicates, and oxides respectively.

Mineralogy	Est. Vol. %	Typical Grain Size
Pyrrhotite	35 to40	10 to 100 μm
Limonite	15 to20	variable aggregates
Quartz	10 to 15	30 to 120 μm
Plagioclase	10 to 12	50 to 150 μm
Magnetite	6 to 8	30 to 100 μm
Amphibole	4 to 6	20 to 80 μm
Biotite/Sericite	1 to 2	< 30 μm
Chlorite	trace	< 50 μm
Epidote	trace	~ 80 μm
Chalcopyrite	trace	30 to 50 μm
Gypsum	trace	~ 40 μm
Calcite	trace	~ 80 μm

This sample (2-6) is similar in nature to the previous two, consisting primarily of pyrrhotite, silicates, and limonite cements. The proportion of pyrrhotite to silicates is approximately equal. There is a higher proportion of limonite cements in this sample, compared to the previous sample (1-6), and a lower proportion of pyrrhotite.

Pyrrhotite typically occurs within loosely to moderately developed, cemented limonite 'clumps'. Individual pyrrhotite grains in the limonite cements range from fresh in appearance to slightly oxidized, showing alteration rims to an Fe-oxyhydroxide (limonite). Only a minor proportion of pyrrhotite occurs as discrete grains, which are typically fresh in appearance. Rare chalcopyrite grains occur as exposed inclusions in silicates.

13

Limonite commonly encloses pyrrhotite and silicate grains, and occurs as loosely cemented 'clumps' or aggregates. Magnetite typically occurs as discrete grains, and rarely as inclusions within limonite cements.

Silicates (30 to 35% of total sample) are similar in nature and composition to the previous samples, and dominantly consist of quartz, plagioclase, amphibole, and biotite. A higher proportion of silicates occur as aggregates in this sample.

Rare grains of gypsum are present, and calcite is also present as a rare carbonate phase.
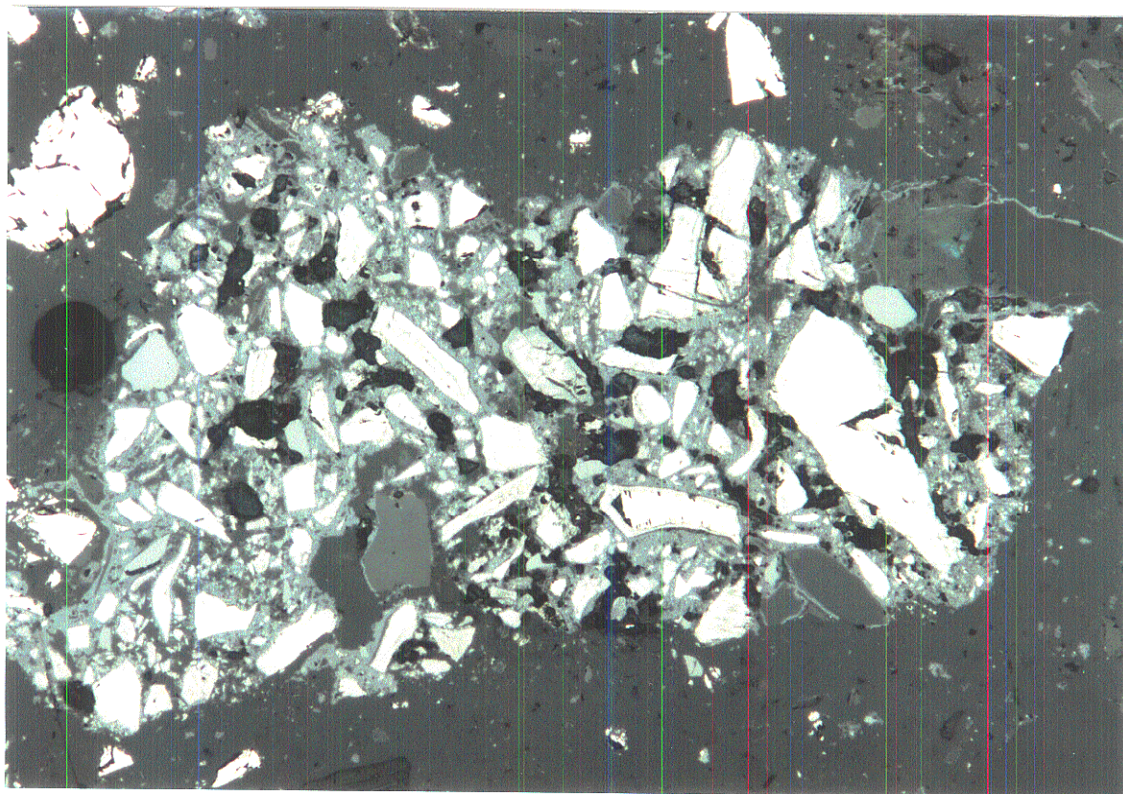
Illustration #6   Magnification 200x   Incident Light   125 µm
Sample 2-6   PS 5761

Photomicrograph of a representative limonite cemented 'clump'. Note almost all pyrrhotite grains occur within the cements. The majority of grains within the limonite cements show incipient effects of oxidation. Pyrrhotite within this cemented aggregate shows minor effects of oxidation with breakdown at the rims to an Fe-oxyhydroxide.
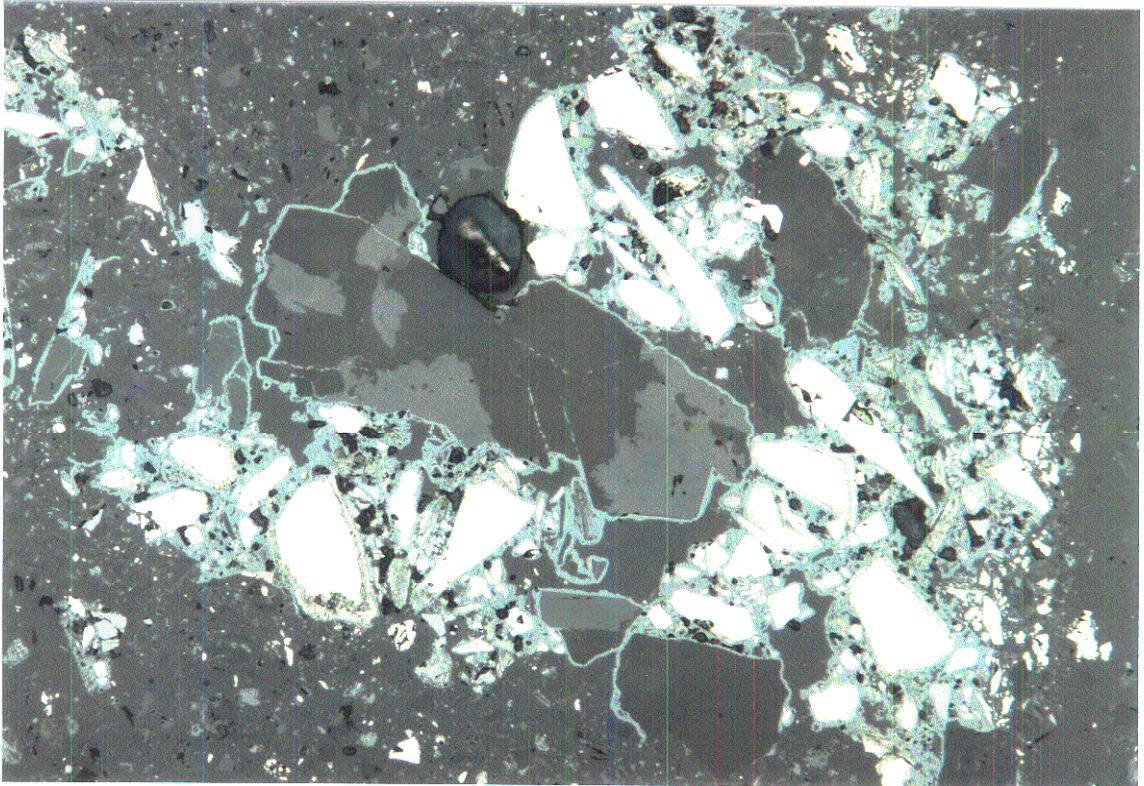
Illustration #7   **Magnification** 200x   **Incident Light**   125 μm
Sample 2-6   **I'S 5761**

Photomicrograph of a representative limonite cemented 'clump'. Limonite cements occur around both pyrrhotite and silicates alike. Pyrrhotite textures range from fresh (sharp boundaries) to slightly oxidized (rims of Fe-oxyhydroxide).

Sample (3-6): Oxidized tailings covered with DST
PS 5762 and PTS 2735

The (3-6) tailings sample is orange-brown in colour, and is composed dominantly of silicates, sulphides, and oxides.

Mineralogy	Est. Vol. %	Typical Grain Size
Plagioclase	25 to 30	50 to 100 μm
Quartz	20 to 25	up to 200 μm
Pyrrhotite	15 to 18	up to 350 pm
Limonite	8 to 10	variable up to 0.6 mm
Amphibole	6 to 8	150 to 200 μm
Magnetite	6 to 8	20 to 70 μm
Chlorite	1 to 2	aggregates 100 to 150 μm
Epidote	1 to 2	~ 50 μm
Ilmenite	- 1	50 to 150 μm
Chalcopyrite	0.5	40 to 150 μm
Pyrite	trace	~ 80 μm
Gypsum/Calcite	trace	< 80 μm

This sample (3-6) is made up of the same components as the previous three, but contains an extremely high proportion of silicates relative to pyrrhotite (with a pyrrhotite:silicate ratio of approximately 1:4), and minor limonite cements. It consists primarily of plagioclase and quartz, with lesser pyrrhotite, limonite, amphibole, magnetite, and phyllosilicates respectively.

Silicates (65 to 70% of total sample) are coarser-grained in this sample compared to previous samples, and typically form coarse dioritic aggregates composed of fresh plagioclase and hornblende, with minor quartz and epidote. These silicate aggregates are commonly surrounded or coated by limonite cements. The above silicates also occur as discrete liberated grains.

Pyrrhotite typically occurs as small (< 60 μm) grains, cemented by earthy to compact limonite cements. Large, rare, relatively fresh pyrrhotite grains (up to 350 μm) also occur dispersed throughout the sample, and are devoid of any cements. Individual pyrrhotite grains within

17

limonite cements commonly show ragged margins and appear leached. These pyrrhotite grains are moderately to highly oxidized, and abundant voids or cavities present in the limonite cements may represent completely leached pyrrhotite. Trace chalcopyrite occurs liberated, or as locked inclusions in silicates.

Limonite cements are variable in nature, and range from earthy to compact, commonly enclosing pyrrhotite and silicate grains. A high proportion of pyrrhotite grains have been leached (or plucked during sample preparation) from the limonite cements.

Gypsum occurs encrusting magnetite, and as partial inclusions on the edges of silicate aggregates, where it appears to be replacing calcite.
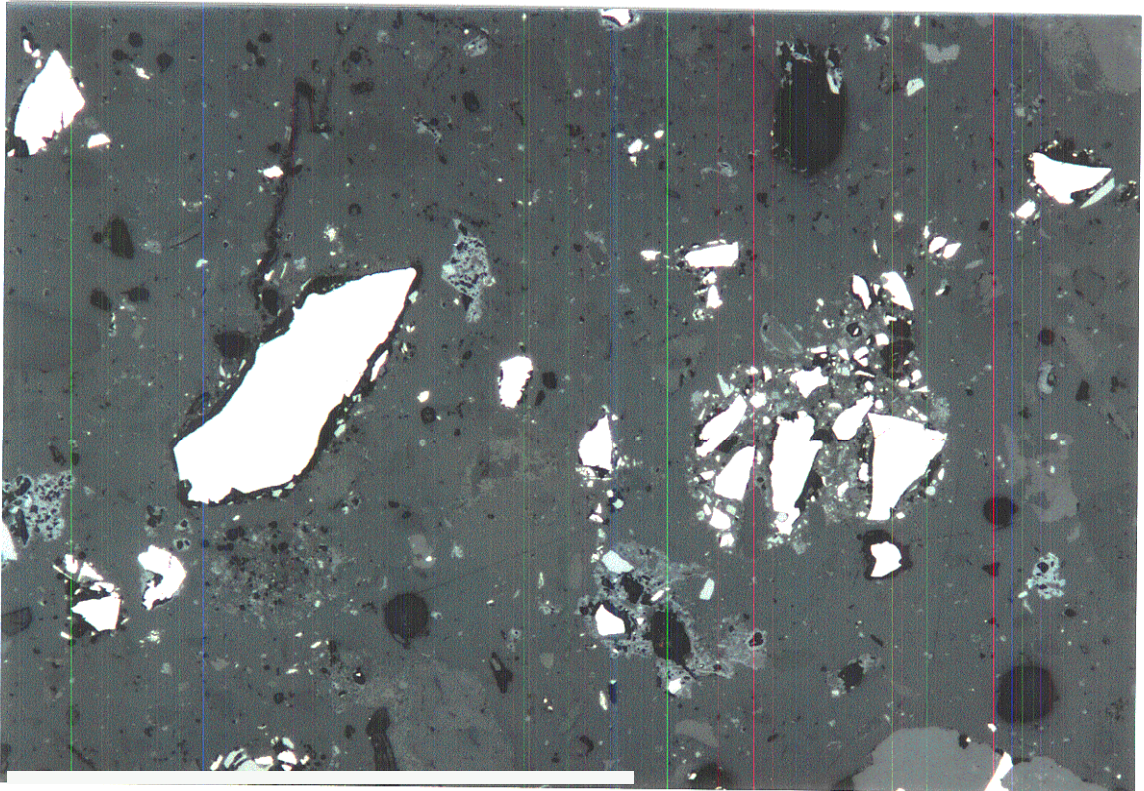
Illustration #8   **Magnification** 200x   **Incident Light**   125 μm
Sample 3-6   **PS 5762**

Photomicrograph of representative **liberated** pyrrhotite **grams. The majority of** pyrrhotite **occurs within loose to compact** limonite **cemented 'clumps'. Pyrrhotite in** this photomicrograph **appears to be leached around its margins.**
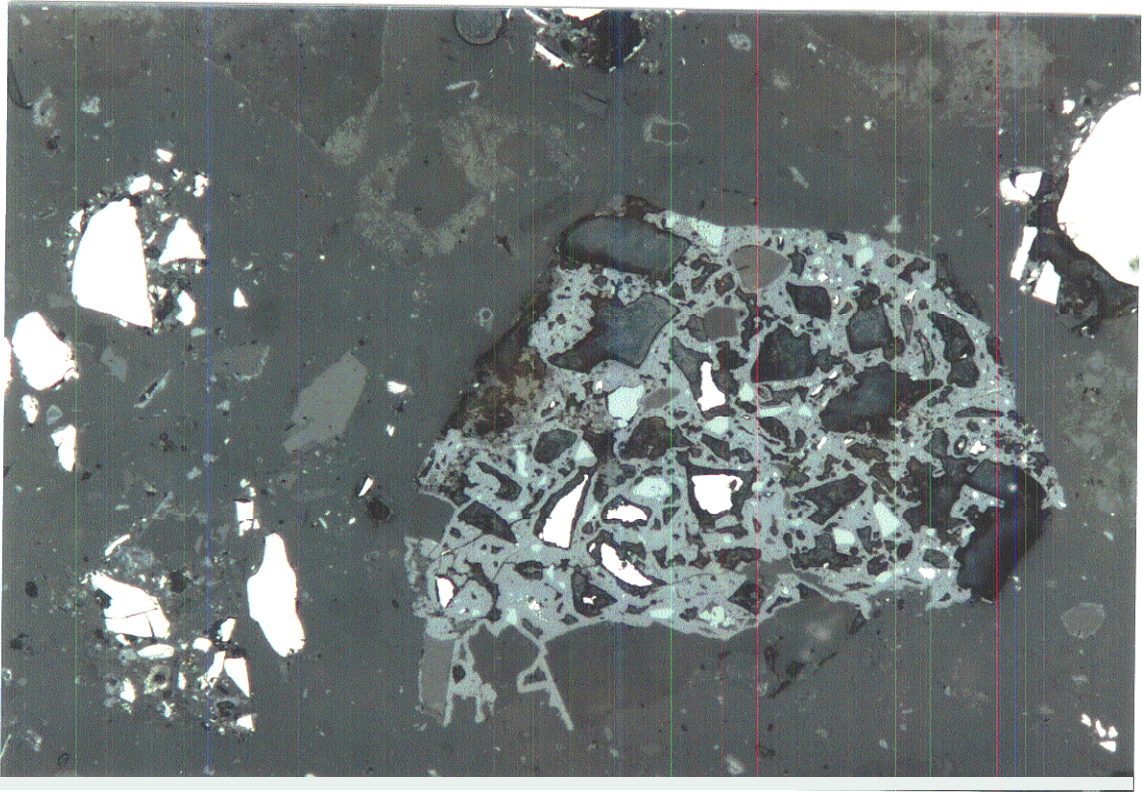
Illustration #9   Magnification 200x   Incident Light   *125* μm
Sample 3-6   **PS 5762**

Photomicrograph of a compact limonite cemented 'clump'. Abundant holes or cavities remain in the limonite, and a few remaining pyrrhotite grains appear leached.

Sample (4-6): Oxidized tailings covered with compost
PS 5763 and PTS 2736

The (4-6) tailings sample is dark-brown to black in colour, and is composed dominantly of sulphides, silicates, and oxides respectively.

Mineralogy	Est. Vol. %	Typical Grain Size
Pyrrhotite	50 to 55	20to 100 μm
Quartz	10 to 12	100 to 120 μm
Plagioclase	8to 10	50 to 120 μm
Limonite	6 to 8	non-compact, variable
Magnetite	4 to 6	40 to 100 μm
Amphibole	4 to 6	80 to 120 μm
Chlorite	1 to 2	aggregates up to 150 μm
Epidote	1 to2	~ 60 μm
Biotite	1 to2	20 to 40 μm
Gypsum	- 1	~ 80 μm
Pyroxene	< 1	100 μm
Chalcopyrite	0.5	30 to 50 μm
Pyrite	trace	up to 150 μm

This sample (4-6) is similar in mineralogy and modal abundance to sample (1-6), with a slightly higher abundance of pyrrhotite to silicates, and lower proportion of limonite cementation. The sample consists primarily of pyrrhotite, quartz, plagioclase, and limonite respectively. A minor proportion of magnetite, amphibole, epidote, and phyllosilicates are also present.

Pyrrhotite typically occurs as small (< 60 μm) discrete grains, the majority of which are cracked, and show evidence of incipient oxidation. Only a small proportion of liberated grains (< 5% of total) show fresh grain boundaries, or extensive effects of oxidation. A minor proportion of pyrrhotite is found within limonite cements, and ranges from fresh to slightly oxidized in appearance (ragged grain margins and alteration to Fe-oxyhydroxide). Trace chalcopyrite occurs as discrete grains, or in binary association with pyrrhotite. Pyrite is found as rare liberated grains.

Limonite cements are typically non-compact in nature, and occur as sporadic clumps suggesting only minor oxidation.

Silicates (30 to 35% of total sample) are similar to those described for previous samples (l-0, 1-6, and 2-6), and include minor pyroxene. The majority of silicates occur as discrete grains,

Gypsum is present as rare discrete grains.
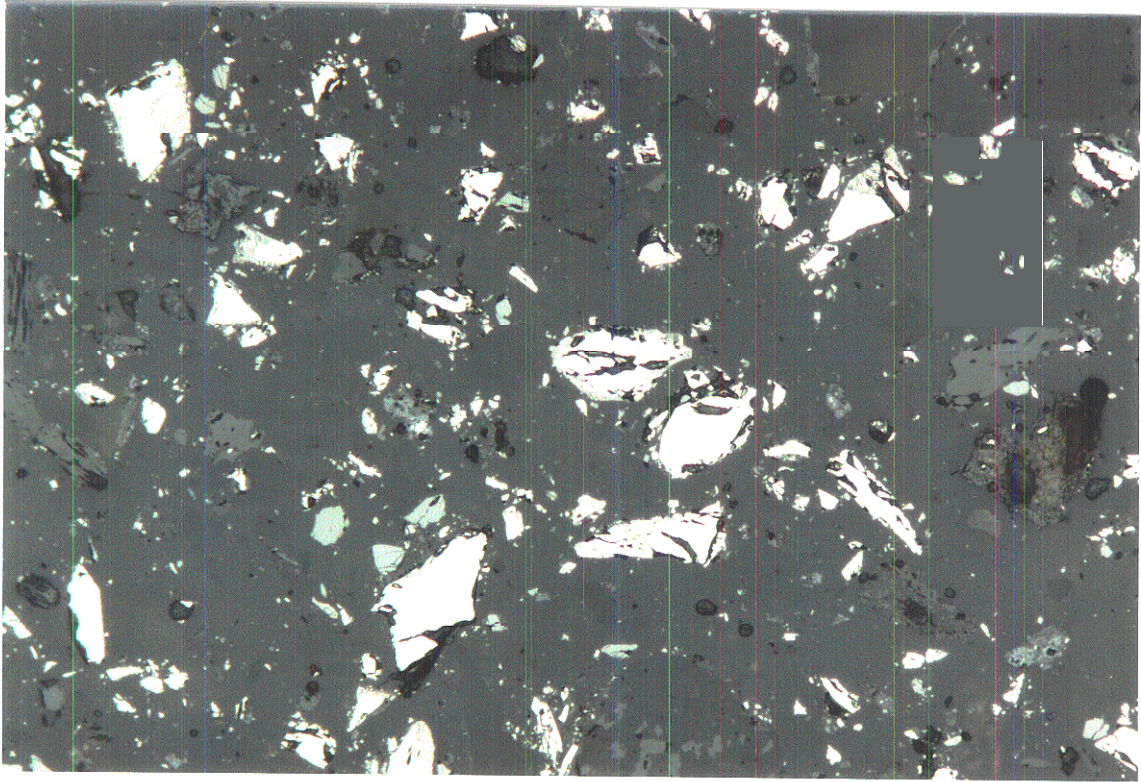
Illustration #10   Magnification 200x   Incident Light   125 μm
Sample 4-6   **PS 5763**

Photomicrograph of representative pyrrhotite grains. The majority of pyrrhotite occurs as liberated grains, which show evidence of incipient oxidation in the form of cracked and ragged grain boundaries. A minor proportion show alteration to an Fe-oxyhydroxide.
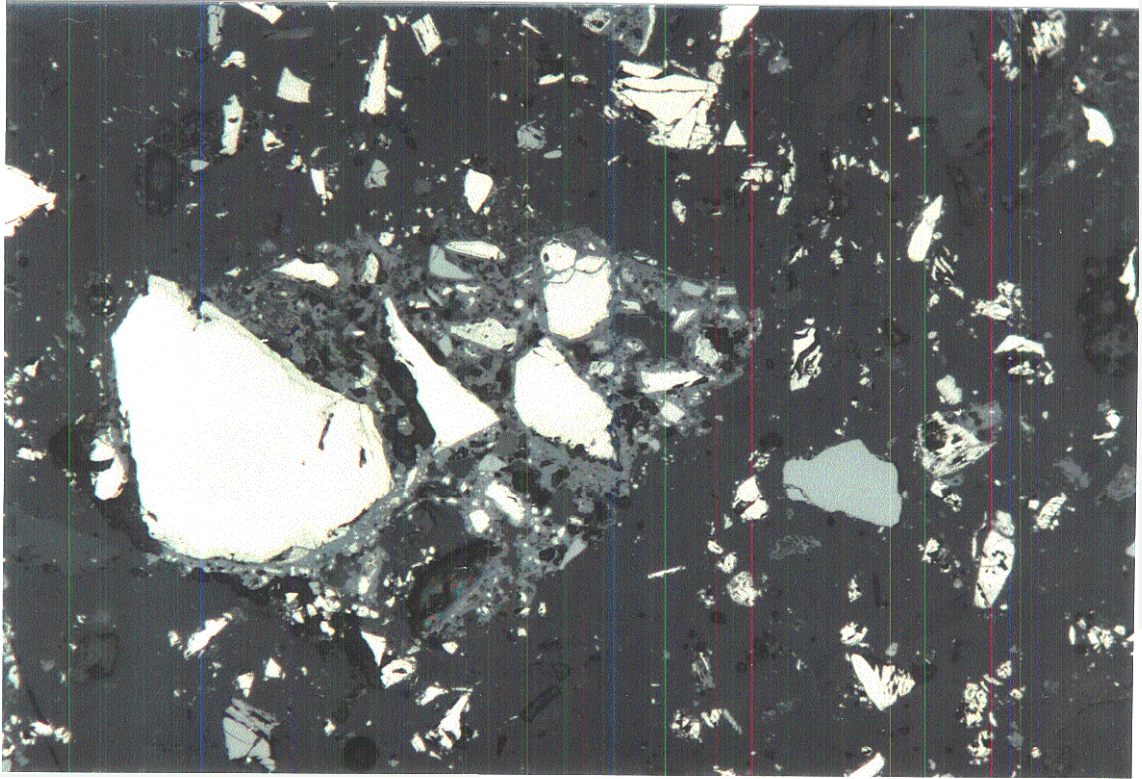
Illustration #11   Magnification 200x   Incident Light   125 μm
Sample 4-6   **PS 5763**

Photomicrograph of a representative limonite cemented 'clump', enclosing pyrrhotite (white) and magnetite (grey). Pyrrhotite shows alteration along the grain margins to an Fe-oxyhydroxide.

Sample (5-6): Oxidized tailings covered with peat
PS 5764 and PTS 2737

The (5-6) tailings sample is dark-orange brown in colour, and is composed dominantly of silicates, sulphides, and oxides respectively.

Mineralogy	Est. Vol. %	Typical Grain Size
Pyrrhotite	35 to 40	20 to 100 μm
Quartz	20 to 25	20 to 150 μm
Plagioclase	10 to 15	50 to 200 μm
Limonite	10 to 12	variable aggregates
Amphibole	4 to 6	40 to 150 μm
Pyroxene	1 to 2	60 to 80 μm
Biotite	1 to 2	20 to 40 μm
Epidote	< 1	20 to 70 μm
Magnetite	< 1	30 to 80 μm
Chalcopyrite	< 0.5	30 to 100 μm
Arsenopyrite	trace	~ 70 μm
Pentlandite	trace	< 30 μm

This sample (5-6) contains approximately equal proportions of pyrrhotite relative to silicates, the latter being slightly more abundant, and minor limonite cements. It is distinct from previous samples in its low abundance of magnetite.

The majority of pyrrhotite occurs as liberated grains which show evidence of incipient oxidation in the form of ragged or cracked grain boundaries. Pyrrhotite within limonite cements ranges from fresh to slightly corroded in texture, and a few rare grains within the cemented 'clumps' appear to be leached around their margins. Other trace sulphides present include chalcopyrite, arsenopyrite, and pentlandite. Arsenopyrite and chalcopyrite occur liberated, and a few chalcopyrite grains occur in binary association with pyrrhotite.

Silicates are abundant in this sample (40 to 45% of total sample) and occur mostly as liberated grains, or encased within limonite cements. The silicate minerals are similar to those described for previous samples, and include minor pyroxene.

Limonite cementation is weak to moderately developed. The sample contains minor limonite cemented 'clumps' which commonly enclose pyrrhotite and silicates. Magnetite is lacking compared to previous samples.
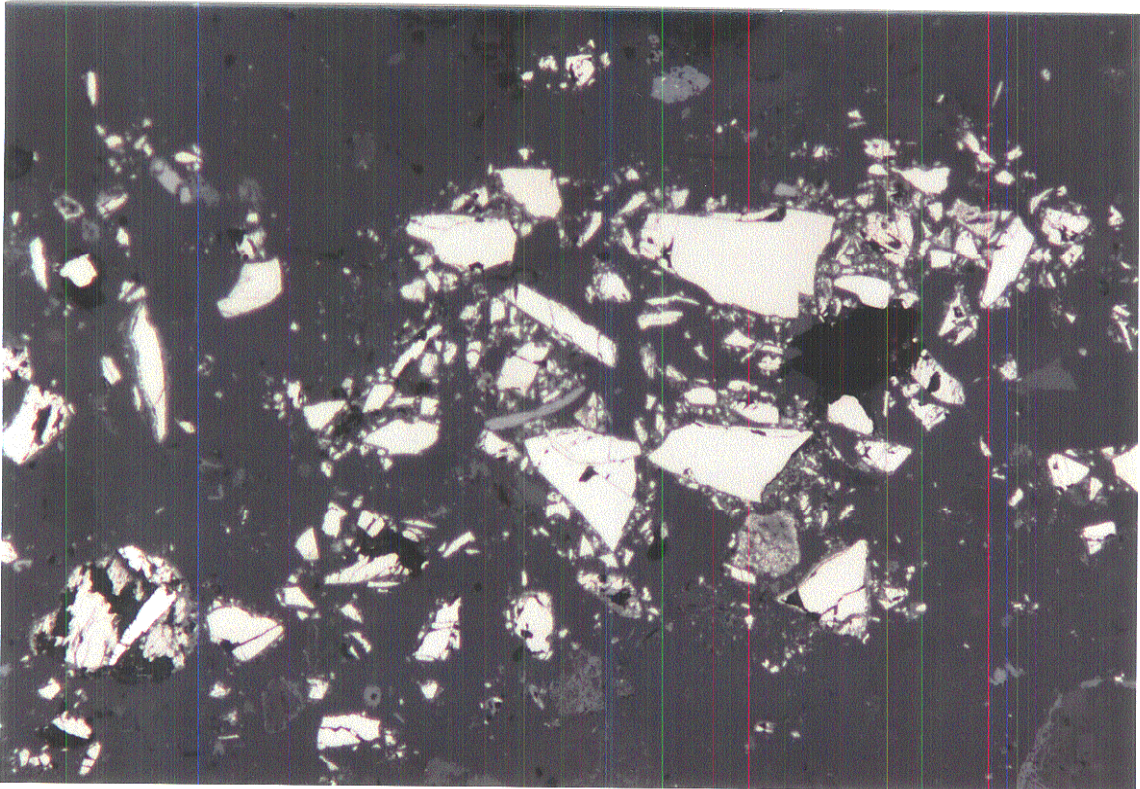
Illustration #12   Magnification 200x   Incident Light   125 μm
Sample 5-6   **PS 5764**

Photomicrograph of representative pyrrhotite grains (creamy white). The majority of pyrrhotite occurs as liberated grains, which show evidence of incipient oxidation in the form of cracked and ragged grain boundaries. A minor proportion show alteration to an Fe-oxyhydroxide (centre-left, and top-centre). Magnetite is rare to absent in this sample (< 1% of total sample).
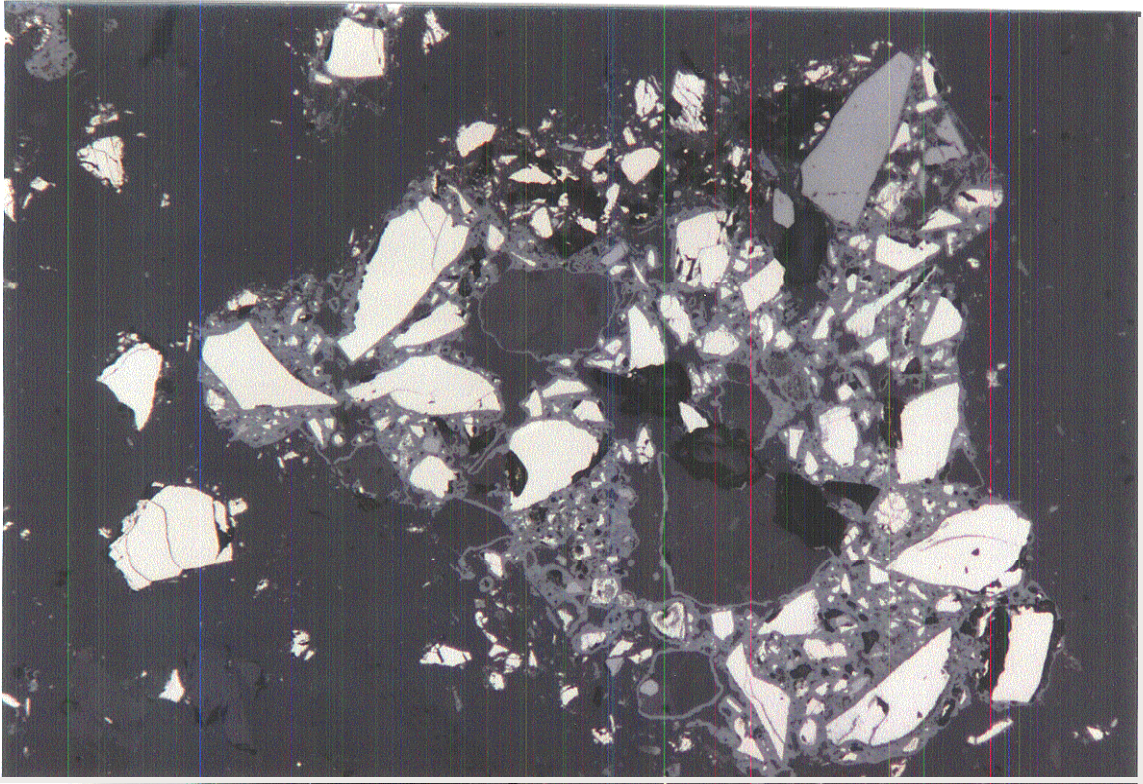
Illustration **#13**   Magnification 200x   Incident Light   *125* µm
Sample 5-6   **PS 5764**

Photomicrograph of pyrrhotite grains within a moderately developed, cemented limonite 'clump'. Limonite cementation occurs around both the sulphide and non-sulphide minerals. The pyrrhotite grains within the cements are relatively fresh in appearance, with sharp grain boundaries

Sample (6-6): Oxidized tailings covered with DST and CB
PS 5765 and PTS 2738

The (6-6) tailings sample is dark-orange to brown in colour, and is composed dominantly of sulphides, silicates, and oxides.

Mineralogy	Est. Vol. %	Typical Grain Size
Pyrrhotite	35 to 40	20 to 100 μm
Limonite	15 to 20	variable aggregates
Quartz	14 to 18	up to 150 μm
Plagioclase	8 to 10	50 to 150 μm
Amphibole	4 to 6	50 to 120 μm
Biotite	2 to 4	20 to 50 μm
Magnetite	2 to 4	60 to 100 μm
Chlorite	1 to 2	50 to 120 μm
Chalcopyrite	0.5	< 50 μm
Pyrite	trace	~ 120 μm
Ilmenite	trace	~ 200 μm

This sample (6-6) is similar to the previous (5-6), containing equal proportions of pyrrhotite to silicates. It contains a slightly higher proportion of limonite cemented 'clumps', and is slightly more oxidized than sample 5-6. It also contains a similar low abundance of magnetite.

Pyrrhotite occurrence is similar to that described for the previous sample (5-6). A relatively high proportion of pyrrhotite fines are present, which exhibit sharp margins and are typically fresh in appearance. A minor proportion are slightly oxidized, showing incipient oxidation in the form of cracked margins with surrounding broken fragments. Pyrrhotite within cemented limonite is moderately to highly oxidized. Individual pyrrhotite grains within the cements commonly show irregular outlines and alteration rims indicative of leaching and oxidation in-situ. Trace pyrite and chalcopyrite are present as discrete grains.

Limonite cementation is fairly extensive in this sample. It varies, however, from compact to non-compact or weakly developed in nature. Minor magnetite occurs as discrete grains, and ilmenite is also found as large (- 200 μm) discrete grains.

29

Silicates (35 to 40% of total sample) are similar to those described in previous samples, and occur mostly as liberated grains. A minor proportion of silicates are found within limonite cemented 'clumps' or occur together as rare aggregates.
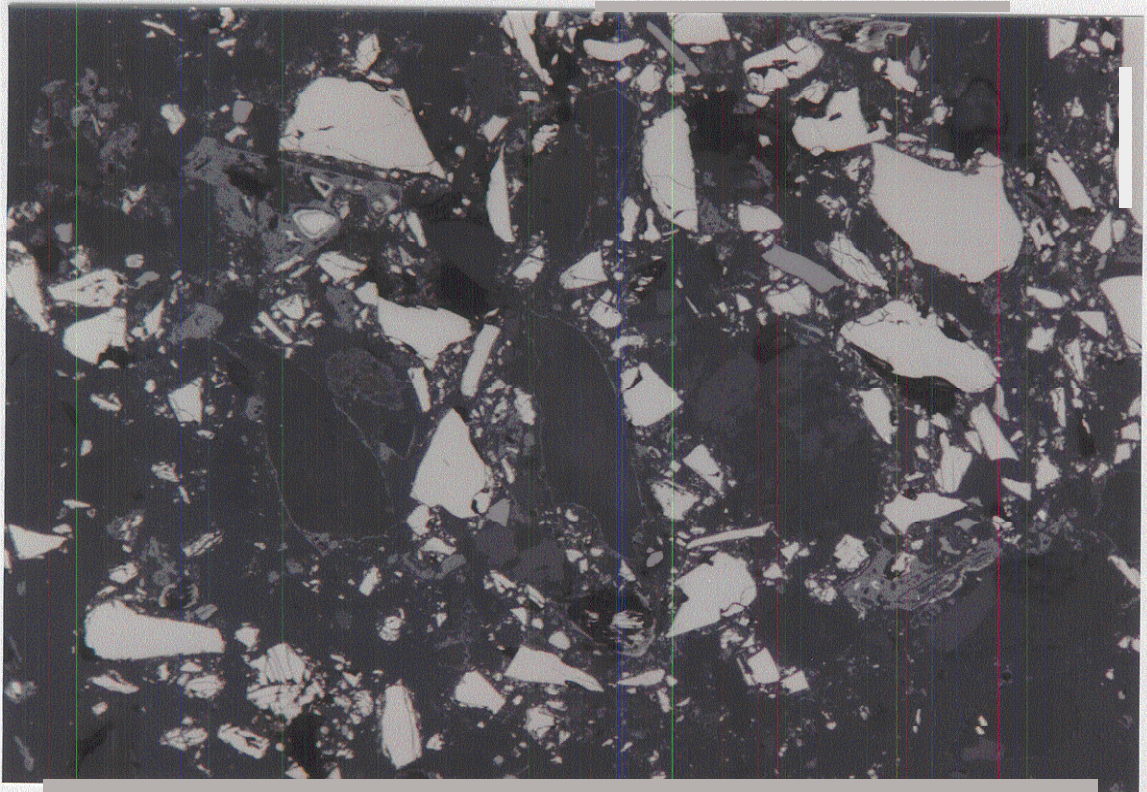
Illustration #14 Magnification 200x Incident Light 125 μm
Sample 6-6 PS 5765

Photomicrograph of a loosely cemented limonite aggregate. Note the relatively fresh appearance of pyrrhotite grains in this photomicrograph, and the abundance of pyrrhotite fines (< 30 μm). A minor proportion of pyrrhotite shows incipient breakdown in the form of ragged grain margins.
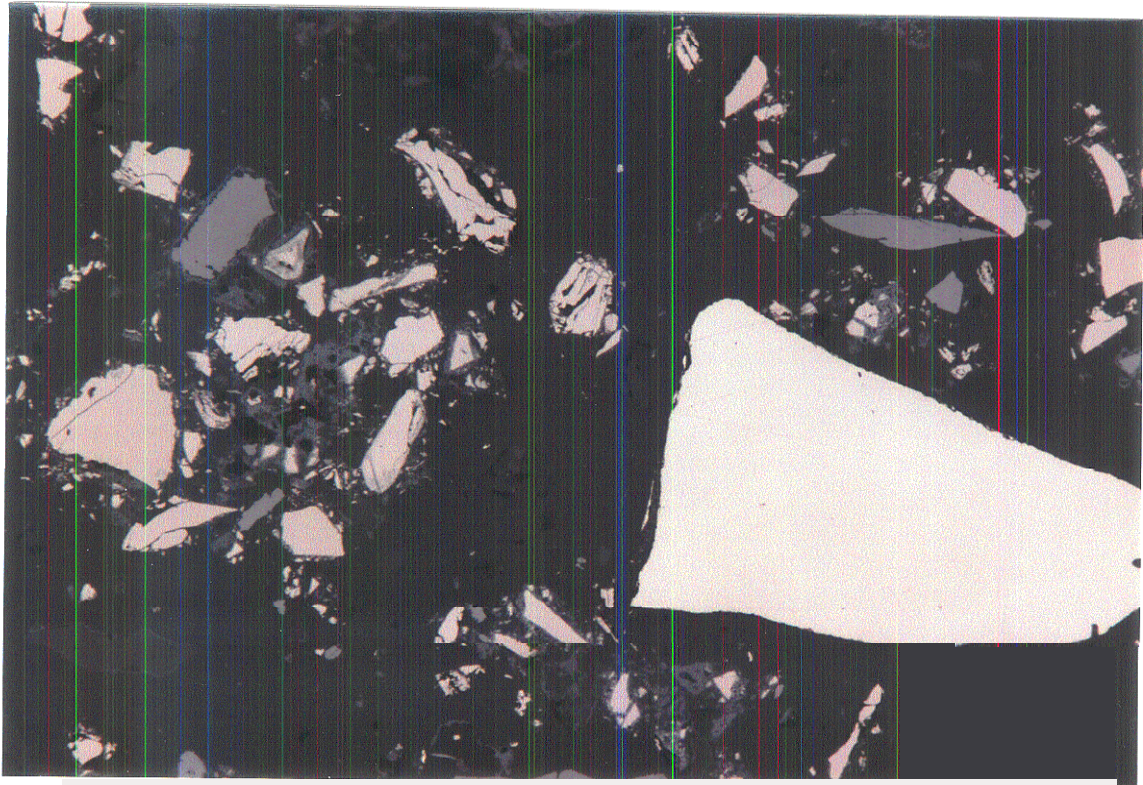
Illustration #15   **Magnification** 200x   **Incident Light**   125 µm
Sample 6-6   **PS 5765**

Photomicrograph of a large (> 200 µm) pyrrhotite grain which is **fresh in appearance** (right-centre). Pyrrhotite grains (left-centre) **show evidence of** minor **to moderate oxidation (cracked and** rims **of Fe-oxyhydroxide). Note the magnetite** (upper-left) **which shows** evidence of breakdown along **its grain boundaries. Magnetite is rare** in this sample (< 4% **of total** sample).

Sample (7-6): Oxidized tailings covered with LSSS and CB
PS 5766 and PTS 2739

The (7-6) tailings sample is dark orange-brown in colour, and is composed of approximately equal proportions of silicates, sulphides, and oxides.

Mineralogy	Est. Vol. %	Typical Grain Size
Pyrrhotite	30 to 35	20to 100 pm
Limonite	25 to 30	variable aggregates
Quartz	10 to 15	30 to 150 μm
Plagioclase	10 to 12	50 to 150 μm
Amphibole	4 to 6	50 to 120 μm
Magnetite	2 to 4	30 to 60 pm
Biotite	1 to 2	30 to 50 pm
Epidote	< 1	~ 70 μm
Chalcopyrite	0.5	20 to 50 pm
Pentlandite	trace	< 30 μm

This sample (7-6) is similar to the previous two, containing approximately equal proportions of pyrrhotite and silicates. It also contains abundant limonite cements. The ratio of limonite to pyrrhotite is high (with an estimated limonite:pyrrhotite ratio of almost 1: 1).

Pyrrhotite occurrence is similar to that described for the previous samples (6-6). A higher proportion of pyrrhotite in this sample is surrounded by limonite cementation. A few individual pyrrhotite grains appear fresh, however, the majority show evidence of incipient to moderate oxidation. The majority of pyrrhotite within compact limonite cemented 'clumps' is extensively corroded, indicative of in-situ oxidation and leaching. Minor chalcopyrite is present as discrete grains, and attached grains to silicates.

As previously described (samples 1-O and 6-6), this sample shows extensive limonite cementation. Limonite cemented 'clumps' are typically compact in nature, and only rarely occur as earthy or non-compact aggregates.

Silicates (30 to 35% of total sample) occur as discrete grains, consisting primarily of quartz, plagioclase, amphibole, and minor biotite and epidote.
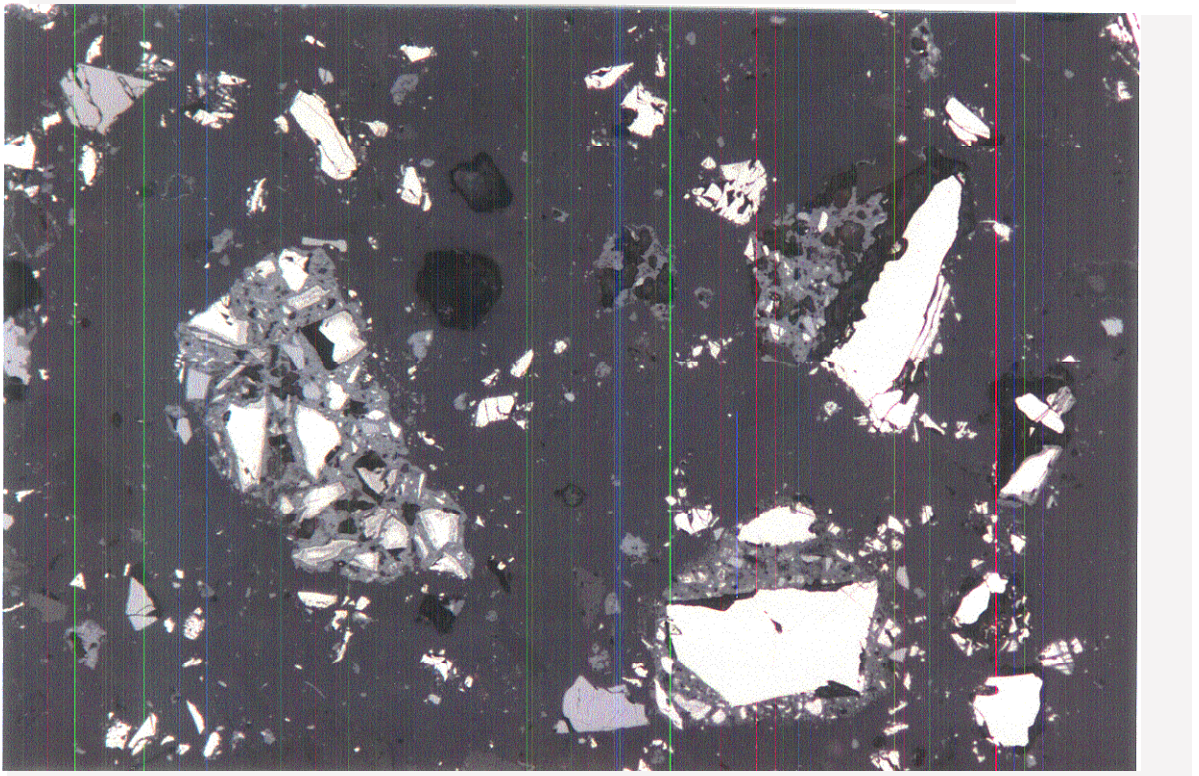
33

Illustration #16   **Magnification** 200x   **Incident Light**   125 μm

Sample 7-6   **PS 5766**

Photomicrograph **of representative pyrrhotite grains. The** majority **of pyrrhotite occurs** within limonite **cemented 'clumps' (left-centre), and a minor proportion** occurs **as liberated grains** (right-bottom, **and right-centrc). Almost all pyrrhotite enclosed** by limonite cements **are moderately oxidized with rims of** Fe-oxyhydroxide or **leached** margins. **Liberated pyrrhotite** grains show **incipient to moderate effects of oxidation (ragged margins and rims of** Fe-oxyhydroxide).
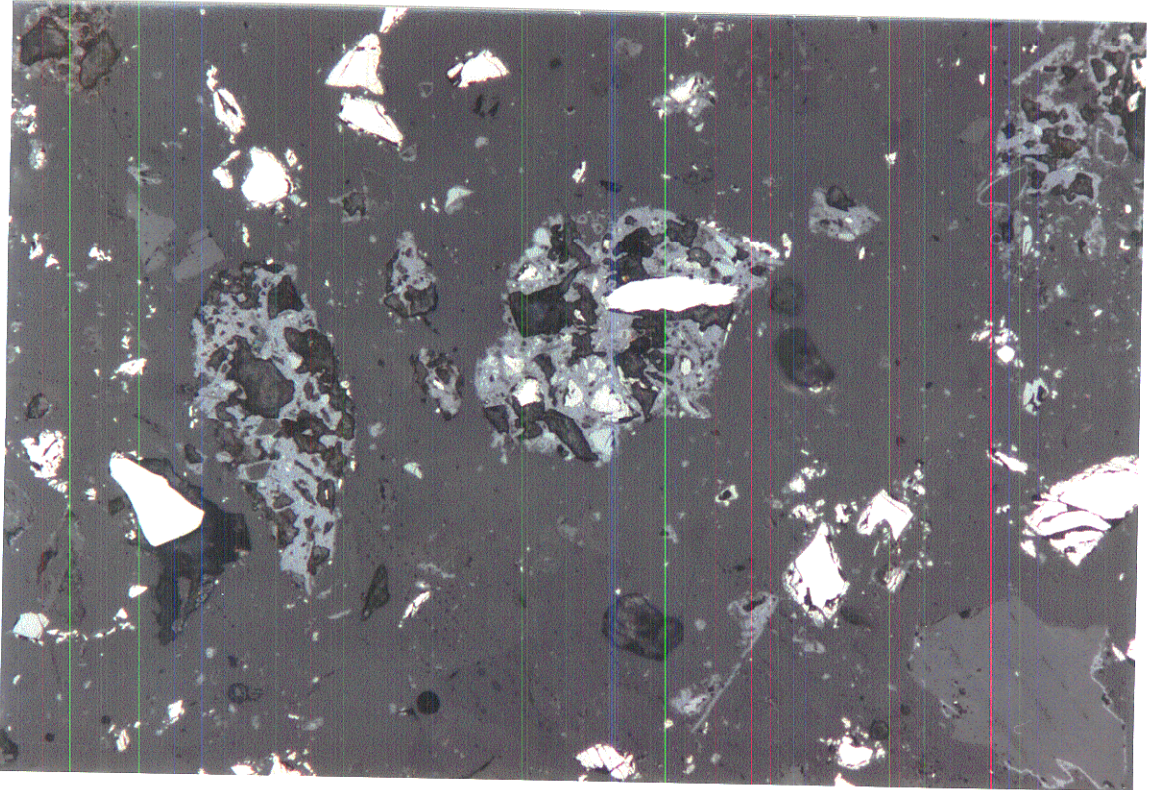
Illustration #17   Magnification 200x   Incident Light   125 μm
Sample 7-6   PS 5766

Photomicrograph of representative limonite cemented clumps Note the absence or rarity of pyrrhotite, and abundant cavities. which may represent dissolved pyrrhotite, or pyrrhotite which has been plucked from the limonite during sample preparation.

Sample (8-6): Fresh PO tailings covered with compost
PS 5767 and PTS 2740

The (S-6) tailings sample is charcoal black in colour, and is composed dominantly of sulphides, with lesser oxides, and minor silicates.

Mineralogy	Est. Vol. %	Typical Grain Size
Pyrrhotite	80 to 85	5 to 75 μm
Magnetite	10 to 12	15 to 40 μm
Quartz	1 to 2	10 to 75 μm
Amphibole	1 to 2	25 to 100 μm
Plagioclase	< 1	20to 100 μm
Chlorite	< 1	< 50 μm
Limonite	< 0.5	< 50 μm
Chalcopyrite	< 0.5	40 to 50 μm
Mica	trace	aggregates up to 50 μm

This sample (S-6) is unique in the suite for its high proportion of fines, extremely high ratio of pyrrhotite to silicates (with a pyrrhotite:silicate ratio of approximately 14: 1), and for the absence of limonite cements. It appears to represent relatively fresh or unoxidized tailings.

Pyrrhotite typically occurs as fresh grains, with sharp margins, and only rarely shows incipient oxidation. A large proportion of pyrrhotite is represented by fines (< 30 μm).

Limonite is rare (< 0.5% of total sample) and occurs as loosely cemented material. Magnetite is fairly abundant (10 to 12% of total sample), and occurs as discrete grains throughout the sample.

Silicates are rare (< 6% of total sample) and consist of minor quartz and amphibole, with trace plagioclase and chlorite.
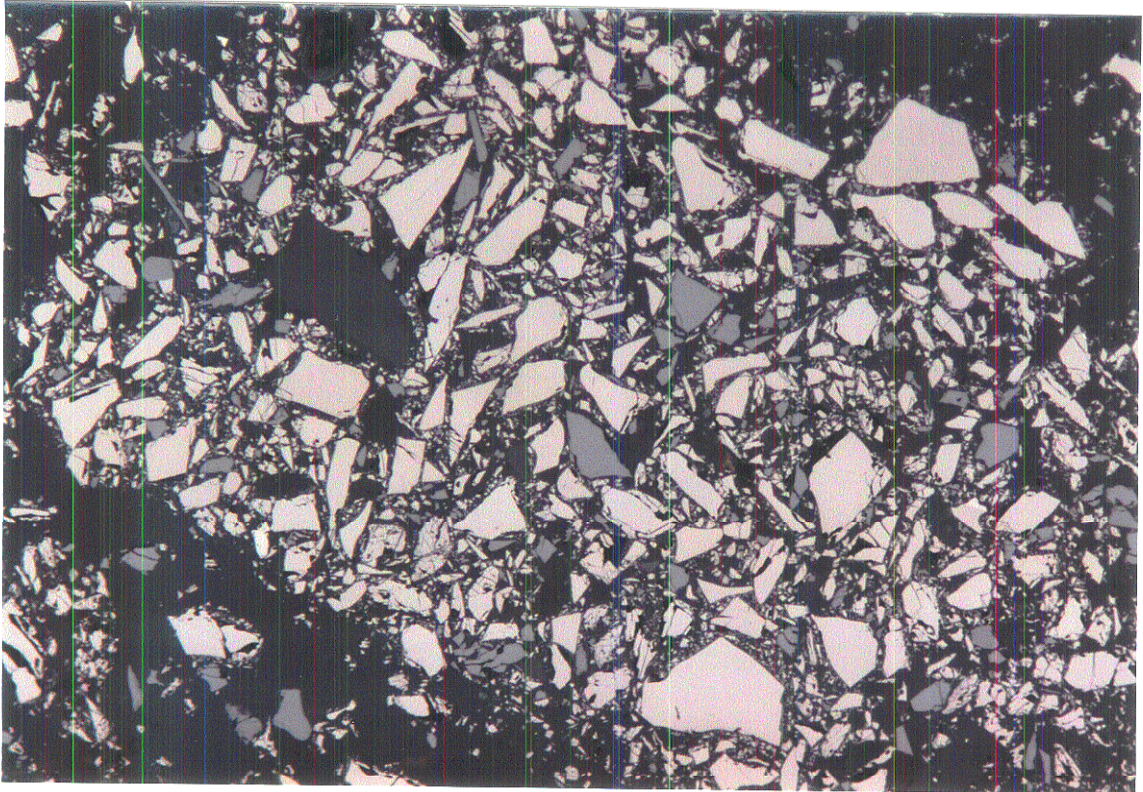
Illustration #18   Magnification   200s   Incident Light   125 pm
Sample 8-6   PS 5767

Photomicrograph of representative fresh pyrrhotite grams (sharp gram boundaries). and fresh magnetite grains (grey). This sample is composed almost entirely of individual liberated pyrrhotite grains. There is only a minor component (< 1% of total sample) of limonite cementation. This sample represents the least oxidized of the suite.

APPENDIX H

RESULTS FOR INCUBATION TEST AND COMPUTER MODELING

Lakefield Research Study
of
RDP Biosolid Cap on DST Minesoil

Organic Amendment Evaluated

RDP Lime Stabilized Biosolid

Soils Used in Evaluation

DST Minesoil

Methods Used in Laboratory Studies

The RDP and DST samples were obtained from Liangxue Liu of Lakefield Research Environmental Services.

RDP and DST were tested for moisture content at low temperature (40-45°C).

A reduced moisture RDP (50% of original moisture) was created by air drying the original RDP in a fume hood for 21 hours. RDP and DST mixtures were created by mixing appropriate volumes of each component to give a 50% RDP:50% DST mixture and a 20% RDP:80% DST mixture.

Each treatment was loaded into a test tube to simulate a column of material and placed in a 500-ml respiration vessel. An empty respiration vessel served as the control. Weights of the test tubes and test tubes plus treatments were recorded. The respiration vessels were then placed in a constant temperature chamber at 25 degrees C. Treatments and controls were duplicated.

Decomposition of the organic amendments was determined by trapping carbon dioxide evolved during the 63 day decomposition period in 1 N NaOH base traps. The base traps were analyzed by weak acid titration after the addition of barium chloride.

At the termination of the experiment the final test tube plus treatment weights were determined to estimate any weight loss that might have occurred. Replicates were then mixed. An undried sample was extracted with distilled water, the extract filtered through Watman #42 filter paper and the filtrate evaluated for soluble organic C. The remainder of each sample was dried at low temperature (40-45°C) and evaluated for % solids, total C by combustion at 900°C and inorganic C at 500°C by trapping evolved carbon dioxide in

ascarite and weighing. Organic C was the difference between total C and inorganic C. Initial samples of the RDP, 50% RPD, and the two RPD:DST mixtures which had be stored in the refrigerator at 4°C were also analyzed so that changes in C species could be assessed.

The organic nitrogen data for the RDP and DST samples were obtained from the UA Diagnostic Services Laboratory.

Laboratory Study Results

The dried RDP sample contained 2.53% organic N, while the dried DST sample contained less than 0.01% organic N. Percent solids (g/100g moist) were 31 and 82, respectively.

Decomposition is the percentage of the original RDP and/or DST organic carbon converted to carbon dioxide is presented below. No decomposition as carbon dioxide evolution was found for any treatment at any time.

Days	% Decomposition			
	RDP	50% moist. RDP	50% RPD 50% DST	20% RDP 80% DST
2	0	0	0	0
4	0	0	0	0
6	0	0	0	0
18	0	0	0	0
30	0	0	0	0
47	0	0	0	0
64	0	0	0	0

initial and final dry weights are reported in the table below. The small differences (+l-1%) are within experimental error and, so, dry weights also suggested that decomposition had not occurred in any of the treatments over the 63 day period.

Sample	Dry Weight, g			
	RDP	50% moist. RDP	50% RPD . 50% DST	20% RDP 80% DST
initial	3.50	4.30	8.20	8.50
final	3.55	4.25	8.10	8.50
difference	+ 0.05	▪ 0.05	▪ 0.10	0

Initial and final soluble organic C contents of the moist samples are reported in the table below. The change in soluble organic C for the RDP treatment was large. The changes in soluble organic C for the other treatments were small and probably within experimental variability.

Sample	Soluble Organic C, %			
	RDP	50% moist. RDP	50% RPD 50% DST	20% RDP 80% DST
initial	3.43	2.00	0.59	0.26
final	2.14	2.21	0.66	0.36
difference	- 1.29	+ 0.21	+ 0.07	+ 0.10

Organic C contents of the dried samples are shown in the table below.. One box is shown for initial and final values as no statistically significant differences were found between initial and final subsamples. While there was no statistically significant difference between initial and final values for RDP, the actual values were 10.2% and **9.6%,** respectively, or a decrease of 0.6% as compared to the 1.3% decline in soluble organic C. This suggested that decomposition of soluble organic C was occurring and that some portion of the soluble organic C was lost during drying at low temperature.

Sample	Organic C, %			
	RDP ..	50% moist. RDP	50% RPD 50% DST	20% RDP 80% DST
initial	9.9	10.5	2.9	1.6
final				
difference	----	---	---	---

Inorganic C contents are shown in the table below. Again, one box is shown for initial and final values as no statistically significant differences were found between initial and final subsamples. While there was no statistically significant difference between initial and final values for RDP, the actual values were 9.7% and **10.1%,** respectively, or an increase of 0.4% as compared to the 1.3% decline in soluble organic C. This suggested that any CO, produced from decomposition of soluble organic C was precipitated as a carbonate by the bases in the lime stabilized biosolid.

Sample	Inorganic C, %			
	RDP	50% moist. RDP	50% RPD 50% DST	20% RDP 00% DST
initial	9.9	9.6	1.8	0.9
final				
difference	---	---	---	---

It is hypothesized that the reaction shown below was occurring in the moist RDP because soluble organic C clearly decreased, organic C showed a trend toward a decrease, and inorganic C showed a trend toward an increase.

$$\text{Organic C} \rightarrow \text{Soluble Organic C} \rightarrow CO, + Ca(OH), \rightleftharpoons CaCO_3 \downarrow + H_2O$$
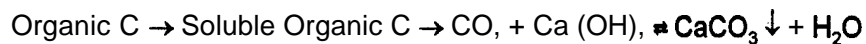
If this decline in soluble organic C was reasonably constant over the 63 day incubation, then the rate of loss of soluble organic C or rate decomposition of moist RDP is calculable.

Some assumptions need to be made to estimate the values of the rate constant and percentage of the organic C in the soluble form. Since the soluble organic C declined by 1.3% of the dry weight of a moist sample of RDP and organic C decreased by 0.6% for the dried RDP sample, it was assumed that about 50% of the soluble organic C was lost when the sample was dried at low temperature. With the latter in mind, the initial organic C content of RDP was set at 9.9% plus 1.7% (from soluble organic C lost during drying) or 11.6% organic C. The initial C:N ratio was 4.6 using the latter value.

If 1.3% of the sample weight was lost in the soluble organic C fraction, then 11% of the initial organic C was also lost (1.3*100/11.6) over the 63 day period. This translates into a first order rate constant of 0.00175 d^{-1} which corresponds to values found for the slow fraction of other, similar biosolids. Thus, it would appear that decomposition **was** occurring, but that it was not detectable due to readsorption of CO, by the lime in the biosolid.

Similar calculations were not made for the other treatments as sufficient evidence for decomposition followed by readsorption of CO, was not obtained.

Description of Computer Simulations

The computer model, DECOMPOSITION, was used in the simulations. The model is actually two computer models. The first creates a physical environment where soil water and temperature relationships are established and decomposition rate constants are corrected for these effects, while the second accounts for the organic amendment carbon and nitrogen mineralization under field conditions.

In the first portion of DECOMPOSITION, soil texture is specified and a water balance for the rootzone is constructed using rainfall and pan evaporation data from NOAA literature. Soil temperatures are estimated using air temperatures from NOAA literature. These data are used to adjust laboratory decomposition rates to field conditions. In this report, optimum soil moisture was assumed for the simulations run at 25°C.

Weather near the site was provided by Liangxue Liu of Lakefield Research Environmental Services.

The second portion of DECOMPOSITION partitions both C and N into the various soil organic carbon pools. During decomposition, the organic amendment fraction that is most decomposable undergoes decomposition first followed by the more slowly decomposable fraction. For RDP, only the slow fraction was assumed. As the organic amendment decomposes, organic N is mineralized or immobilized depending on the C:N of the organic amendment. Soil microbial biomass and soil organic matter or humus pools are also included in these computations.

Computer Simulation of Decomposition and Net N Mineralization

The results of the computer simulation for moist RDP are presented in the two graphs and the table shown below. Decomposition and net N mineralization were predicted during the warmer months with initial annual values of 1516% decomposition and 8-9 lb N/dry ton/acre annually.

The minimum amount of decomposition would be depletion of all the soluble organic C or about 30% (3.4*100/1 1.6) of the organic C in RDP. If this were to take place, decomposition and N mineralization would slow markedly after two years.

Biosolid	First Year		Second Year	
	Decomposition %	Plant Available N lb N per dry ton	Decomposition %	Plant Available N lb N per dry ton
RDP	1 6	9	1 5	8

Conclusions

It is expected that the RDP cap on the DST minesoil will remain in place for some time. Decomposition is slow and decomposition products probably form precipitates remaining in the cap material. The drier RDP and the RDP:DST mixtures appear to be fairly resistant to decomposition.

Net N mineralization is expected to occur and inorganic N in the RDP cap should be assessed although the high pH of the moist RDP biosolid probably precludes much nitrate formation and potential for leaching.

6

RDP Biosolid Applied in July
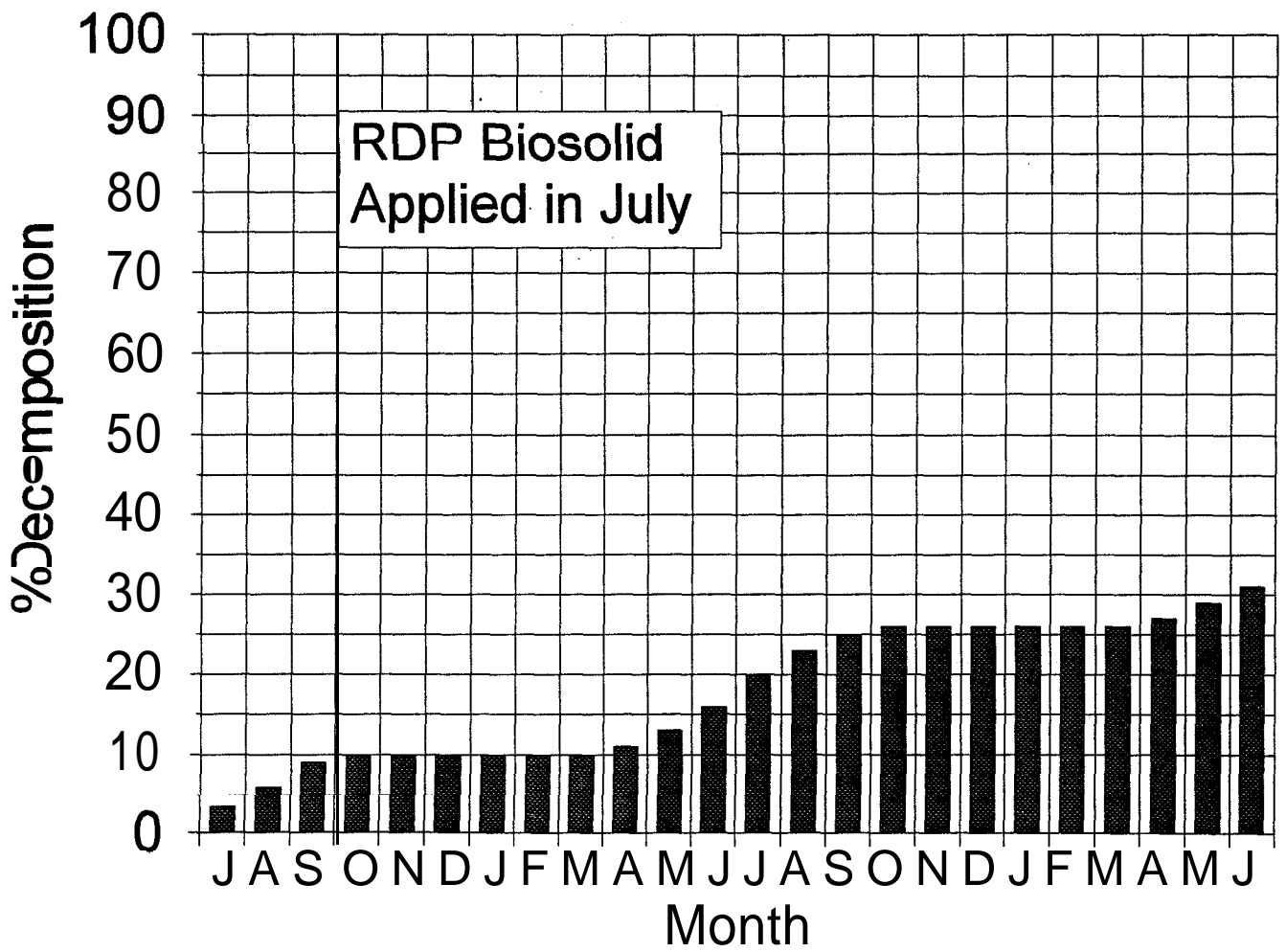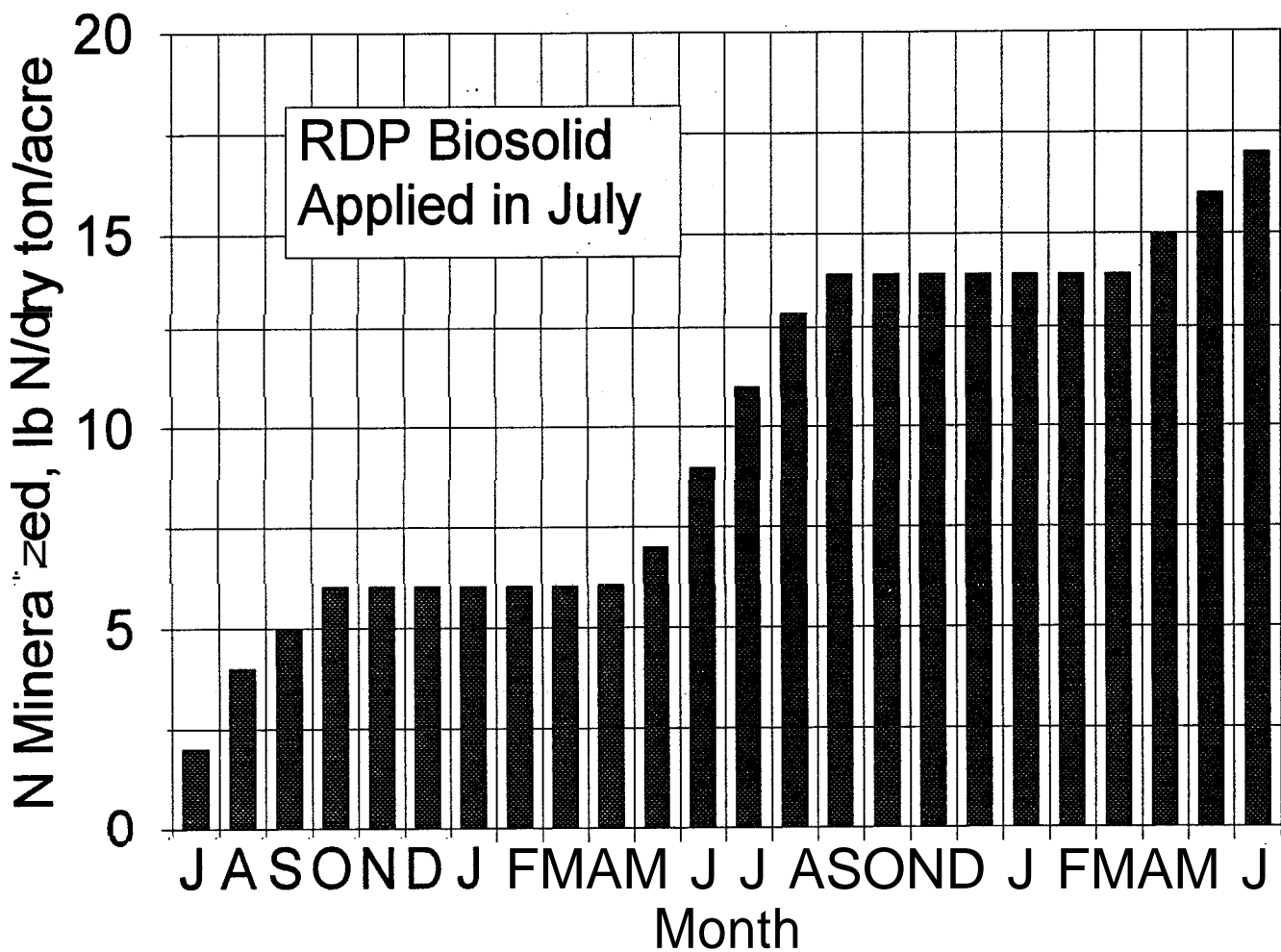
August 13, 1996

TO: **Liangxue Liu**

FROM: John Gilmour

RE: Final Report for the RDP:DST Study

The reason that the 100% **RDP was** the only treatment modeled was that it was the only **treatment** that showed any sign of decomposition as evidenced by the decrease in **soluble** organic C reported on page 3 of the Final Report. The **changes** in soluble organic C for tho other treatments **were very small** and inconsistent, and so, in combination with the other **results** it was assumed that decomposition did not **occur in** 'the other treatments. Thus, they could not be modeled as the model would use rate **constants** equal to zero,

It would appear that some decomposition will occur where 100% **RDP** exists in the cap. At positions where the materials aro **more** like 50% **RDP** or the RDP:DST mixtures, little decomposition is expected based on the laboratory study results. Over a **ten** year period, the total amount of decomposition is going to depend on the relative proportions and water contents of each of the components. If you can estimate the percentage of the cap that is 100% **RDP (RDP** at initial **moisture** and not dried), you can provide a good estimate of what will be left after ten years provided that material that is exposed **(after** decomposition of 100% RDP) does not become **100%** RDP complicating the calculation. I am not trying hedge here • the question regarding what **will** happen in a decade is a **difficult one.**

An approximate estimate of the amount of decomposition of 100% RDP can **be obtained** from the equation below.

$$\% \text{ Decomposition} = 100 \ (I-e">, \text{ where } k=0. 17 \text{ and } t \text{ is years.}$$

After ten years, over 80% of the 100% RDP would be lost as CO,

As before, I have enjoyed working with **Lakefield** Research Limited and hope Predictive Modeling, Inc. can be of service in the **future.**

APPENDIX I

LEACHATE CHARACTERISTICS

Leachate Analysis for Cell #1 Control Cell

Parameter	Unit	Week of Sampling						
		Oct-13-95	Oct-31-95	Nov-29-95	Jan-8-96	Jan-29-96	Feb-19-96	Mar-11-96
SO$_4$	mg/L	51070	71340	60540	52200	62100	64562	27329
Al	mg/L	4.24	1.08	0.15	5.90	1.61	0.34	6.05
As	mg/L	< 0.50	< 0.30	11.3	< 0.05	2.5	< 0.50	< 0.05
Ba	mg/L	0.16	0.23	0.19	0.15	0.19	0.18	0.10
Be	mg/L	< 0.01	< 0.005	< 0.005	< 0.005	<0.005	< 0.005	< 0.005
Ca	mg/L	480	448	538	495	602	528	352
Cd	mg/L	2.17	2.89	2.60	2.25	2.53	3.43	0.81
Co	mg/L	1.31	1.52	1.52	1.32	1.61	1.75	0.90
Cr	mg/L	< 0.04	< 0.02	< 0.02	< 0.02	< 0.02	< 0.02	< 0.02
Cu	mg/L	< 0.03	< 0.02	0.08	0.37	0.24	< 0.015	< 0.02
Fe	mg/L	26330	35800	29750	28000	33900	36100	21715
Mg	mg/L	522	801	534	563	689	638	352
Mn	mg/L	39.6	51.5	41.3	33.3	46.9	48.9	22.4
Mo	mg/L	< 0.10	< 0.05	< 0.05	< 0.04	< 0.035	< 0.035	< 0.04
Na	mg/L	142	201	178	123	179	174	90.6
Ni	mg/L	9.68	5.65	3.99	16.4	4.05	2.00	14.5
P	mg/L	< 0.30	1.02	0.32	0.25	1.03	0.70	< 0.20
Pb	mg/L	2.63	4.04	2.77	< 0.10	3.11	4.35	1.41
S	mg/L	17575	23780	20230	17400	20700	23500	14100
Sb	mg/L	1.06	< 1.00	1.38	< 0.10	< 0.10	< 0.10	< 0.10
Se	mg/L	< 0.20	< 0.10	< 0.10	< 0.10	< 0.10	< 0.10	< 0.10
Si	mg/L	37.9	46.8	34.7	30.3	60.7	69.0	33.1
Sn	mg/L	< 0.20	co.10	< 0.10	< 0.50	< 0.10	< 0.10	< 0.10
Te	mg/L	< 0.40	2.73	< 0.30	< 0.20	< 0.20	< 0.20	< 0.20
Zn	mg/L	4.06	8.96	3.83	4.24	5.18	6.40	3.82
Hardness	mg/L	▪	883	3541	3550	4340	3940	2330
pH	unit	2.39	2.32	2.54	2.71	2.64	2.50	2.54
Conductivity	μmhos/cm	34600	42700	46500	36400	37300	36400	25300

Leachate Analysis for Cell #2 LSSS Over Oxidized Tailings

Parameter	Unit	Week of Sample						
		Oct-13-95	Oct-31-95	Nov-29-95	Jan-8-96	Jan-29-96	Feb-19-96	Mar-11-96
SO$_4$	mg/L	31550	36600	26640	12480	13680	14537	12676
Al	mg/L	<0.20	<0.10	<0.10	4.37	1.02	0.66	1.61
As	mg/L	<0.50	<0.30	2.24	<0.05	<0.5	<0.10	<0.05
Ba	mg/L	0.13	0.16	0.11	0.068	0.096	0.082	0.06
Be	mg/L	<0.01	<0.005	<0.005	<0.005	<0.005	<0.01	<0.005
Ca	mg/L	409	469	444	470	578	640	459'
Cd	mg/L	0.86	0.91	0.58	0.35	0.13	0.12	0.06
C0	mg/L	0.52	0.50	0.37	0.25	0.29	<0.04	0.14
Cr	mg/L	0.05	<0.02	0.03	<0.02	<0.02	<0.040	<0.02
Cu	mg/L	co.03	<0.02	0.37	0.15	0.091	0.058	<0.02
Fe	mg/L	11075	11790	7180	4120	1900	1340	1317
Mg	mg/L	192	216	131	108	52	57.6	53.5
Mn	mg/L	15.5	16.4	10.1	5.65	3.77	4.03	2.96
Mo	mg/L	I <0.10	I co.05	I co.05	I <0.04	<0.035	<0.07	<0.04
Na	g/L m	650	956		79808	659	649	757
Ni	mg/L	0.42	0.44	0.20	0.18	<0.05	0.35	0.32
P	mg/L	3.29	3.85	3.80	3.06	3.21	4.25	2.77
Pb	mg/L	1.43	1.28	0.60	2.25	0.25	<0.20	0.19
S	mg/L	I 10910	12200	8880	5900	4560	5650	5030
Sb	mg/L	0.40	<1.00	0.31	<0.10	<0.10	<0.20	<0.10
Se	mg/L	<0.20	<0.10	<0.10	<0.10	<0.10	<0.20	<0.10
Si	mg/L	24.5	29.1	16.9	15.5	18.6	23	13.4
Sn	mg/L	<0.20	<0.10	<0.10	<0.50	<0.10	<0.20	<0.10
Te	mg/L	<0.40	0.78	<0.30	<0.20	<0.20	<0.40	<0.20
Zn	mg/L	1.14	1.32	0.72	0.87	0.25	0.3	0.33
Hardness	mg/L	-	412	1648	1620	1660	1840	1370
pH	unit	4.05	4.37	4.88	5.24	5.44	5.74	6.21
Conductivity	μmhos/cm	35900	45500	46500	32600	32200	28800	25000

Leachate Analysis for Cell #3 Desulphurized Tailings Over Oxidized Tailings

Parameter	Unit	Week of Sample						
		Oct-13-95	Oct-31-95	Nov-29-95	Jan-8-96	Jan-29-96	Feb-19-96	Mar-11-96
SO_4	mg/L	332	333	429	■	2331	3426	2730
Al	mg/L	1.11	1.09	1.24	-	10.7	14.5	18.1
AS	mg/L	< 0.50	< 0.30	< 0.05	-	<0.50	< 0.05	< 0.05
Ba	mg/L	0.02	0.03	0.03	-	0.028	< 0.01	0.02
Be	mg/L	< 0.01	< 0.005	< 0.005	-	<0.005	< 0.005	< 0.005
Ca	mg/L	91.2	83.8	116	-	134	152	202
Cd	mg/L	< 0.02	0.01	0.03	-	0.077	0.09	0.06
Co	mg/L	0.09	0.02	0.03	-	0.15	0.44	0.25
Cr	mg/L	< 0.04	< 0.02	0.10	-	< 0.02	< 0.02	0.03
Cu	mg/L	0.33	0.21	0.18	-	1.59	1.74	2.48
Fe	mg/L	2.74	6.80	27.3	-	890	959	986
Mg	mg/L	17.3	16.8	24	-	50.3	58.4	64.6
Mn	mg/L	0.49	0.45	0.62	■	3.94	4.37	4.11
Mo	mg/L	< 0.10	< 0.05	0.08	■	< 0.035	< 0.035	< 0.04
Na	mg/L	20.7	21.4	41.5	■	21.6	21.8	30.8
Ni	mg/L	1.01	0.80	**1.01**	■	9.28	12.8	11.5
P	mg/L	< 0.30	co.20	co.20	■	1.21	0.43	0.95
Pb	mg/L	0.30	< 0.10	< 0.10	-	0.12	0.46	0.22
S	mg/L	115	111	145	-	777	919	960
Sb	mg/L	< 0.20	< 1.00	< 0.10	-	< 0.10	< 0.10	< 0.10
Se	mg/L	< 0.20	< 0.10	< 0.10	-	< 0.10	< 0.10	< 0.10
Si	mg/L	< 0.40	1.37	< 0.30	-	7.02	7.11	6.48
Sn	mg/L	< 0.20	< 0.10	< 0.10	-	< 0.10	< 0.10	< 0.10
Te	mg/L	0.50	< 0.20	< 0.30	-	< 0.20	< 0.20	< 0.20
Zn	mg/L	0.48	0.43	0.39		0.71	1.27	0.9
Hardness	mg/L	-	55.6	388	■	542	620	770
pH	unit	3.88	3.30	4.38	■	2.81	2.78	2.87
Conductivity	umhos/cm	791	1105	1172	■	3760	3720	3730

Note:

Leachate was collected immediately after rainfall application, and no leachate from the tailings afterwards.

Leachate analysis for Cell #4 Compost Over Oxidized Tailings

Parameter	unit	Week of Sampling						
		Oct-13-95	Oct-31-95	Nov-29-95	Jan-8-96	Jan-29-96	Feb-19-96	Mar-1 1-96
SO_4	mg/L	29650	34710	19240	29280	34200	35863	31736
Al	mg/L	< 0.20	< 0.10	0.11	3.93	0.26	co.10	0.98
As	mg/L	< 0.50	< 0.30	4.13	< 0.05	<0.5	< 0.50	< 0.05
Ba	mg/L	0.08	0.12	0.09	0.099	0.12	0.095	0.09
Be	mg/L	< 0.01	< 0.005	< 0.005	< 0.005	<0.005	< 0.005	< 0.005
Ca	mg/L	551	461	574	496	459	425	347
Cd	mg/L	1.24	1.42	1.02	1.16	1.41	1.82	0.64
Co	mg/L	0.80	0.81	0.65	0.74	1.02	0.95	0.67
Cr	mg/L	< 0.04	< 0.02	< 0.02	< 0.02	< 0.02	< 0.020	< 0.02
Cu	mg/L	< 0.03	< 0.02	0.06	0.19	0.12	< 0.015	< 0.02
Fe	mg/L	14425	17480	12330	14300	18200	17100	17490
Mg	mg/L	510	574	437	496	433	416	330
Mn	mg/L	23.9	26.3	16.6	15.5	22.3	22.7	15.2
Mo	mg/L	< 0.10	co. 05	60.05	< 0.04	co. 035	< 0.035	< 0.04
Na	mg/L	780	872	1170	883	816	895	819
Ni	mg/L	0.79	0.48	0.58	0.49	< 0.05	0.38	0.23
P	mg/L	0.90	0.77	0.20	0.28	< 0.15	0.96	< 0.20
Pb	mg/L	1.58	2.42	1.13	< 0.10	1.96	1.82	1.24
S	mg/L	10215	11570	8910	9760	11400	12200	11700
sb	mg/L	0.55	< 1.00	0.72	< 0.10	< 0.10	< 0.10	< 0.10
S e	mg/L	< 0.20	< 0.10	GO.10	co.10	co.10	< 0.10	< 0.10
Si	mg/L	27.1	28.6	14	15.2	21.9	27	26.4
Sn	mg/L	< 0.20	< 0.10	< 0.10	< 0.50	< 0.10	< 0.10	< 0.10
Te	mg/L	< 0.40	1.40	co. 30	< 0.20	< 0.20	< 0.20	< 0.20
Zu	mg/L	1.87	2.30	1.60	2.11	2.42	3.21	2.61
Hardness	mg/L	.	703	3232	3280	2930	2770	2220
pH	unit	2.70	2.42	2.93	4.16	3.65	3.49	3.36
Conductivity	μmhos/cm	32200	36400	36100	31300	29900	29400	27000

Leachate Analysis for Cell #5 Peat Over Oxidiied Tailings

Parameter	Unit	Week of Sampling						
		Oct-13-95	Oct-31-95	Nov-29-95	Jan-8-96	Jan-29-96	Feb-19-96	Mar-11-96
SO_4	mg/L	45000	43380	39930	28560	30600	31885	25284
Al	mg/L	0.67	0.33	0.30	3.56	0.83	0.33	1.64
As	mg/L	< 0.50	< 0.30	7.07	12.5	<0.5	< 0.50	< 0.05
Ba	mg/L	0.13	0.13	0.13	0.082	0.1	0.076	0.08
Be	mg/L	< 0.01	< 0.005	< 0.005	< 0.005	<0.005	< 0.005	< 0.005
Ca	mg/L	485	428	478	450	513	478	397
Cd	mg/L	1.74	1.83	1.72	1.27	1.31	1.67	0.57
Co	mg/L	1.17	1.02	1.02	0.74	0.95	1.09	0.61
Cr	mg/L	< 0.04	< 0.02	< 0.02	< 0.02	< 0.02	< 0.020	< 0.02
Cu	mg/L	< 0.03	< 0.02	0.05	0.18	0.14	< 0.015	< 0.02
Fe	mg/L	21135	21870	19860	14600	16600	16100	15935
Mg	mg/L	389	347	296	221	259	220	170
Mn	mg/L	37.5	33.7	30.4	19.6	26.5	24.8	15.8
Mo	mg/L	< 0.10	< 0.05	< 0.05	< 0.04	< 0.035	< 0.035	< 0.04
Na	mg/L	108	97.6	91.3	52.6	61.4	52.5	39.5
Ni	mg/L	0.48	0.27	0.30	< 0.05	< 0.05	< 0.05	< 0.05
P	mg/L	0.70	0.45	0.24	0.26	< 0.15	< 0.15	3.19
Pb	mg/L	2.31	2.66	1.90	< 0.10	1.24	2.12	0.99
S	mg/L	15000	14460	13310	9520	10200	11000	10400
Sb	mg/L	1.36	< 1.00	1.16	< 0.10	< 0.10	< 0.10	< 0.10
Se	mg/L	< 0.20	< 0.10	< 0.10	< 0.10	< 0.10	< 0.10	< 0.10
Si	mg/L	43.7	37.6	30.8	33.6	49	53.4	43.4
Sn	mg/L	< 0.20	< 0.10	< 0.10	< 0.50	< 0.10	< 0.10	< 0.10
Te	mg/L	< 0.40	0.82	< 0.30	< 0.20	< 0.20	< 0.20	< 0.20
Zn	mg/L	2.92	3.11	2.75	2.16	2.84	3.42	2.64
Hardness	mg/L	-	500	2412	2030	2350	2100	1690
pH	unit	2.08	2.26	2.46	2.71	2.59	2.61	2.45
Conductivity	μmhos/cm	33300	34800	32500	23600	23300	22300	20800

c:\data\7-112\leachate.xls

Leachate Analysis for Cell #6 Desulfurized Tailings + CB Over Oxidized Tailings

Parameter	unit	Week of Sampling						
		Oct-13-95	Oct-31-95	Nov-29-95	Jan-8-96	Jan-29-96	Feb-19-96	Mar-1 1-96
SO₄	mg/L	324	330	455	59700	73500	77005	58500
Al	mg/L	1.07	0.15	0.27	6.44	2.45	2.69	2.87
As	mg/L	co.50	< 0.30	< 0.05	12.5	2.5	1.65	< 0.05
Ba	mg/L	0.03	0.02	0.03	0.16	0.22	0.17	0.13
Be	mg/L	< 0.01	< 0.005	< 0.005	< 0,005	<0.005	< 0.005	< 0.005
Ca	mg/L	96	99.1	126	567	620	513	437
Cd	mg/L	< 0.02	< 0.01	0.05	2.44	2.99	3.37	1.24
Co	mg/L	< 0.04	< 0.02	0.12	1.53	2.04	1.97	1.06
Cr	mg/L	0.09	< 0.02	0.09	< 0.02	< 0.02	< 0.020	< 0.02
Cu	mg/L	0.17	0.14	0.13	0.35	0.87	0.07	< 0.02
Fe	mg/L	0.23	2.00	216	31200	40100	36700	29955
Mg	mg/L	15.2	20.2	38.6	710	903	681	475
Mn	mg/L	0.59	0.79	1.80	34.9	53.3	49.1	29.9
Mo	mg/L	< 0.10	< 0.05	0.06	< 0.04	< 0.035	< 0.035	< 0.04
Na	mg/L	16	20.6	37.1	138	176	140	124
Ni	mg/L	0.84	0.85	1.68	369	405	137	55.8
P	mg/L	< 0.30	< 0.20	< 0.20	< 0.20	< 0.15	< 0.15	0.77
Pb	mg/L	< 0.20	< 0.10	< 0.10	< 0.10	3.79	3.8	2.04
S	mg/L	108	110	162	19900	24500	23400	19500
Sb	mg/L	< 0.20	< 1.00	0.16	< 0.10	< 0.10	< 0.10	< 0.10
Se	mg/L	< 0.20	< 0.10	< 0.10	< 0.10	< 0.10	< 0.10	< 0.10
Si	mg/L	< 0.40	0.99	< 0.30	44.6	73.4	72.5	56.7
Sn	mg/L	< 0.20	< 0.10	< 0.10	< 0.50	< 0.10	< 0.10	< 0.10
Te	mg/L	0.53	< 0.20	< 0.30	< 0.20	< 0.20	< 0.20	< 0.20
Zn	mg/L	0.32	0.37	0.48	6.18	8.73	8.63	5.81
pH	unit	.	66.1	474	4340	5260	4080	3050
Conductivity	μmhos/cm	4.65 759	5.56 919	1190 5.64	39100 2.74,	39900 2.40	37300 2.24	31900 2.24

Note:
  During the weeks of Oct. 13, 1995, Oct. 31, 1995 and Nov. 29, 1995, leachate was collected immediately
  After rainfall application, and no leachate from the tailings afterwards.
  Starting Jan.8, 1996, leachate was collected from bottom tailings layer.

Leachate Analysis for Cell #7 LSSS + CB Over Oxidized Tailings

Parameter	unit	Week of Sampling						
		Oct-13-95	Oct-31-95	Nov-29-95	Jan-8-96	Jan-29-96	Feb-19-96	Mar-11-96
SO$_4$	mg/L	37980	35160	21750	20141	9149	23106	24171
Al	mg/L	<0.20	<0.10	0.14	2.51	0.61	0.45	1.37
As	mg/L	<0.50	<0.30	1.22	<0.05	<0.5	<0.05	<0.05
Ba	mg/L	0.17	0.15	0.08	0.062	0.096	0.14	0.11
Be	mg/L	<0.01	<0.005	<0.005	<0.005	<0.005	<0.01	<0.005
Ca	mg/L	454	393	405	414	553	556	459
Cd	mg/L	0.91	0.75	0.34	0.24	0.18	0.42	0.23
Co	mg/L	0.66	0.52	0.28	0.41	0.15	0.58	0.29
Cr	mg/L	<0.04	<0.02	0.06	0.04	<0.02	<0.040	0.03
Cu	mg/L	<0.03	<0.02	0.02	0.13	0.033	0.041	<0.02
Fe	mg/L	11175	10490	4989	3740	3490	4420	5470
Mg	mg/L	243	188	83.6	139	111	160	153
Mn	mg/L	16.8	13	5.69	5.24	5.97	8.95	6.74
Mo	mg/L	<0.10	<0.05	<0.05	<0.04	<0.035	<0.070	<0.04
Na	mg/L	825	872	609	692	684	611	875
Ni	mg/L	0.98	0.50	0.15	1.29	0.41	0.97	0.50
P	mg/L	6.34	4.41	3.06	3.34	3.11	4.19	3.78
Pb	mg/L	1.16	1.11	0.35	2.25	0.35	1.80	0.45
S	mg/L	12660	11720	7250	6960	6690	9200	9260
Sb	mg/L	0.95	<1.00	0.28	<0.10	<0.10	<0.20	<0.10
Se	mg/L	<0.20	<0.10	<0.10	<0.10	<0.10	<0.20	<0.10
Si	mg/L	22.4	22.6	7.69	14.4	19.3	23.8	19.2
Sn	mg/L	<0.20	<0.10	<0.10	<0.50	<0.10	<0.20	<0.10
Te	mg/L	<0.40	<0.20	<0.30	<0.20	<0.20	<0.40	<0.20
Zn	mg/L	1.32	1.21	0.48	0.45	0.4	0.93	0.76
Hardness	mg/L		352	1355	1610	1840	2050	1780
pH	unit	4.74	4.61	5.78	6.75	6.24	5.82	6.12
Conductivity	μmhos/cm	43400	50600	45000	36000	32900	34600	34100

c:\data\7-112\leachate.xls

Leachate Analysis for Cell #8 Compost Over Pyrrhotite Tailings

Parameter	Unit	Week of Sampling						
		Oct-13-95	Oct-31-95	Nov-29-95	Jan-8-96	Jan-29-96	Feb-19-96	Mar-11-96
SO_4	mg/L	7170	10578	5490	6192	7320	6575	8053
Al	mg/L	0.63	0.46	0.83	2.29	1.11	0.50	1.78
As	mg/L	<0.50	<0.30	<0.05	<0.05	<0.5	<0.10	<0.05
Ba	mg/L	0.12,	0.09	0.06	0.057	0.053	0.019	0.03
Be	mg/L	<0.01	<0.005	<0.005	co.005	<0.005	<0.005	<0.005
Ca	mg/L	1014	1195	1346	1030	826	594	615
Cd	mg/L	<0.02	0.02	0.03	<0.01	<0.01	<0.010	<0.01
Co	mg/L	0.05	<0.02	<0.02	<0.02	<0.02	<0.020	0.02
Cr	mg/L	0.13	<0.02	0.10	0.03	co.02	co.020	<0.02
cu	mg/L	co.03	0.04	<0.01	0.064	0.044	0.10	0.08
Fe	mg/L	-	2.12	8.51	2.13	3.96	2.86	2.27
Mg	mg/L	329	352	259	388	503	487	487
Mn	mg/L	1.56	0.88	0.55	0.68	0.41	0.19	0.47
Mo	mg/L	0.28	<0.05	0.18	<0.04	<0.035	0.22	<0.04
Na	mg/L	1235	1430	1280	1440	1840	1850	1950
Ni	mg/L	0.39	0.23	0.17	0.41	0.72	0.83	0.58
P	mg/L	0.38	0.61	0.21	1.73	0.53	1.08	1.37
Pb	mg/L	<0.20	0.13	<0.10	4.50	<0.10	0.23	0.14
S	mg/L	6975	4985	2140	2100	2440	2590	2860
Sb	mg/L	<0.20	<1.00	0.13	<0.10	<0.10	<0.10	<0.10
Se	mg/L	<0.20	<0.10	<0.10	<0.10	<0.10	<0.10	<0.10
Si	mg/L	0.69	3.06	<0.30	6.05	8.72	13.5	9.69
Sn	mg/L	<0.20	0.20	<0.10	<0.50	<0.10	<0.10	<0.10
Te	mg/L	0.73	<0.20	<0.30	<0.20	<0.20	<0.20	<0.20
Zn	mg/L	0.19	0.20	0.06	0.16	<0.20	0.021	<0.02
Hardness	mg/L	-	887	4427	4170	4130	3490	3540
pH	unit	6.12	6.37	7.46	7.25	8.11	8.21	8.35
Conductivity	μmhos/cm	21900	26200	24600	23400	25000	23800	24400